

Durham E-Theses

Neutrino masses and lepton flavour violating phenomena in the MSSM

Rimmer , Steven

How to cite:

Rimmer , Steven (2007) *Neutrino masses and lepton flavour violating phenomena in the MSSM*, Durham theses, Durham University. Available at Durham E-Theses Online:
<http://etheses.dur.ac.uk/2521/>

Use policy

The full-text may be used and/or reproduced, and given to third parties in any format or medium, without prior permission or charge, for personal research or study, educational, or not-for-profit purposes provided that:

- a full bibliographic reference is made to the original source
- a [link](#) is made to the metadata record in Durham E-Theses
- the full-text is not changed in any way

The full-text must not be sold in any format or medium without the formal permission of the copyright holders.

Please consult the [full Durham E-Theses policy](#) for further details.

Neutrino Masses and Lepton Flavour Violating Phenomena in the MSSM

A thesis presented for the degree of

Doctor of Philosophy

by

Steven Rimmer

Institute for Particle Physics Phenomenology

University of Durham

July 2007

The copyright of this thesis rests with the author or the university to which it was submitted. No quotation from it, or information derived from it may be published without the prior written consent of the author or university, and any information derived from it should be acknowledged.

17 OCT 2007



Abstract

The most general supersymmetric model with minimal particle content and an additional discrete \mathcal{Z}_3 symmetry, which allows lepton number violating terms, is considered. In this model, we calculate at the level of one-loop the resulting Majorana neutrino masses and the flavour violating radiative decays of charged leptons, $l \rightarrow l'\gamma$.

We first study the neutral scalar sector of the model, performing a calculable rotation of the scalar fields to a basis in which the sneutrino vacuum expectation values are zero. Lagrangian parameters are initialised without recourse to assumptions concerning trilinear or bilinear terms, CP-conservation or intergenerational mixing and one-loop corrections to the neutrino masses are analysed. We present scenarios in which the experimental data are reproduced. We find that with bilinear lepton number violating couplings in the superpotential of the order 1MeV the atmospheric mass scale can be reproduced. Certain trilinear superpotential couplings, usually of the order of the electron Yukawa coupling can give rise to either atmospheric or solar mass scales and bilinear supersymmetry breaking terms of the order 0.1GeV^2 can set the solar mass scale.

Taking parameters which correctly describe the neutrino sector, we consider their repercussions in flavour violating radiative lepton decays. Such decays have not been observed and upper bounds on their branching ratios exist. We note that certain parameter sets, which correctly describe the neutrino sector, will also generate observable branching ratios and suggest four such sets as Benchmarks scenarios.

We present as Appendices the full set of Feynman Rules for the general supersymmetric standard model with minimal particle content and details of the loop calculations in the Weyl spinor notation.



Acknowledgements

I would like to thank my supervisor, Dr. Athanasios Dedes, for the encouragement and expertise he has enthusiastically provided during the last three years. Our discussions, for which generous amounts of time were always made available, were the most enjoyable part of my study.

It was also a great pleasure to collaborate with Dr. Janusz Rosiek, both in Durham and during a splendid visit to Warsaw, and Mr. Maximilian Schmidt-Sommerfeld. I am glad to acknowledge that I was supported through this work by a PPARC scholarship.

Finally, I would like to thank my parents for years of unending and unwavering encouragement, heartening words and incalculable practical support, all of which mean an enormous amount to me.

Declaration

I declare that no material presented in this thesis has previously been submitted for a degree at this or any other university.

The research described in this thesis was carried out in collaboration with Dr. Athanasios Dedes, Dr. Janusz Rosiek and Mr. Maximilian Schmidt-Sommerfeld. Aspects of Chapters 3, 4, 5 and 6 are based on the following published works.

- A. Dedes, S. Rimmer, J. Rosiek and M. Schmidt-Sommerfeld, “On the neutral scalar sector of the general R-parity violating MSSM,” *Phys. Lett. B* **627** (2005) 161
- A. Dedes, S. Rimmer and J. Rosiek, “Neutrino masses in the lepton number violating MSSM,” *JHEP* **0608** (2006) 005
- S. Rimmer, “ $l \rightarrow l' \gamma$ in the lepton number violating MSSM,” arXiv:hep-ph/0610406.

Contents

1	Introduction	12
2	Constructing Supersymmetric Lagrangians	17
2.1	Superfields	17
2.2	Contributions to the Lagrangian	22
2.3	Constructing the (\mathcal{L})-Minimal Supersymmetric Standard Model . . .	23
3	The \mathcal{L}-MSSM at tree level: Scalar Sector	27
3.1	Basis choice in the neutral scalar sector	29
3.2	Parametrising the neutral scalar mass matrices	35
3.2.1	CP-even neutral scalar masses and couplings	37
3.2.2	CP-odd neutral scalar masses and couplings	41
3.3	Positiveness and stability of the scalar potential	43
3.3.1	Positiveness	43
3.3.2	Stability	43
3.4	Summary	47
4	The \mathcal{L}-MSSM at tree level: Fermionic sector	49

4.1	Basis Choice	50
4.2	Block Diagonalising	53
4.3	Fermion masses and mixing	55
4.3.1	Neutral fermion sector	56
4.3.2	Charged fermion sector	61
4.4	Constructing the MNS matrix	63
4.5	Input parameters	64
5	The \mathbb{U}-MSSM at one-loop: Neutral fermion masses	66
5.1	One-loop neutrino masses in \mathbb{U} -MSSM	67
5.1.1	Renormalization issues	67
5.1.2	One loop contributions to the massless neutrino eigenstates . .	70
5.1.3	Neutral fermion - neutral scalar contribution	72
5.1.4	Charged fermion - charged scalar contribution	75
5.1.5	Quark - squark contribution	79
5.1.6	Neutral fermion - Z gauge boson contribution	81
5.1.7	Charged fermion - W gauge boson contribution	81
5.1.8	Summary of the one-loop radiative corrections to massless neu- trinos	82
5.1.9	Comparison with Literature	82
5.2	Numerical Results	84
5.2.1	Tree level dominance scenario	88
5.2.2	Loop level dominance scenario	91
5.3	Summary	93

6	The \mathbb{U}-MSSM at one loop: Radiative decays	102
6.1	Experimental Results, Bounds and Prospects	104
6.2	Generic Diagrams for $l_i \rightarrow l_j \gamma$	105
6.3	Specific Diagrams for $l_i \rightarrow l_j \gamma$	108
6.3.1	Atmospheric scale set by $\mu_{1,2,3}$	110
6.3.2	Atmospheric scale set by $\mu_{1,2,3}$ – Solar scale set by λ_{ikk} . . .	112
6.3.3	Atmospheric scale set by $\mu_{1,2,3}$ – Solar scale set by λ'_{ikk} . . .	118
6.3.4	Atmospheric scale set by $\mu_{1,2,3}$ – Solar scale set by B_i	119
6.3.5	Atmospheric scale set by λ – Solar scale set by λ'	121
6.3.6	Atmospheric scale set by λ' – Solar scale set by $\lambda^{(')}$	123
6.4	Benchmarks	126
6.5	Summary	129
7	Conclusions	131
A	Weyl Spinors	136
A.1	Notation	136
A.2	Kinetic Terms and Mass Matrices	137
A.3	Diagonalising matrices	138
A.4	Dirac and Majorana Particles	140
A.5	CKM- and PMNS-like matrices	141
B	\mathbb{U}-MSSM Lagrangian: Interaction Basis	143
B.1	Kinetic term for fermion	145
B.2	Kinetic term for gaugino	146
B.3	Kinetic term for scalar	147

B.4	Kinetic term for gauge bosons	151
B.5	Gaugino interactions	153
B.6	Superpotential	154
B.7	Yukawa terms	155
B.8	F-terms	156
B.9	D-terms	158
B.10	Soft Breaking terms	161
B.11	Gauge Fixing terms	161
C	$\mathcal{N}=1$-MSSM Lagrangian: Mass Basis	162
C.1	Kinetic Terms for Gauge Bosons	165
C.2	Kinetic Terms for Scalars	165
C.3	Kinetic Terms for Colourless Fermions	165
C.4	Kinetic Terms for Quarks/Gluino	165
C.5	Kinetic Terms for Ghosts	166
C.6	Mass Terms for Gauge Bosons	166
C.7	Mass Terms for Neutral Scalars	166
C.8	Mass Terms for Charged Scalars	168
C.9	Mass terms for down-type squarks	169
C.10	Mass terms for up-type squarks	170
C.11	Mass terms for quarks	171
C.12	Mass terms for neutrino-neutralino	172
C.13	Mass terms for charged lepton-chargino	173
C.14	Mass terms for gluino	173
C.15	Fermion-Fermion-Photon interactions	174

C.16 Fermion-Fermion-Z interactions	175
C.17 Fermion-Fermion-W interactions	176
C.18 Fermion-Fermion-Gluon interactions	177
C.19 Scalar-Scalar-Photon interactions	177
C.20 Scalar-Scalar-Z interactions	178
C.21 Scalar-Scalar-W	179
C.22 Scalar-Scalar-G	180
C.23 Scalar-Scalar-A-A	181
C.24 Scalar-Scalar-A-Z	181
C.25 Scalar-Scalar-Z-Z	182
C.26 Scalar-Scalar-W-W	184
C.27 Scalar-Scalar-A-W	185
C.28 Scalar-Scalar-Z-W	186
C.29 Scalar-Scalar-G-A	187
C.30 Scalar-Scalar-G-Z	188
C.31 Scalar-Scalar-G-W	189
C.32 Scalar-Scalar-G-G	189
C.33 Scalar-Z-Z	190
C.34 Scalar-W-W	190
C.35 Scalar-A-W	191
C.36 Scalar-Z-W	191
C.37 Gauge boson-Gauge boson-Gauge boson	191
C.38 Gauge boson-Gauge boson-Gauge boson-Gauge boson	192
C.39 Neutral Scalar - Neutral Fermion - Neutral Fermion interactions . . .	194

C.40 Neutral Scalar - Charged Fermion - Charged Fermion interactions . . .	194
C.41 Neutral Scalar-Quark-Quark interactions	195
C.42 Charged Scalar - Neutral Fermion - Charged Fermion interactions . . .	196
C.43 Charged Scalar - Quark - Quark interactions	197
C.44 Squark - Neutral Fermion - Quark interactions	197
C.45 Squark - Charged Fermion - Quark interactions	199
C.46 Squark - Gluino - Quark interactions	200
C.47 Squark - Quark - Quark interactions	201
C.48 Neutral Scalar - Neutral Scalar - Neutral Scalar - Neutral Scalar . . .	201
C.49 Neutral Scalar - Neutral Scalar - Charged Scalar - Charged Scalar . . .	202
C.50 Neutral Scalar - Neutral Scalar - Squark - Squark	204
C.51 Neutral Scalar - Charged Scalar - Squark - Squark	206
C.52 Neutral Scalar - Squark - Squark - Squark	208
C.53 Charged Scalar - Charged Scalar - Charged Scalar - Charged Scalar . . .	208
C.54 Charged Scalar - Charged Scalar - Squark - Squark	209
C.55 Charged Scalar - Squark - Squark - Squark	210
C.56 Squark - Squark - Squark - Squark	211
C.57 Neutral Scalar - Neutral Scalar - Neutral Scalar	214
C.58 Neutral Scalar - Charged Scalar - Charged Scalar	214
C.59 Neutral Scalar - Squark - Squark	217
C.60 Charged Scalar - Squark - Squark	220
C.61 Squark - Squark - Squark	221

D Summary of rotation martrix definitions 223

E	Courant-Fischer theorem	227
E.1	Interlaced eigenvalues	229
F	Self-energy one-loop corrections	231
G	One-loop calculation for radiative decays	234

Chapter 1

Introduction

There is now considerable evidence that neutrinos produced in both the Sun and the upper atmosphere undergo flavour oscillation during their propagation [1]. This observation suggests that neutrinos, in contradiction with their description in the Standard Model (SM), are, in fact, massive particles. Through oscillation experiments it is possible to discern further properties of the neutrino sector; the mass differences between generations are many orders of magnitude smaller than the masses of the charge leptons, the mass difference driving the atmospheric oscillations is much greater than that of the solar oscillations, and the lepton mixing matrix, which appears at the charged-current weak boson vertex, is most unlike the CKM matrix [2,3], its analogue in the quark sector. As such, the Standard Model must be extended in some manner to encompass this new insight.

There remain open questions concerning the nature of the neutrino. It is unknown, for example, whether the neutrino is a Dirac or a Majorana particle. If the neutrino is a Dirac particle, a new field must be introduced to the model, the

right-handed neutrino, which carries a conserved quantum number differentiating the neutrino from the anti-neutrino. If the neutrino is a Majorana particle, lepton number must be violated, giving rise to processes, such as neutrinoless double beta decay, which are as yet unseen by experiment.

Not only does the Standard Model fail to describe these recently observed neutrino phenomena, but it is also blighted by the sensitivity of the Higgs potential to radiative corrections [4]. The mass of the Higgs boson, for example, obtains large corrections at the order of one-loop. This results in the physical mass of the Higgs boson being dependent on energy scales introduced to the theory which are higher than the electroweak scale. As such, we would rely upon an unattractive conspiracy between Lagrangian parameters, producing a delicate cancellation, for the theory to work.

This imposition, that Lagrangian parameters take ‘finely-tuned’ values, is known as the ‘hierarchy problem’, the amelioration of which is a primary reason for incorporating Supersymmetry (SUSY) into theories which extend the SM [4]. By introducing SUSY, a symmetry between particles of different spin, the cancellation of large radiative corrections is ensured due to counteracting contributions from scalar and fermion loops.

In constructing a Supersymmetric model difficulties arise. First, if Supersymmetry is an unbroken symmetry of the model, the fermions and bosons which it relates must be degenerate in mass. This is clearly in contradiction with observation and it follows that supersymmetry must be ‘broken’ in some manner. Secondly, if a model is constructed as follows: assuming a minimal particle content and including all possible operators allowed by Lorentz invariance, the Standard Model gauge symmetries

and renormalizability; it can be seen that tree-level proton decay processes exist. To constrain the values given to these dangerous Lagrangian parameters enough to ensure proton stability is unattractive. Instead, a further discrete symmetry can be imposed when constructing the model to ensure such processes are absent. For this study, a Lagrangian in which lepton number is explicitly broken is chosen; later, we shall fully define this model, the Lepton number-violating Minimal Supersymmetric Standard Model, the \mathcal{L} -MSSM, and present the superpotential.

This thesis concerns the following proposition. Neutrino masses can arise through mixing, at both tree-level and higher order, with heavy neutral particles; in this case, because lepton number is not conserved, the neutrino interaction eigenstates mix with the neutralinos, the supersymmetric partners of the Higgs and vector bosons. Further contributions to neutrino masses arise at the level of one-loop, their magnitude being determined by further lepton number violating parameters in the Lagrangian.

We investigate the \mathcal{L} -MSSM fully. In Chapter 2 we will introduce the algebra of Supersymmetry and the manner in which a SUSY invariant Lagrangian can be constructed. We will write down the most general superpotential for a Lorentz and SUSY invariant, minimal particle content, renormalizable and $SU(3)_C \times SU(2)_L \times U(1)_Y$ model and see explicitly the terms which violate lepton number and baryon number. We then present, in Appendix C, the Lagrangian and Feynman rules of this, most general, R-parity violating model.

In Chapter 3 we consider the scalar sector of the \mathcal{L} -MSSM. We first consider the neutral scalar sector and the spontaneous breaking of the electroweak symmetry, which in turn gives masses to fermions and the weak bosons. In the lepton number violating model, five complex neutral scalar fields acquire vacuum expectation values

(vevs). We solve this system and choose a convenient basis for calculation.

Building on this, in Chapter 4 we investigate the fermionic sector. We discuss the manner in which Lagrangian parameters can be initialised such that the correct mass and mixing parameters for leptons are reproduced. Because the basis has been chosen to simplify the neutral scalar sector and also due to the fact that the charged leptons mix with the charginos, this step deserves careful consideration.

In Chapter 5, renormalisation issues and radiative corrections to the neutrino masses are considered. By considering all possible loop corrections, we are able to describe various scenarios in which the current neutrino observations can be reproduced within this model.

In Chapter 6 we consider whether the sets of parameters which correctly describe the neutrino sector will give rise to flavour violating radiative decays of charged leptons. Such events have not been observed by experiment and, accordingly, strong bounds exist on the branching ratios which are soon to be further improved.

Supporting material is collected and presented in the Appendices. In Appendix A, the Weyl spinor notation is defined and notes are presented on diagonalising matrices, how the resulting mixing matrices arise in vector boson vertices and the manner in which they can be parameterised.

In Appendices B and C, the Lagrangian for the general Minimal Supersymmetric Standard Model (MSSM), being the MSSM without the imposition of an additional discrete symmetry, is presented. In Appendix B, the Lagrangian is presented in terms of interaction eigenstates and before the neutral scalar fields have been expanded around the vacuum expectation value; in Appendix C, the neutral scalar fields acquire vacuum expectation values, and are rotated into the mass eigenbasis. Further, in

Appendix C, the Feynman Rules for the vertices of the theory are given in terms of Lagrangian parameters and the matrices which define the rotation from interaction eigenstate to mass eigenstate. These rotation matrices are collected and presented in Appendix D.

Appendix E contains the proof of the Courant-Fisher theorem, which is required for the analysis of the mass spectrum of neutral scalars. Appendices F and G present the one-loop results for the self-energies of neutral fermions and the radiative decays of charged fermions, respectively.

Chapter 2

Constructing Supersymmetric Lagrangians

2.1 Superfields

The algebra of Supersymmetry [5] is defined by the following (anti)commutation relations,

$$\begin{aligned} [Q_\alpha, P_\mu] &= 0 & [\bar{Q}_{\dot{\alpha}}, P_\mu] &= 0 \\ \{Q_\alpha, Q_\beta\} &= 0 & \{\bar{Q}_{\dot{\alpha}}, \bar{Q}_{\dot{\beta}}\} &= 0 \\ [Q_\alpha, M^{\mu\nu}] &= i\sigma_\alpha^{\mu\nu\beta} Q_\beta & \{Q_\alpha, \bar{Q}_{\dot{\alpha}}\} &= 2\sigma_{\alpha\dot{\alpha}}^\mu P_\mu, \end{aligned} \tag{2.1}$$

where $\mu, \nu = 0, \dots, 3$ are Lorentz four-vector indices; $\alpha, \beta = 1, 2$ and $\dot{\alpha}, \dot{\beta} = 1, 2$ are indices of the left- and right-handed Weyl spinor representations of the Lorentz group, respectively; $M^{\mu\nu}$ and P^μ are the generators of the Poincaré group; and, Q_α

and $\bar{Q}_{\dot{\alpha}}$ are the generators of the group of Supersymmetric transformations. For more details on definitions, notation and spinor algebra see Appendix A.1.

An element from the group of finite Supersymmetry transformations, can then be written as follows,

$$S(x, \theta, \bar{\theta}) = \exp [i (\theta^{\alpha} Q_{\alpha} + \bar{\theta}_{\dot{\alpha}} \bar{Q}^{\dot{\alpha}} - x^{\mu} P_{\mu})] , \quad (2.2)$$

where θ and $\bar{\theta}$ are anti-commuting variables known as Grassman variables. We denote a superfield, $\Phi(x, \theta, \bar{\theta})$, which depends on these Grassman variables as well as the spacetime coordinates, x_{μ} . It then follows that the infinitesimal transformations are given by,

$$P_{\mu} = i\partial_{\mu} , \quad Q_{\alpha} = -i\frac{\partial}{\partial\theta^{\alpha}} + \sigma_{\alpha\dot{\alpha}}^{\mu}\bar{\theta}^{\dot{\alpha}}\partial_{\mu} , \quad \bar{Q}_{\dot{\alpha}} = i\frac{\partial}{\partial\bar{\theta}^{\dot{\alpha}}} - \theta^{\alpha}\sigma_{\alpha\dot{\alpha}}^{\mu}\partial_{\mu} , \quad (2.3)$$

and covariant derivatives are defined as,

$$D_{\alpha} = -i\frac{\partial}{\partial\theta^{\alpha}} - \sigma_{\alpha\dot{\alpha}}^{\mu}\bar{\theta}^{\dot{\alpha}}\partial_{\mu} , \quad \bar{D}_{\dot{\alpha}} = i\frac{\partial}{\partial\bar{\theta}^{\dot{\alpha}}} + \theta^{\alpha}\sigma_{\alpha\dot{\alpha}}^{\mu}\partial_{\mu} . \quad (2.4)$$

Because of the Grassman algebra, a power series expansion of the superfield in terms of θ and $\bar{\theta}$ terminates. As such, the general form can be given by,

$$\begin{aligned} \Phi(x, \theta, \bar{\theta}) = & \varphi(x) + \theta\psi(x) + \bar{\theta}\bar{\chi}(x) + \theta\theta F(x) + \bar{\theta}\bar{\theta}H(x) \\ & + \theta\sigma^{\mu}\bar{\theta}A_{\mu}(x) + \theta\theta\bar{\theta}\bar{\lambda}(x) + \bar{\theta}\bar{\theta}\theta\xi(x) + \theta\theta\bar{\theta}\bar{\theta}D(x) . \end{aligned} \quad (2.5)$$

This general representation is reducible. We require just two irreducible representations, one, the chiral superfield, to describe the standard model fermions and Higgs bosons and their superpartners, the other, the vector superfield, to describe the gauge bosons and their superpartners.

The left-handed chiral superfields are defined by the property,

$$\bar{D}_\alpha \Phi = 0, \quad (2.6)$$

similarly, the right-handed chiral superfields obey,

$$D_\alpha \Phi = 0. \quad (2.7)$$

As such, the chiral superfields can be expanded into components. For example, the left-handed chiral superfield can be given by,

$$\begin{aligned} \Phi(x, \theta, \bar{\theta}) = & \varphi(x) + i\theta\sigma^\mu\bar{\theta}\partial_\mu\varphi(x) + \frac{1}{4}\theta\theta\bar{\theta}\bar{\theta}\partial_\mu\partial^\mu\varphi(x) \\ & + \sqrt{2}\theta\psi(x) - \frac{i}{\sqrt{2}}\theta\theta\partial_\mu\psi(x)\sigma^\mu\bar{\theta} + \theta\theta F(x) \end{aligned} \quad (2.8)$$

where, as we shall see later, φ and ψ are physical scalar and Weyl fermion fields, respectively, and F is an auxiliary field.

The important point to note is that under SUSY transformations it can be shown explicitly that the F-term transforms into a total derivative, bosonic fields transform into fermionic fields and the fermionic fields transform into bosonic fields.

The vector superfield is defined by the property,

$$V(x, \theta, \bar{\theta}) = V^\dagger(x, \theta, \bar{\theta}), \quad (2.9)$$

in addition to this, we require the vector field component of this superfield to be a gauge boson. To ensure that this is the case, a supersymmetric version of gauge invariance,

$$e^{gV} \rightarrow e^{-ig\Lambda^\dagger} e^{gV} e^{ig\Lambda}, \quad (2.10)$$

where Λ is a chiral superfield and g is the gauge coupling, is demanded. This allows the choice of Wess-Zumino gauge to be made. The vector superfield can then be

expanded,

$$V(x, \theta, \bar{\theta}) = -\theta\sigma_\mu\bar{\theta}A^\mu(x) + i\theta\theta\bar{\theta}\bar{\lambda}(x) - i\bar{\theta}\bar{\theta}\theta\lambda(x) + \frac{1}{2}\theta\theta\bar{\theta}\bar{\theta}D(x). \quad (2.11)$$

where A_μ is a real vector field, λ is a Weyl fermion field and D is an auxiliary field which transforms into a total derivative under SUSY transformations.

We move now to construct a Lagrangian which is invariant under SUSY transformations. As such, we construct the Lagrangian from the F- and D-terms in chiral and vector superfields, which themselves transform into total derivatives.

First, consider the product $\Phi\Phi^\dagger$, which is itself a vector superfield. The term given by,

$$\int d^2\theta d^2\bar{\theta}\Phi\Phi^\dagger = FF^* - \partial_\mu\varphi\partial^\mu\varphi^* - i\bar{\psi}\sigma^\mu\partial_\mu\psi, \quad (2.12)$$

is therefore invariant under SUSY transformations, and contributes kinetic terms for scalars and their partner fermions to the Lagrangian. The auxiliary field does not have a kinetic term, and will be integrated out, later, using its equations of motion. To include the gauge interactions, we make the replacement $\partial_\mu \rightarrow D_\mu = \partial_\mu + igA_\mu^a T^a$ where T^a are the group generators, g is the gauge coupling and,

$$\begin{aligned} \int d^2\theta d^2\bar{\theta}\Phi^\dagger\Phi &\rightarrow \int d^2\theta d^2\bar{\theta}\Phi^\dagger e^{2gV}\Phi \\ &= \sum_i (D_\mu\varphi_i D^\mu\varphi_i^* - i\bar{\psi}_i\sigma^\mu D_\mu\psi_i) + g\varphi^* D\varphi + ig\sqrt{2}(\varphi^*\lambda\psi - \bar{\lambda}\bar{\psi}\varphi) + FF^*. \end{aligned} \quad (2.13)$$

The second type of contribution, will come from products of chiral superfields, $\Phi_i\Phi_j, \Phi_i\Phi_j\Phi_k \dots$ which are themselves chiral superfields. From this we can see that the contribution

$$\int d^2\theta \left[\sum_i k_i\Phi_i + \frac{1}{2} \sum_{i,j} m_{ij}\Phi_i\Phi_j + \frac{1}{3} \sum_{i,j,k} g_{ijk}\Phi_i\Phi_j\Phi_k \right], \quad (2.14)$$

is invariant under SUSY transformations and contributes mass terms and scalar-fermion-fermion interactions to the Lagrangian.

Collecting the two previous contributions, and integrating out the FF^* term, the contributions to the Lagrangian can be written,

$$\mathcal{L} \supset \sum_i (\partial_\mu \varphi_i \partial^\mu \varphi_i^* - i \bar{\psi}_i \sigma^\mu \partial_\mu \psi_i) + \left(\sum_{j,k} \frac{\partial^2 \mathcal{W}(\varphi_i)}{\partial \varphi_j \partial \varphi_k} \psi_j \psi_k + \text{H. c.} \right) - \left| \frac{\partial \mathcal{W}(\varphi_i)}{\partial \varphi_i} \right|^2, \quad (2.15)$$

where the interactions are given by the superpotential,

$$\mathcal{W} = \sum_i k_i \Phi_i + \frac{1}{2} \sum_{i,j} m_{ij} \Phi_i \Phi_j + \frac{1}{3} \sum_{i,j,k} g_{ijk} \Phi_i \Phi_j \Phi_k. \quad (2.16)$$

Next, we must add the kinetic terms for gauge bosons to the Lagrangian, we define a chiral superfield, W_α , where

$$W_\alpha = \bar{D} \bar{D} e^{-gV} D_\alpha e^{gV}. \quad (2.17)$$

The product $W_\alpha W^\alpha$ is gauge invariant and can be expanded into component fields as,

$$\frac{1}{32g^2} W_\alpha W^\alpha = -\frac{1}{4} F_{\mu\nu}^a F^{a\mu\nu} + \frac{1}{2} D^a D^a + \left(-\frac{i}{2} \lambda^a \sigma^\mu \partial_\mu \bar{\lambda}^a + \frac{1}{2} g f^{abc} \lambda^a \sigma^\mu A_\mu^b \bar{\lambda}^c + \text{H. c.} \right), \quad (2.18)$$

which contributes kinetic terms for the gauge bosons and gauginos and the interaction between gauginos and gauge bosons. The auxiliary D fields can then be integrated out.

Finally, we add supersymmetry breaking terms. Because mass degenerate scalar and fermion pairs have not been observed, it is clear that SUSY must be broken. A number of mechanisms for this breaking have been suggested, however, it is sufficient

here merely to add all the terms which could break supersymmetry while maintaining the cancellation of quadratic divergences to the Lagrangian. As such, we have not attempted to understand SUSY breaking, but we are able to parameterize its possible effects. Such ‘soft’ SUSY breaking terms are [6]: scalar mass terms, $-m_\varphi^2|\varphi|^2$; gaugino mass terms, $-\frac{1}{2}m_\lambda\lambda\lambda$; trilinear scalar terms, $-A_{ijk}\varphi_i\varphi_j\varphi_k$; bilinear scalar terms, $-B_{ij}\varphi_i\varphi_j$; linear scalar terms, $-C_i\varphi_i$.

2.2 Contributions to the Lagrangian

We can now gather all the contributions defined above together, showing the manner and the origin of terms which appear in the Lagrangian.

Kinetic term for scalar:

$$(\mathcal{D}_\mu\varphi)^\dagger(\mathcal{D}^\mu\varphi)$$

Kinetic term for fermion:

$$i\bar{\psi}_\rho\bar{\sigma}^{\mu\rho\rho}\mathcal{D}_\mu\psi_\rho$$

Both arising from combinations of chiral superfields in the form $\int d^2\theta d^2\bar{\theta}\Phi\Phi^\dagger$

Kinetic term for gaugino:

$$i\bar{\lambda}_\rho^A\bar{\sigma}^{\mu\rho\rho}\mathcal{D}_\mu\lambda_\rho^A$$

Kinetic term for gauge bosons:

$$-\frac{1}{4}F_{\mu\nu}^a F^{a\mu\nu}$$

Gaugino interactions:

$$i\sqrt{2}g\varphi_i^*T^A\psi_i^\rho\lambda_\rho^A - i\sqrt{2}g\bar{\lambda}_\rho^AT^A\varphi_i\bar{\psi}_i^\rho$$

The three terms above arise from $\int d^2\theta d^2\bar{\theta} W^\alpha W_\alpha + \text{H.c}$

Yukawa terms:

$$-\frac{1}{2} \frac{\partial^2 \mathcal{W}}{\partial \varphi_i \partial \varphi_j} \psi_i^\rho \psi_{j\rho} - \frac{1}{2} \frac{\partial^2 \mathcal{W}^\dagger}{\partial \varphi_i^* \partial \varphi_j^*} \bar{\psi}_{i\rho} \bar{\psi}_j^\rho$$

F-terms:

$$-\sum_i \left| \frac{\partial \mathcal{W}}{\partial \varphi_i} \right|^2$$

D-terms:

$$-\sum_l \frac{g_l^2}{2} \sum_A (\varphi_i^{*a} T_l^{Aab} \varphi_i^b)^2$$

Arise from combinations of chiral superfields of the form $\int d^2\theta \Phi_i, \Phi_i \Phi_j, \Phi_i \Phi_j \Phi_k$ and having integrated out auxiliary fields.

SUSY breaking terms:

$$-m_\varphi^2 |\varphi|^2, \quad -\frac{1}{2} m_\lambda \lambda \lambda, \quad -A_{ijk} \varphi_i \varphi_j \varphi_k, \quad -B_{ij} \varphi_i \varphi_j, \quad -C_i \varphi_i$$

We add all possible ‘soft’ terms which do not disrupt the cancellation of quadratic divergences.

2.3 Constructing the (\mathcal{L})-Minimal Supersymmetric Standard Model

We wish to construct a minimal particle content $SU(3)_C \times SU(2)_L \times U(1)_Y$ model which is Lorentz invariant, renormalisable and invariant under SUSY transformations. From the previous section, we know the way in which terms can be added to the Lagrangian and the relations between them. We now need to define the superfields of the model, the quantum numbers they carry and the form of the superpotential.

Chiral Superfield	$SU(3)_C \times SU(2)_L \times U(1)_Y$	Field Components
$Q_i^{a,x}$	$(3, 2, \frac{1}{6})$	$\begin{pmatrix} \tilde{u}_{Li}^x \\ \tilde{d}_{Li}^x \end{pmatrix}, \begin{pmatrix} u_{Li}^x \\ d_{Li}^x \end{pmatrix}$
D_i^{cx}	$(\bar{3}, 1, \frac{1}{3})$	$\tilde{d}_{Ri}^{*x}, d_{Ri}^x$
U_i^{cx}	$(\bar{3}, 1, -\frac{2}{3})$	$\tilde{u}_{Ri}^{*x}, u_{Ri}^x$
L_i^a	$(1, 2, -\frac{1}{2})$	$\begin{pmatrix} \tilde{\nu}_{Li} \\ \tilde{e}_{Li} \end{pmatrix}, \begin{pmatrix} \nu_{Li} \\ e_{Li} \end{pmatrix}$
E_i^c	$(1, 1, 1)$	\tilde{e}_{Ri}^*, e_{Ri}
H_1^a	$(1, 2, -\frac{1}{2})$	$\begin{pmatrix} h_1^0 \\ h_1^- \end{pmatrix}, \begin{pmatrix} \tilde{h}_1^0 \\ \tilde{h}_1^- \end{pmatrix}$
H_2^a	$(1, 2, \frac{1}{2})$	$\begin{pmatrix} h_2^+ \\ h_2^0 \end{pmatrix}, \begin{pmatrix} \tilde{h}_2^+ \\ \tilde{h}_2^0 \end{pmatrix}$
Vector Superfield	$SU(3)_C \times SU(2)_L \times U(1)_Y$	Field Components
V_1	$(1, 1, 0)$	\tilde{B}, B_μ
V_2	$(1, 3, 0)$	$\tilde{W}^{(A)}, W_\mu^{(A)}$
V_3	$(8, 1, 0)$	$\tilde{G}^{(X)}, G_\mu^{(X)}$

Figure 2.1: Particle content of the Minimal Supersymmetric Standard Model. Where $Q_i^{a,x}$, D_i^{cx} , U_i^{cx} , L_i^a , E_i^c , H_1^a , H_2^a are the chiral superfield particle content, $i = 1, 2, 3$ is a generation index, $x = 1, 2, 3$ and $a = 1, 2$ are $SU(3)$ and $SU(2)$ gauge group indices, respectively.

Each standard model particle is placed in its own superfield, as defined in Table 2.1, and the most general superpotential that contains these fields, is given by

$$\begin{aligned}
\mathcal{W} = & Y_E L H_1 E + Y_D H_1 Q D^c + Y_U Q H_2 U^c - \mu H_1 H_2 \\
& + \frac{1}{2} \lambda L L E^c + \lambda' L Q D^c - \kappa L H_2 \\
& + \frac{1}{2} \lambda'' U^c D^c D^c .
\end{aligned} \tag{2.19}$$

The second line will contribute terms to the Lagrangian which violate lepton number and the last line will give rise to baryon number violation. Such lepton or baryon number violation does not arise in the SM, however that fact that none of the terms in the Standard Model violate lepton number (L) is not due to an imposed symmetry, but merely reflects the fact that all such combinations of SM fields are ruled out by consideration of gauge invariance and renormalisability [7]. For supersymmetric extensions of the SM this is no longer true. In the Minimal Supersymmetric Standard Model [4], lepton number and baryon number (B) violating terms appear naturally, giving rise to tree-level processes, proton decay for example, which are already strongly constrained by experiment. Either, bounds can be set on Lagrangian parameters, or a further discrete symmetry can be imposed on the Lagrangian, such that these processes are absent.

It has been shown that there are three preferred discrete symmetries which can be imposed when constructing the model [8, 9], and once any of these symmetries are imposed the proton is stable. The discrete symmetry most commonly imposed is known as R-parity (R_P) [10–12]. Under R-parity the particles of the Standard Model including the scalar Higgs fields are even, while all their superpartners are odd. Imposing this symmetry has a number of effects. First, any interaction terms

which violate lepton number or baryon number will not appear. Second, the decay of the lightest supersymmetric particle (LSP) into SM particles would violate R_P ; the LSP is therefore stable. Third, the sneutrino vacuum expectation values (vevs) are zero; without extending the MSSM field content, spontaneous generation of R_P violating terms is phenomenologically discounted [13]. The second discrete symmetry is a unique, \mathcal{Z}_3 symmetry which results in the MSSM with lepton number violation but not baryon number violation; denoted here as (\mathbb{L} -MSSM). The third is a \mathcal{Z}_6 symmetry referred to as proton hexality.

We consider here the \mathbb{L} -MSSM ¹, the superpotential for which is given by

$$\mathcal{W} = \epsilon_{ab} \left[\frac{1}{2} \lambda_{\alpha\beta k} \mathcal{L}_\alpha^a \mathcal{L}_\beta^b \bar{E}_k + \lambda'_{\alpha j k} \mathcal{L}_\alpha^a Q_j^{b x} \bar{D}_{k x} - \mu_\alpha \mathcal{L}_\alpha^a H_2^b + (Y_U)_{ij} Q_i^{a x} H_2^b \bar{U}_{j x} \right]. \quad (2.20)$$

As lepton number is not conserved, the L and H_1 superfields have no quantum number to differentiate them. As such, we combine them into $\mathcal{L}_{\alpha=0,\dots,3}^a = (H_1^a, L_{i=1,2,3}^a)$ to emphasise the fact that any distinction between the superfields is arbitrary. μ_α is the generalised dimensionful μ -parameter, and $\lambda_{\alpha\beta k}$, $\lambda'_{\alpha j k}$, $\lambda''_{i j k}$, $(Y_U)_{ij}$ are Yukawa matrices with ϵ_{ab} and ϵ_{xyz} being the totally anti-symmetric tensors, with $\epsilon_{12} = \epsilon_{123} = +1$.

The Lagrangian and Feynman rules for the \mathbb{L} -MSSM are obtained by setting the Baryon number violating couplings, λ'' and h'' , to zero in the expressions presented in Appendices B and C.

¹See Ref. [14] for a review of the phenomenology of this model, whose notation we follow here.

Chapter 3

The \mathcal{L} -MSSM at tree level: Scalar Sector

If lepton number conservation is not imposed, bilinear terms exist in the Lagrangian which give rise to mixing between leptons and non-leptons [11, 14–21]. In particular, the neutrinos will mix with the neutralinos and the sneutrinos will mix with the neutral scalar Higgs fields; crucially all five complex neutral scalar fields can acquire vacuum expectation values. Minimising this ten parameter potential in general is not straightforward, it is more convenient to simplify the problem by choosing an appropriate basis in the neutral scalar sector. We have introduced the notation $\mathcal{L}_\alpha = (H_1, L_i)$ where H_1 and L_i are the chiral superfields containing one Higgs doublet and the leptons, respectively ($\alpha = 0, \dots, 3$ and $i = 1, \dots, 3$). Furthermore, starting from the interaction basis, we are free to rotate the fields and choose the direction corresponding to that of the ‘Higgs’ field. Assuming that the system defining the five complex vacuum expectation values of the fields were solved, four complex vevs, v_α ,

would define a direction in the four dimensional (H_1, L_i) space. One can then choose the basis vector which defines the Higgs fields to point in the direction defined by these vacuum expectation values. We refer to this basis, in which the ‘sneutrino’ (as we call the fields perpendicular to the ‘Higgs’ field) vevs are zero, as the ‘vanishing sneutrino vev basis’ [16, 22–24]. This basis has the virtue of simplifying the mass matrices and vertices of the theory and, thus, is better suited for calculations.

Basis independent parameterisations can be chosen which explicitly show the amount of physical lepton number violation [25–27]. Values for physical observables such as sneutrino masses and mass splitting between CP-even and CP-odd sneutrinos have been derived in the literature in terms of these combinations but usually under some approximations (for example the number of generations or CP-conservation). We find this procedure in general complicated for practical applications and we shall not adopt it here.

Instead, we present in the next section a calculable procedure for framing the most general MSSM scalar potential in the vanishing sneutrino vev basis. An advantage of our procedure is to obtain a diagonal ‘slepton’ mass matrix, two real non-zero vacuum expectation values and the neutral scalar potential determined by real parameters in the rotated basis. The latter proves that the neutral scalar sector of the most general L-violating MSSM (and, in fact, R-parity violating MSSM) exhibits neither spontaneous nor explicit CP-violation in agreement with [28]. In Section 3, the tree-level masses and mixing of the neutral scalar sector is investigated. Using the Courant-Fischer theorem for the interlaced eigenvalues, we prove that there is always at least one neutral scalar which is lighter than the tree-level Z -gauge boson. We present approximate formulae which relate the Higgs masses, mixing and Higgs-gauge

boson vertices of the R-parity conserving (RPC) case with the R-parity violating (RPV) one. In Section 4, the positiveness of the scalar mass matrices and stability of the vacuum are discussed. The contents of this chapter are based upon Ref. [24].

3.1 Basis choice in the neutral scalar sector

In this section we develop a procedure connecting a general neutral scalar basis with the vanishing sneutrino vev basis, the latter being more convenient for practical applications. The five neutral scalar fields, $\tilde{\nu}_{L\alpha}$ and h_2^0 , from the $SU(2)$ doublets, $\mathcal{L}_\alpha = (\tilde{\nu}_{L\alpha}, \tilde{e}_{L\alpha}^-)^T$ and $H_2 = (h_2^+, h_2^0)^T$, form the most general neutral scalar potential of the MSSM,

$$\begin{aligned}
V_{\text{neutral}} &= (m_{\tilde{\mathcal{L}}}^2)_{\alpha\beta} \tilde{\nu}_{L\alpha}^* \tilde{\nu}_{L\beta} + \mu_\alpha^* \mu_\beta \tilde{\nu}_{L\alpha}^* \tilde{\nu}_{L\beta} + \mu_\alpha^* \mu_\alpha h_2^{0*} h_2^0 + m_{H_2}^2 h_2^{0*} h_2^0 \\
&- b_\alpha \tilde{\nu}_{L\alpha} h_2^0 - b_\alpha^* \tilde{\nu}_{L\alpha}^* h_2^{0*} + \frac{1}{8} (g^2 + g_2^2) [h_2^{0*} h_2^0 - \tilde{\nu}_{L\alpha}^* \tilde{\nu}_{L\alpha}]^2, \quad (3.1)
\end{aligned}$$

where general complex parameters b_α , an hermitian matrix $(m_{\tilde{\mathcal{L}}}^2)_{\alpha\beta}$ and $m_{H_2}^2$ all arise from the supersymmetry breaking sector of the theory. The last term in (3.1) originates from the D-term contributions of the superfields \mathcal{L}_α and H_2 . Defining

$$(\mathcal{M}_{\tilde{\mathcal{L}}}^2)_{\alpha\beta} \equiv (m_{\tilde{\mathcal{L}}}^2)_{\alpha\beta} + \mu_\alpha^* \mu_\beta, \quad \text{and} \quad m_2^2 \equiv m_{H_2}^2 + \mu_\alpha^* \mu_\alpha, \quad (3.2)$$

one can rewrite the potential in (3.1) in a compact form as

$$\begin{aligned}
V_{\text{neutral}} &= (\mathcal{M}_{\tilde{\mathcal{L}}}^2)_{\alpha\beta} \tilde{\nu}_{L\alpha}^* \tilde{\nu}_{L\beta} + m_2^2 h_2^{0*} h_2^0 - (b_\alpha \tilde{\nu}_{L\alpha} h_2^0 + \text{H.c.}) \\
&+ \frac{1}{8} (g^2 + g_2^2) [h_2^{0*} h_2^0 - \tilde{\nu}_{L\alpha}^* \tilde{\nu}_{L\alpha}]^2. \quad (3.3)
\end{aligned}$$

In order to go to the vanishing sneutrino vev basis, we redefine the ‘Higgs-sneutrino’ fields

$$\tilde{\nu}_{L\alpha} = U_{\alpha\beta} \tilde{\nu}'_{L\beta}, \quad (3.4)$$

where \mathbf{U} is a 4×4 unitary matrix, defined as follows,

$$\mathbf{U} = \mathbf{V} \text{diag}(e^{i\phi_\alpha}) \mathbf{Z}, \quad (3.5)$$

being composed of three other matrices which we define below, \mathbf{V} unitary and \mathbf{Z} real orthogonal. The potential in the primed basis becomes,

$$\begin{aligned} V_{\text{neutral}} &= \left[Z^T \left(\hat{\mathcal{M}}'_{\tilde{\ell}} \right) Z \right]_{\alpha\beta} \tilde{\nu}'_{L\alpha} \tilde{\nu}'_{L\beta} + m_2^2 h_2^{0*} h_2^0 \\ &- \left[(b'Z)_\alpha \tilde{\nu}'_{L\alpha} h_2^0 + \text{H.c} \right] + \frac{1}{8} (g^2 + g_2^2) \left(h_2^{0*} h_2^0 - \tilde{\nu}'_{L\alpha} \tilde{\nu}'_{L\alpha} \right)^2, \end{aligned} \quad (3.6)$$

where

$$\left(\hat{\mathcal{M}}'_{\tilde{\ell}} \right) = \text{diag}(e^{-i\phi_\alpha}) \mathbf{V}^\dagger \left(\mathcal{M}_{\tilde{\ell}} \right) \mathbf{V} \text{diag}(e^{i\phi_\alpha}), \quad b'^T = b^T \mathbf{V} \text{diag}(e^{i\phi_\alpha}). \quad (3.7)$$

The unitary matrix, \mathbf{V} , is chosen such that $\left(\hat{\mathcal{M}}'_{\tilde{\ell}} \right)$ is real and diagonal - the hat ($\hat{}$) is used to denote a diagonal matrix. The phases ϕ_α are chosen such that b'_α is real and positive [they are equal to the phases of $(b^T V)_\alpha^*$]. The minimisation conditions for the scalar fields are now derived, to obtain conditions for the vacuum expectation values,

$$\begin{aligned} \left. \frac{\partial V}{\partial \tilde{\nu}'_{L\alpha}} \right|_{\text{vac}} &= \left[Z^T \left(\hat{\mathcal{M}}'_{\tilde{\ell}} \right) Z \right]_{\alpha\beta} \tilde{\nu}'_{L\beta} - (b'Z)_\alpha h_2^{0*} - \frac{1}{4} (g^2 + g_2^2) \left(h_2^{0*} h_2^0 - \tilde{\nu}'_{L\gamma} \tilde{\nu}'_{L\gamma} \right) \tilde{\nu}'_{L\alpha} \Big|_{\text{vac}} = 0, \\ \left. \frac{\partial V}{\partial h_2^{0*}} \right|_{\text{vac}} &= m_2^2 h_2^0 - (b'Z)_\alpha \tilde{\nu}'_{L\alpha} + \frac{1}{4} (g^2 + g_2^2) \left(h_2^{0*} h_2^0 - \tilde{\nu}'_{L\gamma} \tilde{\nu}'_{L\gamma} \right) h_2^0 \Big|_{\text{vac}} = 0, \end{aligned} \quad (3.8)$$

where ‘vac’ indicates that the fields have to be replaced by their vevs,

$$\langle \tilde{\nu}'_{L\alpha} \rangle = \frac{v_\alpha}{\sqrt{2}} , \quad \langle h_2^0 \rangle = \frac{v_u}{\sqrt{2}} . \quad (3.9)$$

The $U(1)_Y$ symmetry of the unbroken Lagrangian was used to set the phase of v_u to zero, however, at this stage all other vacuum expectation values will be treated as complex variables. By combining Eqs. (3.8,3.9) we obtain

$$\left[Z^T \left(\hat{\mathcal{M}}_{\tilde{L}}^2 \right) Z \right]_{\alpha\beta} v_\beta - (b'Z)_\alpha v_u - \frac{1}{8}(g^2 + g_2^2)(v_u^2 - v_\gamma v_\gamma) v_\alpha = 0 , \quad (3.10)$$

$$m_2^2 v_u - (b'Z)_\alpha v_\alpha + \frac{1}{8}(g^2 + g_2^2)(v_u^2 - v_\gamma v_\gamma) v_u = 0 . \quad (3.11)$$

In a general basis, it is difficult to solve the above system with respect to the vevs without making some approximations, for example assuming small ‘sneutrino’ vevs [14]. In order to simplify calculations we would like to find a basis where the ‘sneutrino’ vevs vanish, $v_1 = v_2 = v_3 = 0$. In other words, we are seeking an orthogonal matrix Z , such that the following equation,

$$\left[Z^T \left(\hat{\mathcal{M}}_{\tilde{L}}^2 \right) Z \right]_{\alpha 0} v_0 - (b'Z)_\alpha v_u - \frac{1}{2} M_Z^2 \frac{v_u^2 - v_0^2}{v_u^2 + v_0^2} v_0 \delta_{0\alpha} = 0 , \quad (3.12)$$

holds. If the above system is satisfied, then a solution with zero ‘sneutrino’ vevs exists. The other solutions, with non-vanishing ‘sneutrino’ vevs will be discussed later. In Eq. (3.12),

$$M_Z^2 = \frac{1}{4} (g^2 + g_2^2) (v_u^2 + v_0^2) , \quad (3.13)$$

is the Z-gauge boson mass squared. It is obvious that when $v_i = 0$, v_0 is real. It is now useful to define

$$\tan \beta \equiv \frac{v_u}{v_0} . \quad (3.14)$$

To determine \mathbf{Z} , multiplying (3.12) by $Z_{\gamma\alpha}$, summing over α and solving for $Z_{\alpha 0}$, yields,

$$Z_{\alpha 0} = \frac{b'_\alpha \tan \beta}{\left(\hat{\mathcal{M}}'_{\tilde{L}}\right)_{\alpha\alpha} - \frac{1}{2} M_Z^2 \frac{\tan^2 \beta - 1}{\tan^2 \beta + 1}}. \quad (3.15)$$

For given set of model parameters, $Z_{\alpha 0}$ depends only on $\tan \beta$ which we can now fix by solving the orthonormality condition,

$$\sum_{\alpha=0}^3 Z_{\alpha 0} Z_{\alpha 0} = \sum_{\alpha=0}^3 \frac{b'_\alpha{}^2 \tan^2 \beta}{\left[\left(\hat{\mathcal{M}}'_{\tilde{L}}\right)_{\alpha\alpha} - \frac{1}{2} M_Z^2 \frac{\tan^2 \beta - 1}{\tan^2 \beta + 1}\right]^2} = 1. \quad (3.16)$$

This equation can be solved numerically for any given set of model parameters.

It is worth noting that when $b_i = 0$ and using notation more typical for this case, $b'_0 \equiv m_{12}^2$, $\left(\hat{\mathcal{M}}'_{\tilde{L}}\right)_{00} \equiv m_1^2$, Eq. (3.16) reduces to one of the standard RPC MSSM equations for the Higgs vevs:

$$m_{12}^2 v_d = v_u \left[m_1^2 - \frac{1}{8} (g^2 + g_2^2) (v_u^2 - v_d^2) \right]. \quad (3.17)$$

For some parameter choices Eq. (3.16) may admit multiple solutions for $\tan \beta$. Each of the possible $\tan \beta$ specify a different basis, and each of these bases has one solution of the minimisation conditions with vanishing ‘sneutrino’ vevs. The subtlety highlighted earlier is the following: all possible solutions of the minimisation conditions can be found in each basis, so, in general, each basis contains a number of extrema equal to the number of possible solutions for $\tan \beta$. Hence, a solution with $v_i = 0$ in one basis, is a solution with $v_i \neq 0$ in another basis. The important point to note is that by considering all possible values of $\tan \beta$, and selecting the value which corresponds to the deepest minima for the solution with vanishing sneutrino vevs, all the solutions will have been accounted for, and the vanishing sneutrino vev

basis will have been determined correctly. The value of the potential at the vacuum, in terms of $\tan\beta$ is given by

$$V(\tan\beta) = -\frac{M_Z^4}{2(g^2 + g_2^2)} \left(\frac{\tan^2\beta - 1}{\tan^2\beta + 1} \right)^2. \quad (3.18)$$

The obvious conclusion from the equation above is that the deepest minimum of the potential is given by the solution for $\tan\beta$ or $\cot\beta$ which is greatest.

Knowing $\tan\beta$, one should fix m_2^2 using Eqs. (3.11,3.13-3.15) (again in the analogy with RPC MSSM where m_2^2 is usually given in terms of M_A and $\tan\beta$). Namely

$$m_2^2 = Z_{\alpha 0} b'_\alpha \cot\beta - \frac{1}{2} M_Z^2 \frac{\tan^2\beta - 1}{\tan^2\beta + 1}. \quad (3.19)$$

In this way m_2^2 is chosen to give the correct value of the the Z -boson mass.

Only the first column of the Z matrix, $Z_{\alpha 0}$, is defined by Eq. (3.15). The remaining elements of \mathbf{Z} must still be determined. Having fixed the first column of the matrix, the other three columns can be chosen to be orthogonal to the first column and to each other. This leaves us with an $O(3)$ invariant subspace, such that the matrix \mathbf{Z} is given by

$$\mathbf{Z} = \mathbf{O} \begin{pmatrix} 1 & 0 \\ 0 & \mathbf{X}_{3 \times 3} \end{pmatrix}, \quad (3.20)$$

where

$$\mathbf{O} = \begin{pmatrix} Z_{00} & -\sqrt{Z_{10}^2 + Z_{20}^2 + Z_{30}^3} & 0 & 0 \\ Z_{10} & \frac{Z_{00}Z_{10}}{\sqrt{Z_{10}^2 + Z_{20}^2 + Z_{30}^3}} & -\frac{\sqrt{Z_{20}^2 + Z_{30}^3}}{\sqrt{Z_{10}^2 + Z_{20}^2 + Z_{30}^3}} & 0 \\ Z_{20} & \frac{Z_{00}Z_{20}}{\sqrt{Z_{10}^2 + Z_{20}^2 + Z_{30}^3}} & \frac{Z_{10}Z_{20}}{\sqrt{Z_{20}^2 + Z_{30}^3}\sqrt{Z_{10}^2 + Z_{20}^2 + Z_{30}^3}} & -\frac{Z_{30}}{\sqrt{Z_{20}^2 + Z_{30}^3}} \\ Z_{30} & \frac{Z_{00}Z_{30}}{\sqrt{Z_{10}^2 + Z_{20}^2 + Z_{30}^3}} & \frac{Z_{10}Z_{30}}{\sqrt{Z_{20}^2 + Z_{30}^3}\sqrt{Z_{10}^2 + Z_{20}^2 + Z_{30}^3}} & \frac{Z_{20}}{\sqrt{Z_{20}^2 + Z_{30}^3}} \end{pmatrix}, \quad (3.21)$$

and \mathbf{X} is an, as yet, undetermined 3×3 orthogonal matrix determined by three angles. This remaining freedom can be used to diagonalise $\left[\mathbf{Z}^T \left(\hat{\mathcal{M}}'_{\tilde{L}} \right) \mathbf{Z} \right]_{ij}$, i.e. the (real symmetric) ‘sneutrino’ part of the $\mathbf{Z}^T \left(\hat{\mathcal{M}}'_{\tilde{L}} \right) \mathbf{Z}$ matrix, with entries $(\hat{M}_{\tilde{L}}^2)_i$. We have now accomplished our aim of finding the matrices \mathbf{V} and \mathbf{Z} which, after inserting into potential of Eq. (3.6) and dropping the primes, reduce the scalar potential to the form

$$\begin{aligned}
V_{\text{neutral}} &= (M_{\tilde{L}}^2)_{\alpha\beta} \tilde{\nu}_{L\alpha}^* \tilde{\nu}_{L\beta} + m_2^2 h_2^{0*} h_2^0 - \left[B_\alpha \tilde{\nu}_{L\alpha} h_2^0 + \text{H.c.} \right] \\
&+ \frac{1}{8} (g^2 + g_2^2) \left(h_2^{0*} h_2^0 - \tilde{\nu}_{L\alpha}^* \tilde{\nu}_{L\alpha} \right)^2, \tag{3.22}
\end{aligned}$$

where

$$(M_{\tilde{L}}^2)_{\alpha\beta} \equiv \left[Z^T \left(\hat{\mathcal{M}}'_{\tilde{L}} \right) Z \right]_{\alpha\beta} \quad \text{and} \quad B_\alpha \equiv (b' Z)_\alpha, \tag{3.23}$$

with $\left(\hat{\mathcal{M}}'_{\tilde{L}} \right)$ and b' given by Eq. (3.7). In this basis the matrix $\mathbf{M}_{\tilde{L}}^2$ adopts a particularly simple form

$$(M_{\tilde{L}}^2)_{\alpha\beta} = \begin{pmatrix} B_0 \tan \beta - \frac{1}{2} M_Z^2 \cos 2\beta & B_j \tan \beta \\ B_i \tan \beta & (\hat{M}_{\tilde{L}}^2)_i \delta_{ij} \end{pmatrix}, \tag{3.24}$$

where there is no sum over i in the down-right part of the matrix. Notice that we did not only succeed to self-consistently go to a basis where the sneutrino vevs are zero, but also we managed to have the sneutrino masses $(\hat{M}_{\tilde{L}}^2)_i$ diagonal and all the parameters of the scalar potential in Eq. (3.22) real.

As a byproduct of our procedure, we note here that the potential of Eq. (3.22) exhibits neither spontaneous nor explicit CP-violation at the tree level. The latter is in agreement with the results of Ref. [28] following a different method. Of course, the

parameters μ_α of the superpotential and the soft supersymmetry breaking couplings stay in general complex. The result that the neutral scalar potential is CP invariant can also be seen directly from Eq. (3.3). By forming the complex basis $(\tilde{\nu}_{L\alpha}, h_2^{0*})$ the first line of the potential can be rewritten as a matrix; a rotation can then be performed such that the matrix is real and diagonal. After the rotation, the second line, being the contribution from D-terms, contains complex parameters in general, but the rotation matrix can be chosen such that these phases are set to zero.

A question arises when we include high order corrections to the potential. Then the vanishing ‘sneutrino’ vevs will be shifted to non-zero values by tadpoles originating, for example, from the $\mathcal{L}QD$ contribution in the superpotential (2.20). The ‘sneutrino’ vevs maybe set back to zero by a renormalization condition such that a counterterm for these vevs set their one particle irreducible (1PI) tadpole corrections to zero.

To conclude, it is worth making a remark about the sign of B_0 . As is clear from the form of Eqs. (3.23,3.7,3.15), if $\left(\hat{\mathcal{M}}_{\tilde{\mathcal{L}}}^2\right)_{\alpha\alpha} - \frac{1}{2} M_Z^2 \frac{\tan^2\beta-1}{\tan^2\beta+1} > 0$ for all α , B_0 is always positive in the vanishing sneutrino vev basis.

3.2 Parametrising the neutral scalar mass matrices

The neutral scalar sector of the R-parity violating MSSM is in general very complicated. This is due to the fact that the scalars mix through the lepton number violating terms proportional to b_i , $\left(m_{\tilde{\mathcal{L}}}^2\right)$ and unless all of these parameters and vevs are real one has a 10×10 matrix to consider. However, for any given set of model parameters, one can always perform the basis change described in the previous section

and arrive at the potential defined by Eq. (3.22), with only real parameters. Consequently, the physical neutral scalars are, at the tree level, exact CP-eigenstates. This implies that the neutral scalar mass matrix decouples into two 5×5 matrices, one for the CP-odd particles and one for CP-even. In the same manner as in the R-parity conserving MSSM, once quantum corrections are considered, the CP invariance will generically be broken [29].

Ultimately, one would like to parametrise the scalar sector resulting from the potential in (3.22) with as few parameters as possible in order to make contact with phenomenology. These parameters in the case of the R-parity conserving MSSM are: the physical mass of the CP-odd Higgs boson

$$M_A^2 = \frac{2 B_0}{\sin 2\beta}, \quad (3.25)$$

and $\tan \beta$. An advantage of the form of potential in Eq. (3.22,3.23,3.24) is that, M_A and $\tan \beta$ can still be used for parametrising the general Higgs sector in the R-parity violating MSSM. M_A^2 is the mass of the lightest CP-odd Higgs boson in the R-parity conserving MSSM; as such, it is used here as a parameter. m_A^2 is used to denote the physical tree-level mass of the lightest CP-odd Higgs in the R-parity violating MSSM (the convention adopted is that masses in the RPC case, parameters in this model, are denoted by M , and the masses in the RPV model are denoted by m).

3.2.1 CP-even neutral scalar masses and couplings

The Lagrangian after spontaneous gauge symmetry breaking contains the terms

$$\mathcal{L} \supset - \begin{pmatrix} \text{Re } h_0^2 & \text{Re } \tilde{\nu}_{L0} & \text{Re } \tilde{\nu}_{Li} \end{pmatrix} \mathcal{M}_{\text{EVEN}}^2 \begin{pmatrix} \text{Re } h_0^2 \\ \text{Re } \tilde{\nu}_{L0} \\ \text{Re } \tilde{\nu}_{Lj} \end{pmatrix}. \quad (3.26)$$

As such, the scalar CP-even Higgs squared mass matrix becomes

$$\mathcal{M}_{\text{EVEN}}^2 = \begin{pmatrix} \cos^2 \beta M_A^2 + \sin^2 \beta M_Z^2 & -\frac{1}{2} \sin 2\beta (M_A^2 + M_Z^2) & -B_j \\ -\frac{1}{2} \sin 2\beta (M_A^2 + M_Z^2) & \sin^2 \beta M_A^2 + \cos^2 \beta M_Z^2 & B_j \tan \beta \\ -B_i & B_i \tan \beta & M_i^2 \delta_{ij} \end{pmatrix}, \quad (3.27)$$

where

$$M_i^2 \equiv (\hat{M}_L^2)_i + \frac{1}{2} \cos 2\beta M_Z^2, \quad (3.28)$$

are in fact the physical sneutrino masses of the RPC case. It is important here to notice that the top-left 2×2 sub-matrix is identical to the RPC case, for which the Higgs masses are given by

$$M_{h,H}^2 = \frac{1}{2} \left(M_Z^2 + M_A^2 \pm \sqrt{(M_Z^2 + M_A^2)^2 - 4M_A^2 M_Z^2 \cos^2 2\beta} \right), \quad (3.29)$$

and will be used as parameters in the RPV model.

The matrix (3.27) *always* has one eigenvalue which is smaller than M_Z^2 . This may be proved as follows: one first observes that the upper left 2×2 submatrix of (3.27), call it A, has at least one eigenvalue smaller than or equal to M_Z^2 . Then using the Courant-Fischer theorem [30], details of which are given in Appendix E applying linear matrix algebra, one proves that, for one flavour, the eigenvalues

of the 3×3 matrix $\mathcal{M}_{\text{EVEN}}^2$, are interlaced with those of A. This means that the matrix $\mathcal{M}_{\text{EVEN}}^2$ with $i = 1$ has at least one eigenvalue smaller or equal than M_Z^2 . Repeating this procedure twice, proves our statement. Furthermore, it is interesting to notice that in the region where $\tan \beta \gg 1$, the eigenvector $(\sin \beta, \cos \beta, 0, 0, 0)^T$ corresponds to the eigenvalue with mass approximately M_Z^2 . Notice that this is the same eigenvector as in the RPC case which corresponds to the Higgs boson which couples almost maximally to the Z-gauge boson.

Lepton flavour violating processes have not been observed as yet and therefore, bearing in mind cancellations, the parameters $B_i \tan \beta$ have to be much smaller than $\min(M_A^2, M_i^2)$. To get a rough estimate, which we will refine later, consider the dominant contribution from neutral scalars and neutralinos in the loop [31–34],

$$m_\nu \sim \frac{a_{ew} B^2 \tan^2 \beta}{16\pi \tilde{m}^3} \lesssim 1 \text{ eV} , \quad (3.30)$$

with $\tilde{m} = \max(M_A, M_i)$ and $B \sim \mathcal{O}(B_i)$. This shows that

$$\frac{B_i \tan \beta}{\tilde{m}^2} \sim \frac{1.2 \cdot 10^{-3}}{\sqrt{\tilde{m}}} \sim 0.1\% . \quad (3.31)$$

With the approximation that $\frac{B_i \tan \beta}{\tilde{m}^2}$ is small it is not hard to find a matrix \mathbf{Z}_R which rotates the fields into the mass basis, by expanding in this combination of parameters, such that

$$\mathbf{Z}_R^T \mathcal{M}_{\text{EVEN}}^2 \mathbf{Z}_R = \text{diag} \left[m_{h^0}^2, m_{H^0}^2, (m_{\tilde{\nu}_+}^2)_i \right] , \quad (3.32)$$

with $m_{h^0}^2$ being the lightest neutral scalar mass and

$$\mathbf{Z}_R = \begin{pmatrix} \cos \alpha & \sin \alpha & -\frac{\cos(\beta-\alpha) \cos \alpha B_j}{\cos \beta (M_j^2 - M_h^2)} + \frac{\sin(\beta-\alpha) \sin \alpha B_j}{\cos \beta (M_j^2 - M_H^2)} \\ -\sin \alpha & \cos \alpha & \frac{\cos(\beta-\alpha) \sin \alpha B_j}{\cos \beta (M_j^2 - M_h^2)} + \frac{\sin(\beta-\alpha) \cos \alpha B_j}{\cos \beta (M_j^2 - M_H^2)} \\ \frac{\cos \beta P_i^h B_i}{\cos(\beta-\alpha)} & \frac{\cos \beta P_i^H B_i}{\sin(\beta-\alpha)} & \delta_{ij} \end{pmatrix} , \quad (3.33)$$

where there is no sum over i and (M_j^2, M_h^2, M_H^2) are defined in (3.28,3.29). In addition,

$$\tan 2\alpha = \tan 2\beta \frac{M_A^2 + M_Z^2}{M_A^2 - M_Z^2} \text{ and } P_i^{h,H} = \frac{M_Z^2 \cos^2 2\beta - M_{h,H}^2}{\cos^2 \beta (M_H^2 - M_h^2)(M_i^2 - M_{h,H}^2)}, \quad (3.34)$$

(the common convention is to choose $0 \leq \beta \leq \pi/2$ and $-\pi/2 \leq \alpha \leq 0$). The mass eigenstates of the RPV model are therefore given by

$$\begin{aligned} h^0 &\simeq \cos \alpha \operatorname{Re} h_0^2 - \sin \alpha \operatorname{Re} \tilde{\nu}_{L0} + \left(\frac{\cos \beta P_i^{h,H} B_i}{\cos(\beta - \alpha)} \right) \operatorname{Re} \tilde{\nu}_{Li}, \quad (3.35) \\ H^0 &\simeq \sin \alpha \operatorname{Re} h_0^2 + \cos \alpha \operatorname{Re} \tilde{\nu}_{L0} + \left(\frac{\cos \beta P_i^{h,H} B_i}{\sin(\beta - \alpha)} \right) \operatorname{Re} \tilde{\nu}_{Li}, \\ (\tilde{\nu}_+)_i &\simeq \left(-\frac{\cos(\beta - \alpha) \cos \alpha B_j}{\cos \beta (M_j^2 - M_h^2)} + \frac{\sin(\beta - \alpha) B_j \sin \alpha B_j}{\cos \beta (M_j^2 - M_H^2)} \right) \operatorname{Re} h_0^2 \\ &\quad + \left(\frac{\cos(\beta - \alpha) \sin \alpha B_j}{\cos \beta (M_j^2 - M_h^2)} + \frac{\sin(\beta - \alpha) \cos \alpha B_j}{\cos \beta (M_j^2 - M_H^2)} \right) \operatorname{Re} \tilde{\nu}_{L0} + \operatorname{Re} \tilde{\nu}_{Li}, \end{aligned}$$

with corresponding masses,

$$m_{h^0}^2 \simeq M_h^2 - \frac{M_Z^2 \cos^2 2\beta - M_h^2}{(M_H^2 - M_h^2) \cos^2 \beta} \sum_{i=1}^3 \frac{B_i^2}{M_i^2 - M_h^2} + \mathcal{O}\left(\frac{B^4}{M^6 \cos^4 \beta}\right), \quad (3.36)$$

$$m_{H^0}^2 \simeq M_H^2 + \frac{M_Z^2 \cos^2 2\beta - M_H^2}{(M_H^2 - M_h^2) \cos^2 \beta} \sum_{i=1}^3 \frac{B_i^2}{M_i^2 - M_H^2} + \mathcal{O}\left(\frac{B^4}{M^6 \cos^4 \beta}\right), \quad (3.37)$$

$$\begin{aligned} (m_{\tilde{\nu}_+}^2)_i &\simeq (\hat{M}_{\tilde{\nu}}^2)_i + \frac{B_i^2}{\cos^2 \beta} \frac{M_i^2 - M_Z^2 \cos^2 2\beta}{\left[M_i^4 - M_i^2 (M_A^2 + M_Z^2) + M_A^2 M_Z^2 \cos^2 2\beta \right]} \\ &\quad + \mathcal{O}\left(\frac{B^4}{M^6 \cos^4 \beta}\right). \quad (3.38) \end{aligned}$$

The above expressions, are useful in relating the masses of the neutral scalars in the RPC and RPV cases in the valid approximation $B \tan \beta \ll \min(M_A^2, M_i^2)$. They are presented here for the first time except the mass in (3.38) which agrees with Ref. [23].

We note here that these formulae are not valid if some of the diagonal entries in the mass matrix are closely degenerate - in such case even small B_i terms lead to the strong mixing of respective fields. However in many types of calculations (e.g. various loop calculations) one can still formally use such expansion. In the final result one often gets expressions of the type $\frac{f(m_1)-f(m_2)}{m_1-m_2}$ which have a well defined and correct limit also for degenerate masses, even if the expansion used in the intermediate steps was, in principle, poorly defined.

It is interesting to note that the rotation matrix \mathbf{U} defined in (3.5), although explicitly calculated in this thesis, does not appear in the neutral scalar vertices. For example, the vertices of the CP-even neutral scalars with the gauge bosons read as¹,

$$\begin{aligned} \mathcal{L}_{\text{VVH}} &= \frac{1}{2} \frac{g_2 M_Z}{\cos \theta_w} (\cos \beta Z_{R2s} + \sin \beta Z_{R1s}) Z^\mu Z_\mu H_s^0 \\ &+ \frac{1}{2} g_2 M_W (\cos \beta Z_{R2s} + \sin \beta Z_{R1s}) W^{+\mu} W_\mu^- H_s^0, \end{aligned} \quad (3.39)$$

where $H_{s=1,\dots,5}^0$ are the Higgs boson fields, $h^0, H^0, (\tilde{\nu}_+)_1, (\tilde{\nu}_+)_2, (\tilde{\nu}_+)_3$ respectively. From (3.33) and \mathcal{L}_{VVH} above, it is easy to see that the light Higgs boson coupling to the vector bosons ($V = Z, W$), is proportional to $\sin(\beta - \alpha)$ as in the RPC case². In fact, the coupling sum rule,

$$\sum_{s=1}^5 g_{VVH_s^0}^2 = g_{VV\phi}^2, \quad (3.40)$$

valid in the RPC case for $s = 1, 2$, persists also here, where $g_{VVH_s^0}$ are the couplings appearing in (3.39) and $g_{VV\phi}$ the corresponding coupling appearing in the Standard Model.

¹Note that the matrix \mathbf{Z} defined in (3.20) has nothing to do with either \mathbf{Z}_R or \mathbf{Z}_A defined in this section.

²We follow the conventions of Ref. [35].

3.2.2 CP-odd neutral scalar masses and couplings

For the CP-odd case one finds,

$$\mathcal{L} \supset - \begin{pmatrix} \text{Im } h_0^2 & \text{Im } \tilde{\nu}_{L0} & \text{Im } \tilde{\nu}_{Li} \end{pmatrix} \mathcal{M}_{\text{ODD}}^2 \begin{pmatrix} \text{Im } h_0^2 \\ \text{Im } \tilde{\nu}_{L0} \\ \text{Im } \tilde{\nu}_{Lj} \end{pmatrix}, \quad (3.41)$$

where the CP-odd mass matrix reads,

$$\mathcal{M}_{\text{ODD}}^2 = \begin{pmatrix} \cos^2 \beta M_A^2 + \xi \sin^2 \beta M_Z^2 & \frac{1}{2} \sin 2\beta (M_A^2 - \xi M_Z^2) & B_j \\ \frac{1}{2} \sin 2\beta (M_A^2 - \xi M_Z^2) & \sin^2 \beta M_A^2 + \xi \cos^2 \beta M_Z^2 & B_j \tan \beta \\ B_i & B_i \tan \beta & M_i^2 \delta_{ij} \end{pmatrix}, \quad (3.42)$$

and ξ is the gauge fixing parameter in R_ξ gauge. In fact, by using an orthogonal rotation

$$\mathcal{V} = \begin{pmatrix} \sin \beta & -\cos \beta & 0 \\ \cos \beta & \sin \beta & 0 \\ 0 & 0 & 1 \end{pmatrix}, \quad (3.43)$$

we can always project out the would-be Goldstone mode, of the CP-odd scalar matrix and thus

$$\mathcal{V}^T \mathcal{M}_{\text{ODD}}^2 \mathcal{V} = \begin{pmatrix} \xi M_Z^2 & 0 & 0 \\ 0 & M_A^2 & \frac{B_j}{\cos \beta} \\ 0 & \frac{B_i}{\cos \beta} & M_i^2 \delta_{ij} \end{pmatrix}. \quad (3.44)$$

Under the approximation of small bilinear RPV couplings [see Eq. (3.31)], a solution is determined for the matrix \mathbf{Z}_A which rotates the fields into the mass basis,

such that

$$\mathbf{Z}_A^T \mathcal{M}_{\text{ODD}}^2 \mathbf{Z}_A = \text{diag} \left[m_{G^0}^2, m_{A^0}^2, (m_{\tilde{\nu}_-}^2)_i \right], \quad (3.45)$$

$$\mathbf{Z}_A = \begin{pmatrix} \sin \beta & \cos \beta & \frac{B_j}{M_j^2 - M_A^2} \\ -\cos \beta & \sin \beta & \frac{B_j \tan \beta}{M_j^2 - M_A^2} \\ 0 & \frac{B_i}{\cos \beta (M_i^2 - M_A^2)} & \delta_{ij} \end{pmatrix}, \quad (3.46)$$

with the mass eigenstates given by

$$\begin{aligned} G^0 &\simeq \sin \beta \text{Im } h_0^2 - \cos \beta \text{Im } \tilde{\nu}_{L0}, \\ A^0 &\simeq \cos \beta \text{Im } h_0^2 + \sin \beta \text{Im } \tilde{\nu}_{L0} + \frac{B_i}{\cos \beta (M_i^2 - M_A^2)} \text{Im } \tilde{\nu}_{Li}, \\ (\tilde{\nu}_-)_i &\simeq \frac{B_i}{M_j^2 - M_A^2} \text{Im } h_0^2 + \frac{B_j \tan \beta}{M_i^2 - M_A^2} \text{Im } \tilde{\nu}_{L0} + \text{Im } \tilde{\nu}_{Li}, \end{aligned} \quad (3.47)$$

with corresponding masses,

$$m_A^2 \simeq M_A^2 - \frac{1}{\cos^2 \beta} \sum_{i=1}^3 \frac{B_i^2}{M_i^2 - M_A^2} + \mathcal{O}\left(\frac{B^4}{M^6 \cos^4 \beta}\right), \quad (3.48)$$

$$(m_{\tilde{\nu}_-}^2)_i \simeq M_i^2 - \frac{B_i^2}{(M_A^2 - M_i^2) \cos^2 \beta} + \mathcal{O}\left(\frac{B^4}{M^6 \cos^4 \beta}\right). \quad (3.49)$$

The coupling of the Z gauge boson to the CP-even and CP-odd neutral scalar fields is given by

$$\mathcal{L}_{ZHA} = \frac{-ig_2}{2c_W} \left[(p_{H_s^0}^\mu - p_{A_p^0}^\mu)_\mu \left(\sum_{\alpha=0}^3 Z_{R(2+\alpha)s} Z_{A(2+\alpha)p} - Z_{R1s} Z_{A1p} \right) \right] Z^\mu H_s^0 A_p^0, \quad (3.50)$$

where the four momenta $p_{H_s^0}^\mu, p_{A_p^0}^\mu$ are incoming and the fields $A_{p=1,\dots,5}^0$ correspond to $G^0, A^0, (\tilde{\nu}_-)_1, (\tilde{\nu}_-)_2, (\tilde{\nu}_-)_3$ respectively. One may check that the coupling $Z - G^0 - h^0$ derived from (3.50) is proportional to $\sin(\alpha - \beta)$ as it should be.

3.3 Positiveness and stability of the scalar potential

3.3.1 Positiveness

In general, one should inspect whether all squared masses in the CP-odd and CP-even sector are positive. For that, all diagonal square subdeterminants of mass matrices should be positive. One can easily check that both CP-odd and CP-even mass matrices in (3.27,3.42) respectively, lead, in the rotated basis, to the same set of conditions,

$$M_i^2 > 0 \text{ with } i = 1, 2, 3 \quad \text{and} \quad M_A^2 > \frac{1}{\cos^2 \beta} \sum_{i=1}^3 \frac{B_i^2}{M_i^2}. \quad (3.51)$$

Using the form of M_A^2 in (3.25), the last equation can be rewritten in the form

$$B_0 > \tan \beta \sum_{i=1}^3 \frac{B_i^2}{M_i^2}. \quad (3.52)$$

Excluding some very singular mass configurations, the above conditions are rather trivially fulfilled if one takes into account the bound of Eq. (3.31).

3.3.2 Stability

The question of whether the potential is stable, i.e. bounded from below, is far more complicated. In most cases the quartic ($D-$)term dominates and there is no problem. The only exception being when the fields follow the direction $|h_2^0|^2 = \sum_{i=0}^4 |\tilde{\nu}_{Li}|^2$. In such a case, one should check whether the remaining part of the potential is positive along this direction.

Denoting $R \equiv \sqrt{\sum_{i=0}^3 |\tilde{\nu}_i|^2}$ and $h_2^0 = R e^{-i\phi}$, where ϕ is a free phase, and using Eqs. (3.19,3.24,3.28), one can write down the scalar potential along this direction in

the vanishing sneutrino vev basis as

$$\begin{aligned}
V_{\text{neutral}} &= \frac{B_0}{\sin \beta \cos \beta} \tilde{\nu}_{L0}^* \tilde{\nu}_{L0} + [M_i^2 + B_0 \cot \beta] \tilde{\nu}_{Li}^* \tilde{\nu}_{Li} \\
&+ B_i \tan \beta (\tilde{\nu}_{L0}^* \tilde{\nu}_{Li} + \tilde{\nu}_{L0} \tilde{\nu}_{Li}^*) - B_\alpha (\tilde{\nu}_{L\alpha} h_0^2 + \text{H.c.}) \\
&\equiv \tilde{\nu}_L^\dagger \mathbf{Q} \tilde{\nu}_L - (\mathbf{B}^T \tilde{\nu}_L \text{Re}^{-i\phi} + \text{H.c.}) .
\end{aligned} \tag{3.53}$$

where the real symmetric matrix \mathbf{Q} is

$$\mathbf{Q} = \begin{pmatrix} M_A^2 & B_i \tan \beta \\ B_j \tan \beta & [M_i^2 + B_0 \cot \beta] \delta_{ij} \end{pmatrix} . \tag{3.54}$$

Finding the stability conditions for the potential (3.53) is difficult, it depends on nine real variables (4 moduli and five phases of the fields). To simplify the problem, we perform one more field rotation to the basis in which the matrix \mathbf{Q} is diagonal. This can be done, in general, by numerical routines (routines were already used in calculating the vanishing sneutrino vev basis, and therefore, finding the stability conditions for the general scalar potential always has to involve some numerical analysis). We thus define the matrix \mathbf{P} , $\tilde{\nu}_L \rightarrow P\tilde{\nu}_L$, as

$$\mathbf{P}^\dagger \mathbf{Q} \mathbf{P} = \text{diag}(X_0, X_1, X_2, X_3) . \tag{3.55}$$

In fact, \mathbf{Q} is real, so we can choose \mathbf{P} to be real orthogonal. Also, we denote $D_\beta \equiv B_\alpha P_{\alpha\beta}$. Obviously, the rotation \mathbf{P} preserves the value of $R = |h_2^0|$.

The potential becomes:

$$V_{\text{neutral}} = \sum_{\alpha=0}^3 [X_\alpha |\tilde{\nu}_{L\alpha}|^2 - D_\alpha R (\tilde{\nu}_{L\alpha} e^{-i\phi} + \text{H.c.})] , \tag{3.56}$$

where X_0 has to be positive, otherwise for $\phi = 0$ along the direction $\tilde{\nu}_{Li} = \text{Im} \tilde{\nu}_{L0} = 0$ the potential $V_{\text{neutral}} = |\text{Re} \tilde{\nu}_{L0}|^2 [X_0 - D_0 \text{sign}(\text{Re} \tilde{\nu}_{L0})]$ falls to $-\infty$ at least for one

direction along the $\text{Re } \tilde{\nu}_{L0}$ axis. In fact the condition on X_α is $X_\alpha \geq 2|D_\alpha|$. Thus our first conclusion is that the matrix \mathbf{Q} has to be positively defined. One can write down appropriate conditions in the same manner as for the scalar mass matrices; comparing with Eq. (3.51), it can be observed that this condition is automatically fulfilled if relation (3.51) holds.

With X_α positive, one can write down the potential as:

$$V_{\text{neutral}} = \sum_{\alpha=0}^3 \left| \sqrt{X_\alpha} \tilde{\nu}_{L\alpha} - \frac{D_\alpha}{\sqrt{X_\alpha}} R e^{i\phi} \right|^2 - R^2 \sum_{\alpha=0}^3 \frac{D_\alpha^2}{X_\alpha}. \quad (3.57)$$

To further simplify the problem, denote $\tilde{\nu}_{L\alpha} = u_\alpha e^{i(\phi - \phi_\alpha)}$, where $u_\alpha \geq 0$ are field moduli and ϕ_α are free phases. Then

$$V_{\text{neutral}} = R^2 \left(\sum_{\alpha=0}^3 \left| \sqrt{X_\alpha} \frac{u_\alpha}{R} - \frac{D_\alpha}{\sqrt{X_\alpha}} e^{i\phi_\alpha} \right|^2 - \sum_{\alpha=0}^3 \frac{D_\alpha^2}{X_\alpha} \right), \quad (3.58)$$

where $R = \sqrt{\sum_{i=0}^3 |\tilde{\nu}_i|^2} = \sqrt{\sum_{i=0}^3 u_i^2}$. Phases ϕ_α can be adjusted independently of u_α . The worst case from the point of view of potential stability, the smallest first term inside the parenthesis, occurs for $D_\alpha e^{i\phi_\alpha} = |D_\alpha|$. Denoting further $\epsilon_\alpha = u_\alpha/R$, $0 \leq \epsilon_\alpha \leq 1$, one can reduce our initial problem to the question whether the function

$$g(\epsilon_\alpha) = \sum_{\alpha=0}^3 \left| \sqrt{X_\alpha} \epsilon_\alpha - \frac{|D_\alpha|}{\sqrt{X_\alpha}} \right|^2 - \sum_{\alpha=0}^3 \frac{D_\alpha^2}{X_\alpha} = \sum_{\alpha=0}^3 (X_\alpha \epsilon_\alpha^2 - 2|D_\alpha| \epsilon_\alpha), \quad (3.59)$$

depending now on four real positive parameters, is non-negative on the unit sphere $\sum_{\alpha=0}^3 \epsilon_\alpha^2 = 1$. In general such problem can be solved numerically using the method of Lagrange multipliers. For $X_i > X_0 - D_0$, the minimum occurs for

$$\epsilon_\alpha = \frac{|D_\alpha|}{X_\alpha + \lambda}, \quad (3.60)$$

where λ can be found numerically as a root of the following equation:

$$\sum_{\alpha=0}^3 \frac{D_\alpha^2}{(X_\alpha + \lambda)^2} = 1. \quad (3.61)$$

For smaller X_i , the minimum is realized for $\epsilon_i = 0$ for one or more values of i and requires analysis of various special cases. Having found the correct minimum, to prove the stability of the potential one needs to show that the function g at the minimum is non-negative.

As shown in Eq. (3.31), B_i terms and thus also D_i terms are usually very small. In this case one can set approximate, sufficient conditions for the stability of the potential, without resorting to solving Eq. (3.61), numerically. Denote $D = \sum_{i=1}^3 D_i^2$ and $X_{min} = \min(X_1, X_2, X_3)$. Then, using the inequality $D_i \epsilon_i \leq \sqrt{\sum_{i=1}^3 D_i^2} \sqrt{\sum_{i=1}^3 \epsilon_i^2} = D \sqrt{1 - \epsilon_0^2}$, one has

$$g(\epsilon_\alpha) \geq X_0 \epsilon_0^2 + X_{min}(1 - \epsilon_0^2) + (X_i - X_{min})\epsilon_i^2 - 2|D_0|\epsilon_0 - 2D\sqrt{1 - \epsilon_0^2} \quad (3.62)$$

Terms $(X_i - X_{min})\epsilon_i^2$ are always non-negative. The worst case being when the vector $(\epsilon_1, \epsilon_2, \epsilon_3)$ is along the minimal X_i axis, where these terms vanish. Other terms are rotation invariant in the 3-dimensional space $(\epsilon_1, \epsilon_2, \epsilon_3)$, so Eq. (3.62) is equivalent to finding parameters X_0, X_{min}, D_0, D for which the expression (3.63), depending on just one real variable, is positive:

$$g'(\epsilon_0) = X_0 \epsilon_0^2 + X_{min}(1 - \epsilon_0^2) - 2|D_0|\epsilon_0 - 2D\sqrt{1 - \epsilon_0^2} \geq 0 . \quad (3.63)$$

Analysis of (3.63) is further simplified by one more approximation, justified for small D :

$$g'(\epsilon_0) \geq X_0 \epsilon_0^2 + X_{min}(1 - \epsilon_0^2) - 2|D_0|\epsilon_0 - 2D . \quad (3.64)$$

The rhs of Eq. (3.64) is now trivial. Following approximate conditions for the stability

of the potential can be summarized as follows:

X_{min} range	Stability requires
$X_{min} \geq X_0 - D_0$	$X_0 \geq 2 D_0 + 2D$
$0 < X_{min} < X_0 - D_0$	$(X_0 - X_{min})(X_{min} - 2D) \geq D_0^2$

Both conditions are sufficient, but not minimal - we have made some approximations and there may be parameters which do not fall into either of the categories above, and yet still give a stable potential. For example, if $X_0 = X_1 = X_2 = X_3 \equiv X$, one can easily derive the exact necessary and sufficient condition for potential stability as $X \geq 2\sqrt{D_0^2 + D^2}$, less strict than $X \geq 2(|D_0| + |D|)$ which would be given by the table above.

For complementary work the reader is referred to Ref. [36].

3.4 Summary

In this chapter, based on Ref. [24], we have presented a procedure for calculating the rotation matrix which brings the neutral scalar fields of the general lepton number violating MSSM into the vanishing sneutrino vev basis. In doing so, we have made no assumption about the complexity of the parameters. We consider the case of three generations, but our approach immediately applies to other cases, apart from obvious modifications of the form of \mathbf{Z} matrix defined in (3.20.3.21). As a byproduct of basis change, we prove that the tree level MSSM potential does not exhibit any form of CP-violation, neither explicit nor spontaneous. Consequently, the neutral scalar fields can be divided into CP-even and CP-odd sectors with the 5×5 neutral scalar squared mass matrices, taking a very simple form with only small lepton number

violating mass terms sitting on their off diagonal elements. We can thus expand along small \mathcal{L} mass terms and find analytic approximate formulae which relate the scalar masses in the R-parity conserving model with the \mathcal{L} -MSSM . Furthermore we also find, that in general there is always at least one neutral scalar field with mass lighter than M_Z which couples maximally to the Z -gauge boson in the case of large $\tan\beta$ and large M_A .

This analysis is an important first step towards our study of the neutrino properties in this model. Having studied the neutral scalar sector, we are now in a position to consider the masses of the fermions at tree level. The vacuum expectation values determined in this chapter give rise to the lepton masses and it is the manner in which lepton masses arise in this model, which is considered in the next chapter.

Chapter 4

The \mathbb{L} -MSSM at tree level: Fermionic sector

In the \mathbb{L} -MSSM a single neutrino mass arises at tree level due to the mixing between neutrinos, gauginos and higgsinos [11, 16, 18, 37, 38]. This tree level mass is proportional to square of the bilinear lepton number violating superpotential parameter, μ_i , which is assumed to be of order of MeV, and is suppressed by the ‘TeV’ supersymmetry breaking gaugino masses, resulting in a low energy see-saw mechanism with light neutrino and heavy neutralino masses. The other two neutrino masses arise from quantum loop corrections made up from lepton number violating superpotential or supersymmetry breaking vertices. We shall refer to neutrinos which only acquire masses due to radiative corrections using the term ‘massless neutrinos’.

Calculations for neutrino masses in the \mathbb{L} -MSSM have been addressed many times in the literature. The tree level set-up of the model was first given in [37], and details worked out later in [16, 18, 38]. Calculations of the one-loop neutrino masses, which

we shall address in full in the next chapter, including only the bilinear superpotential term are given in [17,20,32,33,39]. Corrections involving the trilinear superpotential Yukawa couplings λ, λ' have been considered, mostly in the mass insertion approximation [13, 23, 31, 40] and under the assumption of CP-conservation and flavour diagonal soft SUSY breaking terms. Renormalization group induced corrections to neutrino masses have been studied in [14,41,42]. There is of course a vast number of articles using these calculations, or simplified versions of them, in order to describe the solar and atmospheric neutrino puzzles [43–52].

In this chapter, based on work presented in [53] we show how to define the Lagrangian parameters in the fermion sector of the theory, by starting out with the physical input parameters, being the lepton masses and mixing angles.

4.1 Basis Choice

Physical masses of the fermion fields depend on appropriate λ, λ', μ and Y_U couplings multiplied by the vevs of the neutral scalar fields. As it has been shown in the previous chapter, by unitary rotation in the 4-dimensional space of the neutral scalar components of \mathcal{L}_α , it is possible to set three of the four vacuum expectation values of the \mathcal{L}_α fields to zero, leaving two real non-zero vevs in the neutral scalar sector and, simultaneously, significantly simplifying its structure. It is convenient to apply such a transformation not just to scalars, but to the whole chiral superfield,

$$\mathcal{L}_\alpha = U_{\alpha\beta} \mathcal{L}'_\beta, \quad (4.1)$$

and redefine the Lagrangian parameters to absorb the matrix U in Eq. (4.1) such that it does not appear explicitly in the Lagrangian,

$$\begin{aligned}
\tilde{\lambda}_{\gamma\delta j} &= \lambda_{\alpha\beta j} U_{\alpha\gamma} U_{\beta\delta} , \\
\tilde{\lambda}'_{\gamma ij} &= \lambda'_{\alpha ij} U_{\alpha\gamma} , \\
\tilde{\mu}_{\gamma} &= \mu_{\alpha} U_{\alpha\gamma} .
\end{aligned}
\tag{4.2}$$

The tildes and primes on the fields are then dropped.

In a standard way, both isospin components of Q superfield and of U^c , D^c superfields can each be redefined by a unitary rotation in the flavour space. As such, it is possible to diagonalise the Yukawa couplings (\mathbf{Y}_D) , (\mathbf{Y}_U) (note that $(\mathbf{Y}_D) \equiv \lambda'_{0ij}$ in the basis with two non-vanishing scalar vevs) and absorb the rotation matrices in field redefinitions such that they do not appear explicitly in the Lagrangian, apart from a specific combination of rotation matrices which appear in the gauge and Higgs charged currents which is identified as the CKM matrix. In this basis, it is clear how to initialise the Lagrangian parameters, as the diagonal values are then proportional to the measured values for the up- and down-type quarks. For more details concerning this point the reader should consult Appendix C.

In the lepton sector, however, the same approach cannot be adopted for two reasons. Firstly, even with a diagonal Yukawa matrix, the charged lepton masses are given by three eigenvalues of the larger (5×5) mass matrix which includes mixing between the charged fermionic components of the \mathcal{L} , E^c and the charged gauginos and higgsinos. Thus, the diagonal entries in the Yukawa matrix would not correspond exactly to the masses of the physical mass eigenstates which describe the charged leptons. Secondly, the \mathcal{L} -basis has already been fixed by the property that three

neutral scalar vevs should be zero, so we are not free to absorb a rotation matrix¹.

Still, there is some freedom remaining due to the fact that the E^c -basis has not, as yet, been fixed. Flavour rotation in the E^c -space can be used to remove some of the unphysical degrees of freedom in $\mathbf{Y}_L \equiv \lambda_{0ij}$ coupling². As every general, complex matrix, λ_{0ij} can be uniquely decomposed (polar decomposition theorem [30]) into a product of positive semi-definite Hermitian matrix $\hat{\lambda}_0$ and unitary matrix V_E :

$$\lambda_{0ij} = \hat{\lambda}_{0ik} (V_E)_{kj} , \quad (4.3)$$

V_E can be then absorbed in the chiral superfield \bar{E} redefinition and the ‘hat’ over λ is dropped.

After all the transformations described above, we arrived at the form of the superpotential (2.20) where $(\mathbf{Y}_D)_{ij} = \lambda'_{0ij}$ and $(\mathbf{Y}_U)_{ij}$ are flavour-diagonal and $(\mathbf{Y}_L)_{ij} = \lambda_{0ij}$ is hermitian. Other coupling constants are free and, in general, complex parameters.

¹This is not entirely true: it is actually possible to perform a rotation into the vanishing sneutrino vev basis and to diagonal Yukawa couplings [22]; it is possible to use the freedom in the 3-dimensional lepton space, which we used in the previous chapter to diagonalise the sneutrino masses, in order to make the lepton Yukawa couplings diagonal. But then one will have a 10×10 mass matrix for the neutral scalars because this 3×3 rotation is, in general, complex (unitary). We want to avoid this complication by all means.

²If the decomposition is unique, then all unphysical degrees of freedom will be removed, because then the full $U(3)$ rotation is absorbed into \bar{E} and every rotation in the \mathcal{L}_α -space will “destroy” some of the properties we want to keep.

4.2 Block Diagonalising

In the following sections we outline the procedure by which the parameters of the general hermitian matrix $(\mathbf{Y}_L)_{ij}$ can be initialised such that the correct values are obtained for the charged lepton masses and the MNS mixing matrix [54]. In order to do that, it will be convenient to diagonalise the neutralino-neutrino and chargino-charged lepton mass matrices in two stages. First an approximate, unitary or bi-unitary transformation will result in matrices in block diagonal form; the standard model and supersymmetric fermion masses being split into separate blocks. Then, a second transformation will diagonalize the blocks.

The block diagonalisation can be performed for any complex matrix. Every general matrix M can be diagonalised by two unitary matrices V, U :

$$V^\dagger M U = \hat{M} = \text{diag}(m_1, m_2, \dots, m_n) = \begin{pmatrix} M_1 & 0 \\ 0 & M_2 \end{pmatrix}, \quad (4.4)$$

where m_i^2 are eigenvalues of MM^\dagger and M_1, M_2 are two diagonal sub-matrices of a chosen size. Hence, one can always rewrite M in the form

$$M = V \hat{M} U^\dagger = V A^\dagger A \hat{M} B^\dagger B U^\dagger, \quad (4.5)$$

where A and B are some unitary matrices of the form

$$A = \begin{pmatrix} A_1 & 0 \\ 0 & A_2 \end{pmatrix}, \quad B = \begin{pmatrix} B_1 & 0 \\ 0 & B_2 \end{pmatrix}, \quad (4.6)$$

with sub-matrices $A_{1,2}, B_{1,2}$ which are also unitary. Thus we can write

$$M = Q M_B P^\dagger, \quad (4.7)$$

where

$$M_B = A\hat{M}B^\dagger = \begin{pmatrix} A_1M_1B_1^\dagger & 0 \\ 0 & A_2M_2B_2^\dagger \end{pmatrix}, \quad (4.8)$$

is block diagonal in form and $Q = VA^\dagger$, $P = UB^\dagger$. Of course, M_B is not uniquely defined.

Block diagonalisation is particularly useful the in case of hierarchical matrices, when one can find analytical approximate formulae for P, Q matrices in eq.(4.7). Consider for example a hermitian matrix (other cases can be considered analogously) of the form:

$$M = \begin{pmatrix} m_A & m_B \\ m_B^\dagger & m_C \end{pmatrix}, \quad (4.9)$$

where $m_A = m_A^\dagger$, $m_C = m_C^\dagger$ and $\|m_A\| \gg \|m_B\|, \|m_C\|$. In such a case, the approximately (up to the terms $\mathcal{O}(\|m_{B,C}\|^2/\|m_A\|^2)$) unitary matrix U ,

$$U = \begin{pmatrix} 1 & -(m_A)^{-1}m_B \\ m_B^\dagger(m_A)^{-1} & 1 \end{pmatrix}, \quad (4.10)$$

transforms M into approximately block-diagonal form:

$$\begin{aligned} U^\dagger M U &= \begin{pmatrix} m_A + (m_A)^{-1}m_B m_B^\dagger + m_B m_B^\dagger (m_A)^{-1} & (m_A)^{-1}m_B m_C \\ m_C^\dagger m_B^\dagger (m_A)^{-1} & m_C - m_B^\dagger (m_A)^{-1}m_B \end{pmatrix} + \mathcal{O}\left(\frac{\|m_{B,C}\|^3}{\|m_A\|^2}\right) \\ &\approx \begin{pmatrix} m_A & 0 \\ 0 & m_C - m_B^\dagger (m_A)^{-1}m_B \end{pmatrix} + \mathcal{O}\left(\frac{\|m_{B,C}\|^2}{\|m_A\|}\right). \end{aligned} \quad (4.11)$$

We kept explicitly the $\mathcal{O}\left(\frac{\|m_{B,C}\|^2}{\|m_A\|}\right)$ term in (22) element of block-diagonalised form of M as in many models $m_C \equiv 0$ and in this case it will be the only term which

survives (the see-saw mechanism [55, 56] for neutrino masses being the most famous example of this hierarchical structure).

As a next step one needs to find matrices that diagonalise the sub-blocks in eq.(4.11). We employ this method in the next sections where we present explicit perturbative (first order) results for analogues of the matrices Q and P in Eq. (4.7), in both neutral and charged fermion masses in the \mathbb{L} -MSSM. It should be noted at this point that, although we use only the approximate analytical expressions for the see-saw type expansions above, in our numerical analysis we perform exact block diagonalization, iteratively finding the correct, and strictly unitary, matrices P, Q of eq.(4.7).

4.3 Fermion masses and mixing

In the following section we shall present the tree level phenomena of the fermion sector in the \mathbb{L} -MSSM. We consider in turn, the neutral and charged fermion sectors and the patterns of the mass matrices. We consider the tree level eigenvalues, particularly for the neutral sector and the approximate block diagonalisation of the matrices. In section 4.4, we use the approximate block diagonalisation to consider the way in which the MNS matrix appears in this model. The MNS matrix is now a sub-block of a larger unitary matrix and therefore the MNS matrix itself is not unitary.

This analysis is then used to ensure the correct low energy parameters are reproduced, despite mixing between the leptons and heavy fermion fields.

In section 5.1 we consider the effect of radiative corrections at the order of one-

loop. After setting out the renormalisation framework, we present in turn various loop diagrams and highlight the important contributions. The full numerical analysis has been completed, however approximate expressions are presented for each contribution which demonstrate from where the important effects arise. We will consider the case where the tree-level effect dominates and gives rise to the larger, atmospheric mass squared difference, in which case the solar mass squared difference is generated by the loop effects. We also show that it is possible for loop effects to be greater than the tree level effects, in which case both mass squared differences are generated at the level of one-loop.

4.3.1 Neutral fermion sector

In the lepton number violating extension of the minimal supersymmetric standard model (\mathcal{U} -MSSM) the neutrinos ($\nu_{L1,2,3}$), neutral higgsinos (ν_{L0} and \tilde{h}_2^0) and neutral colourless gauginos (\tilde{W}_0 and \tilde{B}) mix. To transform the fields into the mass basis, the 7×7 neutralino mass matrix must be diagonalised. In the interaction basis,

$$\mathcal{L} \supset -\frac{1}{2} \begin{pmatrix} -i\tilde{B}, & -i\tilde{W}_0, & \tilde{h}_2^0, & \nu_{L\alpha} \end{pmatrix} \mathcal{M}_N \begin{pmatrix} -i\tilde{B} \\ -i\tilde{W}_0 \\ \tilde{h}_2^0 \\ \nu_{L\beta} \end{pmatrix} + \text{H.c.}, \quad (4.12)$$

where the full 7×7 mass matrix reads

$$\mathcal{M}_N = \begin{pmatrix} M_{N4 \times 4} & d_{N4 \times 3} \\ d_{N3 \times 4}^T & 0_{3 \times 3} \end{pmatrix}, \quad (4.13)$$

and the sub-blocks are, in the basis $(-i\tilde{B}, -i\tilde{W}_0, \tilde{h}_2^0, \nu_{L\alpha} \equiv \tilde{h}_1^0, \nu_i)$

$$M_{N4\times4} = \begin{pmatrix} M_1 & 0 & \frac{g v_u}{2} & -\frac{g v_d}{2} \\ 0 & M_2 & -\frac{g_2 v_u}{2} & \frac{g_2 v_d}{2} \\ \frac{g v_u}{2} & -\frac{g_2 v_u}{2} & 0 & -\mu_0 \\ -\frac{g v_d}{2} & \frac{g_2 v_d}{2} & -\mu_0 & 0 \end{pmatrix}, \quad (4.14)$$

and

$$d_{N4\times3} = \begin{pmatrix} 0 & 0 & 0 \\ 0 & 0 & 0 \\ -\mu_1 & -\mu_2 & -\mu_3 \\ 0 & 0 & 0 \end{pmatrix}. \quad (4.15)$$

There is no quantum number to differentiate between neutralinos and neutrinos, the states of definite mass do not have definite lepton number and, as such, there is no reason to think of neutrinos and neutralinos separately. However, for realistic values of parameters, four of the mass eigenstates are heavy and three are very light, so it is convenient to refer to them as to neutralinos and neutrinos, respectively. In addition to this, it can be seen that the mixing is sufficiently small that these three light neutral states are the states which dominantly appear in the decay of the W boson to charged leptons, differentiating between the eigenstates we refer to as neutrinos from those we refer to as neutralinos.

The matrix, Z_N , which rotates the fields in (4.12) from the interaction basis to

the mass eigenstate basis is given by

$$\begin{pmatrix} -i\tilde{B} \\ -i\tilde{W}^0 \\ \tilde{h}_2^0 \\ \nu_{L\alpha} \end{pmatrix} = Z_N \begin{pmatrix} \kappa_1^0 \\ \vdots \\ \kappa_7^0 \end{pmatrix}. \quad (4.16)$$

where $\kappa_{1,\dots,7}^0$ are seven, neutral two component spinors.

The matrix \mathcal{M}_N , as it has been split in eq.(4.13), contains block diagonal terms that conserve lepton number and off-diagonal blocks which violate lepton number. The latter are expected to be very small, as they are strongly constrained by the bounds on neutrino masses or other lepton number violating processes. Thus, one can use the block diagonalization procedure of section 4.2, neglecting terms of the order $\frac{d_N^2}{M_N^2}$, and consider Z_N to be of the form

$$Z_N = \begin{pmatrix} 1 & -M_N^{-1}d_N \\ d_N^\dagger M_N^{\dagger-1} & 1 \end{pmatrix} \begin{pmatrix} \mathcal{Z}_N & 0 \\ 0 & \mathcal{Z}_\nu \end{pmatrix}. \quad (4.17)$$

The first matrix on the RHS of eq.(4.17) which is the analogue of the matrix Q^\dagger in (4.7) block diagonalises the neutrino-neutralino mass matrix:

$$\begin{pmatrix} 1 & M_N^{\dagger-1}d_N^* \\ -d_N^T M_N^{-1} & 1 \end{pmatrix} \mathcal{M}_N \begin{pmatrix} 1 & -M_N^{-1}d_N \\ d_N^\dagger M_N^{\dagger-1} & 1 \end{pmatrix} \approx \begin{pmatrix} M_{N4\times4} & 0 \\ 0 & m_\nu^{eff}{}_{3\times3} \end{pmatrix} \quad (4.18)$$

where the ‘TeV’ see-saw suppressed effective 3×3 neutrino mass matrix is given by [16, 18, 38]

$$m_\nu^{eff} = -d_N^T M_N^{-1} d_N = \frac{v_d^2 (M_1 g_2^2 + M_2 g^2)}{4 \text{Det}[M_N]} \begin{pmatrix} \mu_1^2 & \mu_1 \mu_2 & \mu_1 \mu_3 \\ \mu_1 \mu_2 & \mu_2^2 & \mu_2 \mu_3 \\ \mu_1 \mu_3 & \mu_2 \mu_3 & \mu_3^2 \end{pmatrix}. \quad (4.19)$$

Physical neutralino masses and mixing matrix \mathcal{Z}_N can be found in a standard manner by numerical diagonalization of the matrix M_N . Diagonalization on m_ν^{eff} can be easily done analytically, leading to two massless and one massive neutrino, with its mass given by:

$$m_\nu^{tree} = \left| \frac{v_d^2(M_1 g_2^2 + M_2 g^2)}{4\text{Det}[M_N]} \right| (|\mu_1|^2 + |\mu_2|^2 + |\mu_3|^2), \quad (4.20)$$

and the mixing matrix \mathcal{Z}_ν is

$$\mathcal{Z}_\nu = \begin{pmatrix} \frac{|\mu_2|}{\sqrt{|\mu_1|^2 + |\mu_2|^2}} & \frac{|\mu_1||\mu_3|}{\sqrt{|\mu_1|^2 + |\mu_2|^2}\sqrt{|\mu_1|^2 + |\mu_2|^2 + |\mu_3|^2}} & \frac{|\mu_1|}{\sqrt{|\mu_1|^2 + |\mu_2|^2 + |\mu_3|^2}} \\ \frac{-|\mu_2|\mu_1}{\mu_2\sqrt{|\mu_1|^2 + |\mu_2|^2}} & \frac{\mu_1\mu_3^*|\mu_3|}{|\mu_1|\sqrt{|\mu_1|^2 + |\mu_2|^2}\sqrt{|\mu_1|^2 + |\mu_2|^2 + |\mu_3|^2}} & \frac{|\mu_1|\mu_2^*}{\mu_1^*\sqrt{|\mu_1|^2 + |\mu_2|^2 + |\mu_3|^2}} \\ 0 & -\frac{\mu_1|\mu_3|\sqrt{|\mu_1|^2 + |\mu_2|^2}}{\mu_3|\mu_1|\sqrt{|\mu_1|^2 + |\mu_2|^2 + |\mu_3|^2}} & \frac{|\mu_1|\mu_3^*}{\mu_1^*\sqrt{|\mu_1|^2 + |\mu_2|^2 + |\mu_3|^2}} \end{pmatrix} \begin{pmatrix} X_{2 \times 2} & 0 \\ 0 & 1 \end{pmatrix}, \quad (4.21)$$

where $X_{2 \times 2}$ is an $SU(2)$ rotation. At tree level, the five massive eigenstates are unambiguously defined by diagonalising the mass matrix. The two massless eigenstates, due to the fact that they are degenerate in mass, are not fully defined. The eigenstates are chosen to be orthogonal, but it is still possible to perform a rotation on the eigenstates. As such, statements about the lightest neutrinos, $\nu_{1,2}$, are basis dependent. Because of this, the one loop contributions to $\hat{\mathcal{M}}_{Npq}$ are also basis dependent. By choosing a different linear superposition of the tree level eigenstates, the one-loop contributions to the 2×2 sub-block $\hat{\mathcal{M}}_{N(5,6)(5,6)}$ referring to the massless neutrinos would be redistributed between themselves. This freedom of basis choice is only present at tree level and is not physical. Thus, we start from $X_{2 \times 2} = 1_{2 \times 2}$ and after calculating the radiative corrections to the neutralino-neutrino mass matrix we adjust $X_{2 \times 2}$ such that the off-diagonal one-loop contribution δM_{N56} is approximately zero (this can be done iteratively). As such the effect of rediagonalising the neutrino

sector after loop corrections are added is small. As we discuss in section 4.4, choosing the basis in this manner helps also to define the lepton Yukawa couplings in terms of measured quantities like lepton masses and the U_{MNS} mixing matrix.

The result that two of the neutrino masses vanish at the tree level is not the effect of the approximations made [16,18,38]. The explicit calculation of the secular equation for the full neutralino-neutrino mass matrix \mathcal{M}_N , results in

$$\begin{aligned} \det(\mathcal{M}_N - \lambda) &= -\lambda^2 [\lambda \det(M_N - \lambda) \\ &- (\mu_1^2 + \mu_2^2 + \mu_3^2) \left(\lambda(M_1 - \lambda)(M_2 - \lambda) + \frac{g_2^2 v_d^2}{4}(M_1 - \lambda) + \frac{g^2 v_d^2}{4}(M_2 - \lambda) \right)] . \end{aligned} \quad (4.22)$$

Hence, \mathcal{M}_N always has at least two zero modes. This can be seen directly, by noting that the final three columns of the 7×7 mass matrix are proportional to each other.

Finally, the physical eigenstates of neutralinos and neutrinos are approximately given by, respectively:

$$\mathcal{Z}_N \begin{pmatrix} \kappa_1^0 \\ \kappa_2^0 \\ \kappa_3^0 \\ \kappa_4^0 \end{pmatrix} = \begin{pmatrix} -i\tilde{B} \\ -i\tilde{W}_0 \\ \tilde{h}_2^0 \\ \nu_{L0} \end{pmatrix} + M_N^{-1} d_N \nu_{Li} , \quad (4.23)$$

and

$$\mathcal{Z}_\nu \begin{pmatrix} \kappa_5^0 \\ \kappa_6^0 \\ \kappa_7^0 \end{pmatrix} = -d_N^\dagger M_N^{\dagger-1} \begin{pmatrix} -i\tilde{B} \\ -i\tilde{W}_0 \\ \tilde{h}_2^0 \\ \nu_{L0} \end{pmatrix} + \nu_{Li} , \quad (4.24)$$

with $\nu_{L0} = \tilde{h}_1^0$, the down type Higgsino.

4.3.2 Charged fermion sector

In a similar fashion to the neutral sector, charged leptons, gauginos and higgsinos mix. The full 5×5 chargino mass matrix in the zero sneutrino mass basis is given by

$$\mathcal{M}_C = \begin{pmatrix} M_{C 2 \times 2} & 0 \\ d_{C 3 \times 2} & m_{C 3 \times 3} \end{pmatrix}, \quad (4.25)$$

with the lepton number conserving sub-blocks

$$M_{C 2 \times 2} = \begin{pmatrix} M_2 & \frac{g_2 v_u}{\sqrt{2}} \\ \frac{g_2 v_d}{\sqrt{2}} & \mu_0 \end{pmatrix}, \quad m_{C ij} = \frac{v_d}{\sqrt{2}} \lambda_{0ij}, \quad (4.26)$$

and the lepton number violating being

$$d_{C 3 \times 2} = \begin{pmatrix} 0 & \mu_1 \\ 0 & \mu_2 \\ 0 & \mu_3 \end{pmatrix}. \quad (4.27)$$

The rotation matrices which transform between interaction eigenstates and mass eigenstates are given by

$$\begin{pmatrix} -i\widetilde{W}^+ \\ \tilde{h}_2^+ \\ e_{Ri} \end{pmatrix} = Z_+ \begin{pmatrix} \kappa_1^+ \\ \vdots \\ \kappa_5^+ \end{pmatrix}, \quad (4.28)$$

$$\begin{pmatrix} -i\widetilde{W}^- \\ e_{L\alpha} \end{pmatrix} = Z_-^* \begin{pmatrix} \kappa_1^- \\ \vdots \\ \kappa_5^- \end{pmatrix}, \quad (4.29)$$

and, as such, the mass matrix is diagonalised

$$\hat{\mathcal{M}}_C = Z_-^\dagger \mathcal{M}_C Z_+, \quad (4.30)$$

where the ‘hat’ denotes that the matrix is diagonal.

The matrices Z_+ and Z_- can be determined by the requirement that they should diagonalise the Hermitian matrices $\mathcal{M}_C^\dagger \mathcal{M}_C$ and $\mathcal{M}_C \mathcal{M}_C^\dagger$, respectively. The off-diagonal blocks in the latter two combinations are small comparing to the diagonal ones, so one can again use block-diagonalising approximation of section 4.2. Keeping just the leading terms in $1/M_C$ expansion, one obtains

$$\begin{aligned} Z_- &\approx \begin{pmatrix} 1 & -M_C^{-1} d_C^\dagger \\ d_C M_C^{-1} & 1 \end{pmatrix} \begin{pmatrix} \mathcal{Z}_- & 0 \\ 0 & \mathcal{Z}_{l^-} \end{pmatrix}, \\ Z_+ &\approx \begin{pmatrix} \mathcal{Z}_+ & 0 \\ 0 & \mathcal{Z}_{l^+} \end{pmatrix}. \end{aligned} \quad (4.31)$$

Substitution of (4.31) in (4.30) results in the physical effective mass matrix

$$\hat{\mathcal{M}}_C = \begin{pmatrix} \mathcal{Z}_-^\dagger M_C \mathcal{Z}_+ + \mathcal{O}\left(\frac{d_C^2}{M_C}\right) & \mathcal{O}\left(\frac{d_C m_C}{M_C}\right) \\ \mathcal{O}\left(\frac{d_C^2}{M_C^1}\right) & \mathcal{Z}_{l^-}^\dagger m_C \mathcal{Z}_{l^+} + \mathcal{O}\left(\frac{d_C^2 m_C}{M_C^2}\right) \end{pmatrix} \approx \begin{pmatrix} \mathcal{Z}_-^\dagger M_C \mathcal{Z}_+ & 0 \\ 0 & \mathcal{Z}_{l^-}^\dagger m_C \mathcal{Z}_{l^+} \end{pmatrix}. \quad (4.32)$$

Then the matrices \mathcal{Z}_+ , \mathcal{Z}_- can be again determined as diagonalising matrices for the $M_C^\dagger M_C$, $M_C M_C^\dagger$ products, with the additional requirement that physical fermion masses are real and positive. Matrix m_C in our basis is hermitian and as such $\mathcal{Z}_{l^+} = \mathcal{Z}_{l^-} \equiv \mathcal{Z}_l$. Furthermore, physical eigenstates of fermion fields are given by

$$\begin{aligned} \mathcal{Z}_+ \begin{pmatrix} \kappa_1^+ \\ \kappa_2^+ \end{pmatrix} &\approx \begin{pmatrix} -i\widetilde{W}^+ \\ \tilde{h}_2^+ \end{pmatrix}, \\ \mathcal{Z}_l \begin{pmatrix} \kappa_3^+ \\ \kappa_4^+ \\ \kappa_5^+ \end{pmatrix} &\approx \begin{pmatrix} e_{R1} \\ e_{R2} \\ e_{R3} \end{pmatrix}, \end{aligned} \quad (4.33)$$

and

$$\begin{aligned}
\mathcal{Z}_-^* \begin{pmatrix} \kappa_1^- \\ \kappa_2^- \end{pmatrix} &\approx \begin{pmatrix} -i\widetilde{W}^- \\ e_{L0} \end{pmatrix} + M_C^{-1T} d_C^T \begin{pmatrix} e_{L1} \\ e_{L2} \\ e_{L3} \end{pmatrix}, \\
\mathcal{Z}_l^* \begin{pmatrix} \kappa_3^- \\ \kappa_4^- \\ \kappa_5^- \end{pmatrix} &\approx -d_C^* M_C^{-1*} \begin{pmatrix} -i\widetilde{W}^- \\ e_{L0} \end{pmatrix} + \begin{pmatrix} e_{L1} \\ e_{L2} \\ e_{L3} \end{pmatrix}.
\end{aligned} \tag{4.34}$$

For a quick view of the full charged fermion mass matrix see Appendix B.

4.4 Constructing the MNS matrix

The lepton mixing matrices appear in the charged current gauge boson vertex. Whereas in the lepton number conserving case the U_{MNS} matrix is a 3×3 matrix describing the mixing of three charged leptons into three neutral leptons, the R-parity violating case has the mixing of five charged fermions into seven neutral fermions, of which the U_{MNS} is a 3×3 sub-matrix, only approximately unitary. Thus,

$$\mathcal{L} \supset \frac{g_2}{\sqrt{2}} W_\mu^+ \bar{\nu}'_{Li} \bar{\sigma}^\mu e'_{Li} + \text{H.c} = \frac{g_2}{\sqrt{2}} W_\mu^+ \bar{\kappa}_p^0 \bar{\sigma}^\mu (U_{\text{MNS}})_{pq} \kappa_q^- + \text{H.c}, \tag{4.35}$$

where primes refer to interaction eigenstates, and the MNS matrix,

$$U_{\text{MNS}} = \mathcal{Z}_\nu^\dagger \mathcal{Z}_l^* + \mathcal{O} \left(\frac{d_c d_N}{M_C M_N} \right), \tag{4.36}$$

is defined in terms of the mixing matrices introduced in (4.21) and below (4.32).

As the first term in Eq. (4.36) is unitary, unitarity violation in U_{MNS} is at most of the order of $\frac{d_c d_N}{M_C M_N} \sim \frac{m_\nu^{\text{tree}} M_{\text{SUSY}}}{M_\Sigma^2} \tan^2 \beta \sim 10^{-12} \tan^2 \beta$, which is well below sensitivity of current (or planned) experiments determining the MNS matrix.

4.5 Input parameters

The parameters characterising the light charged fermions are already very well known; masses are measured with very good accuracy. In contrast to this, the neutrino sector is not, as yet, known with the same precision. There is however, information about the mass square difference between neutrinos and the mixing between different interaction states, and upcoming experiments should improve our knowledge of neutrino parameters in the near future. Furthermore, supersymmetric fermions have not yet been discovered, and their masses and couplings (those which are not determined by supersymmetric structure of the model) are entirely unknown. In the \mathcal{U} -MSSM both sectors mix, and thus the question of effective and convenient parameterisation arises. In this section, we will consider the parameters in the Lagrangian which effect the tree level masses and mixing. In the next chapter, we discuss parameters which affect the neutral fermions at the order of one loop.

As the SUSY sector has not been measured directly, it is convenient to take as an input the following set of Lagrangian parameters: $M_1, M_2, \tan\beta, \mu \equiv \mu_0$. With μ_i of the order of MeV, corrections to the supersymmetric sector from the light fermion sector are see-saw suppressed and negligible. Chargino and neutralino masses and lepton-number conserving couplings are thus, to a very good accuracy, determined by the above four parameters. Reconstructing their values from the actual experimental measurements has already been discussed in the literature [57].

In the next step, neutrino masses can be parameterised at tree level by setting the lepton-number violating parameters $\mu_i, i = 1, 2, 3$. In the future, when the neutrino mass matrix is known to better accuracy, it could become more convenient to reconstruct μ_i from the experimental data - for that, the knowledge of radiative

corrections to the neutrino masses would be vital.

To initialize the Lagrangian parameters in the light charged lepton sector, one needs to input the lepton masses, m_e , m_μ , m_τ and the mixing matrix U_{MNS} . The lepton rotation matrix \mathcal{Z}_l can be then calculated from (4.36)

$$\mathcal{Z}_l \approx \mathcal{Z}_\nu^* U_{MNS}^* . \quad (4.37)$$

As we have seen from (4.21), the neutrino mixing matrix, \mathcal{Z}_ν is defined at tree level up to a $U(2)$ rotation for a given set of μ_i . The same matrix is then defined completely at one-loop where all the neutrinos are no longer degenerate. Thus, a complete definition of \mathcal{Z}_l requires a one-loop corrected neutrino mixing matrix. Then, the light charged fermion mass matrix m_C in (4.26), which is hermitian and proportional to the Yukawa matrix $\lambda_{0ij} = \frac{\sqrt{2}}{v_d} m_C ij$ is given by:

$$m_C = \mathcal{Z}_l \text{diag}(m_e, m_\mu, m_\tau) \mathcal{Z}_l^\dagger . \quad (4.38)$$

Eq. (4.38) holds under the assumption that one-loop corrections to \mathcal{Z}_l are small. Otherwise, one needs to find m_C iteratively, such that physical (i.e. loop corrected) \mathcal{Z}_ν and \mathcal{Z}_l produce the correct experimentally measured U_{MNS} matrix of eq.(4.37).

As we have repeatedly mentioned so far, it is important to notice that the matrix m_C is not diagonal.

Having understood and parameterised the model at tree-level, we now look to calculate the radiative corrections. For the neutrino masses and mixing, this is essential. We cannot generate two distinct mass differences at tree-level, and the degenerate neutrinos cause the mixing angle to be undefined. We show in the preceding chapter that the inclusion of radiative corrections at one-loop ameliorates these problems.

Chapter 5

The \mathbb{L} -MSSM at one-loop: Neutral fermion masses

In this chapter, we shall calculate the complete set of the one-loop corrections to the massless neutrinos without assuming CP-conservation or bilinear superpotential operator dominance. In section 5.1 we describe our renormalization procedure and present analytical results for the one-loop corrections together with approximate formulae for individual diagrams. We compare with the current literature. In section 5.2 we present numerical results which show the size of the input parameters required to account for the neutrino experimental data.

zero for the two massless neutrinos). Our renormalization analysis is similar to the one in Ref. [17]. We have also studied an on-shell renormalization analogous to the one in [59]. In this scheme, the physical mass formula is similar to (5.3).

Some additional remarks are important at this stage:

- a) The two one-loop induced neutrino masses are perfectly defined at one-loop through Eq. (5.3). We have proven both analytically and numerically that these masses are finite and numerically that they are gauge independent at one-loop order. This result remains valid also when one takes into account mixing between them.
- b) The one-loop formula for neutralino masses (5.3), receives, in addition to diagonal corrections, off diagonal ones, $m_{Nqq}^{\text{pole}} \rightarrow m_{Nqp}^{\text{pole}}$. Physical neutralino and neutrino masses are then obtained from the diagonalization of m_{Nqp}^{pole} as $\hat{m}_N^{\text{pole}} = (1 + \delta Z_N^\dagger) m_N^{\text{pole}} (1 + \delta Z_N)$. Then the corrected mixing matrix Z_N has to be replaced by $Z_N \rightarrow (1 + \delta Z_N) Z_N$ everywhere in our expressions for the self energies. However, the corrections to Z_N matrix are of the order $\delta Z_{Npq} \sim \delta m_{Npq} / (m_{Npp} - m_{Nqq})$ and are small if the tree level masses are not degenerate. In our case this happens only for the two massless neutrinos, so we include off-diagonal corrections, shifting $\mathcal{Z}_\nu \rightarrow (1 + \delta \mathcal{Z}_\nu) \mathcal{Z}_\nu$ where $\delta \mathcal{Z}_\nu$ has only the upper 2×2 block non-trivial². As discussed previously in section 4.3, this is actually necessary to fix the neutrino basis. The resulting corrections

²Possible exception is the case when μ_i parameters are very small, so that one-loop corrections to the neutrino masses are of the order of tree level neutrino mass or bigger. In this case one needs to re-diagonalise the full 3×3 neutrino mass matrix. This is done numerically in section 5.2 when presenting our results for $\mu_i = 0$.

to lighter neutrino masses are formally two-loop, but numerically important and have to be taken into account. One should note that, as mentioned in the previous point, one-loop corrections to the light neutrino mass sub-matrix are finite - going beyond the approximation described above would require performing formal renormalization on the neutral fermion mass matrix. Finally, similar considerations apply to the case of the charged fermion mixing matrix Z_l in (4.37).

- c) As we have already mentioned, in our neutral scalar basis the sneutrino vevs are zero at tree level. Non-zero sneutrino vevs will appear, in general, at one-loop. As a result, the neutrino tree level mass in Eq. (4.20) should be corrected. However, loop induced vev contributions *do not arise* for the massless neutrinos – they are generated outside the 2×2 light neutrino mass matrix – which is the case we are interested in.
- d) We choose $\mu_R = M_Z$ as renormalization scale in (5.3) were we input the \overline{DR} parameters for $m_{Nq}^{\text{bare}}(\mu_R)$ at tree level. These parameters are taken after diagonalising the full neutralino mass matrix in Eq. (4.13).
- e) The infinities which arise in the calculation of the one loop corrections, must be absorbed in parameters of the tree-level Lagrangian. It is possible to check that there are no infinities which must be absorbed where the mass matrix contains zero entries. The divergent parts of the integrals do not depend on the masses of the particles in the loop integral and as such the infinities only arise when a diagram exists in the interaction picture with only a mass insertion on the fermion in the loop. That is, the symmetry which prevents a term existing in

the classical Lagrangian also causes the divergent part to cancel in the mass basis. This guarantees that it is always possible to absorb the infinite part of the integral in the bare parameters of the classical Lagrangian.

Having considered the above points we find that for the calculation of the one-loop corrections to the eigenstates that are massless at tree level, it is sufficient to consider corrections to the bilinear terms purely between these eigenstates. We find that it is possible to neglect the one-loop effects which correct other entries of the neutral fermion mass matrix, describing neutralino masses or neutralino-neutrino mixing.

5.1.2 One loop contributions to the massless neutrino eigenstates

The mixing of neutrino, neutral Higgsino and neutral gaugino interaction eigenstates has been shown to result in two mass eigenstates with zero mass. It is important to note the composition of the massless eigenstates; they consist solely of neutrino interaction states, not containing any contribution from the fermionic components of the gauge supermultiplets or the Higgs supermultiplets. This can be stated, entirely equivalently as the rotation matrix in Eq. (4.17) becomes [38]

$$Z_{N\{1\rightarrow 4\}\{5\rightarrow 6\}} = 0. \quad (5.4)$$

Radiative corrections at one-loop will affect all three of the light mass eigenstates (‘neutrinos’) and will lift the degeneracy between the massless eigenstates. The possibility that the hierarchy of mass differences in the neutrino sector can be explained in the \mathcal{L} -MSSM is considered. If the ‘atmospheric’ mass difference were to result

from the tree level splitting and the ‘solar’ mass difference originated from loop effects, the distinct hierarchy could be accommodated within the model. If the solar mass difference is to originate purely from loop corrections to massless eigenstates, we must find loop corrections from diagrams with external legs comprised purely of neutrino interaction states. A small caveat is required to compare with the literature. In a general basis where the sneutrino vacuum expectation values are not zero, the massless neutrinos are comprised of interaction state neutrinos and the interaction state Higgsino that carries the same quantum numbers. In the ‘mass insertion’-type diagrams, this means that only diagrams without mass insertion or with a mass insertion which changes the original neutrino external leg to the down-type Higgsino can contribute to the solar mass [32], if the assumption is made that the solar mass arises purely from loop corrections to eigenstates which were massless at tree level.

The one-loop, one-particle irreducible self energies needed in (5.3) are calculated in Appendix F, see (F-1,F-2,F-5,F-6). Results are presented for general vertices and for a general R_ξ gauge. One then has to simply replace these vertices with the appropriate Feynman rules given in Appendix C in order to obtain $\Sigma^{D,L}$. Since this rather trivial replacement leads to rather lengthy formulae for the self energies, we refrain for presenting the full expressions here. Instead we examine in detail the dominant contributions to the massless neutrinos, which are the contributions to Σ^D . Of course, the numerical analysis exploits the full expressions.

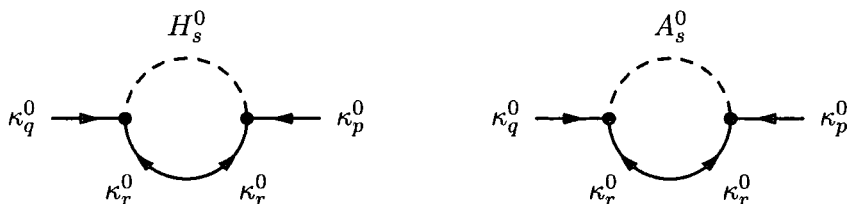
From the expressions (F-1,F-2), it can be seen that these corrections are proportional to the mass of the fermion in the loop. As such, the diagrams that give a large contribution are the diagrams with sufficiently heavy fermions compared to any suppression from the vertices. In addition, standard model neutral fermion masses arise

entirely due to Supersymmetry breaking in the \mathbb{U} -MSSM so corrections are expected to be large for individual diagrams or a certain amount of fine tuning is required for large SUSY soft breaking masses.

In the next section of this chapter we analyze all the possible contributions to Σ_N^D for the massless neutrinos, isolating the dominant ones. For simplicity, we shall confine ourselves only to the diagonal parts of Σ_N^D , although our numerics account also for the off diagonal effects in the massless neutrino sub-block.

5.1.3 Neutral fermion - neutral scalar contribution

Diagrammatically this contribution reads as:



This can be easily calculated by using the formula (F-1) and with the Feynman rules read from Appendix C. The result for the full contribution to the massless neutrinos, $p = q = \{5, 6\}$, is :

$$\begin{aligned} \Sigma_{Npp}^D &= - \sum_{r=1}^7 \sum_{s=1}^5 \sum_{i,j=1}^3 \frac{m_{\kappa_r^0}}{(4\pi)^2} \times \\ &\left[\frac{e}{2c_W} Z_{N(4+i)p} Z_{N1r} - \frac{e}{2s_W} Z_{N2r} Z_{N(4+i)p} \right] \left[\frac{e}{2c_W} Z_{N(4+j)p} Z_{N1r} - \frac{e}{2s_W} Z_{N2r} Z_{N(4+j)p} \right] \\ &\left[Z_{R(2+i)s} Z_{R(2+j)s} B_0(m_{\kappa_p^0}^2, m_{H_s^0}^2, m_{\kappa_r^0}^2) - Z_{A(2+i)s} Z_{A(2+j)s} B_0(m_{\kappa_p^0}^2, m_{A_s^0}^2, m_{\kappa_r^0}^2) \right] , \quad (5.5) \end{aligned}$$

where $H_{1,\dots,5}^0$ and $A_{1,\dots,5}^0$ are the CP-even and CP-odd neutral scalar fields, respectively, each containing a mixture of Higgs and sneutrino fields. The matrices Z_N, Z_R, Z_A are those that diagonalize the neutralino, CP-even, and CP-odd Higgs boson mass matrices and are defined in (4.21) and (C.7,C.7), respectively (for analytic expressions for Z_R, Z_A see Eq. (3.32) and (3.45)). Individually, the neutral fermion - neutral scalar diagrams in (5.5) are large, however, if there were no splitting between the mass of CP-even and CP-odd neutral scalar eigenstates there would be an exact cancellation between the two diagrams. Notice also that the whole contribution is multiplied by a neutralino mass which is generically of the order of the electroweak scale. It is rather instructive to simplify Eq. (5.5) by expanding around $m_{H_{s>2}^0}^2$ and $m_{A_{s>2}^0}^2$ as,

$$\Sigma_{Npp}^D \simeq - \sum_{r=1}^7 \sum_{i=1}^3 \frac{m_{\kappa_r^0}^3}{4(4\pi)^2} \mathcal{Z}_{\nu ip}^2 \left[\frac{e}{c_W} \mathcal{Z}_{N1r} - \frac{e}{s_W} \mathcal{Z}_{N2r} \right]^2 \frac{\Delta m_{\tilde{\nu}i}^2}{(m_{\tilde{\nu}i}^2 - m_{\kappa_r^0}^2)^2} \ln \frac{m_{\kappa_r^0}^2}{m_{\tilde{\nu}i}^2} \quad (5.6)$$

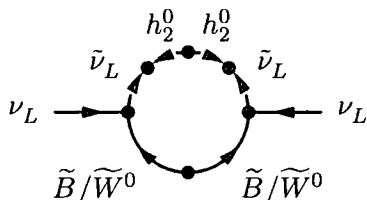
where $\Delta m_{\tilde{\nu}i}^2 = m_{\tilde{\nu}_{+i}}^2 - m_{\tilde{\nu}_{-i}}^2$ is the CP even - CP odd sneutrino square mass difference. Its analytical form can be derived from Eqs. (3.37) and (3.48) of [24] to be

$$\Delta m_{\tilde{\nu}i}^2 = \frac{B_i^2 \tan^2 \beta}{M_A^2 - M_i^2} + O(B_i^4/M_i^6), \quad (5.7)$$

where M_A is the CP-odd Higgs mass and M_i the soft breaking slepton masses which are diagonal in our basis, as discussed in Section 3. A similar expression has been derived in Ref. [23]. \mathcal{Z}_{ν} and \mathcal{Z}_N are defined in (4.17) and (4.21). The contribution (5.6) is driven by the lepton number violating terms in the soft supersymmetry breaking sector, B_i and the whole expression for the neutral scalar contribution collapses approximately to

$$\Sigma^D \sim \left(\frac{\alpha}{4\pi} \right) m_{\kappa^0} \left(\frac{m_{\kappa^0}}{M} \right)^2 \frac{B_i^2 \tan^2 \beta}{(m_{\kappa^0}^2 - M^2)^2}, \quad (5.8)$$

where M is the sneutrino or Higgs and m_{κ^0} the neutralino masses in the loop, respectively. The importance of this contribution has already been pointed out in Refs. [13,32]. The mass insertion approximation diagram reads as



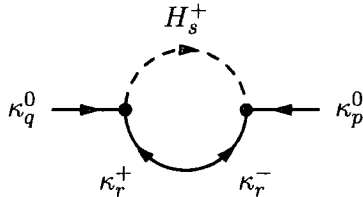
where the ‘blobs’ indicate insertions of B_i s, scalar and gaugino masses. The neutral scalar-fermion contribution is thus *a)* suppressed from the CP-even-CP odd sneutrino mass square difference, i.e, the lepton number violating soft SUSY breaking parameter B_i , *b)* is enhanced by $\tan^2 \beta$, and finally *c)* suppressed by three powers of SUSY breaking masses.

The approximate formula (5.6) does not, in general, capture the full neutral fermion-scalar correction. There are other corrections of the same order of magnitude, including the Higgs bosons in $s = 1, 2$ states. This expansion is more complicated than (5.6) and is given explicitly in section 5.2, Eq. (5.30), where we discuss our numerical results and compare with approximate formulae of this chapter.

Ignoring possible accidental cancellations from other diagrams, $[B_i \tan \beta]$ must be smaller than the 0.1% of the sneutrino mass squared, M^2 , in order to have $m_\nu \leq 1$ eV. On the other hand, numerically, if the ‘solar’ neutrino mass difference were to be generated by this diagram, then $B_i \sim \mathcal{O}(1)\text{GeV}^2$. Because B_i is in principle not constrained from above by other means, we conclude that this diagram dominates the whole contribution especially when the trilinear couplings, λ, λ' , are negligible.

5.1.4 Charged fermion - charged scalar contribution

This contribution reads diagrammatically as:



Using the generic formula the self energy, (F-1), the Feynman rules from Appendix C, and also by applying Eq. (5.4), we find that the full diagonal contribution for $p = q = \{5, 6\}$, is :

$$\begin{aligned} \Sigma_{Npp}^D &= \sum_{s=1}^8 \sum_{r=1}^5 \sum_{i,j,k,l=1}^3 \sum_{\alpha,\beta=0}^3 \frac{m_{\kappa_r^-}}{(4\pi)^2} (\lambda_{\alpha l k} Z_{H(2+\alpha)s}^* Z_{+(2+k)r} Z_{N(4+l)p}) \times \\ &\quad \left[\frac{e}{s_w} Z_{H(2+i)s} Z_{-1r}^* Z_{N(4+i)p} - \lambda_{\beta i j} Z_{H(5+j)s} Z_{-(2+\beta)r}^* Z_{N(4+i)p} \right] B_0(m_{\kappa_p^0}^2, m_{H_s^+}^2, m_{\kappa_r^-}^2), \end{aligned} \quad (5.9)$$

where Z_N, Z_+, Z_-, Z_H are rotation matrices in the neutral fermion, charged fermion, and charged scalar sectors, and defined in (4.17), (4.30), and (C.8), respectively. It is important to notice that following (4.30) we obtain, $Z_{+(2+k)r} \simeq \mathcal{Z}_{lk_r}$, with $r > 2$ and hence the contribution (5.9) is proportional to the mass of a light fermion, $m_{\kappa_r^-}$. In addition, since $Z_{N(4+l)p} \simeq \mathcal{Z}_{\nu lp}$, (4.17) shows that the contribution (5.9) contains the rotation mixing matrix \mathcal{Z}_{ν} , which has been presented analytically in (4.21). In order to analyze the dominant pieces from the charged scalar - fermion contribution, it is instructive to consider two cases : $\lambda_{ijk} = 0$ and $\lambda_{ijk} \neq 0$.

In the case where the trilinear superpotential couplings are absent the charged lepton loop has a small contribution to the massless neutrino eigenstates. From the

discussion above and (5.9), we obtain at the limit of small lepton masses (compared to the SUSY breaking ones),

$$\Sigma_{Npp}^D = \sum_{s=1}^8 \sum_{i,j,k,l=1}^3 \sum_{r>2}^5 \frac{m_{\kappa_r^-}}{(4\pi)^2} (\lambda_{0lk} Z_{H2s}^* Z_{lkr} Z_{\nu lp}) \times \left[\frac{e}{S_W} Z_{H(2+i)s} Z_{-1r}^* Z_{\nu ip} - \lambda_{0ij} Z_{H(5+j)s} Z_{-2r}^* Z_{\nu ip} \right] B_0(0, m_{H_s^+}^2, 0) \quad (5.10)$$

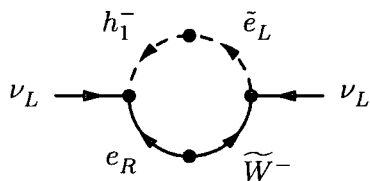
where $\lambda_{i0j} = -\lambda_{0ij}$ is the lepton Yukawa coupling obtained from Eq. (4.26). We can analyse further equation (5.10) by Taylor expansion with respect to $m_{H_s^+}^2$ (commonly named ‘‘Mass Insertion Approximation’’, or MIA, see, for example, review in Ref. [60]) and using (4.27,4.30) and (C.8,C.8) ,

$$Z_{-1r} \simeq \left(\frac{d_C^\dagger}{M_C} Z_l \right)_{1r} \simeq \frac{\mu_i}{M_C} , \quad (5.11)$$

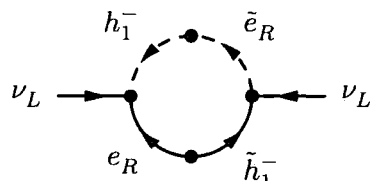
$$Z_{H2s}^* Z_{H(2+i)s} m_{H_s^+}^2 = \mathcal{M}_{H^+ 2,2+i}^2 \simeq \mu_i m_l \tan \beta , \quad (5.12)$$

$$Z_{H2s}^* Z_{H(5+i)s} m_{H_s^+}^2 = \mathcal{M}_{H^+ 2,5+i}^2 \simeq B_i \tan \beta , \quad (5.13)$$

where m_l is the lepton mass and M_C a generic gaugino mass. Hence, the neutrino couples to either the right handed component of the electron, the \widetilde{W}^- or the Higgsino with couplings proportional to μ_i . All the above can be diagrammatically depicted with mass insertions as :



$$\sim m_l \frac{\mu_i}{M_C} \frac{B_i}{M_{H^+}^2} \tan \beta , \quad (5.14)$$



$$\sim m_l \frac{\mu_i}{M_C} \frac{\mu_i m_l}{M_{H^+}^2} \tan \beta , \quad (5.15)$$

where $M_{H^+}^2$ is a generic charged Higgs mass. Obviously, both the fermion and the scalar propagator are suppressed by lepton number violating couplings. This contri-

bution is then compared with the one previously considered with neutral particles in the loop. Indeed, in order to account for the atmospheric neutrino mass scale it must be $\mu_i \ll \sqrt{B_i} \sim O(1 \text{ GeV})$ and hence the charged particle contribution is *always* smaller than the neutral one. Our finding here is in general agreement with the discussion in Refs. [13, 21]. Finally, notice the Goldstone contribution vanishes since this always conserves lepton number.

If the trilinear superpotential lepton number violating coupling λ_{ijk} is turned on, then a lepton - slepton loop contribution is generated. In contrast with the pure bilinear case, the trilinear contribution may dominate depending on the magnitude of λ . In this case the full contribution in (5.9) results in

$$\begin{aligned} \Sigma_{Npp}^D &= \sum_{s=1}^8 \sum_{r=1}^5 \sum_{i,j,k,l,m,n=1}^3 \frac{m_{\kappa_r^-}}{(4\pi)^2} \times [\lambda_{mik} Z_{H(2+m)s}^* Z_{+(2+k)r} Z_{N(4+i)p}] \times \\ &[\lambda_{lnj} Z_{H(5+j)s} Z_{-(2+n)r}^* Z_{N(4+l)p}] B_0(m_{\kappa_p^0}^2, m_{H_s^+}^2, m_{\kappa_r^-}^2). \end{aligned} \quad (5.16)$$

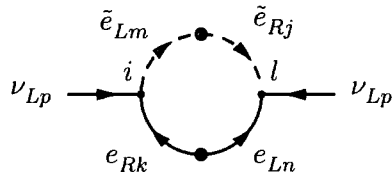
Again, making use of (4.21, 4.30) we see that the contribution is proportional to the light lepton masses and involves the neutrino mixing matrix. We can go a little bit further and perform MIA expansion of (5.16) as we did before. The contribution then reads,

$$\begin{aligned} \Sigma_{Npp}^D &= \sum_{i,j,k,l,m,n=1}^3 \frac{m_{l_q}}{(4\pi)^2} \lambda_{mik} \lambda_{lnj} Z_{\nu ip} Z_{\nu lp} Z_{lkq} Z_{lnq}^* \times \\ &\left[\frac{(\mathcal{M}_{H^+}^2)_{2+m,5+j}}{(\hat{\mathcal{M}}_{H^+}^2)_{2+m} - (\hat{\mathcal{M}}_{H^+}^2)_{5+j}} \ln \frac{(\hat{\mathcal{M}}_{H^+}^2)_{2+m}}{(\hat{\mathcal{M}}_{H^+}^2)_{5+j}} \right], \end{aligned} \quad (5.17)$$

where m_{l_q} is a light charged lepton mass, $(\mathcal{M}_{H^+}^2)$ is the charged scalar mass matrix in the interaction basis and is given by (C.8). In our notation $(\hat{\mathcal{M}}_{H^+}^2)_{5+j} \equiv (\hat{\mathcal{M}}_{H^+}^2)_{5+j,5+j}$, and so on. In the denominator and logarithm of (5.17) one has the

difference of diagonal elements mm and jj of LL and RR slepton mass matrices, respectively. The approximation (5.17) is proportional to the mixing matrix elements $(\mathcal{M}_{H^+}^2)_{2+m,5+j}$ which is nothing other than the LR mixing elements of the charged slepton mass matrix (C.8). These matrix elements are (almost) unbounded from experiments when $m = j$ in contrast to the case $m \neq j$.

This contribution has been discussed largely in the literature, see for instance [13, 21, 23, 31, 41, 43, 47]. It is instructive to draw the mass insertion approximation diagram corresponding to (5.17) :



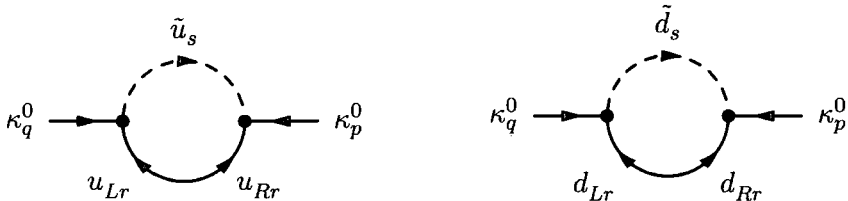
In the case of dominant λ_{ikk} coupling,

$$\Sigma_N^D \sim \lambda^2 m_l^2 \frac{\mu_0 \tan \beta + A_l}{M^2}, \quad (5.18)$$

with A_l being a trilinear SUSY breaking coupling and M a generic soft SUSY breaking mass for a slepton. Comparing (5.18) with (5.14,5.15) of the previous case with $\lambda \rightarrow 0$, we see that the latter is suppressed with at least a factor μ_i/M . In the case where the final two indices are different, λ_{ikl} , $k \neq l$ there is an extra suppression from slepton intergenerational mixing and the couplings must be stronger if the lepton in the loop is lighter. Our calculation is general enough to allow for these effects too. Furthermore, it is obvious from (5.17) that the $\tau - \tilde{\tau}$ -contribution, λ_{i33} , is the dominant one and this coupling tends usually to be strongly bounded.

5.1.5 Quark - squark contribution

In general, this contribution originates from up and down quarks and squarks in the loop:



The up-quark-squark contribution vanishes identically, for the mass eigenstates which are massless at tree level. This can be easily seen by applying the master equation (5.4) to the corresponding [neutralino-up-quark-up-squark] vertex given explicitly in the Appendix C.

The case of down quark-squark contribution (the right Feynman diagram above) can be divided in two cases depending on the dominance of the trilinear superpotential contribution : If $\lambda' \rightarrow 0$ and the only source of lepton number violation is the bilinear term then the contribution vanishes. Note that this does not necessarily disagree with the findings of Refs. [20,39] where apparently this contribution is claimed to be the dominant one. Recall that we are working in the basis where the sneutrino vevs are zero and thus we cannot directly compare, at least graph by graph with this work. In the case of Ref. [39] for example, the bilinear term, $\mu_i L_i H_2$ is rotated away. This rotation generates new, non-negligible superpotential trilinear couplings which is the case we are about to consider. Hence, if $\lambda'_{ijk} \neq 0$, then the situation changes dramatically. Following (F-1), the Feynman rules for the down type quarks of the Appendix C, we find that the most general contribution to the massless neutrinos,

$p = q = \{5, 6\}$, reads as,

$$\Sigma_{Npp}^D = \sum_{i,j,k,n,m=1}^3 \sum_{s=1}^6 \frac{3m_{d_k}}{(4\pi)^2} \left[\lambda'_{jik} \lambda'_{nkm} Z_{\bar{d}_{is}}^* Z_{\bar{d}_{(3+m)s}} Z_{N(4+j)p} Z_{N(4+n)p} \right] B_0(m_{\kappa_p}^2, m_{\bar{d}_s}^2, m_{d_k}^2), \quad (5.19)$$

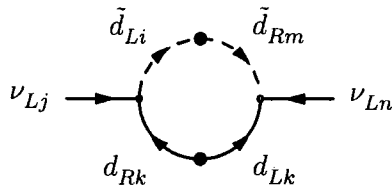
where the rotation matrix in the down squark sector, $Z_{\bar{d}}$, is defined in (C-6), and Z_N in (4.17). It is much more instructive to Taylor expand the full contribution (5.19) around a constant SUSY breaking mass into parameters of the original Lagrangian.

In the limit of small neutrino and quark masses, this results in

$$\Sigma_{Npp}^D = \sum_{j,n,k,m=1}^3 \frac{Z_{\nu jp} Z_{\nu np}}{(4\pi)^2} \left[3 m_{d_k} \lambda'_{jik} \lambda'_{nkm} \frac{(\mathcal{M}_{\bar{d}}^2)_{i,3+m}}{(\hat{\mathcal{M}}_{\bar{d}}^2)_i - (\hat{\mathcal{M}}_{\bar{d}}^2)_{3+m}} \ln \frac{(\hat{\mathcal{M}}_{\bar{d}}^2)_i}{(\hat{\mathcal{M}}_{\bar{d}}^2)_{3+m}} \right] \quad (5.20)$$

where the mass matrix $\mathcal{M}_{\bar{d}}^2$ is defined in (C-7). Notice that $(\mathcal{M}_{\bar{d}}^2)_{i,3+m}$ are the elements of the LR mixing block of $\mathcal{M}_{\bar{d}}^2$ and our notation reads $(\hat{\mathcal{M}}_{\bar{d}}^2)_i \equiv (\mathcal{M}_{\bar{d}}^2)_{ii}$.

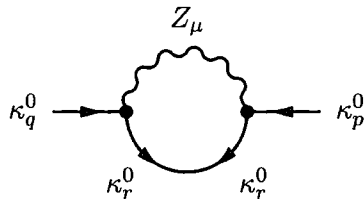
The Feynman diagram with quark and squark mass insertions representing (5.20) is:



Some remarks are in order : First the quark-squark contribution is proportional to neutrino mixing through the matrix (4.21), and hence to possible hierarchies between μ_i s. Second, it is proportional to squark flavour mixing. Experimental results for $K - \bar{K}$, and $B - \bar{B}$ mass difference set severe constraints in the intergenerational squark mixings in the lepton number conserving MSSM [$(\mathcal{M}_{\bar{d}}^2)_{i,3+m}$ must be small for $i \neq m$]. Although, our calculation is as general as possible and allows for these effects we shall assume $(\mathcal{M}_{\bar{d}}^2)_{i,3+m} = 0, i \neq m$ in our numerical results below. The quark-squark contribution may be dominant for sufficient large λ' couplings.

5.1.6 Neutral fermion - Z gauge boson contribution

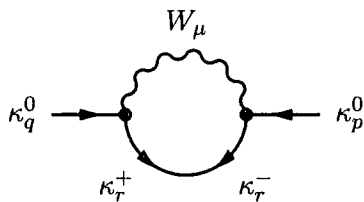
The corresponding Feynman diagram is :



Due to the approximate unitarity of the neutrino sub-block of Z_N , the contribution of this diagram is suppressed either by the lightness of the particle in the loop or by the value of the coupling. However, as we obtain from Eq. (F-2) and Appendix F, this contribution is gauge dependent. The dependence again cancels the neutral fermion-scalar contribution in (5.5) with the Goldstone boson ($s = 1$) in the loop. Although we prove this cancellation numerically, it can be also shown analytically.

5.1.7 Charged fermion - W gauge boson contribution

The Feynman diagram for this contribution is:



Following (5.4) and the Feynman rules of Appendix C, when the external legs are purely neutrino interaction eigenstates ($p, r = 5$ or 6), there is no κ^0 - κ^+ vertex. Hence, the contribution of this diagram vanishes identically.

5.1.8 Summary of the one-loop radiative corrections to massless neutrinos

The total one-loop contribution to massless neutrino masses is given by the sum of the neutral scalar loop in (5.5), the charged scalar loop in (5.9), and the squark loop in (5.19). The gauge boson contributions are negligible. If the trilinear superpotential couplings are tiny then the dominant contribution arises from the neutral scalar fermion loop and is proportional to CP-even – CP-odd sneutrino mixing [see Eq. (5.6)]. If trilinear couplings are not small, then depending upon their nature λ or λ' dominate through *lepton – slepton* [see Eq. (5.16)] and *quark – squark* [see Eq. (5.20)] diagrams.

5.1.9 Comparison with Literature

Our work improves on other work which can be found in the literature as no assumptions or approximations need to be made. Calculations can be performed in the most general supersymmetric model with minimal particle content, without any assumption that matrices are flavour diagonal, or that any complex phases are set to zero. We have not neglected any terms or phases in the neutral scalar sector, a basis was chosen in which to perform the calculation that had a decoupled CP-odd and CP-even sector and two real vevs. In choosing this basis, it is clear that the lepton Yukawa matrix is not, in general, diagonal and the lepton mixing matrix does not come purely from the neutrino sector. This is in contrast to previous work where, in whatever basis the calculation is performed, the lepton Yukawa is chosen to be diagonal. In [33] assumptions are made in the soft sector, such as intergenerational

mixing being zero, which allows a basis to be chosen where the Yukawa matrices are diagonal. Similarly, in [13, 23] there is the assumption of CP conservation in the neutral scalar sector.

Many diagrams are suggested in the literature as being important in generating a correct solar mass difference. Under the assumption that the solar mass difference comes solely from loop corrections to eigenstates which are massless at tree level, in a general basis the external legs must consist purely of neutrino and down-type Higgsino interaction eigenstates (in the basis with sneutrino vevs rotated to zero the external legs must consist purely of interaction state neutrinos). As such, when diagrams are presented with ‘mass insertions’, it is clear that any diagrams with insertions coupling the neutrino to an up-type Higgsino or gaugino on the external leg will not contribute to the solar mass difference at one-loop. In a basis where sneutrino vevs are not zero, the diagrams with an insertion mixing between interaction state neutrinos and the down-type Higgsino contribute to the radiative correction of massless tree level eigenstates. In the basis where sneutrino vevs are zero this contribution is included in the trilinear vertex, $\lambda^{(\prime)}$.

Many papers [13, 21, 23, 31, 41] note the contribution of the loops driven by trilinear couplings $\lambda^{(\prime)}$ and produce expressions, often with flavour mixing suppressed, that agree with the expressions given here.

The contribution to the charged scalar loop from bilinear couplings is also widely noted. Whether a contribution is due to bilinear or trilinear couplings is a basis dependent statement [31]. We agree with the results in [13, 33, 39], however in our basis the diagrams in [33, 39] are accounted for in the trilinear loops.

The importance of the neutral scalar loop has also been noted previously. We

agree with the general result of [40,61] that a sneutrino mass difference will give rise to a radiative correction in the neutrino sector and with [13] that this loop can be the dominant contribution. The neutral scalar contribution is included in the analysis presented in [20], but is not discussed in [33].

The role of tadpole corrections is stressed in [20]. If we assume the solar mass difference arises from the loop corrected ‘massless’ neutrinos, we can see that the tadpoles do not play a role in determining its magnitude. In the interaction picture, there is no ν_α - ν_α -Higgs vertex, so the tadpole contributions vanish. Of course, the tadpoles will affect the other heavy neutral fermions.

A certain class of two-loop diagrams and resulting effects on bounds for lepton number violating couplings have been considered [62]

5.2 Numerical Results

In this section we present our numerical results for the neutrino masses. As we have already explained, in our most general analysis we use the MNS matrix defined by neutrino oscillations as an input. Of course this matrix is not accurately known, but its general ‘picture’ has been emerging during the last five or so years with angles and the 3σ allowed ranges of the neutrino oscillation parameters from a combined, global data, analysis [63], reading,

$$\sin^2 \theta_{12} = 0.24 - 0.40 , \quad \sin^2 \theta_{23} = 0.34 - 0.68 , \quad \sin^2 \theta_{13} \leq 0.046 , \quad (5.21)$$

$$\Delta m_{21}^2 = (7.1 - 8.9) \times 10^{-5} \text{ eV}^2 , \quad |\Delta m_{31}^2| = (1.4 - 3.3) \times 10^{-3} \text{ eV}^2 . \quad (5.22)$$

In our analysis we fix the neutrino mixing angles to reproduce the tri-bimaximal mixing scenario of Ref. [64] ,

$$\sin^2 \theta_{12} = \frac{1}{3}, \quad \sin^2 \theta_{23} = \frac{1}{2}, \quad \sin^2 \theta_{13} = 0, \quad (5.23)$$

in agreement with (5.21); the resulting predictions for neutrino mass squared differences are then compared with (5.22), to see whether the values chosen for the input parameters give results in agreement with current experimental limits. At present, there is no experimental evidence for CP-violation in the leptonic sector; as such, although our analysis is general enough to accommodate these effects, in what follows, we shall assume that they are negligible.

In addition to the experimental inputs for the quark and lepton fermion masses and mixings, soft supersymmetry breaking masses and couplings must also be initialised. We follow the benchmark SPS1a [65] where

$$M_0 = 100 \text{ GeV}, \quad M_{1/2} = 250 \text{ GeV}, \quad A_0 = -100 \text{ GeV}, \quad \tan \beta = 10, \quad \mu_0 > 0, \quad (5.24)$$

and read the low energy SUSY breaking and superpotential parameters at low energies using the code of Ref. [66]. The input parameters of primary interest are those which violate lepton number. In the zero neutrino vev basis, these are,

$$\mu_i, \quad B_i, \quad \lambda_{ijk}, \quad \lambda'_{ijk}, \quad h_{ijk}, \quad h'_{ijk}, \quad (5.25)$$

where the last two, h and h' are the trilinear lepton number violating parameters in the supersymmetry breaking part of the Lagrangian. Apart from these latter parameters, which concern trilinear couplings of scalar particles, all others can be used to set the atmospheric neutrino mass² difference or the solar mass² difference. There are two main cases:

- Tree level dominance : the atmospheric mass² difference originates from tree level contributions to neutrino masses (Fig. 5.1).

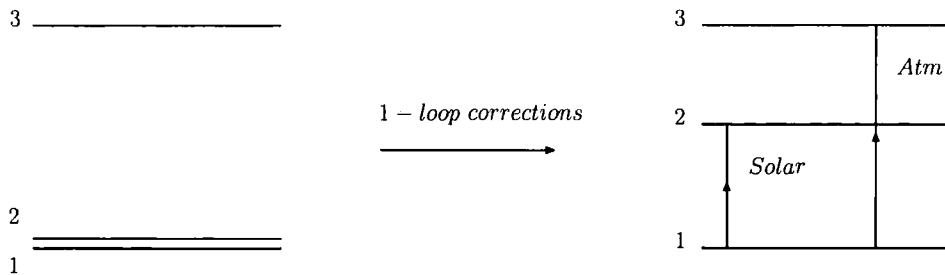


Figure 5.1: *Neutrino mass scales : tree level dominance*

- Loop level dominance : The atmospheric mass² difference originates from one-loop contributions to neutrino masses (Fig. 5.2).

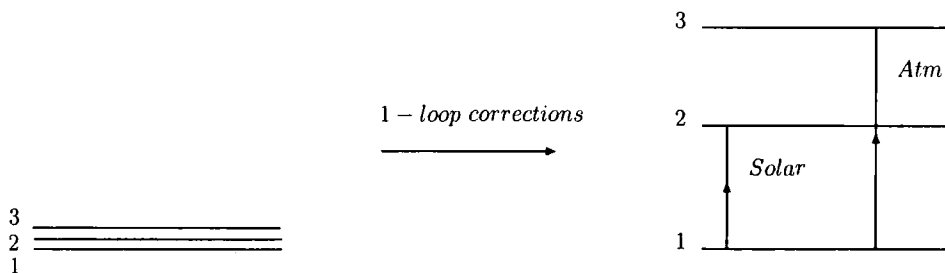


Figure 5.2: *Neutrino mass scales : loop-level dominance*

In either case, the solar mass² difference originates from loop effects from the lepton number violating parameters in (5.25).

The correct neutrino mass hierarchy can be always generated by the proper choice of just two of the lepton number violating parameters from the list of (5.25) – one of which sets the scale of the atmospheric mass² difference, the second setting the solar mass² difference. Of course, in the most general case all parameters can contribute.

After choosing the lepton number violating (LNV) parameters, the method described in section 4.5 is then employed to determine the charged lepton Yukawa matrix. In general it needs to be non-diagonal, in order to reproduce correct masses of both neutral and charged leptons and the U_{MNS} mixing matrix. The non-diagonal Yukawa matrix (thus also non-diagonal charged lepton mass matrix), may easily give rise to effects which are already subject to strong experimental bounds; tree level lepton flavour processes, such as $\mu \rightarrow e\gamma$ or $\mu \rightarrow eee$, are not suppressed and loop corrections to the electron mass will have contributions proportional to the tau mass. To avoid such problems, the specific cases considered in the next sections are those for which the large mixing in the lepton sector, as seen in the MNS matrix, has its origin purely in the neutral sector, and the charged lepton Yukawa couplings remain flavour-diagonal. The formalism we have described thus far allows the correct masses and mixing of charged leptons to be initialised. However, this will lead, in general, to an off-diagonal lepton Yukawa matrix. These, less natural, initial parameters are not necessarily ruled out and within the framework set out above, it is entirely possible to perform the calculations as described. However, we now prefer to consider a set of parameters for which we do not rely on cancellations in the charged lepton sector to make the model phenomenologically viable. The simplest way in which this can be achieved, is to find LNV parameters for which lepton Yukawas are diagonal.

From Eq. (4.36), for the case where the lepton Yukawa is diagonal and therefore \mathcal{Z}_l is the unit matrix, we see that

$$\mathcal{Z}_\nu = U_{MNS}^\dagger, \quad (5.26)$$

up to higher order terms. Using the MNS matrix as an input, it is possible to see which ratios of entries in the mass matrix give rise to the correct leptonic mixing,

being,

$$m_\nu^{\text{eff}} = \mathcal{Z}_\nu^* \text{diag}(m_1, m_2, m_3) \mathcal{Z}_\nu^\dagger = m_k U_{MNS ki} U_{MNS kj}. \quad (5.27)$$

For example, to set the atmospheric scale at tree level, we can see from Eq. (4.19) that as long as the hierarchy of μ_i matches the ratios of any of the rows in the MNS matrix, the mass matrix follow the correct pattern to be consistent with the observed mixing matrix. If a second mass scale is set up using the pattern dictated by one of the other rows of the MNS matrix, the full MNS matrix will be produced upon diagonalisation.

It is worth noting the nontrivial fact that such an approach, i.e. generating correct structure of neutrino masses and mixings, while keeping FCNC processes in charged lepton sector suppressed, is at all possible.

5.2.1 Tree level dominance scenario

At tree level, the mass of a neutrino can be set using μ_i parameters (4.20). The top left panel in Fig. 5.3 shows how the value of $(\Delta m_{\text{ATM}}^2)$ varies with μ_1 only, setting $\mu_{2,3} = 0$. The grey (or red in color) line is the result given by diagonalising the full neutralino matrix in (4.13) and the dark (blue in color) line is given by (4.20). They agree perfectly in Fig. 5.3a and thus only one line is shown. The shaded band shows the current 3σ limits. From Eq. (4.20) it can be seen, however, that it is $|\mu_1|^2 + |\mu_2|^2 + |\mu_3|^2$ which sets the mass of the tree level neutrino and as such it is straightforward to set any hierarchy between the μ_i and still maintain the same value for the atmospheric difference. To correctly reproduce the MNS matrix, we choose

as an input a very simple hierarchy between the μ_i parameters,

$$\text{Hierarchy (A) : } \quad \mu_1 = \frac{\mu_2}{\sqrt{2}} = \frac{\mu_3}{\sqrt{3}}. \quad (5.28)$$

The scale of all three μ_i is set such that a tree level neutrino of the correct mass is generated which result in the observed atmospheric mass difference, being,

$$\mu_1 = 1.47 \text{ MeV} , \quad \mu_2 = \sqrt{2} \times 1.47 \text{ MeV} , \quad \mu_3 = \sqrt{3} \times 1.47 \text{ MeV} . \quad (5.29)$$

At tree level, this choice of hierarchy gives rise to the MNS matrix, up to the $SU(2)$ rotation described earlier, being driven solely by the neutral sector; the charged lepton mass matrix is diagonal, and as such we have chosen a set of parameters within this basis which avoids the possible phenomenological problems.

A further, single lepton number violating parameter can then be chosen to set the scale of the solar mass² difference. The question of the arbitrariness of the tree level neutrino basis is complicated by the requirement that once the loop corrected mass matrix is diagonalised, Z_l being the unit matrix is consistent with the experimentally observed MNS matrix. As only one further lepton number violating coupling is initiated, the ratios in which the loop effects are distributed in the loop corrected mass matrix are approximately determined by the tree level mixing matrix. As such we can determine an approximate expression for the extra contribution to the full rotation matrix from re-diagonalising the loop effects. The further condition that the full rotation must reproduce the MNS matrix allows us to fix the tree level basis.

The three further Figs. 5.3(b,c,d) show the range of possible parameters in this scenario. In each of these plots, the set of μ_i are given the values (5.29) and another, single lepton number violating coupling is varied. In each case, the gray (or red) line shows the full result and the dark (blue) line is the result predicted by the approx-

imate solutions. The fact that λ_{133} and λ'_{133} give the correct solar mass difference over a similar range of parameters is a numerical coincidence. For this example, the factors from the different fermion masses in the quark loop, colour counting and scalar mixing cancel each other.

The contribution of the neutral scalar loop discussed in section 5.1, results from cancellations between the CP-even and the CP-odd diagrams and may includes contributions of approximately the same order. As such, the approximation presented earlier in the text, Eq. (5.6), does not agree well with the full result. The discrepancy between the full result and the approximate result reflects the fact that various contributions arise from different places in the full calculation (e.g. the effect on the mixing matrices, the effect on the sneutrino masses). The approximate result plotted in Fig. 5.3b is given by

$$\begin{aligned}
\Sigma_{Npp}^D \simeq & - \sum_{r=1}^7 \sum_{i,j=1}^3 \frac{m_{\kappa_r^0} \mathcal{Z}_{\nu ip}^2}{4(4\pi)^2} \left[\frac{e}{c_W} \mathcal{Z}_{N 1r} - \frac{e}{s_W} \mathcal{Z}_{N 2r} \right]^2 \left(\left[\frac{\Delta m_{\tilde{\nu}i}^2}{(m_{\tilde{\nu}i}^2 - m_{\kappa_r^0}^2)} - \frac{m_{\kappa_r^0}^2 \Delta m_{\tilde{\nu}i}^2}{(m_{\tilde{\nu}i}^2 - m_{\kappa_r^0}^2)^2} \ln \frac{m_{\kappa_r^0}^2}{m_{\tilde{\nu}i}^2} \right] \delta_{ij} \right. \\
& + \left[\frac{B_i^2 \sin^2(\beta - \alpha)}{\cos^2 \beta (M_H^2 - M_i^2)^2} + \frac{B_i^2 \cos^2(\beta - \alpha)}{\cos^2 \beta (M_h^2 - M_i^2)^2} - \frac{B_i^2 \cos^2 \beta}{(M_A^2 - M_i^2)^2} \right] \delta_{ij} \frac{M_i^2 \ln M_i^2 - m_{\kappa_r^0}^2 \ln m_{\kappa_r^0}^2}{M_i^2 - m_{\kappa_r^0}^2} \\
& + \left[\frac{B_i B_j \cos^2(\beta - \alpha)}{\cos^2 \beta (M_i^2 - M_h^2)(M_j^2 - M_h^2)} \right] \frac{M_h^2 \ln M_h^2 - m_{\kappa_r^0}^2 \ln m_{\kappa_r^0}^2}{M_h^2 - m_{\kappa_r^0}^2} \\
& + \left[\frac{B_i B_j \sin(\beta - \alpha)}{\cos^2 \beta (M_i^2 - M_H^2)(M_j^2 - M_H^2)} \right] \frac{M_H^2 \ln M_H^2 - m_{\kappa_r^0}^2 \ln m_{\kappa_r^0}^2}{M_H^2 - m_{\kappa_r^0}^2} \\
& - \left. \left[\frac{B_i B_j}{\cos^2 \beta (M_i^2 - M_A^2)(M_j^2 - M_A^2)} \right] \frac{M_A^2 \ln M_A^2 - m_{\kappa_r^0}^2 \ln m_{\kappa_r^0}^2}{M_A^2 - m_{\kappa_r^0}^2} \right). \tag{5.30}
\end{aligned}$$

The approximate result for the charged scalar loop, given by Eq. (5.17) agrees well with the full result (Fig. 5.3c). However, as $\lambda_{133} = -\lambda_{313}$, there are other diagrams which contribute to the full result which are not included in the approximation. The approximate expression captures the important effect. The agreement between the

full result and the approximate result, given by Eq. (5.20) when varying λ'_{133} (see Fig 5.3d) is very good, as the diagram highlighted in the text is the only diagram which contributes.

5.2.2 Loop level dominance scenario

It is possible for both the solar and the atmospheric scales to be set by loop corrections. This happens if the bilinear parameters μ_i are small enough. In this section we analyse this case setting strictly $\mu_1 = \mu_2 = \mu_3 = 0$, so that the one-loop corrections to the full 3×3 neutrino mass matrix are finite. Otherwise a more involved renormalisation scheme has to be implemented.

Again, we would like to set the Lagrangian parameters such that one can generate the correct structure of the MNS matrix while keeping the charged Yukawa couplings flavour-diagonal. This can be achieved if the neutrino mass hierarchy is governed by the trilinear λ and λ' couplings. For the diagrams dominated by trilinear couplings the flavour of the external legs of the loop can be “swapped independently” of the flavour of the particles in the loop, just changing the appropriate indices of the λ, λ' matrices in the loop vertices. Setting the λ and λ' entries which control the couplings of the external legs in certain hierarchies, one can ensure that also the ratios of the various entries in the one-loop corrected neutrino mass matrix are such that they give rise to the correct U_{MNS} rotation matrix.

The possible hierarchies are given by the rows of the MNS matrix and are, with

a generic coupling $\lambda_{ijj}^{(\prime)}$ as follows³,

$$\text{Hierarchy (B) :} \quad \lambda'_{1jj} = \frac{\lambda'_{2jj}}{\sqrt{2}} = \frac{\lambda'_{3jj}}{\sqrt{3}} \quad (5.31)$$

$$\text{Hierarchy (C) :} \quad \lambda'_{1jj} = \frac{\lambda'_{2jj}}{\sqrt{2}} = -\frac{\lambda'_{3jj}}{\sqrt{3}} \quad (5.32)$$

$$\text{Hierarchy (D) :} \quad \lambda_{1jj} = -\sqrt{2}\lambda_{2jj} \quad , \quad \lambda_{3jj} = 0 . \quad (5.33)$$

Due to the antisymmetry of the first two indices of λ it can only be chosen to follow hierarchy (D) described above.

As the nature of the loop corrections due to B_i means that the external legs cannot be swapped without affecting the flavour structure inside the loop, it is difficult to fix a hierarchy of B_i in the Lagrangian which will automatically give rise to the correct ratios in the one-loop corrected mass matrix.

We consider first, the case where the atmospheric mass² difference is set by λ_{i33} in hierarchy (D). The range of values for which the correct atmospheric mass difference is given is plotted in Fig. 5.4a. Note that although we plot on the x-axis λ_{133} , the coupling λ_{233} is also varying to keep the hierarchy (D) fixed. The fact that both λ_{133} and λ_{233} contribute is the reason the value of the coupling is only a little greater than the value of λ_{133} which correctly reproduces the solar mass difference in the tree-level dominated scenario.

The further three panels [Fig. 5.4(b-d)] have a fixed set of λ_{i33} in hierarchy (D) giving the atmospheric difference. Being,

$$\lambda_{133} = 6.7 \times 10^{-5} \quad , \quad \lambda_{233} = -\frac{6.7 \times 10^{-5}}{\sqrt{2}} \quad , \quad \lambda_{333} = 0 . \quad (5.34)$$

³Couplings with $\lambda_{ijk}^{(\prime)}$, with $j \neq k$ have only negligible contributions to neutrino masses and excluded from our hierarchy list.

$\lambda_{333} = 0$ due to the antisymmetry between the first two indices, fitting hierarchy (D). In addition to this, Fig. 5.4b varies $\lambda'_{111,211,311}$ in hierarchy (B) giving the solar mass² difference. Again, we plot the solar mass² difference against the value of λ'_{111} , however $\lambda'_{211,311}$ are being varied at the same time. The two remaining panels take in turn different sets of three λ' couplings, λ'_{i22} and λ'_{i33} . The final two indices determine which particle is produced in the loop. As such, with a lighter particle in the loop, the couplings must be greater to compensate. We see that, in moving from one panel to the next Fig. 5.4(b→ d), to produce the same mass difference, a smaller value of the coupling is required with a heavier particle in the loop. With the down quark in the loop (Fig. 5.4b) the value needed for the coupling may result in large contributions to the neutrinoless double beta decay rate as it is already approaching the excluded regime [67].

Finally, Fig. 5.5a, we show how the atmospheric mass² difference can be set by the three λ'_{i33} couplings in hierarchy (B), plotting the result for the atmospheric mass² difference against λ'_{133} . Next, we set λ'_{i33} to take the following values

$$\lambda'_{133} = 3.25 \times 10^{-5}, \quad \lambda'_{233} = \sqrt{2} \times 3.25 \times 10^{-5}, \quad \lambda'_{333} = \sqrt{3} \times 3.25 \times 10^{-5}. \quad (5.35)$$

The remaining three plots, Fig. 5.5(b,c,d), show the change in solar mass² difference, as sets of either $\lambda'_{i11,i22}$ in hierarchy (C) or the set λ_{i33} in hierarchy (D) are varied.

5.3 Summary

An increasingly accurate picture of the neutrino sector, with masses much smaller than the charged leptons and a distinctive mixing matrix in the W -vertex, is being

discerned by current experiments. We note that there are three preferred \mathcal{Z}_N symmetries in the supersymmetric extension of the Standard Model with minimal particle content. Imposing a \mathcal{Z}_2 symmetry results in the widely studied R-parity conserving MSSM, however another preferred symmetry, \mathcal{Z}_3 , gives rise to a Lagrangian which explicitly violates lepton number. These interactions lead to neutrino masses, both through a ‘see-saw’ type suppression at tree level and through radiative corrections. We have considered the most general scenario in this model; no assumptions have been made concerning CP-violation or intergenerational mixing, for example.

In the basis set out in Chapter 3, we find that a non-zero neutrino mass will arise at tree level unless all μ_i are zero and analyse in detail, the further contributions to masses that come from loop corrections. We show that the magnitude of the contributions due to neutral fermion loops, examined in section 5.1.3 are determined by the size of the bilinear supersymmetry breaking parameter, B_i ; that loops with charged fermions, described in section 5.1.4, have a contribution due to trilinear lepton number violating couplings in the superpotential, λ_{ijk} ; and that quark loops, section 5.1.5, are determined by the trilinear lepton number violating coupling λ'_{ijk} . Each of these contributions can be dominant. In sections 5.1.6 and 5.1.7, we consider the gauge loops and why they do not give large contributions to neutrinos which are massless at tree level. We derive expressions for the full calculation, which form the basis of our numerical analysis. We also present approximate expressions in each section, which are simple, compact formulas encoding the important information pertaining to each diagram. In our presentation of the results, as seen in Figs. 5.3,5.4,5.5 these simple expressions are shown to be in good agreement with the full result.

The lepton sector in the \mathbb{Z}_3 -MSSM is much more involved than the lepton number conserving MSSM. Mixing between leptons, gauginos and higgsinos ensures the question of initialising Lagrangian parameters must be carefully considered. A framework has been constructed in section 4 to correctly reproduce the charged lepton masses and MNS matrix for any set of lepton number violating couplings.

In constructing the framework in which to perform the calculation it is clear that there will be, in general, large intergenerational mixing in the lepton Yukawa matrix, this allows the possibility of unsuppressed tree level flavour violating processes, already subjected to strong bounds. To circumvent this problem we considered sets of Lagrangian parameters for which the MNS matrix has its origin solely in the neutral sector, the lepton Yukawa matrix being diagonal. The three rows of the MNS matrix correspond to three sets of ratios between entries in the loop corrected mass matrix which will give the correct MNS angles. It is possible to set these ratios by setting hierarchies in the couplings between generations. With the condition that it must be possible to change the flavour of the external legs of the diagram without affecting the flavour structure of the loop, there is some freedom in choosing which group of Lagrangian parameters we set in each hierarchy.

Lepton number conserving parameters were fixed to be the SPS1a benchmark point, and we have investigated the effect of varying the lepton number violating couplings, as seen in Figs. 5.3,5.4,5.5. We have shown that values for lepton number violating couplings exist, which give the correct atmospheric and solar mass² difference, charged lepton masses and mixing, which are not already excluded by existing studies of low energy bounds. There are two distinct scenarios that achieve this: the tree level dominance scenario, in which the atmospheric scale is set at tree

level and the solar scale set by radiative effects, and another, the loop level dominance scenario, in which both the atmospheric and solar scales are set by radiative corrections.

In the tree level dominance scenario, we choose the μ_i parameters to be of the order of 1 MeV, such that the correct result for the atmospheric mass² difference is obtained. They are chosen to obey a certain hierarchy, which ensures the mixing matrix is consistent with observed MNS.

In addition to this, a further, single lepton number violating coupling can set the scale of the solar mass² difference by determining the contribution of the appropriate loop diagram. It is possible to generate loop diagrams of the appropriate scale, by including either a non-zero λ, λ' or B coupling. We find that the correct solar scale can then be set by any of

$$\begin{aligned}
 B_1 &\sim 0.21 \text{ GeV}^2 \sim \left[300 \mu_1 \right]^2, \\
 \lambda_{133} &\sim 3.4 \times 10^{-5} \sim y_e, \\
 \lambda'_{133} &\sim 3.2 \times 10^{-5} \sim 0.1 y_d,
 \end{aligned}
 \tag{5.36}$$

where $y_{e,d}$ is the Yukawa coupling of either the electron or the down quark, presented here merely for the sake of comparison.

In the second case, the correct masses and mixing for both charged and neutral fermions can be achieved without a massive neutrino at tree level. The solar and atmospheric mass² differences both arise from radiative corrections at one-loop, using loop contributions whose value is determined by sets of λ or λ' couplings in given hierarchies, such that the observed MNS is generated. Firstly, we show that we can set the atmospheric scale with a set of λ couplings of the order of the electron Yukawa

coupling, then find the solar scale is correctly set by λ' couplings of the order of the down quark Yukawa coupling.

Alternatively, the atmospheric scale can be set by λ' couplings,

$$\lambda'_{133} = \frac{\lambda'_{233}}{\sqrt{2}} = \frac{\lambda'_{333}}{\sqrt{3}} = 3.25 \times 10^{-5} \sim 0.1y_d, \quad (5.37)$$

and the solar mass² difference can be generated by another set of λ' couplings,

$$\lambda'_{122} = \frac{\lambda'_{222}}{\sqrt{2}} = -\frac{\lambda'_{322}}{\sqrt{3}} \sim 6.5 \times 10^{-4} \sim 2y_d, \quad (5.38)$$

or a set of λ couplings of the order of the electron Yukawa.

The study of neutrino masses provides the basis for further work concerning lepton number violating phenomena. The ranges of values for lepton number violating parameters required to produce the correct masses and mixing, will be reflected in processes such as tree level lepton flavour violating decays and will have repercussions concerning rare events such as neutrinoless double beta decay and measurements of electric and magnetic dipole moments. In fact, it has been shown in [68] that contributions to the electric dipole moments of the electron and neutron from trilinear R-parity violating superpotential terms only contribute at the two-loop level; however, for Majorana particles they will give rise to one-loop effects leading to constraints on R-parity violating parameters by neutrino electric and magnetic dipole moment bounds. Such correlations make a valuable link between collider experiments and upcoming neutrino experiments. In the next chapter, we examine a particular set of decays, the radiative flavour-violating charged lepton decays. If these decays are driven solely by the neutrino sector, the resulting branching ratio will be too small to measure, however in many extensions of the Standard Model, particularly supersymmetric extensions, decays of this type can become large. We investigate the

possibility that the type and magnitude of operators required to generate neutrino masses in the \mathbb{Z}_4 -MSSM will also generate observable decay rates for radiative lepton decays.

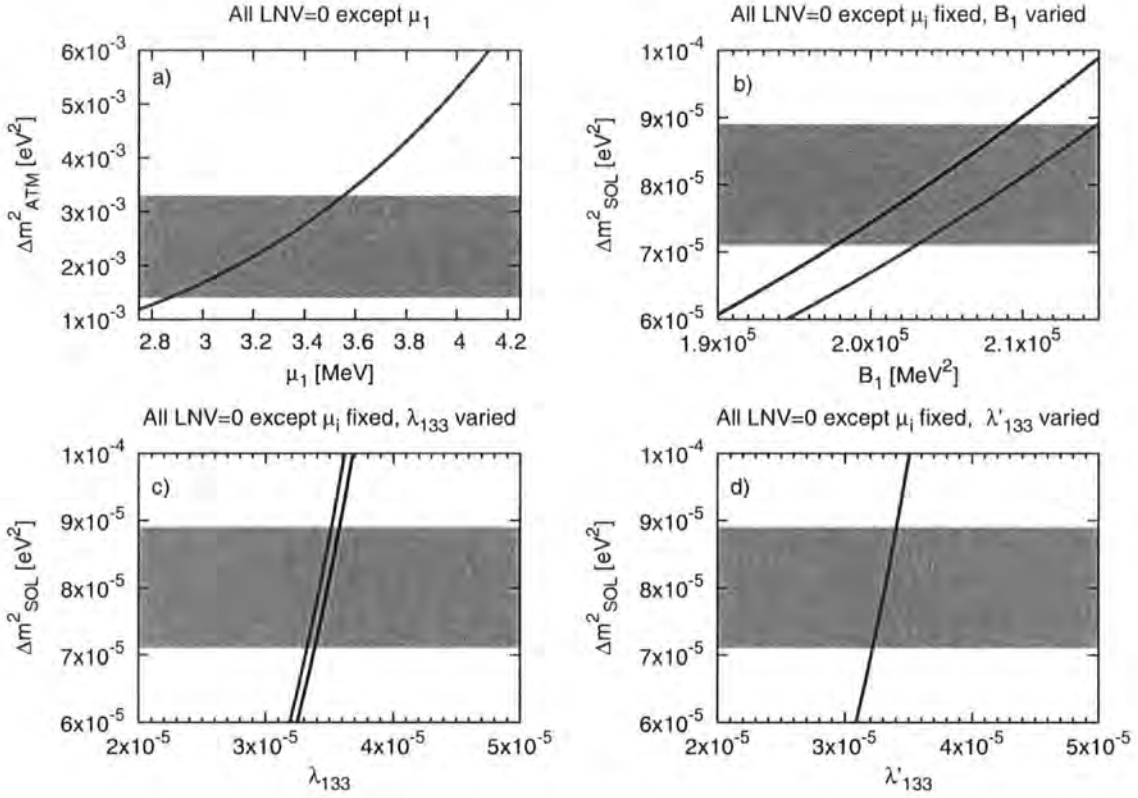


Figure 5.3: Predictions for atmospheric and solar neutrino mass² differences (Δm^2_{ATM}) and (Δm^2_{SOL}) for the tree level dominance scenario vs. variations of Lepton Number Violating (LNV) parameters as displayed in figure titles. The 3σ gray (green) band consistent with experiment is displayed for comparison, as well as the full (gray or red curve) and approximate (dark or blue curve) results. a) Only μ_1 is varied. For all other figures, μ_i is fixed as in hierarchy (A) as explained in the text and b) B_1 , or c) λ_{133} , or d) λ'_{133} , is varied respectively.

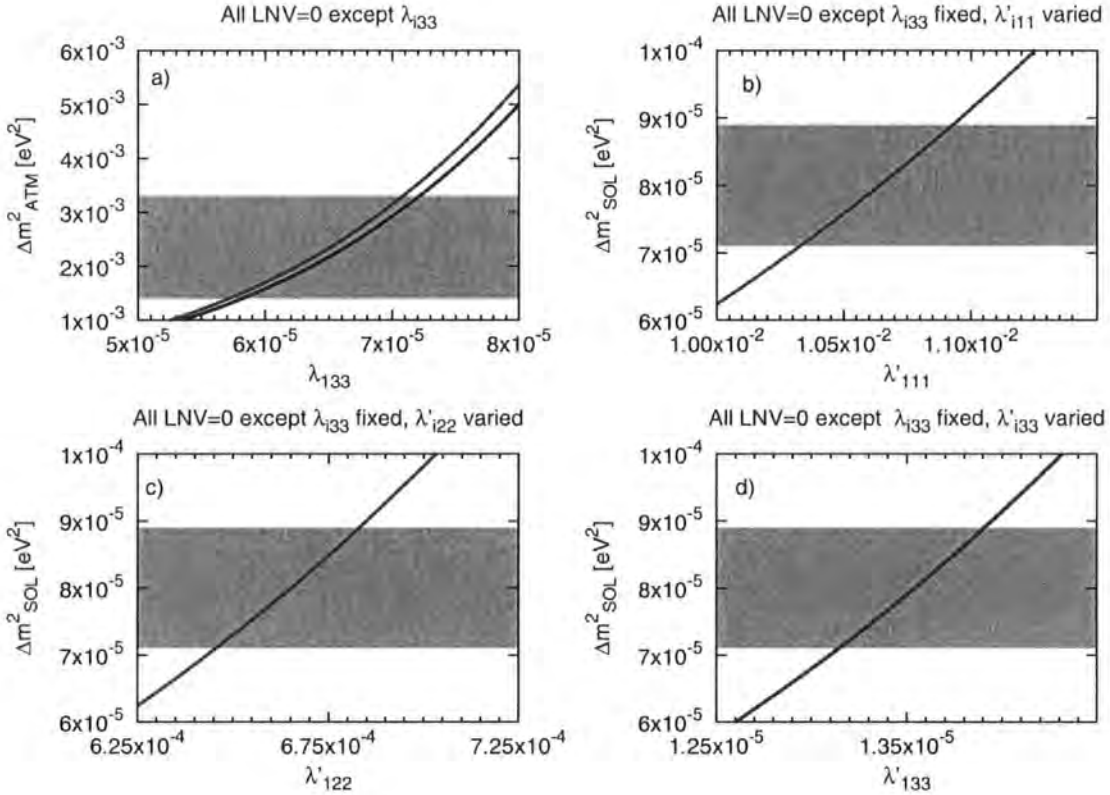


Figure 5.4: Same as in Fig. 3 but for the loop-level dominance scenario. All LNV parameters are zero apart from a) λ_{i33} that is varied in hierarchy (D). For all other figures, λ_{i33} is fixed to a value (see the text) consistent with the atmospheric mass² difference and b) only λ'_{i11} is varied in hierarchy (B) or c) only λ'_{i22} in hierarchy (B) or d) only λ'_{i33} in hierarchy (B) in order to accommodate the solar mass² difference.

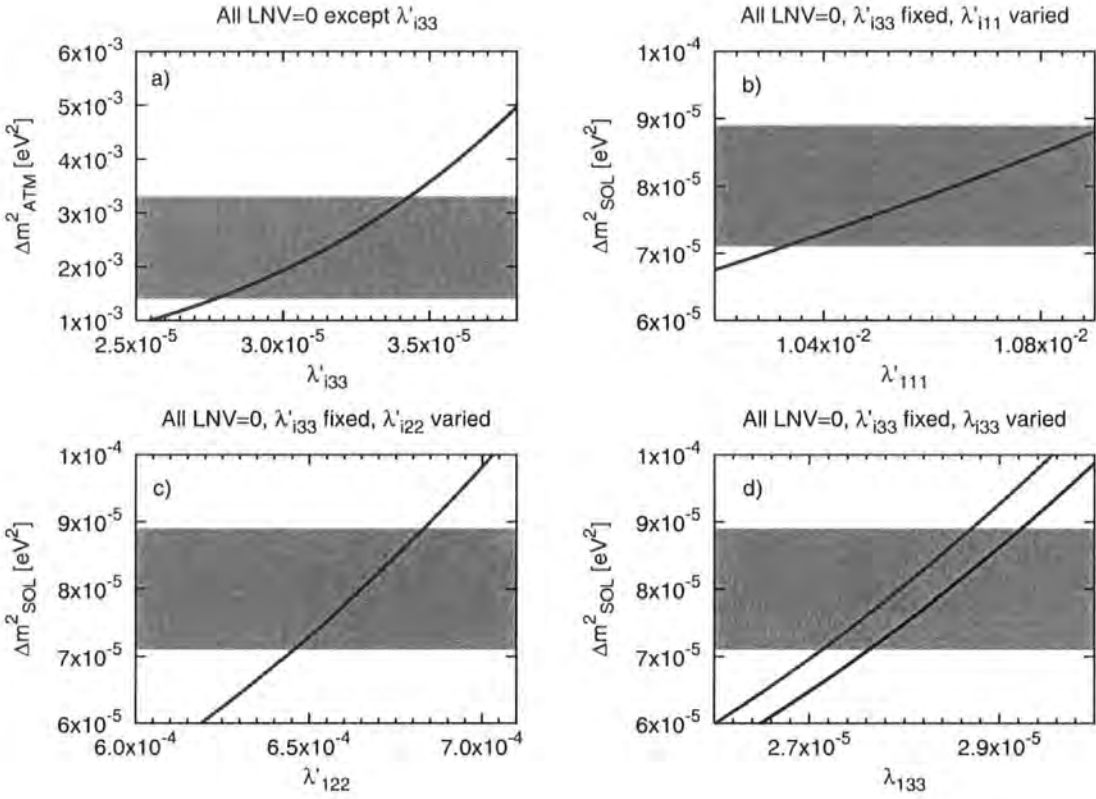


Figure 5.5: Same as in Fig. 3 but for the loop-level dominance scenario. All LNV parameters are zero apart from a) λ'_{i33} that is varied in hierarchy (B). For all other figures, λ'_{i33} is fixed to a value (see the text) consistent with the atmospheric mass² difference and b) only λ'_{i11} is varied in hierarchy (C) or c) only λ'_{i22} in hierarchy (C) or d) only λ_{i33} in hierarchy (D) in order to accommodate the solar mass² difference.



Chapter 6

The \mathbb{L} -MSSM at one loop: Radiative decays

Processes which do not conserve lepton flavour, the flavour oscillations in the neutrino sector, have been observed [69]. This is in contrast with the charged sector, where no such observation has been made. The decays $\tau \rightarrow \mu\gamma, e\gamma$ and $\mu \rightarrow e\gamma$ can be driven solely by the known lepton flavour violation in the neutral sector, the branching ratio will be small [70], however, well below current experimental limits, due to the magnitude of the neutrino mass. Noticing that in many extensions of the Standard Model this branching ratio increases greatly,¹ together with the fact

¹The effect of lepton flavour non-conservation from the charged slepton mass matrix in supersymmetric extensions of the Standard Model where a seesaw mechanism results in light Majorana neutrinos is noted in Ref. [71], this work is extended in Ref [72], where bounds for off-diagonal terms are calculated. In Ref. [73] the results for this model are correlated with neutrino masses and the $(g_\mu - 2)$ data and in Ref. [74] the possibility of discriminating between different supersymmetric seesaw models is investigated. A bottom-up approach is considered in Ref. [75], resulting in predictions for the $\mu \rightarrow e\gamma$ branching ratio. Methods for discerning models with heavy right

that experimental bounds for these decays will soon be improved by several orders of magnitude, suggests that these decays are a valuable place to scrutinise the Standard Model and test theories which extend it.

In the previous chapter, it has been shown that the current experimental values of neutrino mass squared differences and mixing can be accommodated within the model, being determined by the value of lepton number violating couplings in either the superpotential, or the supersymmetry breaking terms of the Lagrangian.

Crucially, the operators which give rise to neutrino masses in this model may also give rise to lepton flavour violation in the charged sector. In this chapter, based on [77], we shall consider combinations of lepton number violating parameters that correctly reproduce the observations made in oscillation experiments. For these sets of parameters we shall investigate whether they would result in branching ratios of rare leptonic decays which would already have been observed, or would be observed by forthcoming experimental studies. If the rare leptonic decays are not observed, the improving bound will be valuable in precluding certain scenarios. We select scenarios in which the off-diagonal terms in the supersymmetry breaking scalar mass matrices are zero. It is possible, of course, even in the R-parity conserving MSSM, that this is not the case and that these terms will lead to large branching ratios for lepton flavour violating decays [72]. The aim of this study is to examine, specifically, the effects of lepton number violating terms in the Lagrangian and the interplay between the charged and neutral sector. As such, we will examine the scenarios which are only handed neutrinos from R-parity violating models using a number of decays are studied in Ref. [76]. Renormalisation group effects due to R-parity violating couplings and their effect on the $\mu \rightarrow e\gamma$ branching ratio are considered in Ref. [41].

present in the \mathcal{U} -MSSM and will not examine phenomena which have their origin in the R-parity conserving part of the Lagrangian.

6.1 Experimental Results, Bounds and Prospects

The results from oscillation experiments combine to describe the mass squared differences and mixing angles of the neutrino sector increasing accurately. The current² 3σ allowed ranges are [69]

$$\sin^2 \theta_{12} = 0.24 - 0.40, \quad \sin^2 \theta_{23} = 0.34 - 0.68, \quad \sin^2 \theta_{13} \leq 0.041, \quad (6.1)$$

$$\Delta m_{21}^2 = (7.1 - 8.9) \times 10^{-5} \text{ eV}^2, \quad |\Delta m_{31}^2| = (1.9 - 3.2) \times 10^{-3} \text{ eV}^2. \quad (6.2)$$

In our analysis we choose Lagrangian parameters such that the neutrino mixing angles match the tri-bimaximal mixing scenario of Ref. [64],

$$\sin^2 \theta_{12} = \frac{1}{3}, \quad \sin^2 \theta_{23} = \frac{1}{2}, \quad \sin^2 \theta_{13} = 0. \quad (6.3)$$

The following bounds have been set on the branching ratios of $\mu \rightarrow e\gamma$ [78], $\tau \rightarrow \mu\gamma$ [79] and $\tau \rightarrow e\gamma$ [80].

$$\text{Br}(\mu \rightarrow e\gamma) < 1.2 \times 10^{-11} \quad \text{at 90\% CL} \quad (6.4)$$

$$\text{Br}(\tau \rightarrow \mu\gamma) < 6.8 \times 10^{-8} \quad \text{at 90\% CL} \quad (6.5)$$

$$\text{Br}(\tau \rightarrow e\gamma) < 1.1 \times 10^{-7} \quad \text{at 90\% CL} \quad (6.6)$$

²During the completion of this final chapter, the updated results of [69] were published. As such, the ranges for neutrino masses and angles differ from the results quoted in (5.21,5.22)

Future experiments will probe these decays further. It is suggested [81–83] that the sensitivity to $\mu \rightarrow e\gamma$ will be improved to $\sim 10^{-13,-14}$, and that the sensitivities to $\tau \rightarrow \mu\gamma$ and $\tau \rightarrow e\gamma$ will reach $\sim 10^{-8,-9}$. To conclude, we present the current experimental values for the branching ratios of $\tau \rightarrow \mu\nu_\tau\bar{\nu}_\mu$, $\tau \rightarrow e\nu_\tau\bar{\nu}_e$ and $\mu \rightarrow e\nu_\mu\bar{\nu}_e$ [1],

$$\text{Br}(\tau \rightarrow \mu\nu_\tau\bar{\nu}_\mu) = 0.1736 \pm 0.0005 \quad (6.7)$$

$$\text{Br}(\tau \rightarrow e\nu_\tau\bar{\nu}_e) = 0.1784 \pm 0.0005 \quad (6.8)$$

$$\text{Br}(\mu \rightarrow e\nu_\mu\bar{\nu}_e) \approx 1 \quad (6.9)$$

6.2 Generic Diagrams for $l_i \rightarrow l_j\gamma$

At the level of one loop, three basic types of diagram contribute to the decay $l_i \rightarrow l_j\gamma$ and in each case, there is a fermion - boson loop. Details of this calculation are presented in Appendix G. The external photon can be attached either to the fermion in the loop, the boson in the loop or the external leg (Fig. 6.1). The calculation, as shown in Fig. 6.1, was performed in Weyl notation. In this notation, the four-component spinor $e \equiv \begin{pmatrix} e_L \\ \bar{e}_R \end{pmatrix}$, where e_L and e_R are two-component left-handed spinors and the four-component spinor, $f \equiv \begin{pmatrix} \psi \\ \bar{\eta} \end{pmatrix}$ denotes a generic fermion. The factors associated with the vertices are denoted by either A_{iks} or B_{iks} as shown in the diagrams, the charges of the particles are given by $Q_{\psi,\varphi}$ (for example $Q_{e_L} = e$), the masses of the particles in the loop are $m_{\psi,\varphi}$ and the masses of the charged leptons on the external legs are given by $m_{i,j}$. For more information concerning calculations

using two-component spinors, see Ref. [58]. Taking all possible combinations of arrows and neglecting diagrams with gauge bosons³ it can be seen that, in agreement with Ref. [84, 85], at leading order the branching ratio is given by

$$\Gamma(l_i \rightarrow l_j \gamma) = \frac{48\pi^2}{G_F^2 m_i^2} \left[|\Lambda_L|^2 + |\Lambda_R|^2 \right] \Gamma(l_i \rightarrow l_j \nu_i \bar{\nu}_j), \quad (6.10)$$

where

$$\begin{aligned} \Lambda_R = & \frac{1}{(4\pi)^2} A_{iks} B_{jks} Q_{\psi_k} m_{\psi_k} \left[-\frac{m_{\psi_k}^2 - 3m_{\phi_s}^2}{4(m_{\psi_k}^2 - m_{\phi_s}^2)^2} + \frac{m_{\phi_s}^4}{(m_{\psi_k}^2 - m_{\phi_s}^2)^3} \ln \left[\frac{m_{\phi_s}}{m_{\psi_k}} \right] \right] \\ & + \frac{1}{2(4\pi)^2} A_{iks} B_{jks} Q_{\phi_s} m_{\psi_k} \left[-\frac{m_{\psi_k}^2 + m_{\phi_s}^2}{2(m_{\psi_k}^2 - m_{\phi_s}^2)^2} + \frac{2m_{\psi_k}^2 m_{\phi_s}^2}{(m_{\psi_k}^2 - m_{\phi_s}^2)^3} \ln \left[\frac{m_{\phi_s}}{m_{\psi_k}} \right] \right] \\ & - \frac{1}{2(4\pi)^2} B_{iks}^* B_{jks} Q_{\psi_k} m_i \left[-\frac{m_{\psi_k}^4 - 5m_{\psi_k}^2 m_{\phi_s}^2 - 2m_{\phi_s}^4}{12(m_{\psi_k}^2 - m_{\phi_s}^2)^3} + \frac{m_{\psi_k}^2 m_{\phi_s}^4}{(m_{\psi_k}^2 - m_{\phi_s}^2)^4} \ln \left[\frac{m_{\phi_s}}{m_{\psi_k}} \right] \right] \\ & - \frac{1}{2(4\pi)^2} B_{iks}^* B_{jks} Q_{\phi_s} m_i \left[\frac{m_{\phi_s}^4 - 5m_{\psi_k}^2 m_{\phi_s}^2 - 2m_{\psi_k}^4}{12(m_{\psi_k}^2 - m_{\phi_s}^2)^3} - \frac{m_{\phi_s}^2 m_{\psi_k}^4}{(m_{\psi_k}^2 - m_{\phi_s}^2)^4} \ln \left[\frac{m_{\phi_s}}{m_{\psi_k}} \right] \right] \end{aligned}$$

and

$$\begin{aligned} \Lambda_L = & \frac{1}{(4\pi)^2} A_{jks}^* B_{iks}^* Q_{\psi_k} m_{\psi_k} \left[-\frac{m_{\psi_k}^2 - 3m_{\phi_s}^2}{4(m_{\psi_k}^2 - m_{\phi_s}^2)^2} + \frac{m_{\phi_s}^4}{(m_{\psi_k}^2 - m_{\phi_s}^2)^3} \ln \left[\frac{m_{\phi_s}}{m_{\psi_k}} \right] \right] \\ & + \frac{1}{2(4\pi)^2} A_{jks}^* B_{iks}^* Q_{\phi_s} m_{\psi_k} \left[-\frac{m_{\psi_k}^2 + m_{\phi_s}^2}{2(m_{\psi_k}^2 - m_{\phi_s}^2)^2} + \frac{2m_{\psi_k}^2 m_{\phi_s}^2}{(m_{\psi_k}^2 - m_{\phi_s}^2)^3} \ln \left[\frac{m_{\phi_s}}{m_{\psi_k}} \right] \right] \\ & - \frac{1}{2(4\pi)^2} A_{jks}^* A_{iks} Q_{\psi_k} m_i \left[-\frac{m_{\psi_k}^4 - 5m_{\psi_k}^2 m_{\phi_s}^2 - 2m_{\phi_s}^4}{12(m_{\psi_k}^2 - m_{\phi_s}^2)^3} + \frac{m_{\psi_k}^2 m_{\phi_s}^4}{(m_{\psi_k}^2 - m_{\phi_s}^2)^4} \ln \left[\frac{m_{\phi_s}}{m_{\psi_k}} \right] \right] \\ & - \frac{1}{2(4\pi)^2} A_{jks}^* A_{iks} Q_{\phi_s} m_i \left[\frac{m_{\phi_s}^4 - 5m_{\psi_k}^2 m_{\phi_s}^2 - 2m_{\psi_k}^4}{12(m_{\psi_k}^2 - m_{\phi_s}^2)^3} - \frac{m_{\phi_s}^2 m_{\psi_k}^4}{(m_{\psi_k}^2 - m_{\phi_s}^2)^4} \ln \left[\frac{m_{\phi_s}}{m_{\psi_k}} \right] \right]. \end{aligned}$$

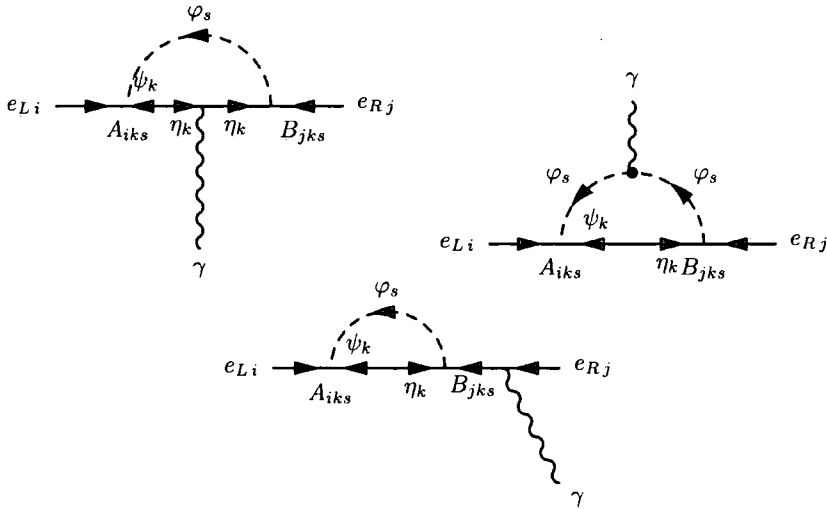


Figure 6.1: *The final state photon can be attached to either of the external fermions, the fermion in the loop, or the scalar in the loop. All combinations of helicities of fermions should be included in the calculation.*

The contribution from each Feynman diagram was expanded under the assumption $m_i^2, m_j^2 \ll m_\varphi^2, m_\psi^2$. On-shell conditions could then be applied and terms proportional to m_j were neglected. The resulting expression can then be re-arranged to be seen to contribute to effective operators of the form⁴

$$\mathcal{L}_{\text{eff}} \supset 2\Lambda_{Rij} e_{Rj} \sigma^{\mu\nu} e_{Li} F_{\mu\nu} + 2\Lambda_{Lij} \bar{e}_{Lj} \bar{\sigma}^{\mu\nu} \bar{e}_{Ri} F_{\mu\nu} . \quad (6.11)$$

Individually, diagrams produce terms contributing to different effective operators, but these cancel when all possible diagrams are considered. Following Ref. [84] and

³It can be seen that diagrams will be suppressed either by the magnitude of the neutrino mass or, in diagrams which contain lepton number violating operators, by the amount of mixing between the neutrinos/neutralinos and charged leptons/charginos.

⁴We define $\sigma^{\mu\nu} \equiv \frac{1}{4}(\sigma^\mu \bar{\sigma}^\nu - \sigma^\nu \bar{\sigma}^\mu)$ and $\bar{\sigma}^{\mu\nu} \equiv \frac{1}{4}(\bar{\sigma}^\mu \sigma^\nu - \bar{\sigma}^\nu \sigma^\mu)$

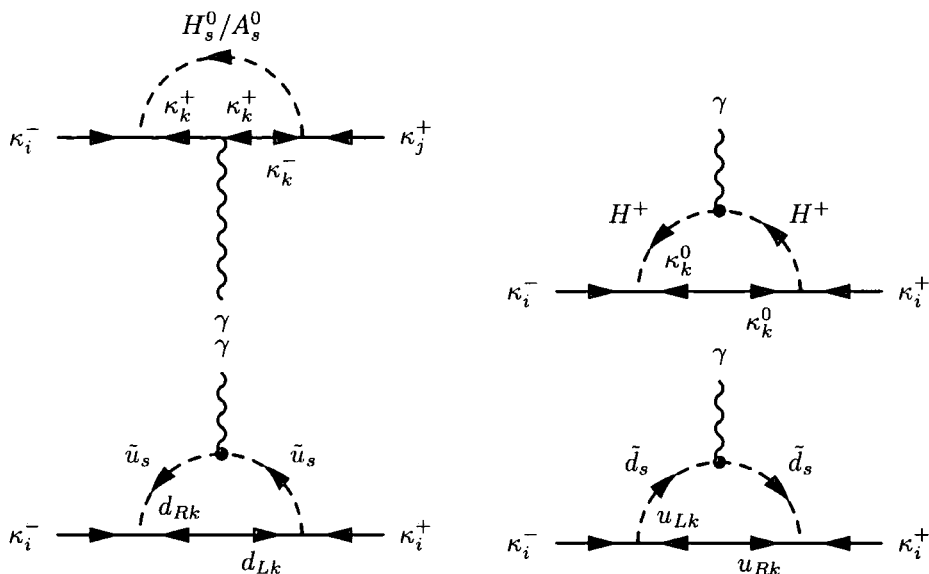


Figure 6.2: *The various possible combinations of particles which can be produced in the loop: chargino and neutral scalar; neutralino and charged scalar; down quark and up-type squark; up quark and down-type squark.*

inserting the experimental values given in Eqs. (6.7,6.8,6.9), it is then possible to move from this effective operator to a branching ratio for the rare decay, given by Eq. (6.10).

6.3 Specific Diagrams for $l_i \rightarrow l_j \gamma$

The following combinations of particles can be produced inside the loop: chargino and neutral scalar; neutralino and charged scalar; quark and squark, as shown in Fig. 6.2. In the \mathcal{U} -MSSM, mixing occurs between charged leptons/charginos and

between neutrinos/neutralinos. For example, there are five charged fermions,

$$\chi_i^\pm = \begin{pmatrix} \kappa_i^\pm \\ \bar{\kappa}_i^\mp \end{pmatrix}, \quad i = 1, \dots, 5,$$

where $i = 3, 4, 5$ are the charged leptons e , μ and τ . Similarly, there are seven neutral fermions,

$$\chi_i^0 = \begin{pmatrix} \kappa_i^0 \\ \bar{\kappa}_i^0 \end{pmatrix}, \quad i = 1, \dots, 7,$$

where $i = 5, 6, 7$ are the neutrinos. The two-component spinors comprising the quarks are denoted,

$$d_i = \begin{pmatrix} d_{L i} \\ \bar{d}_{R i} \end{pmatrix}, \quad i = 1, \dots, 3,$$

$$u_i = \begin{pmatrix} u_{L i} \\ \bar{u}_{R i} \end{pmatrix}, \quad i = 1, \dots, 3.$$

Each of the diagrams in Fig. 6.2 are in the same form as outlined in Sec. 6.2. The generic vertices A_{iks} and B_{jks} can be replaced by the appropriate Feynman rule, which are presented in the Appendix. The calculation is performed in the mass eigenbasis. The full mass matrices are diagonalised and the appropriate rotation matrices are calculated numerically and without approximation. In understanding the important physical contributions it is more useful, however, to present diagrams in the mass insertion approximation containing interaction state particles. The plots are based on a Fortran code which computes the full result.

We will consider the role played by combinations of lepton number violating parameters by, first, investigating the case in which the bilinear lepton number violating coupling in the superpotential correctly produces the atmospheric mass difference

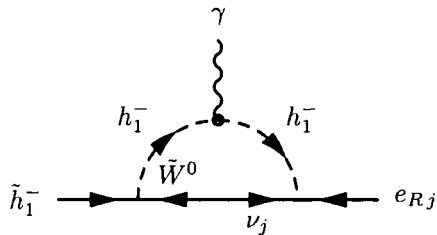


Figure 6.3: *Diagram contributing to $l \rightarrow l'\gamma$ with the only source of lepton number violating being the bilinear lepton number violating couplings in the superpotential, μ_i .*

(and the ratios between the three components ensure the mixing angles are reproduced correctly) and another, single, lepton number violating coupling sets the solar mass difference. Both sources of lepton number violation will then combine to produce a diagram which contributes to a lepton flavour violating decay. Second, we will consider the scenario in which both the scale of the atmospheric mass difference and the solar scale are set by radiative corrections, and the bilinear lepton number violating parameters are set to zero.

6.3.1 Atmospheric scale set by $\mu_{1,2,3}$

With only $\mu_{1,2,3} \neq 0$ and all other lepton number violating couplings set to zero the atmospheric mass squared difference can be correctly reproduced; the solar mass squared difference is not generated and no observable branching ratios for $l \rightarrow l'\gamma$ are generated. The non-zero $\mu_{1,2,3}$ do bring about a branching ratio for $l \rightarrow l'\gamma$, through the diagram shown in Fig. 6.3. The fermion inside the loop is a mixture of the heavy neutralinos and the interaction state neutrinos. The amount of mixing between these interaction states is dependent on $\mu_{1,2,3}$, and also determines the mass of the tree level

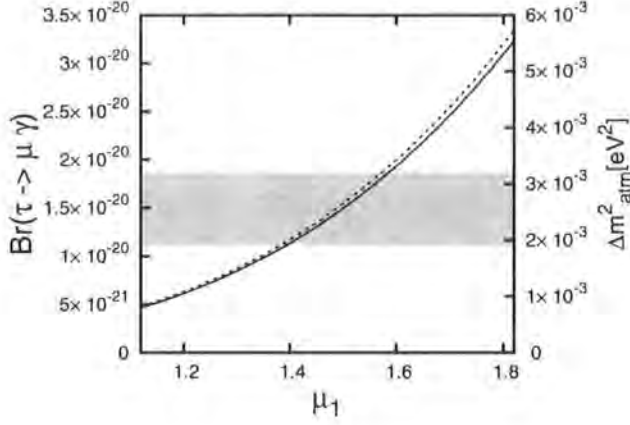


Figure 6.4: $\tau \rightarrow \mu\gamma$ and Δm_{atm}^2 against μ_1 - the dotted line (and right hand axis) show the magnitude of Δm_{atm}^2 with the light grey band indicating the current 3σ allowed range; the full line (and left hand axis) show the branching ratio of $\tau \rightarrow \mu\gamma$.

neutrino. The amount of mixing between the external leg interaction state charged higgsino and left handed charged leptons, is also determined by $\mu_{1,2,3}$. As such, this diagram contributes to the $l_i \rightarrow l_j\gamma$ decay with branching ratio approximately given by,

$$\Gamma(l_i \rightarrow l_j\gamma) \approx \frac{3}{(4\pi)^2} \frac{|\lambda_{0jj}|^2 e^2}{G_F^2 m_i^2 s_w^2} M_{\chi^0}^2 \left[\left(\frac{1}{M_{H^-}^2} \right) \left(\frac{\mu_0 \mu_i}{M_{\chi^\pm}^2} \right) \left(\frac{\mu_j g_2 v_u}{M_{\chi^0}^2} \right) \right]^2 \Gamma(l_i \rightarrow l_j \nu_i \bar{\nu}_j). \quad (6.12)$$

We will consider this scenario. The $\mu_{1,2,3}$ parameter takes the values

$$\mu_1 = \frac{\mu_2}{\sqrt{2}} = \frac{\mu_3}{\sqrt{3}} = 1.12 - 1.82 \text{MeV}, \quad (6.13)$$

where ratios between components of μ_i are chosen such that the mixing angles in the PMNS matrix are generated to take the tri-bimaximal form, which are in agreement with current bounds, and are entirely generated in the neutral sector. The overall

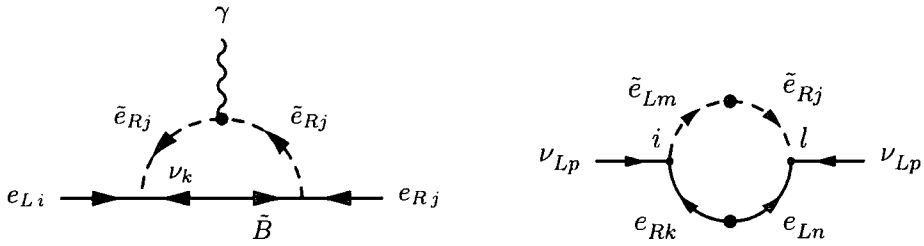


Figure 6.5: Feynman diagrams generated when, firstly, μ_i induces mixing of interaction state neutrinos with gauginos and higgsinos and secondly, $\lambda_{ijk} \neq 0$ generating neutrino masses radiatively.

scale is varied and the resulting mass squared difference and branching ratio for $\tau \rightarrow \mu\gamma$ are calculated and shown in Fig. 6.4. The light grey band (and right hand axis) shows the current 3σ allow region for the atmospheric mass squared difference as given by Eq. (6.2). All other lepton number violating couplings are set to zero, and R-parity conserving parameters are fixed to be the SPS1a benchmark point [65]. We note that, in agreement with Ref. [86], the branching ratios for $l_i \rightarrow l_j\gamma$ are well below current experimental limits, as given in Eq. (6.5), and show the resulting branching ratio for $\tau \rightarrow \mu\gamma$ in Fig. 6.4.

6.3.2 Atmospheric scale set by $\mu_{1,2,3}$ – Solar scale set by λ_{ikk}

For the remaining examples, the bilinear lepton number couplings take the values,

$$\mu_1 = \frac{\mu_2}{\sqrt{2}} = \frac{\mu_3}{\sqrt{3}} = 1.47\text{MeV} , \quad (6.14)$$

which reproduce correctly the atmospheric mass squared difference, as shown in Fig. 6.4. A single, further lepton number violating coupling $\lambda_{ikk}(= -\lambda_{kik})$ is then varied. The branching ratio for lepton flavour violating decays when this coupling

correctly generates the observed solar flavour oscillation are calculated numerically using a Fortran code.⁵ We find that there are scenarios of this form which correctly reproduce all neutrino data and give rise to branching ratios for $l \rightarrow l'\gamma$ which are, or will be, observable in experimental studies.

When $\mu_{1,2,3}, \lambda_{ikk} \neq 0$ then diagrams shown in Fig. 6.5 are generated. It can be seen that the amount of mixing on the fermion line inside the loop, again, corresponds directly to the amount of mixing between interaction state neutrinos and gauginos/higgsinos. It is this mixing which determines the mass of the neutrino produced at tree level and is determined by the values given to the bilinear lepton number violating parameters, μ_i . The left hand vertex is determined by the λ coupling from the superpotential, as defined in Eq. (2.20). This term in the superpotential generates both couplings in the second diagram of Fig. 6.5. In fact, if $\lambda_{ikk} \neq 0$, that is, any λ coupling with the final two indices the same, a single λ coupling will generate this diagram. The branching ratio is approximately given by the following expression,

$$\Gamma(l_i \rightarrow l_j \gamma) \approx \frac{3}{(4\pi)^2} \frac{|\lambda_{ikk}|^2}{G_F^2 m_i^2} \frac{e^2}{c_w^2} M_{\chi^0}^2 \left[\left(\frac{1}{m_e^2} \right) \left(\frac{\mu_k g v_u}{M_{\chi^0}^2} \right) \right]^2 \Gamma(l_i \rightarrow l_j \nu_i \bar{\nu}_j). \quad (6.15)$$

In the following sections, we shall consider in turn all λ couplings with symmetric final indices.

$\mu_{1,2,3}$ and λ_{211}

The first example considered is λ_{211} . As λ_{211} is varied, Fig. 6.6 shows the resulting solar mass squared difference, given by the dashed line, and the $\mu \rightarrow e\gamma$ branching

⁵The same code was used earlier to calculate the neutrino masses.

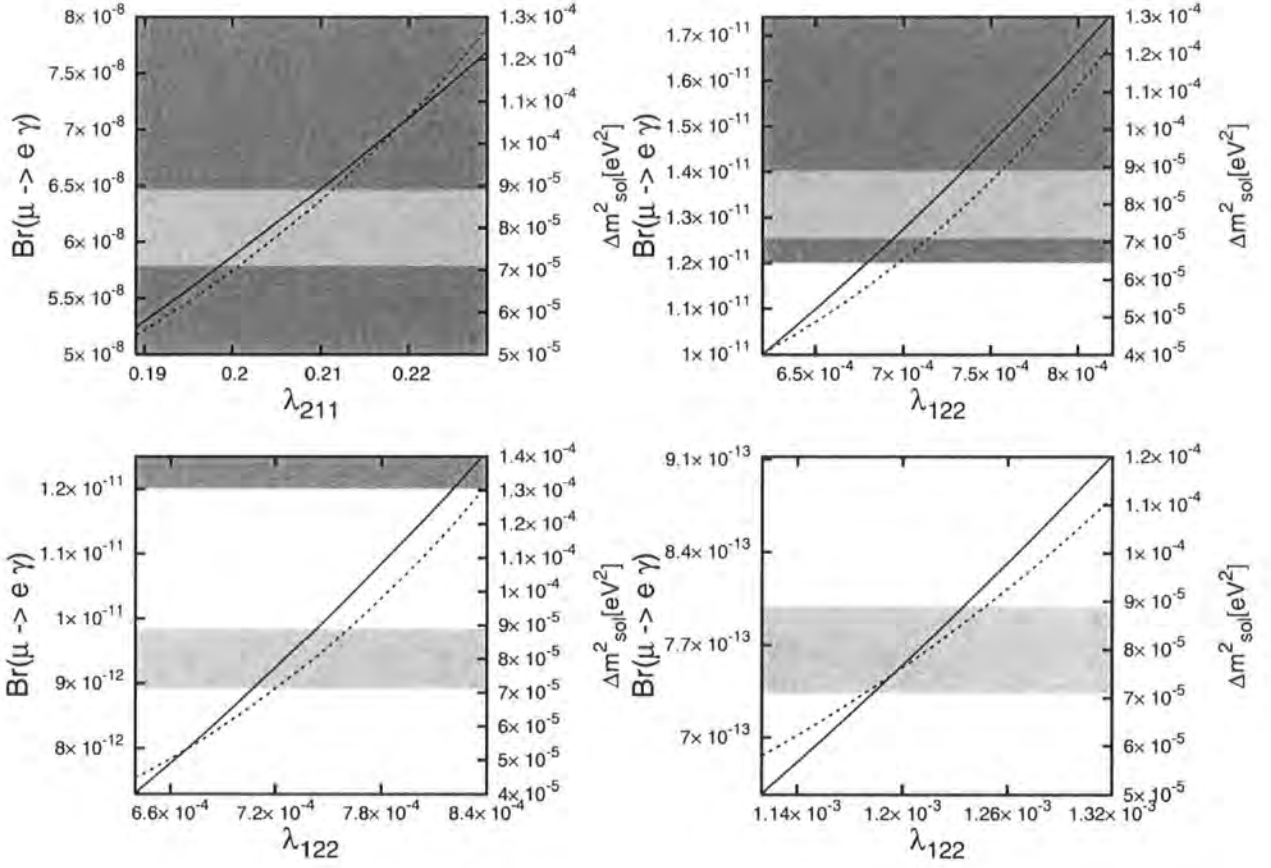


Figure 6.6: $\mu \rightarrow e\gamma$ and Δm_{sol}^2 against λ_{211} or λ_{122} – the dotted line (and right hand axis) show the magnitude of Δm_{sol}^2 with the light grey band indicating the current 3σ allowed range; the full line (and left hand axis) show the branching ratio of $\mu \rightarrow e\gamma$ with the dark grey area showing the values currently excluded at 90% confidence level. For the upper two plots, the R -parity conserving parameters are set by the SPS1a benchmark points, for which the mass of the charged scalar that consists mostly of interaction state $\tilde{\mu}_R$ is approximately 143 GeV. For the lower two plots, the mass of the scalars was increased such that the mass of $\tilde{\mu}_R$ was raised to 145 GeV (bottom left) and 265 GeV (bottom right).

ratio, given by the full line. The light grey strip shows the current experimental value for the solar mass squared difference and the dark grey area is the area presently excluded by $\mu \rightarrow e\gamma$ searches.

The value of λ_{211} required to generate the correct value for the solar mass difference must be comparatively large to compensate for the smallness of the mass of the electron induced in the loop. The $\mu \rightarrow e\gamma$ diagram generated has a large mass in the loop, and there is no suppression in the slepton part of the graph due to intergenerational, or left-right, mixing. As such, it can be seen that this scenario, although correctly explaining neutrino masses, is ruled out as it predicts a $\mu \rightarrow e\gamma$ branching ratio which would have been observed already. Furthermore, it is shown in Ref. [67,87], that a λ_{211} coupling of this magnitude would violate charged current universality.

$\mu_{1,2,3}$ and λ_{122}

In the top right plot of Fig. 6.6, it is shown that the value of λ_{122} required to correctly generate the solar mass squared difference is smaller; a muon is now produced in the loop contributing to the neutrino mass. The lower value of λ_{122} , in turn, makes the $\mu \rightarrow e\gamma$ branching ratio produced lower than the previous example, however it is still at the edge of the region ruled out by experiment with 90% confidence level. For scenarios with slightly heavier scalar masses than the SPS1a benchmark point this would not be ruled out. In the two bottom plots of Fig. 6.6 the mass of the scalars has been increased, such that the mass of the charged scalar which is mostly $\tilde{\mu}_R$ is 143 GeV (bottom left) and 265 GeV (bottom right) compared to approximately 145 GeV which is produced by the SPS1a benchmark values of R-parity conserving

parameters. We note how sensitive the resulting branching ratio is to the mass of the scalar in the loop. As shown in Eq. (6.15), the $\text{Br}(l \rightarrow l' \gamma) \sim 1/m_{\tilde{\mu}}^4$. Because this scenario is at the edge of current limits, and because of this sensitivity to the value of scalar masses, it is a particularly interesting scenario which can be studied in future experiments.

$\mu_{1,2,3}$ and $\lambda_{311,133}$

In the first plot of Fig. 6.7, we note the effect on the branching ratio of $\tau \rightarrow e \gamma$ by varying λ_{311} . The values for λ_{311} which correctly reproduce the neutrino data are not ruled out by current rare decay searches. Not only is the experimental bound less stringent, but the branching ratio is suppressed by a factor of $(m_{\tau}^2/m_{\mu}^2)(\text{Br}(\mu \rightarrow e \nu_{\mu} \bar{\nu}_e)/\text{Br}(\tau \rightarrow e \nu_{\tau} \bar{\nu}_e)) \sim 1600$ compared to the that of Sect. 6.3.2 and the fact that the λ coupling itself is smaller. The predicted branching ratio generated by the λ_{133} coupling that correctly generates the solar mass squared difference, is even smaller due to the lower value of the coupling.

$\mu_{1,2,3}$ and $\lambda_{322,233}$

The right hand plots of Fig. 6.7 demonstrate that the values of λ_{322} or λ_{233} which reproduce the neutrino results are not excluded and well below current experimental sensitivity. We note that the values for λ_{322} which produce the neutrino mass are smaller than for λ_{211} due to mass of the μ produced in the loop and λ_{233} smaller still.

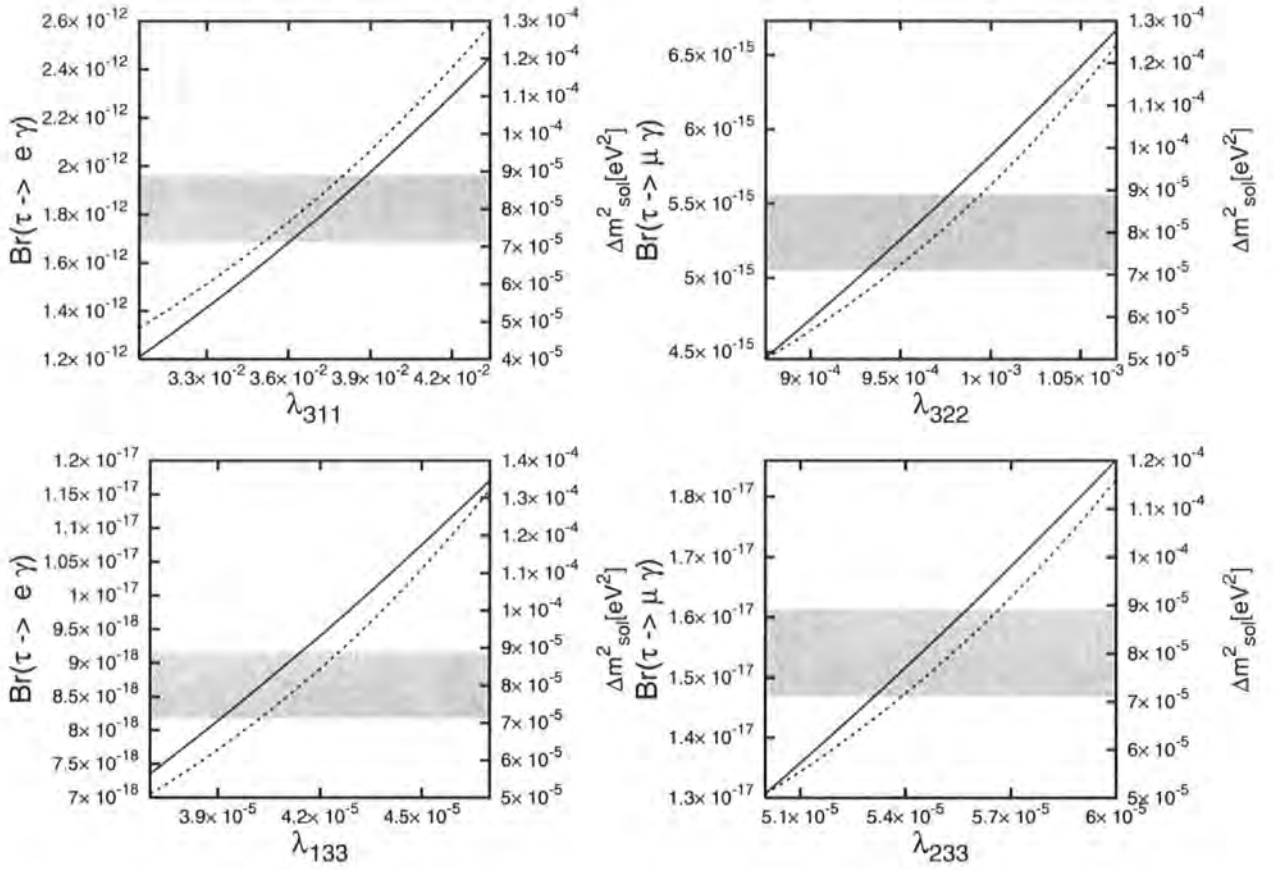


Figure 6.7: $\tau \rightarrow e\gamma$ (full line, left axis) and Δm_{sol}^2 (dotted line, right axis) against $\lambda_{311,133}$ or λ_{133} ; $\tau \rightarrow \mu\gamma$ (full line, left axis) and Δm_{sol}^2 (dotted line, right axis) against λ_{322} or λ_{233}

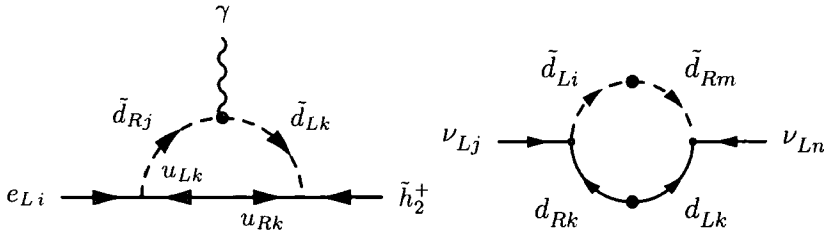


Figure 6.8: *Feynman diagrams generated when λ'_{ikk} generates neutrino masses radiatively and $\mu_{1,2,3}$ induce mixing on the external leg.*

6.3.3 Atmospheric scale set by $\mu_{1,2,3}$ – Solar scale set by λ'_{ikk}

When $\mu_i, \lambda'_{ikk} \neq 0$ the diagrams shown in Fig. 6.8 are generated. In this case, the mixing on the external leg is driven by the μ_i term, again being determined such that the atmospheric mass difference is produced correctly at tree level. In a similar fashion to the previous section, the λ' coupling on the left hand vertex is varied and the resulting solar mass squared difference considered. The branching ratio is approximately given by

$$\Gamma(l_i \rightarrow l_j \gamma) \approx \frac{3}{(4\pi)^2} \frac{|\lambda'_{ikk}|^2}{G_F^2 m_i^2} |(Y_U)_{kk}|^2 m_{u_k}^2 \left[3 \left(\frac{1}{m_{\tilde{d}}^2} \right) \left(\frac{\mu_k m_{e_k}}{m_{\chi^\pm}^2} \right) \left(\frac{\mathcal{M}_{\tilde{d}LR}^2}{\mathcal{M}_{\tilde{d}R}^2 - \mathcal{M}_{\tilde{d}L}^2} \right) \right]^2 \Gamma(l_i \rightarrow l_j \nu_i \bar{\nu}_j), \quad (6.16)$$

where $\mathcal{M}_{\tilde{d}L}^2$ and $\mathcal{M}_{\tilde{d}R}^2$ are diagonal entries in the squark mass matrices and $\mathcal{M}_{\tilde{d}LR}^2$ is the off-diagonal term which determines the mixing between the scalar partners of the left and right handed quarks. We note that the mixing between e_R and charginos is much smaller than the mixing of ν and neutralinos, and as such there is a suppression relative to the λ -driven diagrams. Furthermore, at the SPS1a benchmark point, the squarks are heavier than the charged sleptons; the branching ratios are highly sensitive to the scalar mass and this further suppresses λ' contributions in comparison

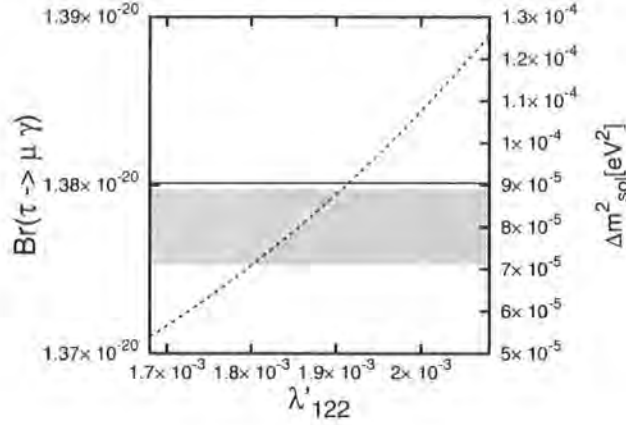


Figure 6.9: $\tau \rightarrow \mu\gamma$ and Δm_{sol}^2 against λ'_{122} .

with λ diagrams. The result being that the λ' vertices produce a negligible effect in this scenario.

With only the $\mu_i \neq 0$, setting the atmospheric mass scale, the diagram shown in Fig. 6.3 gives a contribution to the $\tau \rightarrow \mu\gamma$ branching ratio of the order 1.38×10^{-20} (Fig. 6.4) compared to which we can ignore the contribution from quark loops, as shown in Fig. 6.9 which takes λ'_{122} as an example.

6.3.4 Atmospheric scale set by $\mu_{1,2,3}$ – Solar scale set by B_i

The diagrams shown in Fig. 6.10 are generated when $\mu_i, B_j \neq 0$. In the first diagram of Fig. 6.10, the mixing on the internal fermion is set by μ_j and the mixing on the scalar line is set by B_i . Again, we note that the mass of the particle inside the loop for the rare decay diagram is of the same order of magnitude as of the particle in the radiative correction to the neutrino mass. The contribution to the branching ratio

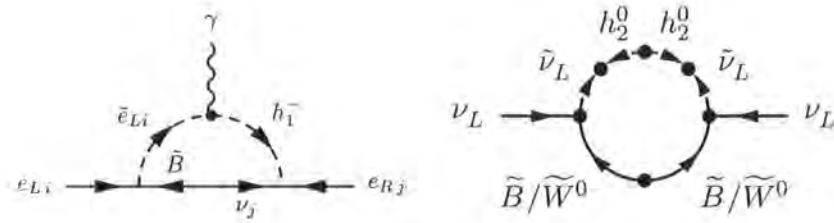


Figure 6.10: Feynman diagrams generated when the bilinear terms in the superpotential and supersymmetry breaking terms, μ_i and B_j respectively, are non-zero

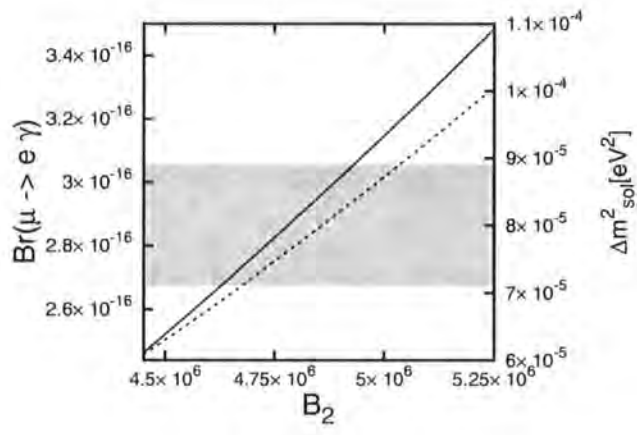


Figure 6.11: $\tau \rightarrow \mu \gamma$ and Δm_{sol}^2 against B_2

is approximately given by,

$$\Gamma(l_i \rightarrow l_j \gamma) \approx \frac{3}{(4\pi)^2} \frac{|\lambda_{0jj}|^2 e^2}{G_F^2 m_i^2 c_w^2} \left[\left(\frac{1}{m_{H^+}^2} \right) \left(\frac{B_i}{m_{H^+}^2} \right) \left(\frac{\mu_j g v_u}{m_{\chi^0}} \right) \right]^2 \Gamma(l_i \rightarrow l_j \nu_i \bar{\nu}_j). \quad (6.17)$$

As such, we see that these diagrams are not ruled out by current experimental bounds, as shown in Fig. 6.11, and are not within reach of upcoming studies.

6.3.5 Atmospheric scale set by λ – Solar scale set by λ'

In the following sections, both the atmospheric and solar mass scales are set by radiative corrections. Again, we can find combinations of parameters which correctly describe the neutrino sector and also give rise to experimentally attainable branching ratios for $l \rightarrow l' \gamma$.

We first consider the case in which λ_{133} and λ_{233} are varied over the following range,

$$\lambda_{133} = -\sqrt{2}\lambda_{233} = 5 \times 10^{-5} - 8 \times 10^{-5}. \quad (6.18)$$

The ratio ensures the correct mixing between neutrino interaction states is reproduced and the magnitude sets in atmospheric masses squared difference. In addition to this, the contribution of the first diagram in Fig. 6.12 to the branching ratio of $l \rightarrow l' \gamma$ is approximately given by,

$$\Gamma(l_i \rightarrow l_j \gamma) \approx \frac{3}{(4\pi)^2} \frac{|\lambda_{ikk}|^2 |\lambda_{jkk}|^2}{G_F^2} \left[\frac{1}{24} \frac{1}{m_{\bar{\nu}}^2} \right]^2 \Gamma(l_i \rightarrow l_j \nu_i \bar{\nu}_j). \quad (6.19)$$

The results are given in the upper left panel on Fig. 6.13. The dashed line (and right hand axis) show the atmospheric mass squared difference and the light grey band shows the values for which $\lambda_{133,233}$ generate an atmospheric mass difference in

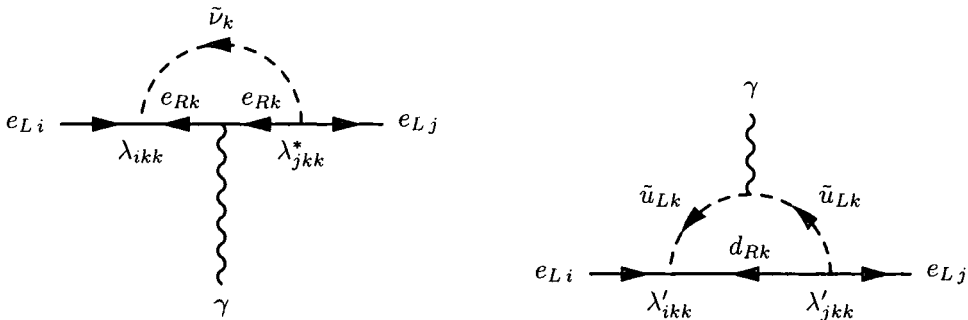


Figure 6.12: *Feynman diagrams which contribute to $l_i \rightarrow l_j \gamma$, in the case where trilinear lepton number violating couplings are dominant.*

agreement with current experimental observations. The full line (and left hand axis) show the corresponding branching ratio for $\mu \rightarrow e \gamma$. The resulting branching ratio is well below current or future experimental sensitivity.

To generate the solar mass squared difference, $\lambda_{1kk,2kk,3kk}$ are varied in the following hierarchy, ensuring the resulting mixing matrix takes the form observed by experiment,

$$\lambda'_{1kk} = \frac{\lambda'_{2kk}}{\sqrt{2}} = -\frac{\lambda'_{3kk}}{\sqrt{3}}. \quad (6.20)$$

The second diagram in Fig. 6.12, produces a contribution to the $l_i \rightarrow l_j \gamma$ branching ratio of approximately,

$$\Gamma(l_i \rightarrow l_j \gamma) \approx \frac{3}{(4\pi)^2} \frac{|\lambda'_{ikk}|^2 |\lambda'_{jkk}|^2}{G_F^2} \left[\frac{1}{3} \frac{1}{m_{\tilde{u}}^2} \right]^2 \Gamma(l_i \rightarrow l_j \nu_i \bar{\nu}_j). \quad (6.21)$$

The results for the three possible cases, that is $k = 1, 2, 3$, are shown in the remaining panels of Fig. 6.13. We note that while $k = 2, 3$ are well below current or planned experimental sensitivity, the scenario in which $\lambda'_{111,211,311}$ generate the solar mass squared difference would be discernible by upcoming experimental studies, al-

though we note that bounds from $\mu-e$ conversion in nuclei already strongly constrain this set of parameters [88]. When the solar mass squared difference is generated by $\lambda'_{133,233,333}$, bottom right panel of Fig. 6.12, the branching ratio is of the same order as that given by $\lambda_{133,233}$, setting the solar scale, and contributes with opposite sign. Resulting in the negative gradient shown.

6.3.6 Atmospheric scale set by λ' – Solar scale set by $\lambda^{(\prime)}$

Again, both the atmospheric and solar mass scales are set by radiative corrections. First, we consider the scenario in which the atmospheric mass squared difference is set by $\lambda'_{111,211,311}$. The parameters are given by,

$$\lambda'_{111} = \frac{\lambda'_{211}}{\sqrt{2}} = \frac{\lambda'_{311}}{\sqrt{3}}. \quad (6.22)$$

The resulting atmospheric mass squared difference and resulting branching ratio for $\mu \rightarrow e\gamma$ are shown in Fig. 6.14, from which it can be seen that the parameter space which brings about the correct atmospheric mass difference is already ruled out by the rare decay searches.

In a similar fashion, we consider the scenario in which the atmospheric mass squared difference is set by $\lambda'_{133,233,333}$, as follows,

$$\lambda'_{133} = \frac{\lambda'_{233}}{\sqrt{2}} = \frac{\lambda'_{333}}{\sqrt{3}}. \quad (6.23)$$

The results are given in the upper left panel of Fig. 6.15. In this case, we note that the values of $\lambda'_{133,233,333}$ which give the correct value for the neutrino mass, generate negligible rates for $\mu \rightarrow e\gamma$.

The solar mass squared difference must now be generated. It can be set either by $\lambda_{133,233}$ or by a different set of λ' couplings. First we examine $\lambda'_{1kk,2kk,3kk}$, which

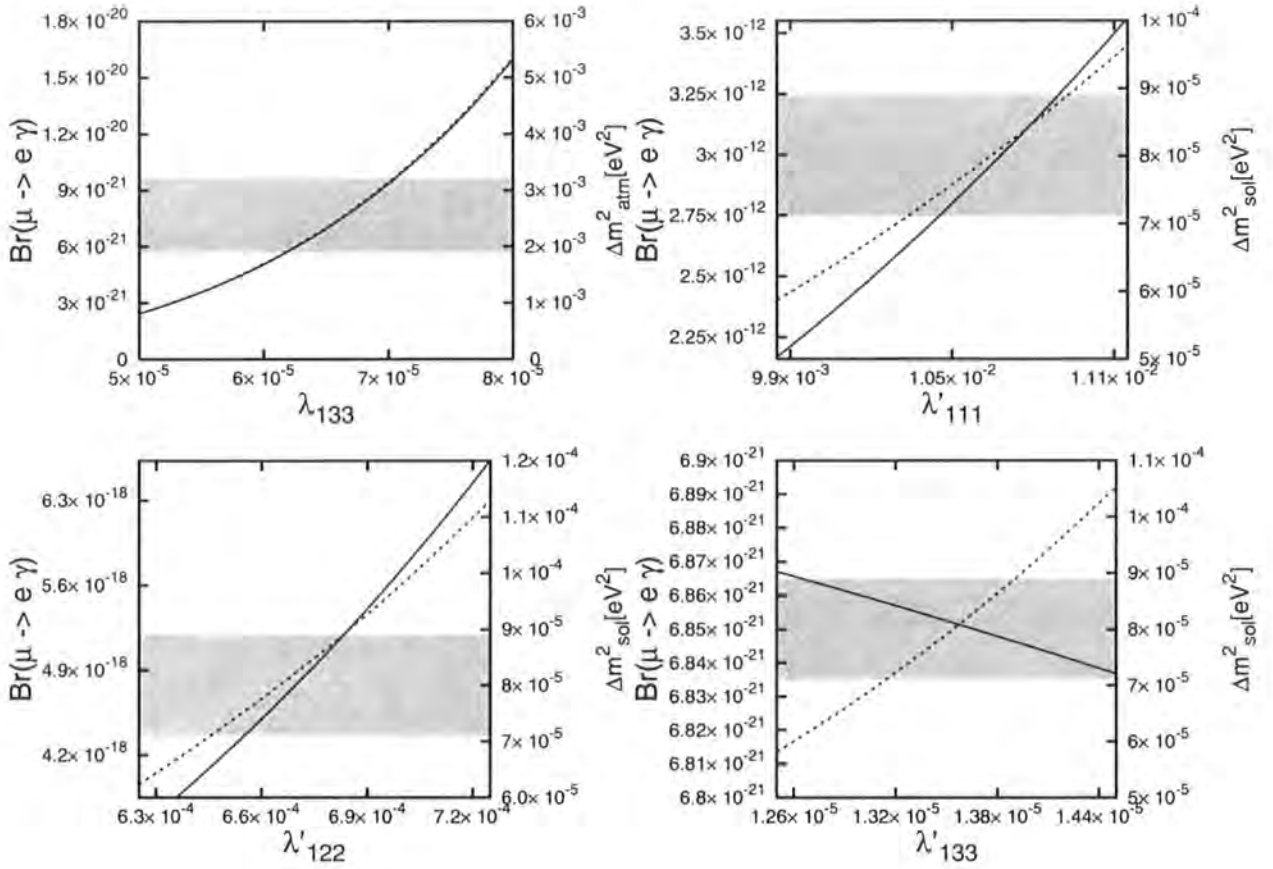


Figure 6.13: $\mu \rightarrow e\gamma$ and $\Delta m_{sol,atm}^2$ against $\lambda^{(i)}$ – In the top left panel $\lambda_{133,233}$ are varied and the resulting branching ratio for $\mu \rightarrow e\gamma$ (full line, left hand axis) and Δm_{atm}^2 (dashed line, right hand axis, grey band showing current 3σ band from experiment) are noted. In the remaining three panels, $\lambda'_{1kk,2kk,3kk}$ are varied and $Br(\mu \rightarrow e\gamma)$ and Δm_{sol}^2 are shown.

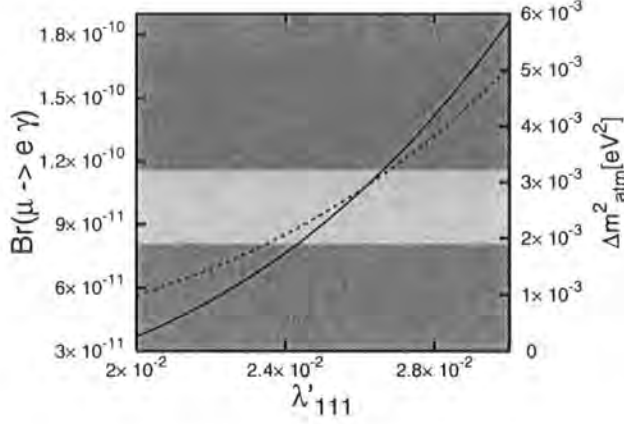


Figure 6.14: $\mu \rightarrow e\gamma$ and Δm_{atm}^2 against $\lambda'_{111} - \lambda'_{111,211,311}$ are varied and the resulting branching ratio for $\mu \rightarrow e\gamma$ (full line, left hand axis, dark grey area showing values excluded by experimental searches) and Δm_{atm}^2 (dashed line, right hand axis, light grey band showing current 3σ band from experiment) are noted.

are varied as follows,

$$\lambda'_{1kk} = \frac{\lambda'_{2kk}}{\sqrt{2}} = -\frac{\lambda'_{3kk}}{\sqrt{3}}. \quad (6.24)$$

The upper right and bottom left panels show the results for these parameters. Again, we note that although the scenario in which the solar scale is set by $\lambda'_{122,222,322}$ (bottom left panel) is not within experimental sensitivity, $\lambda'_{111,211,311}$ (top right panel) is close to the current bounds and would be seen by searches planned for the near future.

The final possibility is that the solar mass squared difference be set by $\lambda_{133,233}$. The parameters are varied in the following hierarchy,

$$\lambda_{133} = -\sqrt{2}\lambda_{233}. \quad (6.25)$$

The results, given in the bottom right panel of Fig. 6.15, show that this scenario is

well below both current and future experimental bounds.

6.4 Benchmarks

Benchmark scenarios for studying R-parity violating models have been suggested [89], for which the mass spectrum, nature of the lightest supersymmetric particle and decays have been studied. The benchmarks presented in [89] are selected as they produce interesting signatures at future colliders and are constrained by measurements of $(g - 2)_\mu$, the $b \rightarrow s\gamma$ decay and mass bounds from direct particle searches.

In addition to these benchmarks, we suggest some other interesting scenarios. Our motivation being that neutrino data is known and we demand that the model correctly reproduces these results. As there are numerous combinations of lepton number violating parameters which satisfy this requirement, we consider scenarios for which the upcoming $l \rightarrow l'\gamma$ searches will constrain the Lagrangian parameters.

The following combinations of lepton number violating parameters are considered, where all R-parity conserving parameters are set at the SPS1a benchmark point,

- *Benchmark Scenario 1* -

$$\mu_1 = \frac{\mu_2}{\sqrt{2}} = \frac{\mu_3}{\sqrt{3}} = 1.47\text{MeV} \quad , \quad \lambda_{211} = 7.4 \times 10^{-4}$$

- *Benchmark Scenario 2* -

$$\mu_1 = \frac{\mu_2}{\sqrt{2}} = \frac{\mu_3}{\sqrt{3}} = 1.47\text{MeV} \quad , \quad \lambda_{311} = 3.7 \times 10^{-2}$$

- *Benchmark Scenario 3* -

$$\lambda_{133} = -\sqrt{2}\lambda_{233} = 6.5 \times 10^{-5} \quad , \quad \lambda'_{111} = \frac{\lambda'_{211}}{\sqrt{2}} = -\frac{\lambda'_{311}}{\sqrt{3}} = 1.05 \times 10^{-2}$$

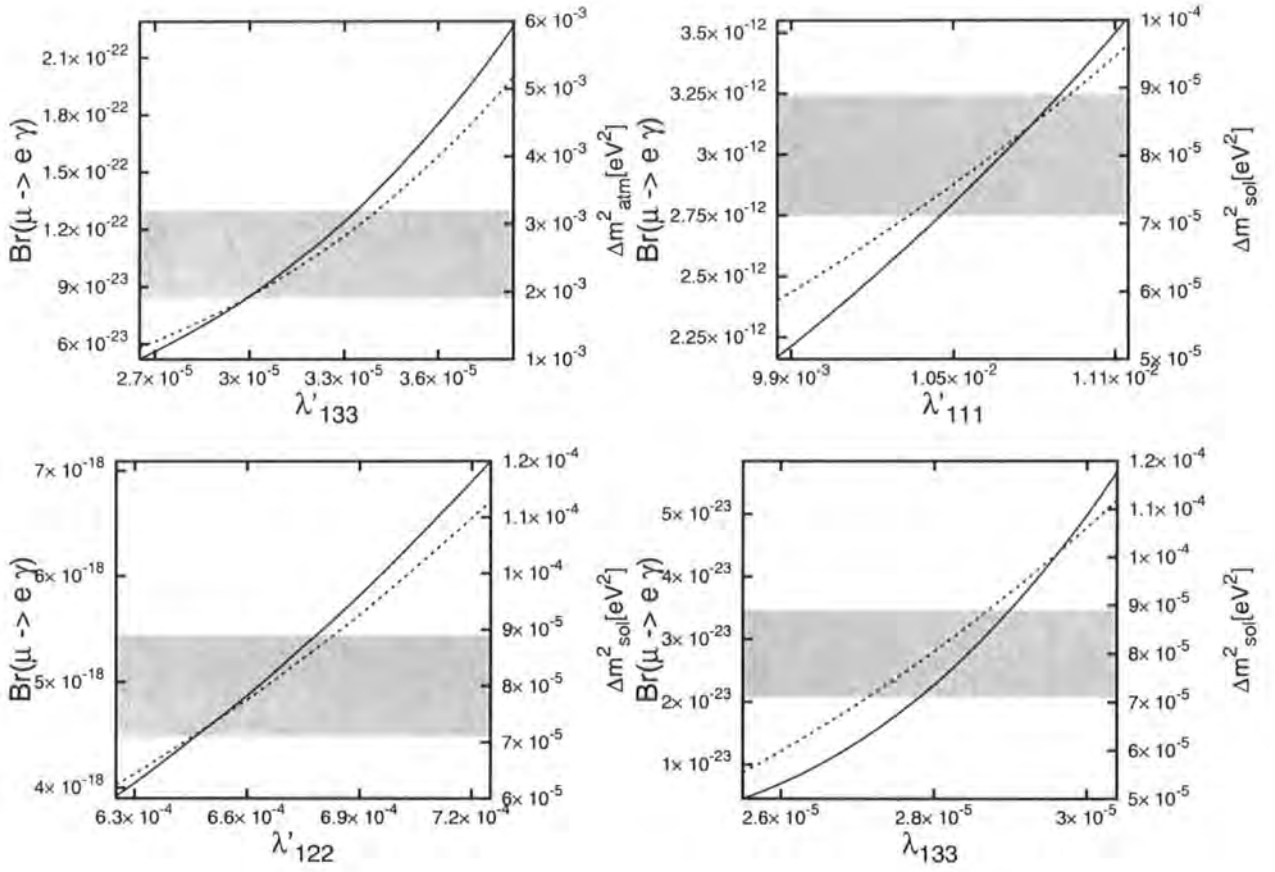


Figure 6.15: $\mu \rightarrow e\gamma$ and $\Delta m_{sol,atm}^2$ against $\lambda^{(\prime)}$ – In the top left panel $\lambda'_{133,233,333}$ are varied and the resulting branching ratio for $\mu \rightarrow e\gamma$ (full line, left hand axis) and Δm_{atm}^2 (dashed line, right hand axis, grey band showing current 3σ band from experiment) are noted. In the top right and bottom left panels, $\lambda'_{111,211,311}$ and $\lambda'_{122,222,322}$ are varied, respectively, and the $\mu \rightarrow e\gamma$ and Δm_{sol}^2 are shown. In the bottom right hand panel $\lambda_{133,233}$ are varied and the $\mu \rightarrow e\gamma$ and Δm_{sol}^2 are given.

- *Benchmark Scenario 4* –

$$\lambda'_{133} = \frac{\lambda'_{233}}{\sqrt{2}} = \frac{\lambda'_{333}}{\sqrt{3}} = 3.25 \times 10^{-5} \quad , \quad \lambda'_{111} = \frac{\lambda'_{211}}{\sqrt{2}} = -\frac{\lambda'_{311}}{\sqrt{3}} = 1.05 \times 10^{-2} \quad .$$

In the first two benchmark scenarios the observed flavour oscillations of atmospheric neutrinos are driven by the bilinear lepton number violating term in the superpotential giving rise to a mass difference at tree level. For this to occur, the μ_i parameters are of the order 1 MeV. In Benchmark Scenario 1, the solar mass squared difference is then generated by setting $\lambda_{211} = 7.4 \times 10^{-4}$. Merely for comparison, we note that this is approximately $\lambda_{211} \sim 25 y_e$, where y_e is the Yukawa coupling associated with a given particle, in this case being the electron. This will give rise to branching ratios for $\mu \rightarrow e\gamma$ which can be probed by upcoming experimental studies. In Benchmark 2 the solar mass squared difference is determined by $\lambda_{311} = 3.7 \times 10^{-2} \sim 1200 y_e$. This combination of parameters will generate a branching ratio for $\tau \rightarrow e\gamma$ which may be probed by future studies of τ decays.

In the Benchmark Scenarios 3 and 4 both the atmospheric and solar mass squared differences are set by radiative corrections. The bilinear lepton number violating terms are set to zero, and the neutrinos are all massless at tree-level. In Benchmark Scenario 3, $|\lambda_{133,233}| \sim 3y_e$ set the atmospheric mass difference and $|\lambda'_{111,211,311}| \sim 40 y_d$ sets the solar mass squared difference. In Benchmark Scenario 4, $|\lambda'_{133,233,333}| \sim 0.1 y_d$ sets the atmospheric scale and $|\lambda'_{111,211,311}| \sim 40 y_d$ gives the solar scale. In both Benchmarks 3 and 4, $\mu \rightarrow e\gamma$ would give branching ratios which will be observed by future experimental studies.

6.5 Summary

That lepton flavour violating decays of charged particles have not been observed is worthy of note. The suppressed branching ratios arise automatically in the Standard Model, but this is not the case in Supersymmetric extensions where it already puts strong bounds on certain parameters. In this chapter, we have examined the effects of lepton number violating couplings on these branching ratios. Combinations of parameters which describe the neutrino sector were chosen to be examined and their subsequent effect on the rare decays considered.

We first investigated the case in which R-parity conserving parameters are set to the SPS1a benchmark point and the bilinear lepton number violating term in the superpotential, μ_i generates the atmospheric mass difference. We showed that the values of μ_i which correctly describe the atmospheric mass difference and mixing angles are not ruled out by the current bounds on $\tau \rightarrow \mu\gamma$, $e\gamma$ or $\mu \rightarrow e\gamma$. As such, the bounds from lepton decays are less stringent than the bounds from neutrino data. We then considered the case in which a further lepton number violating parameter correctly reproduces the solar mass difference and considered the combined effect on the $l \rightarrow l'\gamma$ decays. We note that in this scenario these decays can impose constraints on one of the trilinear lepton number violating parameters in the superpotential, λ . We considered all the examples in which the λ coupling has symmetric final indices, which generate the solar neutrino mass with just one non-zero coupling. λ_{211} and λ_{122} are excluded by experimental searches for $\mu \rightarrow e\gamma$; λ_{311} , λ_{133} , λ_{332} , λ_{233} are not. We note, however, that the branching ratios are sensitive to the masses of the scalar particles in the loop. As such, in scenarios where the scalar masses are heavier than those in SPS1a, the branching ratios can be greatly suppressed.

In this scenario, the limits on $l \rightarrow l'\gamma$ do not place useful constraints on λ' , or the bilinear lepton number violating terms in the supersymmetry breaking part of the Lagrangian, B_i ; generally, the current constraints from the neutrino sector are stronger.

Second, we considered the scenario in which trilinear lepton number violating couplings are dominant. We set all bilinear lepton number violating couplings to zero, and again set R-parity conserving parameters to the SPS1a benchmark point. In this scenario, both neutrino mass scales are determined by radiative corrections and in order to generate the correct mixing matrix in the lepton sector, more than one lepton number violating coupling must be non-zero for each mass scale. Because of this, diagrams which contribute to $l \rightarrow l'\gamma$ are generated. We note that limits already exist when $\lambda'_{111,211,311}$ are used to generate mass differences in this scenario. In general however, for $\lambda'_{x22,x33}$ the constraints from the neutrino masses are stringent.

Chapter 7

Conclusions

The \mathbb{U} -MSSM is well-motivated and worthy of study. As a SUSY model, it solves the hierarchy problem and also generates neutrino masses in an attractive fashion. In this thesis, we have determined the different sets of parameters which produce the observed neutrino patterns. The effect of lepton number violating parameters in this range on the branching ratios for $l \rightarrow l'\gamma$ has also been considered.

In Chapter 2, supersymmetry was introduced in the superfield notation. The (anti)commutation relations which define the supersymmetry algebra and the generators of infinitesimal transformations were noted (Eq. 2.1). Properties and field components of the chiral and vector superfields were given (Eqs. 2.6–2.11); noting that the F- and D-terms transform into total derivatives, combinations of terms invariant under SUSY transformations were constructed and used to build a SUSY-invariant Lagrangian. This procedure enabled us to define an invariant Lagrangian in terms of the superpotential (Sec. 2.2). The superpotential for a minimal particle content model can then be written down (Eq. 2.19). The immediate phenomeno-

logical difficulties – the absence of degenerate scalars and fermions in the observed mass spectrum, and the instability of the proton – were discussed. The former being solved by adding ‘soft’ SUSY-breaking terms to the Lagrangian and the latter by imposing a discrete symmetry when constructing the model. Motivated by the phenomenology of the neutrino sector, we considered a superpotential (and soft breaking terms) which explicitly allow lepton number violation (Eq. 2.20).

In Appendix B, the Lagrangian for the full R-parity violating MSSM is included; that is, the Lagrangian as constructed without an additional discrete symmetry being imposed. The \mathbb{Z}_2 -MSSM Lagrangian is a subset of this Lagrangian, which can be easily derived by setting the parameters which determine baryon number violation to zero.

Starting from this Lagrangian, in Chapter 3, we study the neutral scalar sector and the spontaneous breaking of the electroweak symmetry. The lepton number violating terms compel us to treat the sneutrinos and the ‘down-coupling’ Higgs boson equally; further mixing with the neutral ‘up-coupling’ Higgs gives rise to a system of five complex scalars. We have described a procedure, originally presented in [24], which allows us to control this problem and parameterise the Higgs sector. The procedure allows us to select a basis in which the sneutrino interaction eigenstates do not acquire a non-zero vacuum expectation value, and the two neutral Higgs interaction states acquire real non-zero vacuum expectation values. In this basis, the mass spectrum of the neutral scalar sector is considered, which requires the Courant-Fischer theorem, the derivation of which is given in Appendix E.

Having understood the Higgs sector, it is possible to derive the Feynman rules of the model. Many fields now mix and the vertices contain rotation matrices, themselves determined by the mass matrices of the theory; the definitions of these rotation

matrices are collected together in Appendix D. In Appendix C, we provide the Lagrangian in this mass basis and define the Feynman Rules for vertices of the theory.

We performed all the calculations using Weyl spinors, which we define in Appendix A. Although not as widely used as Dirac notation, in my opinion, for calculations of this nature they are more convenient and demonstrate more clearly the underlying physics. This is, of course, a matter of taste.

The neutrino sector, the phenomenology of which was a primary motivation for this study, was then considered. The tree-level phenomena are presented in Chapter 4 and the effects of radiative corrections are added in Chapter 5. This work was first presented in [53].

Questions concerning the initialisation of Lagrangian parameters, such that the charged lepton masses and MNS matrix are initialised correctly are addressed. To accomplish this, approximate formulae (Eq. 4.18) are derived which allow the mass matrices to be block diagonalised, making use of the large hierarchy between the known leptons and the heavy higgsinos and gauginos. From this analysis we note that two neutrinos are, without approximation, massless at tree level and an approximate expression (Eq. 4.19) for the massive neutrino is determined, making explicit the observation that its mass has a seesaw-like suppression; the high mass scale being provided by the higgsinos and gauginos.

In Chapter 5, we calculate the neutrino masses completely at the order of one-loop. First, the relevant renormalisation issues were addressed and the physical neutrino masses defined to be the poles of the inverse propagator. Generic expressions, given explicitly in Appendix F, for the one-loop contributions were derived and then the effect due to the different possible particles appearing in the loop were

considered.

We were successful in showing that all neutrino parameters could be accommodated in the model using various different sets of parameters, and interesting bounds could be put on these parameters. Computer code for their calculation was produced.

Finally, in Chapter 6, the flavour violating radiative decays of leptons were considered; this calculation was first presented in [77]. We note that some of the operators which drive the neutrino masses in the previous chapter, can also give rise to flavour violating processes in the charged lepton sector. The branching ratios for these process are calculated, explicit results are noted in Appendix G, and the numerical results for the parameter sets noted earlier are plotted. We see that scenarios which describe the neutrino sector are precluded due to bounds from experimental searches for these rare decays. Certain sets of parameters are highlighted as Benchmark Scenarios, which correctly reproduce the neutrino sector and would give rise to observable charged lepton flavour violating events at experiments in the near future.

To extend this work a number of other observables could have been considered. Neutrinoless double-beta decay is widely discussed in the literature and a number of new experiments are planned to probe this process further and confirm or repudiate current experimental claims. As such, although the result at tree-level is well-known, a full one-loop study may be of value.

A further extension of this work would be to set it within a unified model and consider the running of parameters from a high scale using renormalisation group methods. The unification of the gauge couplings suggests that supersymmetry is embedded in a unified model. In the simplest such model, the breaking of supersymmetry occurs in a sector decoupled from the Standard Model gauge interactions.

The large number of parameters in the Minimal Supersymmetric Standard Model can be restricted by making well-motivated simplifying assumptions at the unification scale. It would be interesting to see how many high-energy parameters are required to reproduce the observed, low-energy, neutrino parameters.

It is the aim of future experimental and theoretical study to understand physics beyond that described by the Standard Model. Many models have been, and will be, suggested. To discern the models, the correlations between physical observables are identified, calculated and measured. In this thesis we selected a model that is well-motivated from theoretical considerations, and calculated two correlated physical observables: the neutrino mass and mixing parameters on one hand, and branching ratios for radiative flavour-violating decays on the other. We have shown that there are certain cases in which this appealing description of the neutrino masses may be supported or ruled out by searches for rare decays.

Appendix A

Weyl Spinors

A.1 Notation

The following conventions will be adopted. Dotted indices transform under $(0, \frac{1}{2})$ representation and undotted indices transform under $(\frac{1}{2}, 0)$ representation of the Lorentz group. Indices can be raised and lowered using the antisymmetric $\varepsilon_{\alpha\beta}$ tensor.

$$\varepsilon_{21} = \varepsilon^{12} = 1, \quad \psi^\alpha = \varepsilon^{\alpha\beta}\psi_\beta, \quad \psi_\alpha = \varepsilon_{\alpha\beta}\psi^\beta.$$

Spinors are contracted using the convention $\alpha \ \alpha$ for undotted indices and $\dot{\alpha} \ \dot{\alpha}$ for dotted indices. A four-component Dirac spinor, Ψ can then be constructed in the form,

$$\Psi = \begin{pmatrix} \xi_\alpha \\ \bar{\chi}^{\dot{\alpha}} \end{pmatrix}.$$

The projection operators P_L and P_R are given by,

$$\Psi_L = P_L \Psi = \frac{1}{2}(1 - \gamma_5) \Psi, \quad \Psi_R = P_R \Psi = \frac{1}{2}(1 + \gamma_5) \Psi,$$

and charge conjugation can be represented as follows,

$$\Psi^C = i\gamma^2\Psi^* .$$

Using the above definitions, we see that the operations can be understood easily in terms of Weyl spinors,

$$\Psi_L = \begin{pmatrix} \xi_\alpha \\ 0 \end{pmatrix} , \quad \Psi_R = \begin{pmatrix} 0 \\ \bar{\chi}^{\dot{\alpha}} \end{pmatrix} , \quad \Psi_L^c = \begin{pmatrix} 0 \\ \bar{\xi}^{\dot{\alpha}} \end{pmatrix} , \quad \Psi_R^c = \begin{pmatrix} \chi_\alpha \\ 0 \end{pmatrix} ,$$

$$\bar{\Psi}_L = \begin{pmatrix} 0 & \bar{\xi}_{\dot{\alpha}} \end{pmatrix} , \quad \bar{\Psi}_R = \begin{pmatrix} \chi^\alpha & 0 \end{pmatrix} , \quad \bar{\Psi}_L^c = \begin{pmatrix} \xi^\alpha & 0 \end{pmatrix} , \quad \bar{\Psi}_R^c = \begin{pmatrix} 0 & \bar{\xi}_{\dot{\alpha}} \end{pmatrix} .$$

A.2 Kinetic Terms and Mass Matrices

Consider a Lagrangian in the form,

$$\begin{aligned} \mathcal{L} = & i\bar{\xi}'_{\dot{\alpha}i}\sigma^{\mu\dot{\alpha}\alpha}\partial_\mu\xi'_{\alpha i} + i\bar{\chi}'_{\dot{\alpha}i}\sigma^{\mu\dot{\alpha}\alpha}\partial_\mu\chi'_{\alpha i} + (M_1)_{ij}\chi'^\alpha_i\chi'_{j\alpha} + (M_2)_{ij}\bar{\chi}'_{\dot{\alpha}i}\bar{\chi}'^{\dot{\alpha}}_j \\ & + (M_3)_{ij}\xi'^\alpha_i\xi'_{j\alpha} + (M_4)_{ij}\bar{\xi}'_{\dot{\alpha}i}\bar{\xi}'^{\dot{\alpha}}_j + (M_5)_{ij}\chi'^\alpha_i\xi'_{j\alpha} + (M_6)_{ij}\bar{\chi}'_{\dot{\alpha}i}\bar{\xi}'^{\dot{\alpha}}_j \end{aligned}$$

We have written down all possible bilinear combinations of two families of Weyl spinors, χ_i and ξ_i , and parameterised them in the most general way. We can now derive constraints on the parameters, such that the condition, $\mathcal{L}^\dagger = \mathcal{L}$, is satisfied.

$$M_1 = M_2^* , \quad M_3 = M_4^* , \quad M_5 = M_6^* .$$

We further note that the terms involving $(M_{1,2,3,4})$ can be re-arranged, such that,

$$(M_1)_{ij}\chi'_i\chi'_j = \left[\frac{1}{2}(M_1)_{ij} + \frac{1}{2}(M_1)_{ji} \right] \chi'_i\chi'_j = (\bar{M}_1)_{ij}\chi'_i\chi'_j .$$

That is, we can always rearrange parameters such that,

$$M_1^T = M_1 , \quad M_2^T = M_2 , \quad M_3^T = M_3 , \quad M_4^T = M_4 ,$$

without any loss of generality. Substituting these results into the Langrangian gives the most general Lagranian,

$$\begin{aligned} \mathcal{L} = & i\bar{\xi}'_{\dot{\alpha}i}\sigma^{\mu\dot{\alpha}\alpha}\partial_{\mu}\xi'_{\alpha i} + i\bar{\chi}'_{\dot{\alpha}i}\sigma^{\mu\dot{\alpha}\alpha}\partial_{\mu}\chi'_{\alpha i} + (M_1)_{ij}\chi'^{\alpha}_i\chi'_{j\alpha} + (M_1^*)_{ij}\bar{\chi}'_{\dot{\alpha}i}\bar{\chi}'^{\dot{\alpha}}_j \\ & + (M_3)_{ij}\xi'^{\alpha}_i\xi'_{j\alpha} + (M_3^*)_{ij}\bar{\xi}'_{\dot{\alpha}i}\bar{\xi}'^{\dot{\alpha}}_j + (M_5)_{ij}\chi'^{\alpha}_i\xi'_{j\alpha} + (M_5^*)_{ij}\bar{\chi}'_{\dot{\alpha}i}\bar{\xi}'^{\dot{\alpha}}_j \end{aligned} \quad (\text{A-1})$$

In general, (M_1) and (M_3) are complex, symmetric matrices (and as such, can be defined by $n(n+1)$ real parameters); (M_5) is a complex matrix (can be defined by $2n^2$ real parameters.) The nature of these mass matrices determine the manner in which the matrices can be diagonalised, as discussed in the next section.

A.3 Diagonalising matrices

Consider a general $n \times n$ complex matrix, M , with eigenvectors \tilde{e}_i and corresponding eigenvalues λ_i . If a matrix, P is constructed to have the form

$$P = \begin{pmatrix} \tilde{e}_1 & \tilde{e}_2 & \tilde{e}_3 & \tilde{e}_4 & \cdots & \tilde{e}_n \end{pmatrix}$$

then

$$MP = \begin{pmatrix} \lambda_1\tilde{e}_1 & \lambda_2\tilde{e}_2 & \lambda_3\tilde{e}_3 & \lambda_4\tilde{e}_4 & \cdots & \lambda_n\tilde{e}_n \end{pmatrix}$$

$$P^{-1}MP = \begin{pmatrix} \lambda_1 & 0 & 0 & 0 & 0 & \cdots \\ 0 & \lambda_2 & 0 & 0 & 0 & \cdots \\ 0 & 0 & \lambda_3 & 0 & 0 & \cdots \\ & & & \ddots & & \\ 0 & 0 & 0 & 0 & \cdots & \lambda_n \end{pmatrix}$$

If M were an Hermitian matrix ($M^\dagger = M$), the eigenvalues, and therefore the diagonal elements, would be real and non-negative and P would be a unitary matrix

($P^\dagger = P^{-1}$). However, we must find a method to diagonalise the general complex mass matrices and self-transpose mass matrices highlighted in the previous section by unitary transformations, which leave kinetic terms unaffected.

Consider a general, complex matrix A . The product $A^\dagger A$ is Hermitian, and, as such, it is possible to diagonalise it with a unitary matrix in the following manner,

$$U^\dagger A^\dagger A U = D^2 ,$$

where D^2 is diagonal, with real, non-negative elements. A new hermitian matrix, H , is defined to take the form,

$$H = U F D F^\dagger U^\dagger ,$$

where $F = \text{diag}(e^{i\varphi_1}, e^{i\varphi_2}, e^{i\varphi_3}, \dots)$ and D is chosen such that it is a diagonal matrix with entries which are the positive square roots of the diagonal elements of D^2 . We consider the product,

$$H^2 = U F D F^\dagger U^\dagger U F D F^\dagger U^\dagger = U F D^2 F^\dagger U^\dagger .$$

As D and F are both diagonal in form, the F commutes past D^2 to give

$$H^2 = A^\dagger A$$

We define unitary matrices, $W = A H^{-1}$ and $V = W U$. Rearranging and substituting for H gives,

$$A = W H = W U F D F^\dagger U^\dagger = V F D F^\dagger U^\dagger = V' D U'^\dagger$$

$$V'^\dagger A U' = D$$

Hence, U' and V' are unitary matrices which diagonalise the general complex matrix, A , such that the diagonal entries are real and non-negative. Also,

$$V'^\dagger A U' = F D = D'$$

Where D' is a diagonal matrix with complex entries.

The specific case where $A = A^T$ is now considered. If

$$\begin{aligned} V'^{\dagger} A U' &= D \Rightarrow U'^T A V'^* = D \\ &\Rightarrow V'^* = U' \end{aligned}$$

A.4 Dirac and Majorana Particles

If ψ' carries a conserved quantum number it must be contracted with a spinor which carries the opposite quantum number, η' . The ψ' and the η' do not mix as they can be differentiated by the quantum number. In this case, terms such as $\psi'\psi'$ and $\eta'\eta'$ do not appear in the Lagrangian. The Lagrangian for Dirac particles takes the form:

$$\mathcal{L}_D = i\bar{\psi}'_{\dot{\alpha}i}\sigma^{\mu\dot{\alpha}\alpha}\partial_{\mu}\psi'_{\alpha i} + i\bar{\eta}'_{\dot{\alpha}i}\sigma^{\mu\dot{\alpha}\alpha}\partial_{\mu}\eta'_{\alpha i} + (M_5)_{ij}\psi'_{i\alpha}\eta'_{j\alpha} + (M_5^*)_{ij}\bar{\psi}'_{\dot{\alpha}i}\bar{\eta}'_{\dot{\alpha}j} \quad (\text{A-2})$$

If none of the quantum numbers ψ' carries are unbroken, ψ' can be contracted with similar spinors. Terms such as $\psi'\psi', \psi'\xi', \xi'\xi'$ all appear in the Lagrangian. Having noted all such terms, they are then brought together as χ_i , where $\chi_1 = \psi$, $\chi_2 = \xi$ etc. There is no quantum number to differentiate between the fields, in general therefore, they will mix. The Lagrangian for such Majorana particles is given by:

$$\mathcal{L}_M = i\bar{\chi}'_{\dot{\alpha}i}\sigma^{\mu\dot{\alpha}\alpha}\partial_{\mu}\chi'_{\alpha i} + (M_1)_{ij}\chi'_{i\alpha}\chi'_{j\alpha} + (M_1^*)_{ij}\bar{\chi}'_{\dot{\alpha}i}\bar{\chi}'_{\dot{\alpha}j} \quad (\text{A-3})$$

The following transformations are now defined

$$\begin{aligned} \chi'_{\alpha i} &= U_{\chi ij}\chi_{\alpha j} , & \bar{\chi}'_{\dot{\alpha}i} &= U_{\chi ij}^*\bar{\chi}_{\dot{\alpha}j} , \\ \psi'_{\alpha i} &= U_{\psi ij}^*\chi_{\alpha j} , & \bar{\psi}'_{\dot{\alpha}i} &= U_{\psi ij}\bar{\chi}_{\dot{\alpha}j} , \\ \eta'_{\alpha i} &= U_{\eta ij}\chi_{\alpha j} , & \bar{\eta}'_{\dot{\alpha}i} &= U_{\eta ij}^*\bar{\chi}_{\dot{\alpha}j} . \end{aligned}$$

Substituting this into the Langrangian, gives

$$\begin{aligned} \mathcal{L} = & iU_{\chi ik}^* \bar{\chi}_{\dot{\alpha}k} \sigma^{\mu\dot{\alpha}\alpha} \partial_\mu U_{\chi il} \chi_{\alpha l} + iU_{\psi ik} \bar{\psi}_{\dot{\alpha}k} \sigma^{\mu\dot{\alpha}\alpha} \partial_\mu U_{\psi il}^* \psi_{\alpha l} + iU_{\eta ij}^* \bar{\eta}_{\dot{\alpha}j} \sigma^{\mu\dot{\alpha}\alpha} \partial_\mu U_{\eta ik} \eta_{\alpha j} \\ & + (M_1)_{ij} U_{\chi ik} \chi_k^\alpha U_{\chi jl} \chi_{l\alpha} + (M_1^*)_{ij} U_{\chi ik}^* \bar{\chi}_{\dot{\alpha}k} U_{\chi jl}^* \bar{\chi}_{\dot{\alpha}l} + (M_5)_{ij} U_{\psi ik}^* \psi_k^\alpha U_{\eta jl} \eta_{l\alpha} + (M_5^\dagger)_{ij} U_{\eta ik}^* \bar{\eta}_{\dot{\alpha}k} U_{\psi jl} \bar{\psi}_{\dot{\alpha}l}^{\dot{\alpha}}, \end{aligned}$$

which can be simplified as follows,

$$\begin{aligned} \mathcal{L} = & i\bar{\chi}_{\dot{\alpha}i} \sigma^{\mu\dot{\alpha}\alpha} \partial_\mu \chi_{\alpha i} + i\bar{\psi}_{\dot{\alpha}i} \sigma^{\mu\dot{\alpha}\alpha} \partial_\mu \psi_{\alpha i} + i\bar{\eta}_{\dot{\alpha}i} \sigma^{\mu\dot{\alpha}\alpha} \partial_\mu \eta_{\alpha i} \\ & + [U_\chi^T (M_1) U_\chi]_{kl} \chi_k^\alpha \chi_{l\alpha} + [U_\chi^\dagger (M_1^*) U_\chi^*]_{kl} \bar{\chi}_{\dot{\alpha}k} \bar{\chi}_{\dot{\alpha}l} + [U_\psi^\dagger (M_5) U_\eta]_{kl} \psi_k^\alpha \eta_{l\alpha} + [U_\eta^\dagger (M_5^\dagger) U_\psi]_{kl} \bar{\eta}_{\dot{\alpha}k} \bar{\psi}_{\dot{\alpha}l}^{\dot{\alpha}}. \end{aligned}$$

We observe that the unitary matrices can be defined such that the matrices are diagonal, following the procedure defined above.

A.5 CKM- and PMNS-like matrices

Consider the following Langrangian which is composed of a single family of Majorana particles, three different families of Dirac particle and two gauge bosons defined as follows,

$$\Psi_{\chi\bar{\chi}} = \begin{pmatrix} \chi_\alpha \\ \bar{\chi}^{\dot{\alpha}} \end{pmatrix} \quad \Psi_{\psi\bar{\eta}} = \begin{pmatrix} \psi_\alpha \\ \bar{\eta}^{\dot{\alpha}} \end{pmatrix} \quad \Psi_{\lambda\bar{\xi}} = \begin{pmatrix} \lambda_\alpha \\ \bar{\xi}^{\dot{\alpha}} \end{pmatrix} \quad \Psi_{\rho\bar{\zeta}} = \begin{pmatrix} \rho_\alpha \\ \bar{\zeta}^{\dot{\alpha}} \end{pmatrix} \quad X_\mu \quad Y_\mu .$$

Resulting in a (diagonalised) Lagrangian in the following form,

$$\begin{aligned} \mathcal{L} = & i\bar{\chi}_i \sigma^\mu \partial_\mu \chi_i + i\bar{\psi}_i \sigma^\mu \partial_\mu \psi_i + i\bar{\eta}_i \sigma^\mu \partial_\mu \eta_i \\ & + i\bar{\lambda}_i \sigma^\mu \partial_\mu \lambda_i + i\bar{\xi}_i \sigma^\mu \partial_\mu \xi_i + i\bar{\rho}_i \sigma^\mu \partial_\mu \rho_i + i\bar{\zeta}_i \sigma^\mu \partial_\mu \zeta_i \\ & + (\hat{M}_\chi)_{ij} \chi_i \chi_j + (\hat{M}_\chi)_{ij} \bar{\chi}_i \bar{\chi}_j + (\hat{M}_{\psi\eta})_{ij} \psi_i \eta_j + (\hat{M}_{\psi\eta})_{ij} \bar{\eta}_i \bar{\psi}_j \end{aligned}$$

$$\begin{aligned}
& + \left(\hat{M}_{\lambda\xi} \right)_{ij} \lambda_i \xi_j + \left(\hat{M}_{\lambda\xi} \right)_{ij} \bar{\xi}_i \bar{\lambda}_j + \left(\hat{M}_{\rho\zeta} \right)_{ij} \rho_i \zeta_j + \left(\hat{M}_{\rho\zeta} \right)_{ij} \bar{\zeta}_i \bar{\rho}_j \\
& + g_1 \bar{\chi}_k U_{\chi ki}^\dagger \sigma^\mu X_\mu U_{\psi im}^* \psi_m + g_2 \bar{\rho}_k U_{\rho ki}^T \sigma^\mu Y_\mu U_{\lambda im}^* \lambda_m
\end{aligned}$$

Here, it can be seen that by moving to the mass eigenstates there will be flavour mixing in the gauge interaction.

$$V_{DM} = U_{\chi ki}^\dagger U_{\psi im}^* \quad V_{DD} = U_{\rho ki}^T U_{\lambda im}^*$$

Both V_{DM} and V_{DD} are unitary matrices. We can specify a general $n \times n$ complex matrix by $2n^2$ real parameters; the condition of unitarity removes n^2 ; an orthogonal matrix is specified by $\frac{1}{2}n(n-1)$ angles, leaving the remaining $\frac{1}{2}n(n+1)$ parameters as phases. However, not all of these phases are physically observable. It is possible to redefine the phase of the Dirac spinors

$$\Psi_{\psi\bar{\eta}} \rightarrow e^{i\varphi} \Psi_{\psi\bar{\eta}} \Rightarrow \psi \rightarrow e^{i\varphi} \psi, \eta \rightarrow e^{-i\varphi} \eta$$

An overall phase is not observable, so $2n-1$ phases can be removed from V_{DD} , leaving $\frac{1}{2}(n-1)(n-2)$. It is not possible to redefine the phase of a Majorana spinor, so only n phases can be removed from V_{DM} , leaving $\frac{1}{2}n(n-1)$. The CKM matrix is of the form $V_D D$; we have $\frac{1}{2} \times 3 \times (3-1) = 3$ CKM angles and $\frac{1}{2} \times (3-1) \times (3-2)$ and one phase. The PMNS matrix of the lepton sector takes the same form as the V_{DM} , leaving $\frac{1}{2} \times 3 \times (3-1) = 3$ PMNS angles and $\frac{1}{2} \times 3 \times (3-1) = 3$ phases. It is conventional to describe the 3 PMNS phases as one ‘Dirac’ phase and two ‘Majorana’ phases.

Appendix B

\mathcal{L} -MSSM Lagrangian: Interaction Basis

The \mathcal{L} -MSSM Lagrangian contains the following kinetic and interactions terms.

Kinetic term for scalar:

$$(\mathcal{D}_\mu\varphi)^\dagger (\mathcal{D}^\mu\varphi) \tag{B-1}$$

Kinetic term for fermion:

$$i\bar{\psi}_\rho\bar{\sigma}^{\mu\rho\rho}\mathcal{D}_\mu\psi_\rho \tag{B-2}$$

Kinetic term for gaugino:

$$i\bar{\lambda}_\rho^A\bar{\sigma}^{\mu\rho\rho}\mathcal{D}_\mu\lambda_\rho^A \tag{B-3}$$

Kinetic term for gauge bosons:

$$-\frac{1}{4}F_{\mu\nu}^a F^{a\mu\nu} \tag{B-4}$$

Gaugino interactions:

$$i\sqrt{2}g\varphi_i^*T^A\psi_i^\rho\lambda_\rho^A - i\sqrt{2}g\bar{\lambda}_\rho^AT^A\varphi_i\bar{\psi}_i^\rho \tag{B-5}$$

Yukawa terms:

$$-\frac{1}{2} \frac{\partial^2 \mathcal{W}}{\partial \varphi_i \partial \varphi_j} \psi_i^\rho \psi_{j\rho} - \frac{1}{2} \frac{\partial^2 \mathcal{W}^\dagger}{\partial \varphi_i^* \partial \varphi_j^*} \bar{\psi}_{i\dot{\rho}} \bar{\psi}_j^{\dot{\rho}} \quad (\text{B-6})$$

F-terms:

$$-\sum_i \left| \frac{\partial \mathcal{W}}{\partial \varphi_i} \right|^2 \quad (\text{B-7})$$

D-terms:

$$-\sum_l \frac{g_l^2}{2} \sum_A (\varphi_i^{*a} T_l^{Aab} \varphi_i^b)^2 \quad (\text{B-8})$$

SUSY breaking terms:

$$-m_\varphi^2 |\varphi|^2, \quad -\frac{1}{2} m_\lambda \lambda \lambda, \quad -A_{ijk} \varphi_i \varphi_j \varphi_k, \quad -B_{ij} \varphi_i \varphi_j, \quad -C_i \varphi_i \quad (\text{B-9})$$

The covariant derivative is defined as,

$$\mathcal{D}_\mu = \partial_\mu - ig A_\mu^A T^A,$$

where $\mu, \nu = 0, \dots, 3$ are Lorentz indices; $\rho, \dot{\rho}, \sigma, \dot{\sigma} = 1, 2$ are Weyl indices; $i, j = 1, 2, \dots$ are generational indices; and, $A = 1, \dots, n^2 - 1$ labels the generators of the $SU(N)$ group.

The derivation of these terms is presented in Sec. 2, which is based upon the introductions and reviews of Supersymmetry presented in Refs. [4, 5].

B.1 Kinetic term for fermion

$$i\bar{\psi}_{\dot{\alpha}}\bar{\sigma}^{\mu\dot{\alpha}\alpha}\mathcal{D}_{\mu}\psi_{\alpha}$$

$$\begin{aligned}\mathcal{L}_{\text{Kinetic, Fermion}} &= i\bar{\mathcal{L}}_{\alpha\dot{\rho}}^a\bar{\sigma}^{\mu\dot{\rho}\rho}\mathcal{D}_{\mu}^ab\mathcal{L}_{\alpha\rho}^b + i\bar{E}_{i\dot{\rho}}^c\bar{\sigma}^{\mu\dot{\rho}\rho}\mathcal{D}_{\mu}E_{i\rho}^c + i\bar{H}_2^a\bar{\sigma}^{\mu\dot{\rho}\rho}\mathcal{D}_{\mu}^abH_{2\rho}^bi \\ &+ i\bar{Q}_{i\dot{\rho}}^{ax}\bar{\sigma}^{\mu\dot{\rho}\rho}\mathcal{D}_{\mu}^abQ_{i\rho}^{bx} + i\bar{D}_{i\dot{\rho}}^{cx}\bar{\sigma}^{\mu\dot{\rho}\rho}\mathcal{D}_{\mu}D_{i\rho}^{cx} + i\bar{U}_{i\dot{\rho}}^{cx}\bar{\sigma}^{\mu\dot{\rho}\rho}\mathcal{D}_{\mu}U_{i\rho}^{cx}\end{aligned}$$

where

$$\mathcal{D}_{\mu}^{ab} = \partial_{\mu}1^{ab} - \frac{ig}{\sqrt{2}}(W_{\mu}^+T^{+ab} + W_{\mu}^-T^{-ab}) - \frac{ig_2}{\cos\theta_W}Z_{\mu}(T_3^{ab} - \sin^2\theta_W Q^{ab}) - ieQ^{ab}A_{\mu}$$

$$\begin{aligned}\mathcal{L}_{\text{Kinetic, Fermion}} &= i\bar{\nu}_{L\alpha}\bar{\sigma}^{\mu}\partial_{\mu}\nu_{L\alpha} + i\bar{e}_{L\alpha}\bar{\sigma}^{\mu}\partial_{\mu}e_{L\alpha} + i\bar{e}_{Ri}\bar{\sigma}^{\mu}\partial_{\mu}e_{Ri} + i\bar{h}_2^+\bar{\sigma}^{\mu}\partial_{\mu}\tilde{h}_2^+ + i\bar{h}_2^0\bar{\sigma}^{\mu}\partial_{\mu}\tilde{h}_2^0 \\ &+ i\bar{u}_{Li}^x\bar{\sigma}^{\mu}\partial_{\mu}u_{Li}^x + i\bar{d}_{Li}^x\bar{\sigma}^{\mu}\partial_{\mu}d_{Li}^x + i\bar{u}_{Ri}^x\bar{\sigma}^{\mu}\partial_{\mu}u_{Ri}^x + i\bar{d}_{Ri}^x\bar{\sigma}^{\mu}\partial_{\mu}d_{Ri}^x \\ &- e\bar{e}_{L\alpha}\bar{\sigma}^{\mu}A_{\mu}e_{L\alpha} + e\bar{e}_{Ri}\bar{\sigma}^{\mu}A_{\mu}e_{Ri} + e\bar{h}_2^+\bar{\sigma}^{\mu}A_{\mu}\tilde{h}_2^+ \\ &+ \frac{2e}{3}\bar{u}_{Li}^x\bar{\sigma}^{\mu}A_{\mu}u_{Li}^x - \frac{e}{3}\bar{d}_{Li}^x\bar{\sigma}^{\mu}A_{\mu}d_{Li}^x - \frac{2e}{3}\bar{u}_{Ri}^x\bar{\sigma}^{\mu}A_{\mu}u_{Ri}^x + \frac{e}{3}\bar{d}_{Ri}^x\bar{\sigma}^{\mu}A_{\mu}d_{Ri}^x \\ &+ \frac{g_2}{2c_W}\bar{\nu}_{L\alpha}\bar{\sigma}^{\mu}Z_{\mu}\nu_{L\alpha} - \frac{g_2}{c_W}\left(\frac{1}{2} - s_W^2\right)\bar{e}_{L\alpha}\bar{\sigma}^{\mu}Z_{\mu}e_{L\alpha} - g_s w\bar{e}_{Ri}\bar{\sigma}^{\mu}Z_{\mu}e_{Ri} \\ &+ \frac{g_2}{c_W}\left(\frac{1}{2} - s_W^2\right)\bar{h}_2^+\bar{\sigma}^{\mu}Z_{\mu}\tilde{h}_2^+ - \frac{g_2}{2c_w}\bar{h}_2^0\bar{\sigma}^{\mu}Z_{\mu}\tilde{h}_2^0 \\ &+ \frac{g_2}{c_w}\left(\frac{1}{2} - \frac{2}{3}s_W^2\right)\bar{u}_{Li}^x\bar{\sigma}^{\mu}Z_{\mu}u_{Li}^x - \frac{g_2}{c_w}\left(\frac{1}{2} - \frac{1}{3}s_W^2\right)\bar{d}_{Li}^x\bar{\sigma}^{\mu}Z_{\mu}d_{Li}^x \\ &+ \frac{2}{3}g_s w\bar{u}_{Ri}^x\bar{\sigma}^{\mu}Z_{\mu}u_{Ri}^x - \frac{1}{3}g_s w\bar{d}_{Ri}^x\bar{\sigma}^{\mu}Z_{\mu}d_{Ri}^x \\ &+ \frac{g_2}{\sqrt{2}}\bar{\nu}_{L\alpha}\bar{\sigma}^{\mu}W_{\mu}^+e_{L\alpha} + \frac{g_2}{\sqrt{2}}\bar{e}_{L\alpha}\bar{\sigma}^{\mu}W_{\mu}^-\nu_{L\alpha} + \frac{g_2}{\sqrt{2}}\bar{h}_2^+\bar{\sigma}^{\mu}W_{\mu}^+\tilde{h}_2^0 + \frac{g_2}{\sqrt{2}}\bar{h}_2^0\bar{\sigma}^{\mu}W_{\mu}^-\tilde{h}_2^+ \\ &+ \frac{g_2}{\sqrt{2}}\bar{u}_{Li}^x\bar{\sigma}^{\mu}W_{\mu}^+d_{Li}^x + \frac{g_2}{\sqrt{2}}\bar{d}_{Li}^x\bar{\sigma}^{\mu}W_{\mu}^-u_{Li}^x \\ &+ \frac{g_3}{2}\bar{u}_{Li}^x\bar{\sigma}^{\mu}G_{\mu}^{(R)}\lambda^{(R)xy}u_{Li}^y + \frac{g_3}{2}\bar{d}_{Li}^x\bar{\sigma}^{\mu}G_{\mu}^{(R)}\lambda^{(R)xy}d_{Li}^y + \frac{g_3}{2}\bar{u}_{Ri}^x\bar{\sigma}^{\mu}G_{\mu}^{(R)}\lambda^{*(R)xy}u_{Ri}^y + \frac{g_3}{2}\bar{d}_{Ri}^x\bar{\sigma}^{\mu}G_{\mu}^{(R)}\lambda^{*(R)xy}d_{Ri}^y\end{aligned}$$

B.2 Kinetic term for gaugino

$$i\bar{\lambda}_\rho^A \bar{\sigma}^{\mu\rho\rho} \mathcal{D}_\mu \lambda_\rho^A$$

$$\mathcal{L}_{\text{Kinetic, Gaugino}} = i\bar{\tilde{B}}_\rho \bar{\sigma}^{\mu\rho\rho} \mathcal{D}_\mu \tilde{B}_\rho + i\bar{\tilde{W}}_\rho^{(\Gamma)} \bar{\sigma}^{\mu\rho\rho} \mathcal{D}_\mu \tilde{W}_\rho^{(\Gamma)} + i\bar{\tilde{G}}_\rho^{(R)} \bar{\sigma}^{\mu\rho\rho} \mathcal{D}_\mu \tilde{G}_\rho^{(R)}$$

$$\begin{aligned} \mathcal{L}_{\text{Kinetic, Gaugino}} &= i\bar{\tilde{B}}_\rho \bar{\sigma}^{\mu\rho\rho} \partial_\mu \tilde{B}_\rho + i\bar{\tilde{W}}_\rho^0 \bar{\sigma}^{\mu\rho\rho} \partial_\mu \tilde{W}_\rho^0 \\ &+ i\bar{\tilde{W}}_\rho^+ \bar{\sigma}^{\mu\rho\rho} \partial_\mu \tilde{W}_\rho^+ + i\bar{\tilde{W}}_\rho^- \bar{\sigma}^{\mu\rho\rho} \partial_\mu \tilde{W}_\rho^- + i\bar{\tilde{G}}_\rho^{(R)} \bar{\sigma}^{\mu\rho\rho} \partial_\mu \tilde{G}_\rho^{(R)} \\ &+ g_2 s_w \bar{\tilde{W}}^+ \bar{\sigma}^\mu A_\mu \tilde{W}^+ - g_2 s_w \bar{\tilde{W}}^- \bar{\sigma}^\mu A_\mu \tilde{W}^- \\ &+ g_2 c_w \bar{\tilde{W}}^+ \bar{\sigma}^\mu Z_\mu \tilde{W}^+ - g_2 c_w \bar{\tilde{W}}^- \bar{\sigma}^\mu Z_\mu \tilde{W}^- \\ &+ g_2 \bar{\tilde{W}}^- \bar{\sigma}^\mu W_\mu^- \tilde{W}^0 - g_2 \bar{\tilde{W}}^+ \bar{\sigma}^\mu W_\mu^+ \tilde{W}^0 \\ &+ g_2 \bar{\tilde{W}}^0 \bar{\sigma}^\mu W_\mu^+ \tilde{W}^- - g_2 \bar{\tilde{W}}^0 \bar{\sigma}^\mu W_\mu^- \tilde{W}^+ \\ &+ i g_3 \varepsilon_{RSQ} \bar{\tilde{G}}^{(R)} \bar{\sigma}^\mu G_\mu^{(S)} \tilde{G}^{(Q)} \end{aligned}$$

B.3 Kinetic term for scalar

$$(\mathcal{D}_\mu \varphi)^\dagger (\mathcal{D}^\mu \varphi)$$

$$\begin{aligned} \mathcal{L}_{\text{Kinetic, Scalar}} = & \left(\mathcal{D}_\mu^{ab} \tilde{\mathcal{L}}_\alpha^b \right)^\dagger \left(\mathcal{D}^{\mu ad} \tilde{\mathcal{L}}_\alpha^d \right) + \left(\mathcal{D}_\mu \tilde{E}_i^c \right)^* \left(\mathcal{D}^\mu \tilde{E}_i^c \right) + \left(\mathcal{D}_\mu^{ab} H_2^b \right)^\dagger \left(\mathcal{D}^{\mu ad} H_2^d \right) \\ & + \left(\mathcal{D}_\mu^{ab} \tilde{Q}_i^b \right)^\dagger \left(\mathcal{D}^{\mu ad} \tilde{Q}_i^d \right) + \left(\mathcal{D}_\mu \tilde{D}_i^c \right)^* \left(\mathcal{D}^\mu \tilde{D}_i^c \right) + \left(\mathcal{D}_\mu \tilde{U}_i^c \right)^* \left(\mathcal{D}^\mu \tilde{E}_i^c \right) \end{aligned}$$

$$\begin{aligned} \mathcal{L}_{\text{Kinetic, Scalar}} = & + \partial_\mu \tilde{\nu}_{L\alpha}^* \partial^\mu \tilde{\nu}_{L\alpha} + \partial_\mu \tilde{e}_{L\alpha}^* \partial^\mu \tilde{e}_{L\alpha} + \partial_\mu \tilde{e}_{Ri}^* \partial^\mu \tilde{e}_{Ri} \\ & + \partial_\mu h_2^{+*} \partial^\mu h_2^+ + \partial_\mu h_2^{0*} \partial^\mu h_2^0 + \partial_\mu \tilde{u}_{Li}^{*x} \partial^\mu \tilde{u}_{Li}^x + \partial_\mu \tilde{d}_{Li}^{*x} \partial^\mu \tilde{d}_{Li}^x \\ & + \partial_\mu \tilde{u}_{Ri}^x \partial^\mu \tilde{u}_{Ri}^{*x} + \partial_\mu \tilde{d}_{Ri}^x \partial^\mu \tilde{d}_{Ri}^{*x} \\ & + ie \partial_\mu \tilde{e}_{L\alpha}^* A^\mu \tilde{e}_{L\alpha} - ie A_\mu \tilde{e}_{L\alpha}^* \partial^\mu \tilde{e}_{L\alpha} - ie \partial_\mu \tilde{e}_{Ri} A^\mu \tilde{e}_{Ri}^* + ie A_\mu \tilde{e}_{Ri} \partial^\mu \tilde{e}_{Ri}^* \\ & - ie \partial_\mu h_2^{+*} A^\mu h_2^+ + ie A_\mu h_2^{+*} \partial^\mu h_2^+ \\ & - \frac{2ie}{3} \partial_\mu \tilde{u}_{Li}^{*x} A^\mu \tilde{u}_{Li}^x + \frac{2ie}{3} A^\mu \tilde{u}_{Li}^{*x} \partial_\mu \tilde{u}_{Li}^x - \frac{ie}{3} \partial_\mu \tilde{d}_{Li}^{*x} A^\mu \tilde{d}_{Li}^x - \frac{ie}{3} A^\mu \tilde{d}_{Li}^{*x} \partial_\mu \tilde{d}_{Li}^x \\ & + \frac{2ie}{3} \partial_\mu \tilde{u}_{Ri}^x A^\mu \tilde{u}_{Ri}^{*x} - \frac{2ie}{3} A^\mu \tilde{u}_{Ri}^x \partial_\mu \tilde{u}_{Ri}^{*x} - \frac{ie}{3} \partial_\mu \tilde{d}_{Ri}^x A^\mu \tilde{d}_{Ri}^{*x} + \frac{ie}{3} A^\mu \tilde{d}_{Ri}^x \partial_\mu \tilde{d}_{Ri}^{*x} \\ & - \frac{ig_2}{2c_W} \partial_\mu \tilde{\nu}_{L\alpha}^* Z^\mu \tilde{\nu}_{L\alpha} + \frac{ig_2}{2c_W} Z_\mu \tilde{\nu}_{L\alpha}^* \partial^\mu \tilde{\nu}_{L\alpha} + \frac{ig_2}{c_W} \left(\frac{1}{2} - s_w^2 \right) \partial_\mu \tilde{e}_{L\alpha}^* Z^\mu \tilde{e}_{L\alpha} - \frac{ig_2}{c_W} \left(\frac{1}{2} - s_w^2 \right) Z_\mu \tilde{e}_{L\alpha}^* \partial^\mu \tilde{e}_{L\alpha} \\ & - ig s_w Z_\mu \tilde{e}_{Ri} \partial^\mu \tilde{e}_{Ri}^* + ig s_w \partial_\mu \tilde{e}_{Ri} Z^\mu \tilde{e}_{Ri}^* - \frac{ig_2}{c_w} \left(\frac{1}{2} - s_w^2 \right) \partial_\mu h_2^{+*} Z^\mu h_2^+ + \frac{ig_2}{c_w} \left(\frac{1}{2} - s_w^2 \right) Z_\mu h_2^{+*} \partial^\mu h_2^+ \\ & + \frac{ig_2}{2c_w} \partial_\mu h_2^{0*} Z^\mu h_2^0 - \frac{ig_2}{2c_w} Z_\mu h_2^{0*} \partial^\mu h_2^0 \\ & - \frac{ig_2}{c_w} \left(\frac{1}{2} - \frac{2}{3} s_w^2 \right) \partial_\mu \tilde{u}_{Li}^{*x} Z^\mu \tilde{u}_{Li}^x + \frac{ig_2}{c_w} \left(\frac{1}{2} - \frac{2}{3} s_w^2 \right) Z_\mu \tilde{u}_{Li}^{*x} \partial^\mu \tilde{u}_{Li}^x \\ & + \frac{ig_2}{c_w} \left(\frac{1}{2} - \frac{1}{3} s_w^2 \right) \partial_\mu \tilde{d}_{Li}^{*x} Z^\mu \tilde{d}_{Li}^x - \frac{ig_2}{c_w} \left(\frac{1}{2} - \frac{1}{3} s_w^2 \right) Z_\mu \tilde{d}_{Li}^{*x} \partial^\mu \tilde{d}_{Li}^x \\ & - \frac{2i}{3} g s_w \partial_\mu \tilde{u}_{Ri}^x Z^\mu \tilde{u}_{Ri}^{*x} + \frac{2i}{3} g s_w Z_\mu \tilde{u}_{Ri}^x \partial^\mu \tilde{u}_{Ri}^{*x} - \frac{i}{3} g s_w Z_\mu \tilde{d}_{Ri}^x \partial^\mu \tilde{d}_{Ri}^{*x} + \frac{i}{3} g s_w \partial_\mu \tilde{d}_{Ri}^x Z^\mu \tilde{d}_{Ri}^{*x} \end{aligned}$$

$$\begin{aligned}
& + \frac{ig_2}{\sqrt{2}} W_\mu^- \tilde{e}_{L\alpha}^* \partial^\mu \tilde{\nu}_{L\alpha} - \frac{ig_2}{\sqrt{2}} \partial_\mu \tilde{\nu}_{L\alpha}^* W^{+\mu} \tilde{e}_{L\alpha} + \frac{ig_2}{\sqrt{2}} W_\mu^+ \tilde{\nu}_{L\alpha}^* \partial^\mu \tilde{e}_{L\alpha} - \frac{ig_2}{\sqrt{2}} \partial_\mu \tilde{e}_{L\alpha}^* W^{-\mu} \tilde{\nu}_{L\alpha} \\
& + \frac{ig_2}{\sqrt{2}} W_\mu^- h_2^{0*} \partial^\mu h_2^+ - \frac{ig_2}{\sqrt{2}} \partial_\mu h_2^{+\mu} W^{+\mu} h_2^0 + \frac{ig_2}{\sqrt{2}} W_\mu^+ h_2^{+\mu} \partial^\mu h_2^0 - \frac{ig_2}{\sqrt{2}} \partial_\mu h_2^{0*} W^{-\mu} h_2^+ \\
& + \frac{ig_2}{\sqrt{2}} W_\mu^- \tilde{d}_{Li}^{*x} \partial^\mu \tilde{u}_{Li}^x - \frac{ig_2}{\sqrt{2}} \partial_\mu \tilde{d}_{Li}^{*x} W^{-\mu} \tilde{u}_{Li}^x + \frac{ig_2}{\sqrt{2}} W_\mu^+ \tilde{u}_{Li}^{*x} \partial^\mu \tilde{d}_{Li}^x - \frac{ig_2}{\sqrt{2}} \partial_\mu \tilde{u}_{Li}^{*x} W^{+\mu} \tilde{d}_{Li}^x \\
& + \frac{ig_3}{2} G_\mu^{(R)} \tilde{u}^{*z} \lambda^{\dagger(R)zx} \partial^\mu \tilde{u}_{Li}^x - \frac{ig_3}{2} \partial_\mu \tilde{u}_{Li}^{*x} G^{\mu(R)} \lambda^{(R)xy} \tilde{u}_{Li}^y \\
& + \frac{ig_3}{2} G_\mu^{(R)} \tilde{d}^{*z} \lambda^{\dagger(R)zx} \partial^\mu \tilde{d}_{Li}^x - \frac{ig_3}{2} \partial_\mu \tilde{d}_{Li}^{*x} G^{\mu(R)} \lambda^{(R)xy} \tilde{d}_{Li}^y \\
& + \frac{ig_3}{2} G_\mu^{(R)} \tilde{u}_{Ri}^z \lambda^{(R)zx} \partial^\mu \tilde{u}_{Ri}^{*x} - \frac{ig_3}{2} \partial_\mu \tilde{u}_{Ri}^x G^{\mu(R)} \lambda^{\dagger(R)xy} \tilde{u}_{Ri}^{*y} \\
& + \frac{ig_3}{2} G_\mu^{(R)} \tilde{d}_{Ri}^z \lambda^{(R)zx} \partial^\mu \tilde{d}_{Ri}^{*x} - \frac{ig_3}{2} \partial_\mu \tilde{d}_{Ri}^x G^{\mu(R)} \lambda^{\dagger(R)xy} \tilde{d}_{Ri}^{*y} \\
& + e^2 A_\mu \tilde{e}_{L\alpha}^* A^\mu \tilde{e}_{L\alpha} + e^2 A_\mu \tilde{e}_{Ri} A^\mu \tilde{e}_{Ri}^* + e^2 A_\mu h_2^{+\mu} A^\mu h_2^+ \\
& + \frac{4e^2}{9} A_\mu \tilde{u}_{Li}^{*x} A^\mu \tilde{u}_{Li}^x + \frac{e^2}{9} A_\mu \tilde{d}_{Li}^{*x} A^\mu \tilde{d}_{Li}^x + \frac{4e^2}{9} A_\mu \tilde{u}_{Ri}^x A^\mu \tilde{u}_{Ri}^{*x} + \frac{e^2}{9} A_\mu \tilde{d}_{Ri}^x A^\mu \tilde{d}_{Ri}^{*x} \\
& + \frac{g_2^2}{4c_w^2} Z_\mu \tilde{\nu}_{L\alpha}^* Z^\mu \tilde{\nu}_{L\alpha} + \frac{g_2^2}{c_w^2} \left(\frac{1}{2} - s_w^2 \right)^2 Z_\mu \tilde{e}_{L\alpha}^* Z^\mu \tilde{e}_{L\alpha} \\
& + g^2 s_w^2 Z_\mu \tilde{e}_{Ri} Z^\mu \tilde{e}_{Ri}^* + \frac{g_2^2}{4c_w^2} Z_\mu h_2^{0*} Z^\mu h_2^0 \\
& + \frac{g_2^2}{c_w^2} \left(\frac{1}{2} - s_w^2 \right)^2 Z_\mu h_2^{+\mu} Z^\mu h_2^+ + \frac{g_2^2}{c_w^2} \left(\frac{1}{2} - \frac{2}{3} s_w^2 \right)^2 Z_\mu \tilde{u}_{Li}^{*x} Z^\mu \tilde{u}_{Li}^x \\
& + \frac{g_2^2}{c_w^2} \left(\frac{1}{2} - \frac{1}{3} s_w^2 \right)^2 Z_\mu \tilde{d}_{Li}^{*x} Z^\mu \tilde{d}_{Li}^x + \frac{4}{9} g^2 s_w^2 Z_\mu \tilde{u}_{Ri}^x Z^\mu \tilde{u}_{Ri}^{*x} \\
& + \frac{1}{9} g^2 s_w^2 Z_\mu \tilde{d}_{Ri}^x Z^\mu \tilde{d}_{Ri}^{*x} \\
& + \frac{eg_2}{c_w} \left(\frac{1}{2} - s_w^2 \right)^2 A_\mu \tilde{e}_{L\alpha}^* Z^\mu \tilde{e}_{L\alpha} + \frac{eg_2}{c_w} \left(\frac{1}{2} - s_w^2 \right)^2 Z_\mu \tilde{e}_{L\alpha}^* A^\mu \tilde{e}_{L\alpha} - eg s_w Z_\mu \tilde{e}_{Ri} A^\mu \tilde{e}_{Ri}^* - eg s_w A_\mu \tilde{e}_{Ri} Z^\mu \tilde{e}_{Ri}^* \\
& + \frac{eg_2}{c_w} \left(\frac{1}{2} - s_w^2 \right)^2 Z_\mu h_2^{+\mu} A^\mu h_2^+ + \frac{eg_2}{c_w} \left(\frac{1}{2} - s_w^2 \right)^2 A_\mu h_2^{+\mu} Z^\mu h_2^+ \\
& + \frac{2eg_2}{3c_w} \left(\frac{1}{2} - \frac{2}{3} s_w^2 \right) Z_\mu \tilde{u}_{Li}^{*x} A^\mu \tilde{u}_{Li}^x + \frac{2eg_2}{3c_w} \left(\frac{1}{2} - \frac{2}{3} s_w^2 \right) A_\mu \tilde{u}_{Li}^{*x} Z^\mu \tilde{u}_{Li}^x
\end{aligned}$$

$$\begin{aligned}
& + \frac{eg_2}{3c_w} \left(\frac{1}{2} - \frac{1}{3}s_w^2 \right) Z_\mu \tilde{d}_{Li}^{*x} A^\mu \tilde{d}_{Li}^x + \frac{eg_2}{3c_w} \left(\frac{1}{2} - \frac{1}{3}s_w^2 \right) A_\mu \tilde{d}_{Li}^{*x} Z^\mu \tilde{d}_{Li}^x \\
& - \frac{4}{9} eg_s w Z_\mu \tilde{u}_{Ri}^x A^\mu \tilde{u}_{Ri}^{*x} - \frac{4}{9} eg_s w A_\mu \tilde{u}_{Ri}^x Z^\mu \tilde{u}_{Ri}^{*x} - \frac{1}{9} eg_s w Z_\mu \tilde{d}_{Ri}^x A^\mu \tilde{d}_{Ri}^{*x} - \frac{1}{9} eg_s w A_\mu \tilde{d}_{Ri}^x Z^\mu \tilde{d}_{Ri}^{*x} \\
& + \frac{g_2^2}{2} W_\mu^+ \tilde{\nu}_{L\alpha}^* W^{-\mu} \tilde{\nu}_{L\alpha} + \frac{g_2^2}{2} W_\mu^- \tilde{e}_{L\alpha}^* W^{+\mu} \tilde{e}_{L\alpha} + \frac{g_2^2}{2} W_\mu^- h_2^{0*} W^{+\mu} h_2^0 + \frac{g_2^2}{2} W_\mu^+ h_2^{+*} W^{-\mu} h_2^+ \\
& \quad + \frac{g_2^2}{2} W_\mu^- \tilde{d}_{Li}^{*x} W^{+\mu} \tilde{d}_{Li}^x + \frac{g_2^2}{2} W_\mu^+ \tilde{u}_{Li}^{*x} W^{-\mu} \tilde{u}_{Li}^x \\
& - \frac{eg_2}{\sqrt{2}} A_\mu \tilde{e}_{L\alpha}^* W^{-\mu} \tilde{\nu}_{L\alpha} - \frac{eg_2}{\sqrt{2}} W_\mu^+ \tilde{\nu}_{L\alpha}^* A^\mu \tilde{e}_{L\alpha} + \frac{eg_2}{\sqrt{2}} A_\mu h_2^{+*} W^{-\mu} h_2^0 + \frac{eg_2}{\sqrt{2}} W_\mu^+ h_2^{0*} A^\mu h_2^+ \\
& + \frac{\sqrt{2}}{3} eg_2 A_\mu \tilde{u}_{Li}^{*x} W^{+\mu} \tilde{d}_{Li}^x + \frac{\sqrt{2}}{3} eg_2 W^{-\mu} \tilde{d}_{Li}^{*x} A_\mu \tilde{u}_{Li}^x - \frac{1}{3\sqrt{2}} eg_2 A_\mu \tilde{d}_{Li}^{*x} W^{-\mu} \tilde{u}_{Li}^x - \frac{1}{3\sqrt{2}} eg_2 W^{+\mu} \tilde{u}_{Li}^{*x} A_\mu \tilde{d}_{Li}^x \\
& \quad + \frac{g_2^2}{2\sqrt{2}c_w} Z_\mu \tilde{\nu}_{L\alpha}^* W^{+\mu} \tilde{e}_{L\alpha} + \frac{g_2^2}{2\sqrt{2}c_w} W^{-\mu} \tilde{e}_{L\alpha}^* Z_\mu \tilde{\nu}_{L\alpha} \\
& - \frac{g_2^2}{\sqrt{2}c_w} \left(\frac{1}{2} - s_w^2 \right) W^{+\mu} \tilde{\nu}_{L\alpha}^* Z_\mu \tilde{e}_{L\alpha} - \frac{g_2^2}{\sqrt{2}c_w} \left(\frac{1}{2} - s_w^2 \right) Z_\mu \tilde{e}_{L\alpha}^* W^{-\mu} \tilde{\nu}_{L\alpha} \\
& + \frac{g_2^2}{\sqrt{2}c_w} \left(\frac{1}{2} - s_w^2 \right) Z_\mu h_2^{+*} W^{+\mu} h_2^0 + \frac{g_2^2}{\sqrt{2}c_w} \left(\frac{1}{2} - s_w^2 \right) W^{-\mu} h_2^{0*} Z_\mu h_2^+ \\
& \quad - \frac{g_2^2}{2\sqrt{2}c_w} W^{+\mu} h_2^{+*} Z_\mu h_2^0 - \frac{g_2^2}{2\sqrt{2}c_w} Z_\mu h_2^{0*} W^{-\mu} h_2^+ \\
& + \frac{g_2^2}{\sqrt{2}c_w} \left(\frac{1}{2} - \frac{2}{3}s_w^2 \right) Z_\mu \tilde{u}_{Li}^{*x} W^{+\mu} \tilde{d}_{Li}^x + \frac{g_2^2}{\sqrt{2}c_w} \left(\frac{1}{2} - \frac{2}{3}s_w^2 \right) W^{-\mu} \tilde{d}_{Li}^{*x} Z_\mu \tilde{u}_{Li}^x \\
& - \frac{g_2^2}{\sqrt{2}c_w} \left(\frac{1}{2} - \frac{1}{3}s_w^2 \right) W^{+\mu} \tilde{u}_{Li}^{*x} Z_\mu \tilde{d}_{Li}^x - \frac{g_2^2}{\sqrt{2}c_w} \left(\frac{1}{2} - \frac{1}{3}s_w^2 \right) Z_\mu \tilde{d}_{Li}^{*x} W^{-\mu} \tilde{u}_{Li}^x \\
& + \frac{g_2 g_3}{2c_w} \left(\frac{1}{2} - \frac{2}{3}s_w^2 \right) G_\mu^{(R)} \tilde{u}_{Li}^{*z} \lambda^{\dagger(R)zx} Z^\mu \tilde{u}_{Li}^x + \frac{g_2 g_3}{2c_w} \left(\frac{1}{2} - \frac{2}{3}s_w^2 \right) Z_\mu \tilde{u}_{Li}^{*z} G^{\mu(R)} \lambda^{(R)zx} \tilde{u}_{Li}^x \\
& \quad + \frac{g_2 g_3}{2\sqrt{2}} G_\mu^{(R)} \tilde{u}_{Li}^{*z} \lambda^{\dagger(R)zx} W^{+\mu} \tilde{d}_{Li}^x + \frac{g_2 g_3}{2\sqrt{2}} W_\mu^- \tilde{d}_{Li}^{*z} G^{\mu(R)} \lambda^{\dagger(R)zx} \tilde{u}_{Li}^x \\
& \quad + \frac{g_2 g_3}{2\sqrt{2}} G_\mu^{(R)} \tilde{d}_{Li}^{*z} \lambda^{\dagger(R)zx} W^{-\mu} \tilde{u}_{Li}^x + \frac{g_2 g_3}{2\sqrt{2}} W_\mu^+ \tilde{u}_{Li}^{*z} G^{\mu(R)} \lambda^{(R)xy} \tilde{d}_{Li}^y \\
& - \frac{g_2 g_3}{2c_w} \left(\frac{1}{2} - \frac{1}{3}s_w^2 \right) G_\mu^{(R)} \tilde{d}_{Li}^{*z} \lambda^{\dagger(R)zx} Z^\mu \tilde{d}_{Li}^x - \frac{g_2 g_3}{2c_w} \left(\frac{1}{2} - \frac{1}{3}s_w^2 \right) Z_\mu \tilde{d}_{Li}^{*z} G^{\mu(R)} \lambda^{(R)xy} \tilde{d}_{Li}^y \\
& \quad + \frac{g g_3 s_w}{3} G_\mu^{(R)} \tilde{u}_{Ri}^z \lambda^{\dagger(R)zx} Z^\mu \tilde{u}_{Ri}^{*x} + \frac{g g_3 s_w}{3} Z_\mu \tilde{u}_{Ri}^x G^{\mu(R)} \lambda^{\dagger(R)xy} \tilde{u}_{Ri}^y
\end{aligned}$$

$$\begin{aligned}
& -\frac{gg_3s_w}{6}G_\mu^{(R)}\tilde{d}_{Ri}^z\lambda^{(R)zx}Z^\mu\tilde{d}_{Ri}^{*x}-\frac{gg_3s_w}{6}Z_\mu\tilde{d}_{Ri}^xG^{(R)\mu}\lambda^{\dagger(R)xy}\tilde{d}_{Ri}^{*y} \\
& +\frac{eg_3}{3}G_\mu^{(R)}\tilde{u}_{Li}^{*z}\lambda^{\dagger(R)zx}A^\mu\tilde{u}_{Li}^x+\frac{eg_3}{3}A_\mu\tilde{u}_{Li}^{*x}G^{\mu(R)}\lambda^{(R)xy}\tilde{u}_{Li}^y \\
& -\frac{eg_3}{6}G_\mu^{(R)}\tilde{d}_{Li}^{*z}\lambda^{\dagger(R)zx}A^\mu\tilde{d}_{Li}^x-\frac{eg_3}{6}A_\mu\tilde{d}_{Li}^{*x}G^{\mu(R)}\lambda^{(R)xy}\tilde{d}_{Li}^y \\
& -\frac{eg_3}{3}G_\mu^{(R)}\tilde{u}_{Ri}^z\lambda^{(R)zx}A^\mu\tilde{u}_{Ri}^{*x}-\frac{eg_3}{3}A_\mu\tilde{u}_{Ri}^xG^{\mu(R)}\lambda^{\dagger(R)xy}\tilde{u}_{Ri}^{*y} \\
& +\frac{eg_3}{6}G_\mu^{(R)}\tilde{d}_{Ri}^z\lambda^{(R)zx}A^\mu\tilde{d}_{Ri}^{*x}+\frac{eg_3}{6}A_\mu\tilde{d}_{Ri}^xG^{(R)\mu}\lambda^{\dagger(R)xy}\tilde{d}_{Ri}^{*y} \\
& +\frac{g_3^2}{4}G_\mu^{(R)}\tilde{u}_{Li}^{*z}\lambda^{\dagger(R)zx}G^\mu(S)\lambda^{(S)xy}\tilde{u}_{Li}^y+\frac{g_3^2}{4}G_\mu^{(R)}\tilde{d}_{Li}^{*z}\lambda^{\dagger(R)zx}G^\mu(S)\lambda^{(S)xy}\tilde{d}_{Li}^y \\
& +\frac{g_3^2}{4}G_\mu^{(R)}\tilde{u}_{Ri}^z\lambda^{(R)zx}G^\mu(S)\lambda^{\dagger(S)xy}\tilde{u}_{Ri}^{*y}+\frac{g_3^2}{4}G_\mu^{(R)}\tilde{d}_{Ri}^z\lambda^{(R)zx}G^\mu(S)\lambda^{\dagger(S)xy}\tilde{d}_{Ri}^{*y}
\end{aligned}$$

B.4 Kinetic term for gauge bosons

$$-\frac{1}{4}F_{\mu\nu}^a F^{a\mu\nu}$$

$$\mathcal{L}_{\text{kinetic, gauge boson}} =$$

$$-\frac{1}{4}(\partial_\mu B_\nu - \partial_\nu B_\mu)(\partial^\mu B^\nu - \partial^\nu B^\mu)$$

$$-\frac{1}{4}(\partial_\mu W_\nu^{(\Gamma)} - \partial_\nu W_\mu^{(\Gamma)} + g_2 \varepsilon_{\Gamma\Theta\Pi} W_\mu^{(\Theta)} W_\nu^{(\Pi)}) (\partial_\mu W^{(\Gamma)\nu} - \partial_\nu W^{(\Gamma)\mu} + g_2 \varepsilon_{\Gamma\Theta\Pi} W^{(\Theta)\mu} W^{(\Pi)\nu})$$

$$-\frac{1}{4}(\partial_\mu G_\nu^{(R)} - \partial_\nu G_\mu^{(R)} + g_3 f_{RSQ} G_\mu^{(S)} G_\nu^{(Q)}) (\partial^\mu G^{(R)\nu} - \partial^\nu G^{(R)\mu} + g_3 f_{RSQ} G^{(S)\mu} G^{(Q)\nu})$$

$$W_\mu^1 = \frac{1}{\sqrt{2}}(W_\mu^+ + W_\mu^-) \quad W_\mu^3 = c_w Z_\mu + s_w A_\mu$$

$$W_\mu^2 = \frac{i}{\sqrt{2}}(W_\mu^+ - W_\mu^-) \quad B_\mu = -s_w Z_\mu + c_w A_\mu$$

$$\mathcal{L}_{\text{kinetic, gauge boson}} =$$

$$-\frac{1}{4}(\partial_\mu Z_\nu - \partial_\nu Z_\mu)(\partial^\mu Z^\nu - \partial^\nu Z^\mu) - \frac{1}{4}(\partial_\mu A_\nu - \partial_\nu A_\mu)(\partial^\mu A^\nu - \partial^\nu A^\mu)$$

$$-\frac{1}{2}(\partial_\mu W_\nu^+ - \partial_\nu W_\mu^+)(\partial^\mu W^{-\nu} - \partial^\nu W^{-\mu})$$

$$+2g_2 s_w \partial_\mu A_\nu W^{+\mu} W^{-\nu} - 2g_2 s_w \partial_\mu A_\nu W^{-\mu} W^{+\nu} + 2g_2 s_w \partial_\mu W_\nu^+ W^{-\mu} A_\nu - 2g_2 s_w \partial_\mu W_\nu^+ A_\mu W^{-\nu}$$

$$+2g_2 s_w \partial_\mu W_\nu^- A^\mu W^{+\nu} - 2g_2 s_w \partial_\mu W_\nu^- W^{+\mu} A^\nu$$

$$+2g_2 c_w \partial_\mu Z_\nu W^{+\mu} W^{-\nu} - 2g_2 c_w \partial_\mu Z_\nu W^{-\mu} W^{+\nu} + 2g_2 c_w \partial_\mu W_\nu^+ W^{-\mu} Z_\nu - 2g_2 c_w \partial_\mu W_\nu^+ Z_\mu W^{-\nu}$$

$$+2g_2 c_w \partial_\mu W_\nu^- Z^\mu W^{+\nu} - 2g_2 c_w \partial_\mu W_\nu^- W^{+\mu} Z^\nu$$

$$-g_2^2 c_w^2 Z_\mu Z^\mu W_\nu^- W^{+\nu} - g_2^2 c_w^2 Z_\mu Z^\nu W_\nu^- W^{+\mu} - g_2^2 s_w^2 A_\mu A^\mu W_\nu^- W^{+\nu} - g_2^2 s_w^2 A_\mu A^\nu W_\nu^- W^{+\mu}$$

$$\begin{aligned}
& -2g_2^2 c_w s_w A_\mu Z^\mu W_\nu^- W^{+\nu} - g_2^2 c_w s_w Z_\mu A^\nu W_\nu^- W^{+\mu} - g_2^2 c_w s_w Z_\mu A^\nu W_\nu^+ W^{-\mu} \\
& + \frac{3}{2} g_2^2 W_\mu^+ W^{+\mu} W_\nu^- W^{-\nu} - \frac{3}{2} g_2^2 W_\mu^+ W^{-\mu} W_\nu^+ W^{-\nu} \\
& - \frac{1}{4} (\partial_\mu G_\nu^{(R)} - \partial_\nu G_\mu^{(R)}) (\partial^\mu G^{(R)\nu} - \partial^\nu G^{(R)\mu}) \\
& - \frac{g_3}{2} f_{RSQ} \partial^\mu G^{(R)\nu} G_\mu^{(S)} G_\nu^{(Q)} + \frac{g_3}{2} f_{RSQ} \partial^\nu G^{(R)\mu} G_\mu^{(S)} G_\nu^{(Q)} - \frac{g_3^2}{4} f_{RSQ} f_{RTW} G_\mu^{(S)} G_\nu^{(Q)} G^{(T)\mu} G^{(W)\nu}
\end{aligned}$$

B.5 Gaugino interactions

$$i\sqrt{2}g\varphi_i^*T^A\psi_i^\rho\lambda_\rho^A - i\sqrt{2}g\bar{\lambda}_\rho T^A\varphi_i\bar{\psi}_i^\rho$$

$$\mathcal{L}_{\text{Gaugino interaction}} =$$

$$\begin{aligned} & -\frac{ig}{\sqrt{2}}\tilde{\nu}_{L\alpha}^*\nu_{L\alpha}\tilde{B} - \frac{ig}{\sqrt{2}}\tilde{e}_{L\alpha}^*e_{L\alpha}\tilde{B} + \frac{ig}{\sqrt{2}}\tilde{e}_{Ri}^*e_{Ri}\tilde{B} + \frac{ig}{\sqrt{2}}h_2^{+*}\tilde{h}_2^+\tilde{B} + \frac{ig}{\sqrt{2}}h_2^{0*}\tilde{h}_2^0\tilde{B} \\ & + \frac{ig}{\sqrt{2}}\tilde{\nu}_{L\alpha}\bar{\nu}_{L\alpha}\tilde{\bar{B}} + \frac{ig}{\sqrt{2}}\tilde{e}_{L\alpha}\bar{e}_{L\alpha}\tilde{\bar{B}} - \frac{ig}{\sqrt{2}}\tilde{e}_{Ri}^*\bar{e}_{Ri}\tilde{\bar{B}} - \frac{ig}{\sqrt{2}}h_2^+\tilde{h}_2^+\tilde{\bar{B}} - \frac{ig}{\sqrt{2}}h_2^0\tilde{h}_2^0\tilde{\bar{B}} \\ & + \frac{ig}{3\sqrt{2}}\tilde{u}_{Li}^*u_{Li}\tilde{B} + \frac{ig}{3\sqrt{2}}\tilde{d}_{Li}^*d_{Li}\tilde{B} + \frac{ig\sqrt{2}}{3}\tilde{d}_{Ri}d_{Ri}\tilde{B} - \frac{ig\sqrt{2}}{3}\tilde{u}_{Ri}u_{Ri}\tilde{B} \\ & - \frac{ig}{3\sqrt{2}}\tilde{u}_{Li}\bar{u}_{Li}\tilde{\bar{B}} - \frac{ig}{3\sqrt{2}}\tilde{d}_{Li}\bar{d}_{Li}\tilde{\bar{B}} - \frac{ig\sqrt{2}}{3}\tilde{d}_{Ri}^*\bar{d}_{Ri}\tilde{\bar{B}} + \frac{ig\sqrt{2}}{3}\tilde{u}_{Ri}^*\bar{u}_{Ri}\tilde{\bar{B}} \\ & + \frac{ig_2}{\sqrt{2}}h_2^{+*}\tilde{W}^0\tilde{h}_2^+ + \frac{ig_2}{\sqrt{2}}h_2^{+*}\tilde{W}^+\tilde{h}_2^0 + \frac{ig_2}{\sqrt{2}}h_2^{0*}\tilde{W}^-\tilde{h}_2^+ - \frac{ig_2}{\sqrt{2}}h_2^{0*}\tilde{W}^0\tilde{h}_2^0 \\ & - \frac{ig_2}{\sqrt{2}}h_2^+\tilde{W}^0\tilde{h}_2^+ - \frac{ig_2}{\sqrt{2}}h_2^+\tilde{W}^+\tilde{h}_2^0 - \frac{ig_2}{\sqrt{2}}h_2^0\tilde{W}^-\tilde{h}_2^+ + \frac{ig_2}{\sqrt{2}}h_2^0\tilde{W}^0\tilde{h}_2^0 \\ & + \frac{ig_2}{\sqrt{2}}\tilde{\nu}_{L\alpha}^*\tilde{W}^0\nu_{L\alpha} + \frac{ig_2}{\sqrt{2}}\tilde{\nu}_{L\alpha}^*\tilde{W}^+e_{L\alpha} + \frac{ig_2}{\sqrt{2}}\tilde{e}_{L\alpha}^*\tilde{W}^-\nu_{L\alpha} - \frac{ig_2}{\sqrt{2}}\tilde{e}_{L\alpha}^*\tilde{W}^0e_{L\alpha} \\ & - \frac{ig_2}{\sqrt{2}}\tilde{\nu}_{L\alpha}\tilde{W}^0\bar{\nu}_{L\alpha} - \frac{ig_2}{\sqrt{2}}\tilde{\nu}_{L\alpha}\tilde{W}^+\bar{e}_{L\alpha} - \frac{ig_2}{\sqrt{2}}\tilde{e}_{L\alpha}\tilde{W}^-\bar{\nu}_{L\alpha} + \frac{ig_2}{\sqrt{2}}\tilde{e}_{L\alpha}\tilde{W}^0\bar{e}_{L\alpha} \\ & + \frac{ig_2}{\sqrt{2}}\tilde{u}_{Li}^*\tilde{W}^0u_{Li} + \frac{ig_2}{\sqrt{2}}\tilde{u}_{Li}^*\tilde{W}^+d_{Li} + \frac{ig_2}{\sqrt{2}}\tilde{d}_{Li}^*\tilde{W}^-u_{Li} - \frac{ig_2}{\sqrt{2}}\tilde{d}_{Li}^*\tilde{W}^0d_{Li} \\ & - \frac{ig_2}{\sqrt{2}}\tilde{u}_{Li}\tilde{W}^0\bar{u}_{Li} - \frac{ig_2}{\sqrt{2}}\tilde{u}_{Li}\tilde{W}^+\bar{d}_{Li} - \frac{ig_2}{\sqrt{2}}\tilde{d}_{Li}\tilde{W}^-\bar{u}_{Li} + \frac{ig_2}{\sqrt{2}}\tilde{d}_{Li}\tilde{W}^0\bar{d}_{Li} \\ & + \frac{ig_3}{\sqrt{2}}\tilde{u}_{Li}^{*x}\lambda^{Axy}u_{Li}^y\tilde{G}^A + \frac{ig_3}{\sqrt{2}}\tilde{d}_{Li}^{*x}\lambda^{Axy}d_{Li}^y\tilde{G}^A + \frac{ig_3}{\sqrt{2}}\tilde{u}_{Ri}^{*x}\lambda^{*Axy}u_{Ri}^y\tilde{G}^A + \frac{ig_3}{\sqrt{2}}\tilde{d}_{Ri}^{*x}\lambda^{*Axy}d_{Ri}^y\tilde{G}^A \\ & - \frac{ig_3}{\sqrt{2}}\tilde{u}_{Li}^x\lambda^{*Axy}\bar{u}_{Li}^y\tilde{\bar{G}}^A - \frac{ig_3}{\sqrt{2}}\tilde{d}_{Li}^x\lambda^{*Axy}\bar{d}_{Li}^y\tilde{\bar{G}}^A - \frac{ig_3}{\sqrt{2}}\tilde{u}_{Ri}^x\lambda^{Axy}\bar{u}_{Ri}^y\tilde{\bar{G}}^A - \frac{ig_3}{\sqrt{2}}\tilde{d}_{Ri}^x\lambda^{Axy}\bar{d}_{Ri}^y\tilde{\bar{G}}^A \end{aligned}$$

B.6 Superpotential

$$\begin{aligned} \mathcal{W} = & \frac{1}{2} \varepsilon_{ab} \lambda_{\alpha\beta j} \mathcal{L}_\alpha^a \mathcal{L}_\beta^b E_j^c + \varepsilon_{ab} \lambda'_{\alpha ij} \mathcal{L}_\alpha^a Q_i^{bx} D_j^{cx} - \varepsilon_{ab} \mu_\alpha \mathcal{L}_\alpha^a H_2^b \\ & + (Y_U)_{ij} \varepsilon_{ab} Q_i^{ax} H_2^b U_j^{cx} + \frac{1}{2} \varepsilon_{xyz} \lambda''_{ijk} U_i^{cx} D_j^{cy} D_k^{cz} \end{aligned}$$

$$\frac{\partial \mathcal{W}}{\partial \tilde{\nu}_{L\gamma}} = \frac{1}{2} \lambda_{\gamma\beta j} \tilde{e}_{L\beta} \tilde{e}_{Rj}^* - \frac{1}{2} \lambda_{\alpha\gamma j} \tilde{e}_{L\alpha} \tilde{e}_{Rj}^* + \lambda'_{\gamma ij} \tilde{d}_{Li}^y \tilde{d}_{Rj}^{*y} - \mu_\gamma h_2^0$$

$$\frac{\partial \mathcal{W}}{\partial \tilde{e}_{L\gamma}} = \frac{1}{2} \lambda_{\alpha\gamma j} \tilde{\nu}_{L\alpha} \tilde{e}_{Rj}^* - \frac{1}{2} \lambda_{\gamma\beta j} \tilde{\nu}_{L\beta} \tilde{e}_{Rj}^* - \lambda'_{\gamma ij} \tilde{u}_{Li}^y \tilde{d}_{Rj}^{*y} + \mu_\gamma h_2^+$$

$$\frac{\partial \mathcal{W}}{\partial \tilde{e}_{Rk}^*} = \frac{1}{2} \lambda_{\alpha\beta k} \tilde{\nu}_{L\alpha} \tilde{e}_{L\beta} - \frac{1}{2} \lambda_{\alpha\beta k} \tilde{e}_{L\alpha} \tilde{\nu}_{L\beta}$$

$$\frac{\partial \mathcal{W}}{\partial h_2^+} = \mu_\alpha \tilde{e}_{L\alpha} - (Y_U)_{ij} \tilde{d}_{Li}^y \tilde{u}_{Rj}^{*y}$$

$$\frac{\partial \mathcal{W}}{\partial h_2^0} = -\mu_\alpha \tilde{\nu}_{L\alpha} + (Y_U)_{ij} \tilde{u}_{Li}^y \tilde{u}_{Rj}^{*y}$$

$$\frac{\partial \mathcal{W}}{\partial \tilde{u}_{Lk}^z} = -\lambda'_{\alpha kj} \tilde{e}_{L\alpha} \tilde{d}_{Rj}^{*z} + (Y_U)_{kj} h_2^0 \tilde{u}_{Rj}^{*z}$$

$$\frac{\partial \mathcal{W}}{\partial \tilde{u}_{Rk}^{*z}} = (Y_U)_{ik} \tilde{u}_{Li}^z h_2^0 - (Y_U)_{ik} \tilde{d}_{Li}^z h_2^+ + \frac{1}{2} \varepsilon_{xyz} \lambda''_{kij} \tilde{d}_{Ri}^{*x} \tilde{d}_{Rj}^y$$

$$\frac{\partial \mathcal{W}}{\partial \tilde{d}_{Lk}^{*z}} = \lambda'_{\alpha kj} \tilde{\nu}_{L\alpha} \tilde{d}_{Rj}^{*z} - (Y_U)_{kj} h_2^+ \tilde{u}_{Rj}^{*z}$$

$$\frac{\partial \mathcal{W}}{\partial \tilde{d}_{Rk}^{*z}} = \lambda'_{\alpha ik} \tilde{\nu}_{L\alpha} \tilde{d}_{Li}^z - \lambda'_{\alpha ik} \tilde{e}_{L\alpha} \tilde{u}_{Li}^z + \frac{1}{2} \varepsilon_{xzy} \lambda''_{ikj} \tilde{u}_{Ri}^{*x} \tilde{d}_{Rj}^{*y} + \frac{1}{2} \varepsilon_{xyz} \lambda''_{ijk} \tilde{u}_{Ri}^{*x} \tilde{d}_{Rj}^{*y}$$

B.7 Yukawa terms

$$-\frac{1}{2} \frac{\partial^2 \mathcal{W}}{\partial \varphi_i \partial \varphi_j} \psi_i^p \psi_{j\rho} - \frac{1}{2} \frac{\partial^2 \mathcal{W}^\dagger}{\partial \varphi_i^* \partial \varphi_j^*} \bar{\psi}_{i\rho} \bar{\psi}_j^p$$

$$\mathcal{L}_{\text{Yukawa}} =$$

$$\begin{aligned} & -\lambda_{\alpha\beta j} \tilde{e}_{Rj}^* e_{L\beta} \nu_{L\alpha} - \lambda_{\alpha\beta j} \tilde{e}_{L\beta} e_{Rj} \nu_{L\alpha} + \mu_\alpha \nu_{L\alpha} \tilde{h}_2^0 \\ & -\lambda'_{\alpha ij} \tilde{d}_{Rj}^{*y} e_{L\alpha} u_{Li}^y - \lambda'_{\alpha ij} \tilde{d}_{Li}^y \nu_{L\alpha} d_{Rj}^y + \lambda_{\alpha\beta j} \tilde{\nu}_{L\beta} e_{L\alpha} e_{Rj} - \mu_\alpha e_{L\alpha} \tilde{h}_2^+ \\ & \quad + \lambda'_{\alpha ij} \tilde{d}_{Rj}^{*y} e_{L\alpha} u_{Li}^y + \lambda'_{\alpha ij} \tilde{u}_{Li}^y e_{L\alpha} d_{Rj}^y \\ & + (Y_U)_{ij} \tilde{d}_{Li}^y u_{Rj}^y \tilde{h}_2^+ + (Y_U)_{ij} \tilde{u}_{Rj}^y d_{Li}^y \tilde{h}_2^+ - (Y_U)_{ij} \tilde{u}_{Rj}^y u_{Li}^y \tilde{h}_2^+ \\ & - (Y_U)_{ij} \tilde{u}_{Li}^y u_{Rj}^y \tilde{h}_2^+ - (Y_U)_{ij} h_2^0 u_{Rj}^y u_{Li}^y + (Y_U)_{ij} h_2^+ d_{Li}^z u_{Rj}^z \\ & + \lambda'_{\alpha ij} \tilde{e}_{L\alpha} d_{Rj}^z u_{Li}^z + \varepsilon_{xyz} \lambda''_{ijk} \tilde{d}_{Rk}^{*z} u_{Ri}^x d_{Rj}^y - \lambda'_{\alpha ij} \tilde{\nu}_{L\alpha} d_{Li}^z d_{Rj}^z - \varepsilon_{xyz} \lambda''_{ijk} \tilde{u}_{Ri}^{*x} d_{Rj}^y d_{Rk}^z \\ & \quad - \lambda_{\alpha\beta j}^* \tilde{e}_{Rj} \bar{e}_{L\beta} \bar{\nu}_{L\alpha} - \lambda_{\alpha\beta j}^* \tilde{e}_{L\beta} \bar{e}_{Rj} \bar{\nu}_{L\alpha} + \mu_\alpha^* \bar{\nu}_{L\alpha} \bar{h}_2^0 \\ & - \lambda'_{\alpha ij} \tilde{d}_{Rj}^y \bar{e}_{L\alpha} \bar{u}_{Li}^y - \lambda'_{\alpha ij} \tilde{d}_{Li}^{*y} \bar{\nu}_{L\alpha} \bar{d}_{Rj}^y + \lambda_{\alpha\beta j}^* \tilde{\nu}_{L\beta} \bar{e}_{L\alpha} \bar{e}_{Rj} - \mu_\alpha^* \bar{e}_{L\alpha} \bar{h}_2^+ \\ & + \lambda'_{\alpha ij} \tilde{d}_{Rj}^y \bar{e}_{L\alpha} \bar{u}_{Li}^y + \lambda'_{\alpha ij} \tilde{u}_{Li}^{*y} \bar{e}_{L\alpha} \bar{d}_{Rj}^y + (Y_U)_{ij}^* \tilde{d}_{Li}^{*y} \bar{u}_{Rj}^y \bar{h}_2^+ + (Y_U)_{ij}^* \tilde{u}_{Rj}^y \bar{d}_{Li}^y \bar{h}_2^+ - (Y_U)_{ij}^* \tilde{u}_{Rj}^y \bar{u}_{Li}^y \bar{h}_2^+ \\ & - (Y_U)_{ij}^* \tilde{u}_{Li}^{*y} \bar{u}_{Rj}^y \bar{h}_2^+ - (Y_U)_{ij}^* h_2^{0*} \bar{u}_{Rj}^y \bar{u}_{Li}^y + (Y_U)_{ij}^* h_2^{+*} \bar{d}_{Li}^z \bar{u}_{Rj}^z \\ & + \lambda'_{\alpha ij} \tilde{e}_{L\alpha}^* \bar{d}_{Rj}^z \bar{u}_{Li}^z + \varepsilon_{xyz} \lambda''_{ijk} \tilde{d}_{Rk}^z \bar{u}_{Ri}^x \bar{d}_{Rj}^y - \lambda'_{\alpha ij} \tilde{\nu}_{L\alpha}^* \bar{d}_{Li}^z \bar{d}_{Rj}^z - \varepsilon_{xyz} \lambda''_{ijk} \tilde{u}_{Ri}^{*x} \bar{d}_{Rj}^y \bar{d}_{Rk}^z \end{aligned}$$

B.8 F-terms

$$-\sum_i \left| \frac{\partial \mathcal{W}}{\partial \varphi_i} \right|^2$$

$$\mathcal{L}_F =$$

$$\begin{aligned} & - \left| \lambda_{\alpha\beta j} \tilde{e}_{L\beta} \tilde{e}_{Rj}^* + \lambda'_{\alpha ij} \tilde{d}_{Li}^y \tilde{d}_{Rj}^{*y} - \mu_\alpha h_2^0 \right|^2 - \left| -\lambda_{\alpha\beta j} \tilde{\nu}_{L\beta} \tilde{e}_{Rj}^* - \lambda'_{\alpha ij} \tilde{u}_{Li}^y \tilde{d}_{Rj}^{*y} + \mu_\alpha h_2^+ \right|^2 \\ & - \left| \lambda_{\alpha\beta k} \tilde{\nu}_{L\alpha} \tilde{e}_{L\beta} \right|^2 - \left| -(Y_U)_{ij} \tilde{d}_{Li}^y \tilde{u}_{Rj}^{*y} + \mu_\alpha \tilde{e}_{L\alpha} \right|^2 \\ & - \left| (Y_U)_{ij} \tilde{u}_{Li}^y \tilde{u}_{Rj}^{*y} - \mu_\alpha \tilde{\nu}_{L\alpha} \right|^2 - \left| (Y_U)_{ij} h_2^0 \tilde{u}_{Rj}^{*y} - \lambda'_{\alpha ij} \tilde{e}_{L\alpha} \tilde{d}_{Rj}^{*y} \right|^2 \\ & - \left| (Y_U)_{ij} \tilde{u}_{Li}^y h_2^0 - (Y_U)_{ij} \tilde{d}_{Li}^y + \frac{1}{2} \varepsilon_{xyz} \lambda''_{ijk} \tilde{d}_{Rj}^{*y} \tilde{d}_{Rk}^{*z} \right|^2 - \left| -(Y_U)_{ij} h_2^+ \tilde{u}_{Rj}^{*y} + \lambda'_{\alpha ij} \tilde{\nu}_{L\alpha} \tilde{d}_{Rj}^{*y} \right|^2 \\ & - \left| \lambda'_{\alpha ik} \tilde{\nu}_{L\alpha} \tilde{d}_{Li}^y - \lambda'_{\alpha ik} \tilde{e}_{L\alpha} \tilde{u}_{Li}^y + \varepsilon_{xyz} \lambda''_{ijk} \tilde{u}_{Ri}^{*x} \tilde{d}_{Rj}^{*y} \right|^2 \end{aligned}$$

$$\mathcal{L}_F =$$

$$\begin{aligned} & -\lambda_{\alpha\beta j} \lambda_{\alpha\gamma q}^* \tilde{e}_{L\beta} \tilde{e}_{Rj}^* \tilde{e}_{L\gamma}^* \tilde{e}_{Rq} - \lambda_{\alpha\beta j} \lambda_{\alpha pq}^* \tilde{e}_{L\beta} \tilde{e}_{Rj}^* \tilde{d}_{Lp}^{*z} \tilde{d}_{Rq}^z + \lambda_{\alpha\beta j} \mu_\alpha^* \tilde{e}_{L\beta} \tilde{e}_{Rj}^* h_2^{0*} \\ & -\lambda'_{\alpha ij} \lambda_{\alpha\gamma q}^* \tilde{d}_{Li}^y \tilde{d}_{Rj}^{*y} \tilde{e}_{L\gamma}^* \tilde{e}_{Rq} - \lambda'_{\alpha ij} \lambda_{\alpha pq}^* \tilde{d}_{Li}^y \tilde{d}_{Rj}^{*y} \tilde{d}_{Lp}^{*z} \tilde{d}_{Rq}^z + \lambda'_{\alpha ij} \mu_\alpha^* \tilde{d}_{Li}^y \tilde{d}_{Rj}^{*y} h_2^{0*} \\ & + \mu_\alpha \lambda_{\alpha\gamma q}^* h_2^0 \tilde{e}_{L\gamma}^* \tilde{e}_{Rq} + \mu_\alpha \lambda_{\alpha pq}^* h_2^0 \tilde{d}_{Lp}^{*z} \tilde{d}_{Rq}^z - \mu_\alpha \mu_\alpha^* h_2^0 h_2^{0*} \\ & -\lambda_{\alpha\beta j} \lambda_{\alpha\gamma q}^* \tilde{\nu}_{L\beta} \tilde{e}_{Rj}^* \tilde{\nu}_{L\gamma}^* \tilde{e}_{Rq} - \lambda_{\alpha\beta j} \lambda_{\alpha pq}^* \tilde{\nu}_{L\beta} \tilde{e}_{Rj}^* \tilde{u}_{Lp}^{*z} \tilde{d}_{Rq}^z + \lambda_{\alpha\beta j} \mu_\alpha^* \tilde{\nu}_{L\beta} \tilde{e}_{Rj}^* h_2^{+*} \\ & -\lambda'_{\alpha ij} \lambda_{\alpha\gamma q}^* \tilde{u}_{Li}^y \tilde{d}_{Rj}^{*y} \tilde{\nu}_{L\gamma}^* \tilde{e}_{Rq} - \lambda'_{\alpha ij} \lambda_{\alpha pq}^* \tilde{u}_{Li}^y \tilde{d}_{Rj}^{*y} \tilde{u}_{Lp}^{*z} \tilde{d}_{Rq}^z + \lambda'_{\alpha ij} \mu_\alpha^* \tilde{u}_{Li}^y \tilde{d}_{Rj}^{*y} h_2^{+*} \\ & + \mu_\alpha \lambda_{\alpha\gamma q}^* h_2^+ \tilde{\nu}_{L\gamma}^* \tilde{e}_{Rq} + \mu_\alpha \lambda_{\alpha pq}^* h_2^+ \tilde{u}_{Lp}^{*z} \tilde{d}_{Rq}^z - \mu_\alpha \mu_\alpha^* h_2^+ h_2^{+*} \\ & -\lambda_{\alpha\beta k} \lambda_{\delta\gamma k}^* \tilde{\nu}_{L\alpha} \tilde{e}_{L\beta} \tilde{\nu}_{L\delta}^* \tilde{e}_{L\gamma}^* \\ & - (Y_U)_{ij} (Y_U)_{pq}^* \tilde{d}_{Li}^y \tilde{u}_{Rj}^{*y} \tilde{d}_{Lp}^{*z} \tilde{u}_{Rq}^z + (Y_U)_{ij} \mu_\beta^* \tilde{d}_{Li}^y \tilde{u}_{Rj}^{*y} \tilde{e}_{L\beta}^* \end{aligned}$$

$$\begin{aligned}
& +\mu_\alpha (Y_U)_{pq}^* \tilde{e}_{L\alpha} \tilde{d}_{Lp}^{*z} \tilde{u}_{Rq}^z - \mu_\alpha \mu_\beta^* \tilde{e}_{L\alpha} \tilde{e}_{L\beta}^* \\
& - (Y_U)_{ij} (Y_U)_{pq}^* \tilde{u}_{Li}^y \tilde{u}_{Rj}^{*y} \tilde{u}_{Lp}^{*z} \tilde{u}_{Rq}^z + (Y_U)_{ij} \mu_\beta^* \tilde{u}_{Li}^y \tilde{u}_{Rj}^{*y} \tilde{v}_{L\beta}^* \\
& +\mu_\alpha (Y_U)_{pq}^* \tilde{v}_{L\alpha} \tilde{u}_{Lp}^{*z} \tilde{u}_{Rq}^z - \mu_\alpha \mu_\beta^* \tilde{v}_{L\alpha} \tilde{v}_{L\beta}^* \\
& - (Y_U)_{ij} (Y_U)_{iq}^* h_2^0 \tilde{u}_{Rj}^{*y} h_2^{0*} \tilde{u}_{Rq}^y + (Y_U)_{ij} \lambda_{\alpha iq}^* h_2^0 \tilde{u}_{Rj}^{*y} \tilde{e}_{L\alpha}^* \tilde{d}_{Rq}^y \\
& +\lambda'_{\alpha ij} (Y_U)_{iq}^* \tilde{e}_{L\alpha} \tilde{d}_{Rj}^{*y} h_2^{0*} \tilde{u}_{Rq}^y - \lambda'_{\alpha ij} \lambda_{\alpha iq}^* \tilde{e}_{L\alpha} \tilde{d}_{Rj}^{*y} \tilde{e}_{L\alpha}^* \tilde{d}_{Rq}^y \\
& - (Y_U)_{ik} (Y_U)_{pk}^* \tilde{u}_{Li}^x h_2^0 \tilde{u}_{Lp}^{*x} h_2^{0*} + (Y_U)_{ik} (Y_U)_{pk}^* \tilde{u}_{Li}^x h_2^0 \tilde{d}_{Lp}^{*x} - (Y_U)_{ik} \frac{1}{2} \varepsilon_{xvw} \lambda_{kpq}^{**} \tilde{u}_{Li}^x h_2^0 \tilde{d}_{Rp}^v \tilde{d}_{Rq}^w \\
& + (Y_U)_{ik} (Y_U)_{pk}^* \tilde{d}_{Li}^x \tilde{u}_{Lp}^{*x} h_2^{0*} - (Y_U)_{ik} (Y_U)_{pk}^* \tilde{d}_{Li}^x \tilde{d}_{Lp}^{*x} + (Y_U)_{ik} \frac{1}{2} \varepsilon_{xvw} \lambda_{kpq}^{**} \tilde{d}_{Li}^x \tilde{d}_{Rp}^v \tilde{d}_{Rq}^w \\
& - \frac{1}{2} \varepsilon_{xyz} \lambda''_{kij} (Y_U)_{pk}^* \tilde{d}_{Ri}^{*y} \tilde{d}_{Rj}^{*z} \tilde{u}_{Lp}^{*x} h_2^{0*} + \frac{1}{2} \varepsilon_{xyz} \lambda''_{kij} (Y_U)_{pk}^* \tilde{d}_{Ri}^{*y} \tilde{d}_{Rj}^{*z} \tilde{d}_{Lp}^{*x} - \frac{1}{4} \varepsilon_{xyz} \varepsilon_{xvw} \lambda''_{kij} \lambda_{kpq}^{**} \tilde{d}_{Ri}^{*y} \tilde{d}_{Rj}^{*z} \tilde{d}_{Rp}^v \tilde{d}_{Rq}^w \\
& - (Y_U)_{ij} (Y_U)_{iq}^* h_2^+ \tilde{u}_{Rj}^{*y} h_2^{+*} \tilde{u}_{Rq}^y + (Y_U)_{ij} \lambda_{\alpha iq}^* h_2^+ \tilde{u}_{Rj}^{*y} \tilde{v}_{L\alpha}^* \tilde{d}_{Rq}^y \\
& +\lambda'_{\alpha ij} (Y_U)_{iq}^* \tilde{v}_{L\alpha} \tilde{d}_{Rj}^{*y} h_2^{+*} \tilde{u}_{Rq}^y - \lambda'_{\alpha ij} \lambda_{\alpha iq}^* \tilde{v}_{L\alpha} \tilde{d}_{Rj}^{*y} \tilde{v}_{L\alpha}^* \tilde{d}_{Rq}^y \\
& -\lambda'_{\alpha ik} \lambda_{\alpha pk}^* \tilde{v}_{L\alpha} \tilde{d}_{Li}^z \tilde{v}_{L\alpha}^* \tilde{d}_{Lp}^{*w} + \lambda'_{\alpha ik} \lambda_{\alpha pk}^* \tilde{v}_{L\alpha} \tilde{d}_{Li}^z \tilde{e}_{L\alpha}^* \tilde{u}_{Lp}^{*w} - \lambda'_{\alpha ik} \varepsilon_{vwz} \lambda_{pqk}^{**} \tilde{v}_{L\alpha} \tilde{d}_{Li}^z \tilde{u}_{Rp}^v \tilde{d}_{Rq}^w \\
& +\lambda'_{\alpha ik} \lambda_{\alpha pk}^* \tilde{e}_{L\alpha} \tilde{u}_{Li}^z \tilde{v}_{L\alpha}^* \tilde{d}_{Lp}^{*w} - \lambda'_{\alpha ik} \lambda_{\alpha pk}^* \tilde{e}_{L\alpha} \tilde{u}_{Li}^z \tilde{e}_{L\alpha}^* \tilde{u}_{Lp}^{*w} + \lambda'_{\alpha ik} \varepsilon_{vwz} \lambda_{pqk}^{**} \tilde{e}_{L\alpha} \tilde{u}_{Li}^z \tilde{u}_{Rp}^v \tilde{d}_{Rq}^w \\
& -\varepsilon_{xyz} \lambda''_{ijk} \lambda_{\alpha pk}^* \tilde{u}_{Ri}^{*x} \tilde{d}_{Rj}^{*y} \tilde{v}_{L\alpha}^* \tilde{d}_{Lp}^{*w} + \varepsilon_{xyz} \lambda''_{ijk} \lambda_{\alpha pk}^* \tilde{u}_{Ri}^{*x} \tilde{d}_{Rj}^{*y} \tilde{e}_{L\alpha}^* \tilde{u}_{Lp}^{*w} - \varepsilon_{xyz} \lambda''_{ijk} \varepsilon_{vwz} \lambda_{pqk}^{**} \tilde{u}_{Ri}^{*x} \tilde{d}_{Rj}^{*y} \tilde{u}_{Rp}^v \tilde{d}_{Rq}^w
\end{aligned}$$

B.9 D-terms

$$-\sum_l \frac{g_l^2}{2} \sum_A (\varphi_i^{*a} T_l^{Aab} \varphi_i^b)^2$$

$$\mathcal{L}_D =$$

$$\begin{aligned}
& -\frac{g^2}{8} \tilde{e}_{L\alpha}^* \tilde{e}_{L\alpha} \tilde{e}_{L\beta}^* \tilde{e}_{L\beta} - \frac{g^2}{8} \tilde{e}_{L\alpha}^* \tilde{e}_{L\alpha} \tilde{\nu}_{L\beta}^* \tilde{\nu}_{L\beta} + \frac{g^2}{4} \tilde{e}_{L\alpha}^* \tilde{e}_{L\alpha} \tilde{e}_{Rj}^* \tilde{e}_{Rj} + \frac{g^2}{8} \tilde{e}_{L\alpha}^* \tilde{e}_{L\alpha} h_2^{+*} h_2^+ + \frac{g^2}{8} \tilde{e}_{L\alpha}^* \tilde{e}_{L\alpha} h_2^{0*} h_2^0 \\
& \quad + \frac{g^2}{24} \tilde{e}_{L\alpha}^* \tilde{e}_{L\alpha} \tilde{u}_{Lj}^{*y} \tilde{u}_{Lj}^y + \frac{g^2}{24} \tilde{e}_{L\alpha}^* \tilde{e}_{L\alpha} \tilde{d}_{Lj}^{*y} \tilde{d}_{Lj}^y - \frac{g^2}{6} \tilde{e}_{L\alpha}^* \tilde{e}_{L\alpha} \tilde{u}_{Rj}^{*y} \tilde{u}_{Rj}^y + \frac{g^2}{12} \tilde{e}_{L\alpha}^* \tilde{e}_{L\alpha} \tilde{d}_{Rj}^{*y} \tilde{d}_{Rj}^y \\
& -\frac{g^2}{8} \tilde{\nu}_{L\alpha}^* \tilde{\nu}_{L\alpha} \tilde{e}_{L\beta}^* \tilde{e}_{L\beta} - \frac{g^2}{8} \tilde{\nu}_{L\alpha}^* \tilde{\nu}_{L\alpha} \tilde{\nu}_{L\beta}^* \tilde{\nu}_{L\beta} + \frac{g^2}{4} \tilde{\nu}_{L\alpha}^* \tilde{\nu}_{L\alpha} \tilde{e}_{Rj}^* \tilde{e}_{Rj} + \frac{g^2}{8} \tilde{\nu}_{L\alpha}^* \tilde{\nu}_{L\alpha} h_2^{+*} h_2^+ + \frac{g^2}{8} \tilde{\nu}_{L\alpha}^* \tilde{\nu}_{L\alpha} h_2^{0*} h_2^0 \\
& \quad + \frac{g^2}{24} \tilde{\nu}_{L\alpha}^* \tilde{\nu}_{L\alpha} \frac{1}{3} \tilde{u}_{Lj}^{*y} \tilde{u}_{Lj}^y + \frac{g^2}{24} \tilde{\nu}_{L\alpha}^* \tilde{\nu}_{L\alpha} \frac{1}{3} \tilde{d}_{Lj}^{*y} \tilde{d}_{Lj}^y - \frac{g^2}{6} \tilde{\nu}_{L\alpha}^* \tilde{\nu}_{L\alpha} \frac{4}{3} \tilde{u}_{Rj}^{*y} \tilde{u}_{Rj}^y + \frac{g^2}{12} \tilde{\nu}_{L\alpha}^* \tilde{\nu}_{L\alpha} \frac{2}{3} \tilde{d}_{Rj}^{*y} \tilde{d}_{Rj}^y \\
& + \frac{g^2}{4} \tilde{e}_{Ri}^* \tilde{e}_{Ri} \tilde{e}_{L\beta}^* \tilde{e}_{L\beta} + \frac{g^2}{4} \tilde{e}_{Ri}^* \tilde{e}_{Ri} \tilde{\nu}_{L\beta}^* \tilde{\nu}_{L\beta} - \frac{g^2}{2} \tilde{e}_{Ri}^* \tilde{e}_{Ri} \tilde{e}_{Rj}^* \tilde{e}_{Rj} - \frac{g^2}{4} \tilde{e}_{Ri}^* \tilde{e}_{Ri} h_2^{+*} h_2^+ - \frac{g^2}{4} \tilde{e}_{Ri}^* \tilde{e}_{Ri} h_2^{0*} h_2^0 \\
& \quad - \frac{g^2}{12} \tilde{e}_{Ri}^* \tilde{e}_{Ri} \tilde{u}_{Lj}^{*y} \tilde{u}_{Lj}^y - \frac{g^2}{12} \tilde{e}_{Ri}^* \tilde{e}_{Ri} \tilde{d}_{Lj}^{*y} \tilde{d}_{Lj}^y + \frac{g^2}{3} \tilde{e}_{Ri}^* \tilde{e}_{Ri} \tilde{u}_{Rj}^{*y} \tilde{u}_{Rj}^y - \frac{g^2}{6} \tilde{e}_{Ri}^* \tilde{e}_{Ri} \tilde{d}_{Rj}^{*y} \tilde{d}_{Rj}^y \\
& + \frac{g^2}{8} h_2^{+*} h_2^+ \tilde{e}_{L\beta}^* \tilde{e}_{L\beta} + \frac{g^2}{8} h_2^{+*} h_2^+ \tilde{\nu}_{L\beta}^* \tilde{\nu}_{L\beta} - \frac{g^2}{4} h_2^{+*} h_2^+ \tilde{e}_{Rj}^* \tilde{e}_{Rj} - \frac{g^2}{8} h_2^{+*} h_2^+ h_2^{+*} h_2^+ - \frac{g^2}{8} h_2^{+*} h_2^+ h_2^{0*} h_2^0 \\
& \quad - \frac{g^2}{24} h_2^{+*} h_2^+ \tilde{u}_{Lj}^{*y} \tilde{u}_{Lj}^y - \frac{g^2}{24} h_2^{+*} h_2^+ \tilde{d}_{Lj}^{*y} \tilde{d}_{Lj}^y + \frac{g^2}{6} h_2^{+*} h_2^+ \tilde{u}_{Rj}^{*y} \tilde{u}_{Rj}^y - \frac{g^2}{12} h_2^{+*} h_2^+ \tilde{d}_{Rj}^{*y} \tilde{d}_{Rj}^y \\
& + \frac{g^2}{8} h_2^{0*} h_2^0 \tilde{e}_{L\beta}^* \tilde{e}_{L\beta} + \frac{g^2}{8} h_2^{0*} h_2^0 \tilde{\nu}_{L\beta}^* \tilde{\nu}_{L\beta} - \frac{g^2}{4} h_2^{0*} h_2^0 \tilde{e}_{Rj}^* \tilde{e}_{Rj} - \frac{g^2}{8} h_2^{0*} h_2^0 h_2^{+*} h_2^+ - \frac{g^2}{8} h_2^{0*} h_2^0 h_2^{0*} h_2^0 \\
& \quad - \frac{g^2}{24} h_2^{0*} h_2^0 \tilde{u}_{Lj}^{*y} \tilde{u}_{Lj}^y - \frac{g^2}{24} h_2^{0*} h_2^0 \tilde{d}_{Lj}^{*y} \tilde{d}_{Lj}^y + \frac{g^2}{6} h_2^{0*} h_2^0 \tilde{u}_{Rj}^{*y} \tilde{u}_{Rj}^y - \frac{g^2}{12} h_2^{0*} h_2^0 \tilde{d}_{Rj}^{*y} \tilde{d}_{Rj}^y \\
& + \frac{g^2}{24} \tilde{u}_{Li}^{*x} \tilde{u}_{Li}^x \tilde{e}_{L\beta}^* \tilde{e}_{L\beta} + \frac{g^2}{24} \tilde{u}_{Li}^{*x} \tilde{u}_{Li}^x \tilde{\nu}_{L\beta}^* \tilde{\nu}_{L\beta} - \frac{g^2}{12} \tilde{u}_{Li}^{*x} \tilde{u}_{Li}^x \tilde{e}_{Rj}^* \tilde{e}_{Rj} - \frac{g^2}{24} \tilde{u}_{Li}^{*x} \tilde{u}_{Li}^x h_2^{+*} h_2^+ - \frac{g^2}{24} \tilde{u}_{Li}^{*x} \tilde{u}_{Li}^x h_2^{0*} h_2^0 \\
& \quad - \frac{g^2}{72} \tilde{u}_{Li}^{*x} \tilde{u}_{Li}^x \tilde{u}_{Lj}^{*y} \tilde{u}_{Lj}^y - \frac{g^2}{72} \tilde{u}_{Li}^{*x} \tilde{u}_{Li}^x \tilde{d}_{Lj}^{*y} \tilde{d}_{Lj}^y + \frac{g^2}{18} \tilde{u}_{Li}^{*x} \tilde{u}_{Li}^x \tilde{u}_{Rj}^{*y} \tilde{u}_{Rj}^y - \frac{g^2}{36} \tilde{u}_{Li}^{*x} \tilde{u}_{Li}^x \tilde{d}_{Rj}^{*y} \tilde{d}_{Rj}^y \\
& + \frac{g^2}{24} \tilde{d}_{Li}^{*x} \tilde{d}_{Li}^x \tilde{e}_{L\beta}^* \tilde{e}_{L\beta} + \frac{g^2}{24} \tilde{d}_{Li}^{*x} \tilde{d}_{Li}^x \tilde{\nu}_{L\beta}^* \tilde{\nu}_{L\beta} - \frac{g^2}{12} \tilde{d}_{Li}^{*x} \tilde{d}_{Li}^x \tilde{e}_{Rj}^* \tilde{e}_{Rj} - \frac{g^2}{24} \tilde{d}_{Li}^{*x} \tilde{d}_{Li}^x h_2^{+*} h_2^+ - \frac{g^2}{24} \tilde{d}_{Li}^{*x} \tilde{d}_{Li}^x h_2^{0*} h_2^0 \\
& \quad - \frac{g^2}{72} \tilde{d}_{Li}^{*x} \tilde{d}_{Li}^x \tilde{u}_{Lj}^{*y} \tilde{u}_{Lj}^y - \frac{g^2}{72} \tilde{d}_{Li}^{*x} \tilde{d}_{Li}^x \tilde{d}_{Lj}^{*y} \tilde{d}_{Lj}^y + \frac{g^2}{18} \tilde{d}_{Li}^{*x} \tilde{d}_{Li}^x \tilde{u}_{Rj}^{*y} \tilde{u}_{Rj}^y - \frac{g^2}{36} \tilde{d}_{Li}^{*x} \tilde{d}_{Li}^x \tilde{d}_{Rj}^{*y} \tilde{d}_{Rj}^y
\end{aligned}$$

$$\begin{aligned}
& -\frac{g^2}{6}\tilde{u}_{Ri}^{*x}\tilde{u}_{Ri}^x\tilde{e}_{L\beta}^*\tilde{e}_{L\beta}-\frac{g^2}{6}\tilde{u}_{Ri}^{*x}\tilde{u}_{Ri}^x\tilde{\nu}_{L\beta}^*\tilde{\nu}_{L\beta}+\frac{g^2}{3}\tilde{u}_{Ri}^{*x}\tilde{u}_{Ri}^x\tilde{e}_{Rj}^*\tilde{e}_{Rj}+\frac{g^2}{6}\tilde{u}_{Ri}^{*x}\tilde{u}_{Ri}^xh_2^{*+}h_2^++\frac{g^2}{6}\tilde{u}_{Ri}^{*x}\tilde{u}_{Ri}^xh_2^{0*}h_2^0 \\
& +\frac{g^2}{18}\tilde{u}_{Ri}^{*x}\tilde{u}_{Ri}^x\tilde{u}_{Lj}^{*y}\tilde{u}_{Lj}^y+\frac{g^2}{18}\tilde{u}_{Ri}^{*x}\tilde{u}_{Ri}^x\tilde{d}_{Lj}^{*y}\tilde{d}_{Lj}^y-\frac{2g^2}{9}\tilde{u}_{Ri}^{*x}\tilde{u}_{Ri}^x\tilde{u}_{Rj}^{*y}\tilde{u}_{Rj}^y+\frac{g^2}{9}\tilde{u}_{Ri}^{*x}\tilde{u}_{Ri}^x\tilde{d}_{Rj}^{*y}\tilde{d}_{Rj}^y \\
& +\frac{g^2}{12}\tilde{d}_{Ri}^{*x}\tilde{d}_{Ri}^x\tilde{e}_{L\beta}^*\tilde{e}_{L\beta}+\frac{g^2}{12}\tilde{d}_{Ri}^{*x}\tilde{d}_{Ri}^x\tilde{\nu}_{L\beta}^*\tilde{\nu}_{L\beta}-\frac{g^2}{6}\tilde{d}_{Ri}^{*x}\tilde{d}_{Ri}^x\tilde{e}_{Rj}^*\tilde{e}_{Rj}-\frac{g^2}{12}\tilde{d}_{Ri}^{*x}\tilde{d}_{Ri}^xh_2^{*+}h_2^+-\frac{g^2}{12}\tilde{d}_{Ri}^{*x}\tilde{d}_{Ri}^xh_2^{0*}h_2^0 \\
& -\frac{g^2}{36}\tilde{d}_{Ri}^{*x}\tilde{d}_{Ri}^x\tilde{u}_{Lj}^{*y}\tilde{u}_{Lj}^y-\frac{g^2}{36}\tilde{d}_{Ri}^{*x}\tilde{d}_{Ri}^x\tilde{d}_{Lj}^{*y}\tilde{d}_{Lj}^y+\frac{g^2}{9}\tilde{d}_{Ri}^{*x}\tilde{d}_{Ri}^x\tilde{u}_{Rj}^{*y}\tilde{u}_{Rj}^y-\frac{g^2}{18}\tilde{d}_{Ri}^{*x}\tilde{d}_{Ri}^x\tilde{d}_{Rj}^{*y}\tilde{d}_{Rj}^y \\
& -\frac{g^2}{8}\tilde{\nu}_{L\alpha}^*\tilde{\nu}_{L\alpha}\tilde{\nu}_{L\beta}^*\tilde{\nu}_{L\beta}-\frac{g^2}{8}\tilde{e}_{L\alpha}^*\tilde{e}_{L\alpha}\tilde{e}_{L\beta}^*\tilde{e}_{L\beta}-\frac{g^2}{4}\tilde{e}_{L\alpha}^*\tilde{\nu}_{L\alpha}\tilde{\nu}_{L\beta}^*\tilde{e}_{L\beta}-\frac{g^2}{4}\tilde{\nu}_{L\alpha}^*\tilde{e}_{L\alpha}\tilde{e}_{L\beta}^*\tilde{\nu}_{L\beta}+\frac{g^2}{4}\tilde{e}_{L\alpha}^*\tilde{e}_{L\alpha}\tilde{\nu}_{L\beta}^*\tilde{\nu}_{L\beta} \\
& -\frac{g^2}{8}\tilde{u}_{Li}^{*y}\tilde{u}_{Li}^y\tilde{u}_{Lj}^{*z}\tilde{u}_{Lj}^z-\frac{g^2}{8}\tilde{d}_{Li}^{*y}\tilde{d}_{Li}^y\tilde{d}_{Lj}^{*z}\tilde{d}_{Lj}^z-\frac{g^2}{4}\tilde{u}_{Li}^{*y}\tilde{d}_{Li}^y\tilde{d}_{Lj}^{*z}\tilde{u}_{Lj}^z \\
& +\frac{g^2}{8}\tilde{u}_{Li}^{*y}\tilde{u}_{Li}^y\tilde{d}_{Lj}^{*z}\tilde{d}_{Lj}^z-\frac{g^2}{8}\tilde{u}_{Li}^{*y}\tilde{d}_{Li}^y\tilde{u}_{Lj}^{*z}\tilde{d}_{Lj}^z-\frac{g^2}{8}h_2^{*+}h_2^+h_2^{*+}h_2^+-\frac{g^2}{8}h_2^{0*}h_2^0h_2^{0*}h_2^0-\frac{g^2}{4}h_2^{0*}h_2^0h_2^{*+}h_2^+ \\
& -\frac{g^2}{2}h_2^{*+}\tilde{\nu}_{L\alpha}h_2^+\tilde{\nu}_{L\alpha}^*-\frac{g^2}{2}h_2^{*+}\tilde{\nu}_{L\alpha}h_2^0\tilde{e}_{L\alpha}^*-\frac{g^2}{2}h_2^{0*}\tilde{e}_{L\alpha}h_2^+\tilde{\nu}_{L\alpha}^*-\frac{g^2}{2}h_2^{0*}\tilde{e}_{L\alpha}h_2^0\tilde{e}_{L\alpha}^* \\
& +\frac{g^2}{4}h_2^{*+}h_2^+\tilde{\nu}_{L\alpha}^*\tilde{\nu}_{L\alpha}+\frac{g^2}{4}h_2^{*+}h_2^+\tilde{e}_{L\alpha}^*\tilde{e}_{L\alpha}+\frac{g^2}{4}h_2^{0*}h_2^0\tilde{\nu}_{L\alpha}^*\tilde{\nu}_{L\alpha}+\frac{g^2}{4}h_2^{0*}h_2^0\tilde{e}_{L\alpha}^*\tilde{e}_{L\alpha} \\
& -\frac{g^2}{2}h_2^{*+}\tilde{u}_{Li}^xh_2^+\tilde{u}_{Li}^{*x}-\frac{g^2}{2}h_2^{*+}\tilde{u}_{Li}^xh_2^0\tilde{d}_{Li}^{*x}-\frac{g^2}{2}h_2^{0*}\tilde{d}_{Li}^xh_2^+\tilde{u}_{Li}^{*x}-\frac{g^2}{2}h_2^{0*}\tilde{d}_{Li}^xh_2^0\tilde{d}_{Li}^{*x} \\
& +\frac{g^2}{4}h_2^{*+}h_2^+\tilde{u}_{Li}^{*x}\tilde{u}_{Li}^x+\frac{g^2}{4}h_2^{*+}h_2^+\tilde{d}_{Li}^{*x}\tilde{d}_{Li}^x+\frac{g^2}{4}h_2^{0*}h_2^0\tilde{u}_{Li}^{*x}\tilde{u}_{Li}^x-\frac{g^2}{4}h_2^{0*}h_2^0\tilde{d}_{Li}^{*x}\tilde{d}_{Li}^x \\
& -\frac{g^2}{2}\tilde{\nu}_{L\alpha}^*\tilde{u}_{Lj}^x\tilde{\nu}_{L\alpha}\tilde{u}_{Lj}^{*x}-\frac{g^2}{2}\tilde{\nu}_{L\alpha}^*\tilde{u}_{Lj}^y\tilde{e}_{L\alpha}\tilde{d}_{Lj}^{*y}-\frac{g^2}{2}\tilde{e}_{L\alpha}^*\tilde{d}_{Lj}^y\tilde{\nu}_{L\alpha}\tilde{u}_{Lj}^{*y}-\frac{g^2}{2}\tilde{e}_{L\alpha}^*\tilde{d}_{Lj}^y\tilde{e}_{L\alpha}\tilde{d}_{Lj}^{*y} \\
& +\frac{g^2}{4}\tilde{\nu}_{L\alpha}^*\tilde{\nu}_{L\alpha}\tilde{u}_{Lj}^{*x}\tilde{u}_{Lj}^x+\frac{g^2}{4}\tilde{\nu}_{L\alpha}^*\tilde{\nu}_{L\alpha}\tilde{d}_{Lj}^{*x}\tilde{d}_{Lj}^x+\frac{g^2}{4}\tilde{e}_{L\alpha}^*\tilde{e}_{L\alpha}\tilde{u}_{Lj}^{*x}\tilde{u}_{Lj}^x+\frac{g^2}{4}\tilde{e}_{L\alpha}^*\tilde{e}_{L\alpha}\tilde{d}_{Lj}^{*x}\tilde{d}_{Lj}^x \\
& -\frac{g^2}{4}\tilde{u}_{Li}^{*x}\tilde{u}_{Li}^x\tilde{u}_{Lj}^{*v}\tilde{u}_{Lj}^v+\frac{g^2}{12}\tilde{u}_{Li}^{*y}\tilde{u}_{Li}^y\tilde{u}_{Lj}^{*v}\tilde{u}_{Lj}^v-\frac{g^2}{4}\tilde{d}_{Li}^{*x}\tilde{d}_{Li}^x\tilde{d}_{Lj}^{*v}\tilde{d}_{Lj}^v+\frac{g^2}{12}\tilde{d}_{Li}^{*y}\tilde{d}_{Li}^y\tilde{d}_{Lj}^{*v}\tilde{d}_{Lj}^v-\frac{g^2}{4}\tilde{u}_{Ri}^{*x}\tilde{u}_{Ri}^x\tilde{u}_{Rj}^{*v}\tilde{u}_{Rj}^v \\
& +\frac{g^2}{12}\tilde{u}_{Ri}^{*y}\tilde{u}_{Ri}^y\tilde{u}_{Rj}^{*v}\tilde{u}_{Rj}^v-\frac{g^2}{4}\tilde{d}_{Ri}^{*x}\tilde{d}_{Ri}^x\tilde{d}_{Rj}^{*v}\tilde{d}_{Rj}^v+\frac{g^2}{12}\tilde{d}_{Ri}^{*y}\tilde{d}_{Ri}^y\tilde{d}_{Rj}^{*v}\tilde{d}_{Rj}^v-\frac{g^2}{4}\tilde{u}_{Li}^{*x}\tilde{u}_{Li}^x\tilde{u}_{Rj}^{*v}\tilde{u}_{Rj}^v \\
& +\frac{g^2}{12}\tilde{u}_{Li}^{*x}\tilde{u}_{Li}^x\tilde{u}_{Rj}^{*v}\tilde{u}_{Rj}^v-\frac{g^2}{4}\tilde{u}_{Li}^{*x}\tilde{u}_{Li}^x\tilde{d}_{Rj}^{*v}\tilde{d}_{Rj}^v+\frac{g^2}{12}\tilde{u}_{Li}^{*x}\tilde{u}_{Li}^x\tilde{d}_{Rj}^{*v}\tilde{d}_{Rj}^v-\frac{g^2}{4}\tilde{d}_{Li}^{*x}\tilde{d}_{Li}^x\tilde{u}_{Rj}^{*v}\tilde{u}_{Rj}^v \\
& +\frac{g^2}{12}\tilde{d}_{Li}^{*x}\tilde{d}_{Li}^x\tilde{u}_{Rj}^{*v}\tilde{u}_{Rj}^v-\frac{g^2}{4}\tilde{d}_{Li}^{*x}\tilde{d}_{Li}^x\tilde{d}_{Rj}^{*v}\tilde{d}_{Rj}^v+\frac{g^2}{12}\tilde{d}_{Li}^{*x}\tilde{d}_{Li}^x\tilde{d}_{Rj}^{*v}\tilde{d}_{Rj}^v-\frac{g^2}{4}\tilde{u}_{Ri}^{*x}\tilde{u}_{Ri}^x\tilde{u}_{Lj}^{*v}\tilde{u}_{Lj}^v \\
& +\frac{g^2}{12}\tilde{u}_{Ri}^{*x}\tilde{u}_{Ri}^x\tilde{u}_{Lj}^{*v}\tilde{u}_{Lj}^v-\frac{g^2}{4}\tilde{u}_{Ri}^{*x}\tilde{u}_{Ri}^x\tilde{d}_{Lj}^{*v}\tilde{d}_{Lj}^v+\frac{g^2}{12}\tilde{u}_{Ri}^{*x}\tilde{u}_{Ri}^x\tilde{d}_{Lj}^{*v}\tilde{d}_{Lj}^v-\frac{g^2}{4}\tilde{u}_{Ri}^{*x}\tilde{u}_{Ri}^x\tilde{d}_{Rj}^{*v}\tilde{d}_{Rj}^v
\end{aligned}$$

$$\begin{aligned}
& + \frac{g_3^2}{12} \tilde{u}_{Ri}^{*x} \tilde{u}_{Ri}^x \tilde{d}_{Rj}^{*v} \tilde{d}_{Rj}^v - \frac{g_3^2}{4} \tilde{d}_{Ri}^{*x} \tilde{d}_{Ri}^v \tilde{u}_{Lj}^{*v} \tilde{u}_{Lj}^x + \frac{g_3^2}{12} \tilde{d}_{Ri}^{*x} \tilde{d}_{Ri}^x \tilde{u}_{Lj}^{*v} \tilde{u}_{Lj}^v - \frac{g_3^2}{4} \tilde{d}_{Ri}^{*x} \tilde{d}_{Ri}^v \tilde{d}_{Lj}^{*v} \tilde{d}_{Lj}^x \\
& + \frac{g_3^2}{12} \tilde{d}_{Ri}^{*x} \tilde{d}_{Ri}^x \tilde{d}_{Lj}^{*v} \tilde{d}_{Lj}^v - \frac{g_3^2}{4} \tilde{d}_{Ri}^{*x} \tilde{d}_{Ri}^v \tilde{u}_{Rj}^{*v} \tilde{u}_{Rj}^x + \frac{g_3^2}{12} \tilde{d}_{Ri}^{*x} \tilde{d}_{Ri}^x \tilde{u}_{Rj}^{*v} \tilde{u}_{Rj}^v
\end{aligned}$$

B.10 Soft Breaking terms

$$\begin{aligned}
\mathcal{L}_{\text{Soft breaking}} = & - \left(m_{\tilde{L}}^2\right)_{\alpha\beta} \tilde{\nu}_{L\alpha}^* \tilde{\nu}_{L\beta} - \left(m_{\tilde{E}}^2\right)_{\alpha\beta} \tilde{e}_{L\alpha}^* \tilde{e}_{L\beta} - m_{H_2}^2 h_2^{0*} h_2^0 - m_{H_2}^2 h_2^{+*} h_2^+ - \left(m_{\tilde{E}^c}^2\right)_{ij} \tilde{e}_{Ri}^* \tilde{e}_{Rj} \\
& - \left(m_{\tilde{Q}}^2\right)_{ij} \tilde{u}_{Li}^{*z} \tilde{u}_{Lj}^z - \left(m_{\tilde{Q}}^2\right)_{ij} \tilde{d}_{Li}^{*z} \tilde{d}_{Lj}^z - \left(m_{\tilde{D}^c}^2\right)_{ij} \tilde{d}_{Ri}^{*z} \tilde{d}_{Rj}^z - \left(m_{\tilde{U}^c}^2\right)_{ij} \tilde{u}_{Ri}^{*z} \tilde{u}_{Rj}^z \\
& - (h_u)_{ij} \tilde{u}_{Li}^y h_2^0 \tilde{u}_{Rj}^{*y} + (h_u)_{ij} \tilde{d}_{Li}^y h_2^+ \tilde{u}_{Rj}^{*y} - h_{\alpha\beta k} \tilde{\nu}_{L\alpha} \tilde{e}_{L\beta} \tilde{e}_{Rk}^* - h'_{\alpha j k} \tilde{\nu}_{L\alpha} \tilde{d}_{Lj} \tilde{d}_{Rk}^* \\
& \quad + h'_{\alpha j k} \tilde{e}_{L\alpha} \tilde{u}_{Lj} \tilde{d}_{Rk}^* - \frac{1}{2} \varepsilon_{xyz} h''_{ijk} \tilde{u}_{Li}^x \tilde{d}_{Rk}^{*z} \tilde{d}_{Rk}^{*z} + b_\alpha \tilde{\nu}_{L\alpha} h_2^0 - b_\alpha \tilde{e}_{L\alpha} h_2^+ \\
& - (h_u^*)_{ij} \tilde{u}_{Li}^{*y} h_2^{0*} \tilde{u}_{Rj}^y + (h_u^*)_{ij} \tilde{d}_{Li}^{*y} h_2^{+*} \tilde{u}_{Rj}^y - h_{\alpha\beta k}^* \tilde{\nu}_{L\alpha}^* \tilde{e}_{L\beta}^* \tilde{e}_{Rk} - h'_{\alpha j k}^* \tilde{\nu}_{L\alpha}^* \tilde{d}_{Lj} \tilde{d}_{Rk}^* \\
& \quad + h'_{\alpha j k}^* \tilde{e}_{L\alpha}^* \tilde{u}_{Lj} \tilde{d}_{Rk}^* - \frac{1}{2} \varepsilon_{xyz} h''_{ijk}^* \tilde{u}_{Li}^{*x} \tilde{d}_{Rk}^z \tilde{d}_{Rk}^z + b_\alpha^* \tilde{\nu}_{L\alpha}^* h_2^{0*} - b_\alpha^* \tilde{e}_{L\alpha}^* h_2^{+*} \\
& \quad + \frac{1}{2} M_1 \tilde{B} \tilde{B} + M_2 \tilde{W}_+ \tilde{W}_- + \frac{1}{2} M_2 \tilde{W}_0 \tilde{W}_0 + \frac{1}{2} M_3 \tilde{G}_R \tilde{G}_R \\
& \quad + \frac{1}{2} M_1^* \tilde{B} \tilde{B} + M_2 \tilde{W}_+ \tilde{W}_- + \frac{1}{2} M_2 \tilde{W}_0 \tilde{W}_0 + \frac{1}{2} M_3 \tilde{G}_R \tilde{G}_R
\end{aligned}$$

B.11 Gauge Fixing terms

$$\begin{aligned}
\mathcal{L}_{GF} = & -\frac{1}{\xi} \partial_\mu W^{+\mu} \partial_\nu W^{-\nu} - \frac{1}{2\xi} (\partial_\mu Z^\mu \partial_\nu Z^\nu + \partial_\mu A^\mu \partial_\nu A^\nu) - \frac{1}{2\xi_3} \partial_\mu G^{(\Omega)\mu} \partial_\nu W^{(\Omega)\nu} \\
& - \frac{1}{\sqrt{2}} \frac{ig_2}{2c_w} \tilde{\nu}_{L\alpha}^* v_\alpha \partial_\mu Z^\mu + \frac{1}{\sqrt{2}} \frac{ig_2}{2c_w} v_\alpha \tilde{\nu}_{L\alpha} \partial_\mu Z^\mu + \frac{1}{\sqrt{2}} \frac{ig_2}{2c_w} h_2^{0*} v_u \partial_\mu Z^\mu - \frac{1}{\sqrt{2}} \frac{ig_2}{2c_w} v_u h_2^0 \partial_\mu Z^\mu \\
& - \frac{ig_2}{2} \tilde{e}_{L\alpha}^* v_\alpha \partial_\mu W^{-\mu} + \frac{ig_2}{2} v_\alpha \tilde{e}_{L\alpha} \partial_\mu W^{+\mu} - \frac{ig_2}{2} h_2^{+*} v_u \partial_\mu W^{+\mu} + \frac{ig_2}{2} v_u h_2^+ \partial_\mu W^{-\mu} \\
& + \frac{1}{16} \xi (g^2 + g_2^2) \{ \tilde{\nu}_{L\alpha}^* v_\alpha \tilde{\nu}_{L\beta} v_\beta + v_\alpha \tilde{\nu}_{L\alpha} v_\beta \tilde{\nu}_{L\beta} + h_2^{0*} v_u h_2^{0*} v_u + v_u h_2^0 v_u h_2^0 \\
& \quad - 2\tilde{\nu}_{L\alpha}^* v_\alpha \tilde{\nu}_{L\beta} v_\beta - 2\tilde{\nu}_{L\alpha}^* v_\alpha h_2^{0*} v_u + 2\tilde{\nu}_{L\alpha}^* v_\alpha v_u h_2^0 \\
& \quad + 2\tilde{\nu}_{L\alpha} v_\alpha h_2^{0*} v_u - 2v_\alpha \tilde{\nu}_{L\alpha} v_u h_2^0 - 2h_2^{0*} v_u v_u h_2^0 \} \\
& + \frac{1}{4} \xi g_2^2 \{ -\tilde{e}_{L\alpha}^* v_\alpha v_\beta \tilde{e}_{L\beta} + \tilde{e}_{L\alpha}^* v_\alpha h_2^{+*} v_u + v_\alpha \tilde{e}_{L\alpha} v_u h_2^+ - h_2^{+*} v_u v_u h_2^+ \}
\end{aligned}$$

Appendix C

\mathbb{L} -MSSM Lagrangian: Mass Basis

In Section 3 we have defined the basis in which the sneutrino vevs are zero, and we apply this rotation to the whole chiral superfield \mathcal{L} . We choose the basis in the quark sector as follows. We rotate the four quark superfields to a basis where both λ'_{0ij} and $(Y_U)_{ij}$ are diagonal

$$\begin{aligned} D'_L &\longrightarrow Z_{d_L}^* D_L, & \bar{D}' &\longrightarrow Z_{d_R} \bar{D}, \\ U'_L &\longrightarrow Z_{u_L} U_L, & \bar{U}' &\longrightarrow Z_{u_R}^* \bar{U}. \end{aligned} \tag{C-1}$$

By absorbing a rotation matrix into the Lagrangian parameters, one can write down the superpotential (2.20) as

$$\begin{aligned} \mathcal{W} &= \frac{1}{2} \varepsilon_{ab} \lambda_{\alpha\beta j} \mathcal{L}_\alpha^a \mathcal{L}_\beta^b \bar{E}_j + \lambda'_{\alpha ij} \mathcal{L}_\alpha^1 Q_i^{2x} \bar{D}_j^x - \lambda'_{\alpha kj} K_{ik}^* \mathcal{L}_\alpha^2 Q_i^{1x} \bar{D}_j^x - \varepsilon_{ab} \mu_\alpha \mathcal{L}_\alpha^a H_2^b \\ &+ (Y_U)_{ij} Q_i^{1x} H_2^{2x} \bar{U}_j^x - (Y_U)_{kj} K_{ki} Q_i^{2x} H_2^{1x} \bar{U}_j^x, \end{aligned} \tag{C-2}$$

where λ'_{0jk} and $(Y_U)_{ij}$ are diagonal matrices and \mathcal{L}^1 (\mathcal{L}^2) is the neutrino (electron) component of the $SU(2)$ doublet. The charged current part of the Lagrangian,

$$\mathcal{L}_W = \frac{e}{\sqrt{2}s_W} \bar{u}_{Li} K_{ij} \bar{\sigma}^\mu W_\mu^+ d_{Lj} + \text{H.c.}, \quad (\text{C-3})$$

diagrammatically reads (in Weyl spinor notation) as,

$$\begin{array}{c} \downarrow d_{Lj} \\ W_\mu \text{ wavy line} \\ \rightarrow u_{Li} \end{array} : \frac{ie}{\sqrt{2}s_W} K_{ij} \bar{\sigma}^\mu \quad (\text{C-4})$$

with $K_{ij} = Z_{u_L ki}^* Z_{d_L kj}^*$ being the CKM matrix. We rotate all fields in the basis where sneutrino vevs are zero. Then the soft supersymmetry breaking terms are,

$$\begin{aligned} \mathcal{L}_{\text{SSB}} = & - (M_L^2)_{\alpha\beta} \tilde{\nu}_{L\alpha}^* \tilde{\nu}_{L\beta} - (M_L^2)_{\alpha\beta} \tilde{e}_{L\alpha}^* \tilde{e}_{L\beta} - m_{H_2}^2 h_2^{0*} h_2^0 - m_{H_2}^2 h_2^{+*} h_2^+ \\ & - (m_{\tilde{E}^c}^2)_{ij} \tilde{e}_{Ri}^* \tilde{e}_{Rj} - (m_{\tilde{Q}}^2)_{kl} K_{ik} K_{jl}^* \tilde{u}_{Li}^{*z} \tilde{u}_{Lj}^z - (m_{\tilde{Q}}^2)_{ij} \tilde{d}_{Li}^{*z} \tilde{d}_{Lj}^z \\ & - (m_{\tilde{D}^c}^2)_{ij} \tilde{d}_{Ri}^{*z} \tilde{d}_{Rj}^z - (m_{\tilde{U}^c}^2)_{ij} \tilde{u}_{Ri}^{*z} \tilde{u}_{Rj}^z \\ & \left[- (h_u)_{ij} \tilde{u}_{Li}^y h_2^0 \tilde{u}_{Rj}^{*y} + (h_u)_{kj} K_{ki} \tilde{d}_{Li}^y h_2^+ \tilde{u}_{Rj}^{*y} - h_{\alpha\beta k} \tilde{\nu}_{L\alpha} \tilde{e}_{L\beta} \tilde{e}_{Rk}^* - h'_{\alpha j k} \tilde{\nu}_{L\alpha} \tilde{d}_{Lj} \tilde{d}_{Rk}^* \right. \\ & \quad \left. + h'_{\alpha k j} K_{ik}^* \tilde{e}_{L\alpha} \tilde{u}_{Li} \tilde{d}_{Rj}^* + B_\alpha \tilde{\nu}_{L\alpha} h_2^0 - B_\alpha \tilde{e}_{L\alpha} h_2^+ \right. \\ & \quad \left. + \frac{1}{2} M_1 \tilde{B} \tilde{B} + M_2 \tilde{W}^+ \tilde{W}^- + \frac{1}{2} M_2 \tilde{W}^0 \tilde{W}^0 + \frac{1}{2} M_3 \tilde{G}^R \tilde{G}^R + \text{H.c.} \right], \quad (\text{C-5}) \end{aligned}$$

where B_α is the four-component bilinear term $B_\alpha = (B_0, B_i)$ and h, h' are trilinear soft breaking couplings.

In the following sections, we bring together terms of the same form, containing interaction states which mix. We first collect bilinear terms: the kinetic terms and mass terms, which determine the mixing between the fields which carry the same quantum numbers after the spontaneous breaking of the electroweak symmetry occurs.

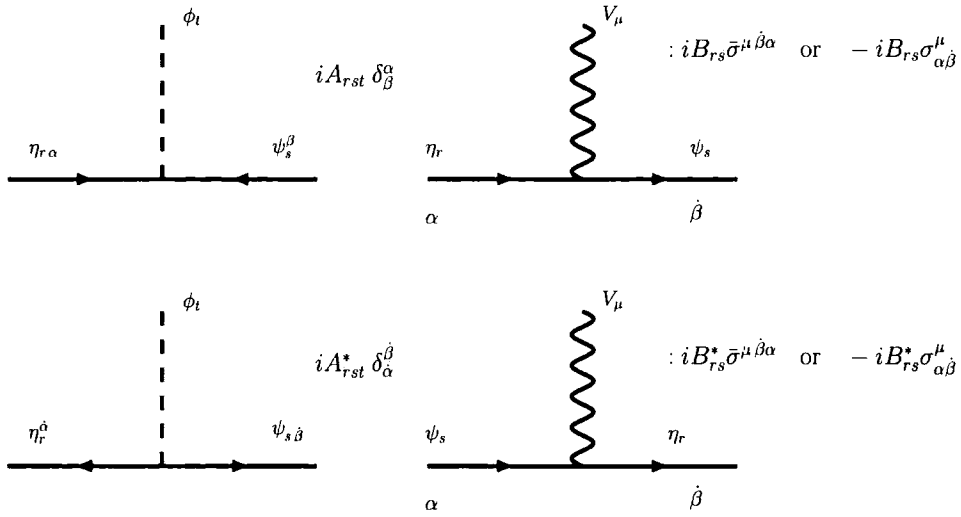


Figure C.1: Vertices on the left arise from $\mathcal{L}_Y = A_{rst}\phi_t\psi_s\eta_r + A_{rst}^*\phi_t^*\bar{\psi}_s\bar{\eta}_r$ and vertices on the right arise from $\mathcal{L} = B_{rs}\bar{\psi}_s\bar{\sigma}^\mu V_\mu\eta_r + B_{rs}^*\bar{\eta}_r\bar{\sigma}^\mu V_\mu^*\psi_s$.

For the mass terms, we present the mass matrices and define the rotation matrices which describe the transformation between the ‘interaction’ eigenstates and the ‘mass’ eigenstates.

For interaction terms, we gather the appropriate terms and display the Feynman rule for the vertex in terms of Lagrangian parameters and rotation matrices. In Fig. C.1, we manner in which Feynman rules for Weyl fermions are defined. In the following Feynman rules we only note the rule for ingoing Weyl fermions for scalar-fermion-fermion vertices and one example for each gauge boson-fermion-fermion vertex. In each case, however all the combinations shown in Fig. C.1 exist.

C.1 Kinetic Terms for Gauge Bosons

$$\begin{aligned}
\mathcal{L} \supset & -\frac{1}{4} (\partial_\mu A_\nu - \partial_\nu A_\mu) (\partial^\mu A^\nu - \partial^\nu A^\mu) - \frac{1}{2\xi} \partial_\mu A^\mu \partial_\nu A^\nu \\
& -\frac{1}{4} (\partial_\mu Z_\nu - \partial_\nu Z_\mu) (\partial^\mu Z^\nu - \partial^\nu Z^\mu) - \frac{1}{2\xi} \partial_\mu Z^\mu \partial_\nu Z^\nu \\
& -\frac{1}{2} (\partial_\mu W_\nu^+ - \partial_\nu W_\mu^+) (\partial^\mu W^{-\nu} - \partial^\nu W^{-\mu}) - \frac{1}{\xi} \partial_\mu W^{+\mu} \partial_\nu W^{-\nu} \\
& -\frac{1}{4} (\partial_\mu G_\nu^{(R)} - \partial_\nu G_\mu^{(R)}) (\partial^\mu G^{(R)\nu} - \partial^\nu G^{(R)\mu}) - \frac{1}{2\xi_3} \partial_\mu G^{(\Omega)\mu} \partial_\nu G^{(\Omega)\nu}
\end{aligned}$$

C.2 Kinetic Terms for Scalars

$$\begin{aligned}
\mathcal{L} \supset & \partial_\mu h_2^{0*} \partial^\mu h_2^0 + \partial_\mu \tilde{\nu}_{L\alpha}^* \partial^\mu \tilde{\nu}_{L\alpha} \\
& + \partial_\mu h_2^{+*} \partial^\mu h_2^+ + \partial_\mu \tilde{e}_{L\alpha}^* \partial^\mu \tilde{e}_{L\alpha} + \partial_\mu \tilde{e}_{Ri} \partial^\mu \tilde{e}_{Ri}^* \\
& + \partial_\mu \tilde{u}_{Li}^{*x} \partial^\mu \tilde{u}_{Li}^x + \partial_\mu \tilde{d}_{Li}^{*x} \partial^\mu \tilde{d}_{Li}^x + \partial_\mu \tilde{u}_{Ri}^x \partial^\mu \tilde{u}_{Ri}^{*x} + \partial_\mu \tilde{d}_{Ri}^x \partial^\mu \tilde{d}_{Ri}^{*x}
\end{aligned}$$

C.3 Kinetic Terms for Colourless Fermions

$$\begin{aligned}
\mathcal{L} \supset & i\tilde{B} \bar{\sigma}^\mu \partial_\mu \tilde{B} + i\tilde{W}^0 \bar{\sigma}^\mu \partial_\mu \tilde{W}^0 + i\tilde{h}_2^0 \bar{\sigma}^\mu \partial_\mu \tilde{h}_2^0 + i\bar{\nu}_{L\alpha} \bar{\sigma}^\mu \partial_\mu \nu_{L\alpha} \\
& + i\tilde{W}^- \bar{\sigma}^\mu \partial_\mu \tilde{W}^- + i\bar{e}_{L\alpha} \bar{\sigma}^\mu \partial_\mu e_{L\alpha} + i\tilde{W}^+ \bar{\sigma}^\mu \partial_\mu \tilde{W}^+ + i\tilde{h}_2^+ \bar{\sigma}^\mu \partial_\mu \tilde{h}_2^+ + i\bar{e}_{Ri} \bar{\sigma}^\mu \partial_\mu e_{Ri}
\end{aligned}$$

C.4 Kinetic Terms for Quarks/Gluino

$$\begin{aligned}
\mathcal{L} \supset & i\bar{u}_{Li}^x \bar{\sigma}^\mu \partial_\mu u_{Li}^x + i\bar{d}_{Li}^x \bar{\sigma}^\mu \partial_\mu d_{Li}^x + i\bar{u}_{Ri}^x \bar{\sigma}^\mu \partial_\mu u_{Ri}^x + i\bar{d}_{Ri}^x \bar{\sigma}^\mu \partial_\mu d_{Ri}^x \\
& + i\tilde{G}^{(R)} \bar{\sigma}^\mu \partial_\mu \tilde{G}^{(R)}
\end{aligned}$$

C.5 Kinetic Terms for Ghosts

$$\mathcal{L} \supset \partial_\mu \bar{\eta}^+ \partial^\mu \eta^+ + \partial_\mu \bar{\eta}^- \partial^\mu \eta^- + \partial_\mu \bar{\eta}_Z \partial^\mu \eta_Z + \partial_\mu \bar{\eta}_A \partial^\mu \eta_A + \partial_\mu \bar{\eta}_G^{(R)} \partial^\mu \eta_G^{(R)}$$

C.6 Mass Terms for Gauge Bosons

$$\begin{aligned} \mathcal{L} \supset & \frac{g_2^2}{8c_w^2} Z_\mu v_0 Z^\mu v_0 + \frac{g_2^2}{8c_w^2} Z_\mu v_u Z^\mu v_u \\ & + \frac{g_2^2}{4} W_\mu^+ v_0 W^{-\mu} v_0 + \frac{g_2^2}{4} W_\mu^- v_u W^{+\mu} v_u \end{aligned}$$

From these terms we see that the masses given to the vector bosons are as follows:

$$M_A^2 = 0, \quad M_Z^2 = \frac{g_2^2}{4c_w^2} (v_0^2 + v_u^2), \quad M_W^2 = \frac{g_2^2}{4} (v_0^2 + v_u^2).$$

C.7 Mass Terms for Neutral Scalars

$$\begin{aligned} \mathcal{L} \supset & h_2^{0*} h_2^0 \left\{ -m_{H_2}^2 - \mu_\alpha^* \mu_\alpha + \frac{1}{8} (g^2 + g_2^2) (v_0^2 - 2v_u^2) - \frac{1}{8} \xi (g^2 + g_2^2) v_u^2 \right\} \\ & + h_2^0 h_2^0 \left\{ -\frac{1}{16} (g^2 + g_2^2) v_u^2 + \frac{1}{16} \xi (g^2 + g_2^2) v_u^2 \right\} \\ & + h_2^{0*} h_2^{0*} \left\{ -\frac{1}{16} (g^2 + g_2^2) v_u^2 + \frac{1}{16} \xi (g^2 + g_2^2) v_u^2 \right\} \\ & + \tilde{\nu}_{L\alpha}^* \tilde{\nu}_{L\beta} \left\{ +\frac{1}{8} (g^2 + g_2^2) (v_u^2 - v_0^2) \delta_{\alpha\beta} - \frac{1}{8} (g^2 + g_2^2) v_0^2 \delta_{0\alpha} \delta_{0\beta} - \frac{1}{8} \xi (g^2 + g_2^2) v_0^2 \delta_{0\alpha} \delta_{0\beta} - \mu_\alpha^* \mu_\beta - (m_{\tilde{L}}^2)_{\alpha\beta} \right\} \\ & + \tilde{\nu}_{L\alpha} \tilde{\nu}_{L\beta} \left\{ -\frac{1}{16} (g^2 + g_2^2) v_0^2 \delta_{0\alpha} \delta_{0\beta} + \frac{1}{16} \xi (g^2 + g_2^2) v_0^2 \delta_{0\alpha} \delta_{0\beta} \right\} \\ & + \tilde{\nu}_{L\alpha}^* \tilde{\nu}_{L\beta}^* \left\{ -\frac{1}{16} (g^2 + g_2^2) v_0^2 \delta_{0\alpha} \delta_{0\beta} + \frac{1}{16} \xi (g^2 + g_2^2) v_0^2 \delta_{0\alpha} \delta_{0\beta} \right\} \end{aligned}$$

$$\begin{aligned}
& +\tilde{\nu}_{L\alpha} h_2^0 \left\{ +\frac{1}{8}(g^2 + g_2^2)v_u v_0 \delta_{0\alpha} + b_\alpha - \frac{1}{8}\xi(g^2 + g_2^2)v_u v_0 \delta_{0\alpha} \right\} \\
& +\tilde{\nu}_{L\alpha}^* h_2^{0*} \left\{ +\frac{1}{8}(g^2 + g_2^2)v_u v_0 \delta_{0\alpha} + b_\alpha - \frac{1}{8}\xi(g^2 + g_2^2)v_u v_0 \delta_{0\alpha} \right\} \\
& +\tilde{\nu}_{L\alpha}^* h_2^0 \left\{ +\frac{1}{8}(g^2 + g_2^2)v_u v_0 \delta_{0\alpha} + \frac{1}{8}\xi(g^2 + g_2^2)v_u v_0 \delta_{0\alpha} \right\} \\
& +\tilde{\nu}_{L\alpha} h_2^{0*} \left\{ +\frac{1}{8}(g^2 + g_2^2)v_u v_0 \delta_{0\alpha} + \frac{1}{8}\xi(g^2 + g_2^2)v_u v_0 \delta_{0\alpha} \right\} \\
& \dots\dots\dots
\end{aligned}$$

We have moved to the basis in which sneutrino vevs vanish $\mathcal{L} \rightarrow U\mathcal{L}$, as described in Section. 3. As such, the sector decouples into exact CP-odd and CP-even mass eigenstates,

$$\mathcal{L} \supset - \begin{pmatrix} \text{Re } h_0^2 & \text{Re } \tilde{\nu}_{L0} & \text{Re } \tilde{\nu}_{Li} \end{pmatrix} Z_R^* Z_R^T \mathcal{M}_H^2 Z_R Z_R^\dagger \begin{pmatrix} \text{Re } h_0^2 \\ \text{Re } \tilde{\nu}_{L0} \\ \text{Re } \tilde{\nu}_{Lj} \end{pmatrix},$$

where

$$\mathcal{M}_H^2 = \begin{pmatrix} \cos^2 \beta M_A^2 + \sin^2 \beta M_Z^2 & -\frac{1}{2} \sin 2\beta (M_A^2 + M_Z^2) & -B_j \\ -\frac{1}{2} \sin 2\beta (M_A^2 + M_Z^2) & \sin^2 \beta M_A^2 + \cos^2 \beta M_Z^2 & B_j \tan \beta \\ -B_i & B_i \tan \beta & M_i^2 \delta_{ij} \end{pmatrix},$$

and

$$M_i^2 \equiv \left[U^\dagger \left((m_{\tilde{L}}^2) + \mu_\alpha^* \mu_\beta \right) U \right]_{ii} + \frac{1}{2} \cos 2\beta M_Z^2, \quad B_\alpha = b_\beta U_{\beta\alpha} \quad \text{and} \quad M_A^2 = \frac{2B_0}{\sin 2\beta},$$

where M_A is the value the lightest CP-odd neutral scalar would have in the R-parity conserving limit. The rotation matrix is then given by

$$Z_R^T \mathcal{M}_H^2 Z_R = \text{diag}[m_{h^0}^2, m_{H^0}^2, (m_{\tilde{\nu}_+}^2)_i]. \quad i = 1, \dots, 3.$$

$$\mathcal{L} \supset - \begin{pmatrix} \text{Im } h_0^2 & \text{Im } \tilde{\nu}_{L0} & \text{Im } \tilde{\nu}_{Li} \end{pmatrix} Z_A^* Z_A^T \mathcal{M}_A^2 Z_A Z_A^\dagger \begin{pmatrix} \text{Im } h_0^2 \\ \text{Im } \tilde{\nu}_{L0} \\ \text{Im } \tilde{\nu}_{Lj} \end{pmatrix},$$

where

$$\mathcal{M}_A^2 = \begin{pmatrix} \cos^2 \beta M_A^2 + \xi \sin^2 \beta M_Z^2 & \frac{1}{2} \sin 2\beta (M_A^2 - \xi M_Z^2) & B_j \\ \frac{1}{2} \sin 2\beta (M_A^2 - \xi M_Z^2) & \sin^2 \beta M_A^2 + \xi \cos^2 \beta M_Z^2 & B_j \tan \beta \\ B_i & B_i \tan \beta & M_i^2 \delta_{ij} \end{pmatrix},$$

$$Z_A^T \mathcal{M}_A^2 Z_A = \text{diag}[m_{G^0}^2, m_{A^0}^2, (m_{\tilde{\nu}_-}^2)_i], \quad i = 1, \dots, 3.$$

C.8 Mass Terms for Charged Scalars

$$\begin{aligned} \mathcal{L} \supset & -h_2^{+\ast} h_2^+ \left(\mu_\alpha \mu_\alpha^\ast + m_{H_2}^2 + \frac{g^2}{8} v_u^2 - \frac{g^2}{8} v_\alpha^2 + \frac{g_2^2}{8} v_u^2 + \frac{g_2^2}{8} v_\alpha^2 + \frac{g_2^2}{4} \xi v_u^2 \right) \\ & - \tilde{e}_{L\alpha}^\ast h_2^{+\ast} \left(b_\alpha^\ast + \frac{g_2^2}{4} (1 - \xi) v_0 v_u \delta_{0\alpha} \right) \\ & - \tilde{e}_{Rj}^\ast h_2^{+\ast} \left(-\frac{1}{\sqrt{2}} \lambda_{\alpha 0j} \mu_\alpha^\ast v_0 \right) \\ & - \tilde{e}_{L\alpha} h_2^+ \left(b_\alpha + \frac{g_2^2}{4} (1 - \xi) v_u v_0 \delta_{0\alpha} \right) \\ & - \tilde{e}_{L\alpha} \tilde{e}_{L\beta}^\ast \left(\mu_\alpha \mu_\beta^\ast + (m_{\tilde{L}}^2)_{\beta\alpha} + \frac{1}{8} (g_2^2 - g^2) (v_u^2 - v_0^2) \delta_{\alpha\beta} \right. \\ & \quad \left. + \frac{g_2^2}{4} (\xi + 1) v_0 \delta_{0\alpha} \delta_{0\beta} + \frac{1}{2} \lambda_{0\alpha k} \lambda_{0\beta k}^\ast v_0 \right) \\ & - \tilde{e}_{L\beta} \tilde{e}_{Rj}^\ast \left(-\frac{1}{\sqrt{2}} \lambda_{\alpha\beta j} \mu_\alpha^\ast v_u + \frac{1}{\sqrt{2}} h_{0\beta j} v_0 \right) \end{aligned}$$

$$\begin{aligned}
& -\tilde{e}_{Rq} h_2^+ \left(-\frac{1}{\sqrt{2}} \mu_\alpha \lambda_{\alpha 0q}^* v_0 \right) \\
& -\tilde{e}_{L\beta}^* \tilde{e}_{Rk} \left(-\frac{1}{\sqrt{2}} \mu_\alpha \lambda_{\alpha\beta k}^* v_u + \frac{1}{\sqrt{2}} h_{0\beta k}^* v_0 \right) \\
& -\tilde{e}_{Ri}^* \tilde{e}_{Rj} \left(\left(m_{\tilde{E}^c}^2 \right)_{ij} + \frac{g^2}{4} v_u^2 \delta_{ij} - \frac{g^2}{4} v_0^2 \delta_{ij} + \frac{1}{2} \lambda_{\alpha 0i} \lambda_{\alpha 0j}^* v_0^2 \right)
\end{aligned}$$

$$\begin{aligned}
\mathcal{L} \supset & - \begin{pmatrix} h_2^{+*} & h_1^- & \tilde{e}_{Lj} & \tilde{e}_{Rk} \end{pmatrix} Z_H Z_H^\dagger \mathcal{M}_{H^+}^2 Z_H Z_H^\dagger \begin{pmatrix} h_2^+ \\ h_1^{-*} \\ \tilde{e}_{Li}^* \\ \tilde{e}_{Rl}^* \end{pmatrix} \\
& = -(\hat{\mathcal{M}}_{H^+}^2)_{pq} H_p^{+*} H_q^+, \quad p, q = 1, \dots, 8,
\end{aligned}$$

where,

$$\mathcal{M}_{H^+}^2 = \begin{pmatrix} M_A^2 \cos^2 \beta + M_W^2 \cos^2 \beta + \xi M_W^2 \sin^2 \beta & M_A^2 \sin \beta \cos \beta + M_W^2 (1 - \xi) \sin \beta \cos \beta & & & \\ M_A^2 \sin \beta \cos \beta + M_W^2 (1 - \xi) \sin \beta \cos \beta & M_A^2 \sin^2 \beta + \xi M_W^2 \cos^2 \beta + M_W^2 \sin^2 \beta & & & \\ & & B_j & & B_j \tan \beta \\ & & \frac{1}{\sqrt{2}} \lambda_{0ml}^* \mu_m v_d & & \frac{1}{\sqrt{2}} \lambda_{0ml}^* \mu_m v_u \\ & & & & \\ & & & & \\ & & B_i & & \frac{1}{\sqrt{2}} \lambda_{0ml} \mu_m^* v_d \\ & & B_i \tan \beta & & \frac{1}{\sqrt{2}} \lambda_{0ml} \mu_m^* v_u \\ M_i^2 \delta_{ij} - M_W^2 \cos^2 2\beta \delta_{ij} + \frac{1}{2} \lambda_{0im}^* \lambda_{0jm} v_d^2 & & & & \frac{1}{\sqrt{2}} (-\lambda_{\alpha jl} \mu_\alpha^* v_u + h_{0jl} v_d) \\ & & \frac{1}{\sqrt{2}} (-\lambda_{\alpha jl}^* \mu_\alpha v_u + h_{0jl}^* v_d) & & \left(m_{\tilde{E}^c}^2 \right)_{lk} + (M_W^2 - M_Z^2) \cos^2 2\beta \delta_{lk} + \frac{1}{2} \lambda_{0ml} \lambda_{0mk}^* v_d^2 \end{pmatrix}.$$

C.9 Mass terms for down-type squarks

$$-\tilde{d}_{Li}^{*z} \tilde{d}_{Lj}^z \left(\left(m_{\tilde{Q}}^2 \right)_{ij} + \left(\frac{g^2}{24} + \frac{g_2^2}{8} \right) (v_u^2 - v_0^2) \delta_{ik} + \lambda'_{0jk} \lambda_{0ik}^* v_0^2 \right)$$

$$\begin{aligned}
& -\tilde{d}_{Li}^{*z} \tilde{d}_{Rj}^z \left(-\frac{1}{\sqrt{2}} \mu_\alpha \lambda'_{\alpha ij} v_u + \frac{1}{\sqrt{2}} h'_{0ij} v_0 \right) \\
& -\tilde{d}_{Ri}^{*y} \tilde{d}_{Lj}^y \left(-\frac{1}{\sqrt{2}} \lambda'_{\alpha ji} \mu_\alpha^* v_u + \frac{1}{\sqrt{2}} h'_{0ji} v_0 \right) \\
& -\tilde{d}_{Ri}^{*x} \tilde{d}_{Rj}^x \left(+ \left(m_{\tilde{D}^c}^2 \right)_{ij} + \frac{g^2}{12} v_u^2 \delta_{ij} + \frac{1}{2} \lambda'_{0qi} \lambda'_{0qj}^* v_0^2 - \frac{g^2}{12} v_0^2 \delta_{ij} \right)
\end{aligned}$$

.....

Mass terms and rotation matrices for down-type squarks arise from the following terms in the Lagrangian:

$$\begin{aligned}
-\mathcal{L} \supset \begin{pmatrix} \tilde{d}_{Li}^{*z} & \tilde{d}_{Rj}^{*z} \end{pmatrix} \mathcal{M}_d^2 \begin{pmatrix} \tilde{d}_{Lk}^z \\ \tilde{d}_{Rl}^z \end{pmatrix} &= \begin{pmatrix} \tilde{d}_{Li}^{*z} & \tilde{d}_{Rj}^{*z} \end{pmatrix} Z_{\tilde{d}}^* Z_{\tilde{d}}^T \mathcal{M}_d^2 Z_{\tilde{d}} Z_{\tilde{d}}^T \begin{pmatrix} \tilde{d}_{Lk}^z \\ \tilde{d}_{Rl}^z \end{pmatrix} \\
&= \hat{\mathcal{M}}_{dpq}^2 \tilde{d}_p^{*z} \tilde{d}_q^z, \quad p, q = 1, \dots, 6 \quad (\text{C-6})
\end{aligned}$$

where

$$\mathcal{M}_d^2 = \begin{pmatrix} \left(m_{\tilde{Q}}^2 \right)_{ik} + \frac{1}{2} \lambda'_{0km} \lambda'_{0im}^* v_0^2 + \left(\frac{g^2}{24} + \frac{g_2^2}{8} \right) (v_u^2 - v_0^2) \delta_{ik} & -\frac{1}{\sqrt{2}} \mu_\alpha \lambda'_{\alpha il} v_u + \frac{1}{\sqrt{2}} h'_{0il} v_0 \\ -\frac{1}{\sqrt{2}} \lambda'_{\alpha kj} \mu_\alpha^* v_u + \frac{1}{\sqrt{2}} h'_{0kj} v_0 & \left(m_{\tilde{D}^c}^2 \right)_{jl} + \frac{1}{2} \lambda'_{0qj} \lambda'_{0ql}^* v_0^2 + \frac{g^2}{12} (v_u^2 - v_0^2) \delta_{jl} \end{pmatrix},$$

Recall that $\lambda'_{0km} = \hat{Y}_{Dk} \delta_{km}$ are diagonal down-quark Yukawa couplings.

C.10 Mass terms for up-type squarks

$$\begin{aligned}
\mathcal{L} \supset & -\tilde{u}_{Li}^{*z} \tilde{u}_{Lj}^z \left(+ \left(m_{\tilde{Q}}^2 \right)_{ij} + \frac{1}{2} (Y_U)_{jk} (Y_U)_{ik}^* v_u^2 + \left(\frac{g^2}{24} - \frac{g_2^2}{8} \right) (v_u^2 - v_0^2) \delta_{ij} \right) \\
& -\tilde{u}_{Ri}^{*y} \tilde{u}_{Lj}^y \left(+ \frac{1}{\sqrt{2}} (h_u)_{ji} v_u - \frac{1}{\sqrt{2}} (Y_U)_{ji} \mu_0^* v_0 \right) \\
& -\tilde{u}_{Li}^{*y} \tilde{u}_{Rj}^y \left(+ \frac{1}{\sqrt{2}} (h_u^*)_{ij} v_u - \frac{1}{\sqrt{2}} \mu_0 (Y_U)_{ij}^* v_0 \right)
\end{aligned}$$

$$-\tilde{u}_{Ri}^{*z}\tilde{u}_{Rj}^z \left(+ \left(m_{\tilde{U}c}^2 \right)_{ij} + \frac{1}{2} (Y_U)_{ki} (Y_U)_{kj}^* v_u^2 - \frac{g^2}{6} (v_u^2 - v_0^2) \delta_{ij} \right)$$

.....

The mass terms for up-type squarks are

$$\begin{aligned} -\mathcal{L} \supset \begin{pmatrix} \tilde{u}_{Li}^{*z} & \tilde{u}_{Rj}^{*z} \end{pmatrix} \mathcal{M}_u^2 \begin{pmatrix} \tilde{u}_{Lk}^z \\ \tilde{u}_{Rl}^z \end{pmatrix} &= \begin{pmatrix} \tilde{u}_{Li}^{*z} & \tilde{u}_{Rj}^{*z} \end{pmatrix} Z_{\tilde{u}} Z_{\tilde{u}}^\dagger \mathcal{M}_u^2 Z_{\tilde{u}} Z_{\tilde{u}}^\dagger \begin{pmatrix} \tilde{u}_{Lk}^z \\ \tilde{u}_{Rl}^z \end{pmatrix} \\ &= \mathcal{M}_{upq}^2 \tilde{u}_p^{*z} \tilde{u}_q^z, \quad p, q = 1, \dots, 6, \quad (\text{C-7}) \end{aligned}$$

where,

$$\mathcal{M}_u^2 = \begin{pmatrix} \left((K m_Q^2 K^\dagger)_{ik} + \frac{1}{2} (Y_U Y_U^\dagger)_{ki} v_u^2 + \left(\frac{g^2}{24} - \frac{g_2^2}{8} \right) (v_u^2 - v_0^2) \delta_{ik} & \frac{1}{\sqrt{2}} (h_u^*)_{jk} v_u - \frac{1}{\sqrt{2}} \mu_0 (Y_U)_{jk}^* v_0 \\ \frac{1}{\sqrt{2}} (h_u)_{li} v_u - \frac{1}{\sqrt{2}} (Y_U)_{li} \mu_0^* v_0 & \left(m_{\tilde{U}c}^2 \right)_{jm} + \frac{1}{2} (Y_U Y_U^\dagger)_{jm} v_u^2 - \frac{g^2}{6} (v_u^2 - v_0^2) \delta_{jm} \end{pmatrix}$$

Recall that $(Y_U)_{ij} = \hat{Y}_{Ui} \delta_{ij}$ are diagonal up quark Yukawa couplings.

C.11 Mass terms for quarks

$$\begin{aligned} \mathcal{L} &- \frac{1}{\sqrt{2}} \lambda'_{0ij} v_0 d_{Li}^z d_{Rj}^z - \frac{1}{\sqrt{2}} \lambda'_{0ij}{}^* v_0 \bar{d}_{Li}^z \bar{d}_{Rj}^z \\ &- \frac{1}{\sqrt{2}} (Y_U)_{ij} v_u u_{Rj}^y u_{Li}^y - \frac{1}{\sqrt{2}} (Y_U)_{ij}^* v_u \bar{u}_{Rj}^y \bar{u}_{Li}^y \end{aligned}$$

.....

$$\begin{aligned} \mathcal{L} \supset & -\frac{1}{\sqrt{2}} \lambda'_{0ij} v_d d_{Li}^z d_{Rj}^z - \frac{1}{\sqrt{2}} \lambda'_{0ij}{}^* v_d \bar{d}_{Li}^z \bar{d}_{Rj}^z \\ & = -m_{di} d_{Li}^z d_{Ri}^z - m_{di} \bar{d}_{Li}^z \bar{d}_{Ri}^z, \quad i = 1, \dots, 3. \quad (\text{C-8}) \end{aligned}$$

C.12 Mass terms for neutrino-neutralino

$$\begin{aligned}
\mathcal{L} \supset & -\frac{1}{2}M_1(-i\tilde{B})(-i\tilde{B}) - \frac{g}{2}v_u\tilde{h}_2^0(-i\tilde{B}) + \frac{g}{2}v_0\nu_{L0}(-i\tilde{B}) \\
& -\frac{1}{2}M_2(-i\tilde{W}^0)(-i\tilde{W}^0) + \frac{g_2}{2}v_u(-i\tilde{W}^0)\tilde{h}_2^0 - \frac{g_2}{2}v_0(-i\tilde{W}^0)\nu_{L0} + \mu_\alpha\nu_{L\alpha}\tilde{h}_2^0 \\
& -\frac{1}{2}M_1^*(i\tilde{B})(i\tilde{B}) - \frac{g}{2}v_u\tilde{h}_2^0(i\tilde{B}) + \frac{g}{2}v_0\bar{\nu}_{L0}(i\tilde{B}) \\
& -\frac{1}{2}M_2^*(i\tilde{W}^0)(i\tilde{W}^0) + \frac{g_2}{2}v_u(i\tilde{W}^0)\tilde{h}_2^0 - \frac{g_2}{2}v_0(i\tilde{W}^0)\bar{\nu}_{L0} + \mu_\alpha^*\bar{\nu}_{L\alpha}\tilde{h}_2^0
\end{aligned}$$

.....

$$\begin{aligned}
\mathcal{L} \supset & -\frac{1}{2} \begin{pmatrix} -i\tilde{B} & -i\tilde{W}^0 & \tilde{h}_2^0 & \nu_{L\alpha} \end{pmatrix} \mathcal{M}_N \begin{pmatrix} -i\tilde{B} \\ -i\tilde{W}^0 \\ \tilde{h}_2^0 \\ \nu_{L\beta} \end{pmatrix} - \text{H.c.} \\
= & -\frac{1}{2} \begin{pmatrix} -i\tilde{B} & -i\tilde{W}^0 & \tilde{h}_2^0 & \nu_{L\alpha} \end{pmatrix} Z_N^* Z_N^T \mathcal{M}_N Z_N Z_N^\dagger \begin{pmatrix} -i\tilde{B} \\ -i\tilde{W}^0 \\ \tilde{h}_2^0 \\ \nu_{L\beta} \end{pmatrix} + \text{H.c.} \\
= & -\frac{1}{2} \hat{\mathcal{M}}_{Npq} \kappa_p^0 \kappa_q^0 - \frac{1}{2} \hat{\mathcal{M}}_{Npq}^* \bar{\kappa}_p^0 \bar{\kappa}_q^0, \quad p, q = 1, \dots, 7. \tag{C-9}
\end{aligned}$$

where

$$\mathcal{M}_N = \begin{pmatrix} M_1 & 0 & \frac{g}{2}v_u & -\frac{g}{2}v_0\delta_{0\beta} \\ 0 & M_2 & -\frac{g_2}{2}v_u & \frac{g_2}{2}v_0\delta_{0\beta} \\ \frac{g}{2}v_u & -\frac{g_2}{2}v_u & 0 & -\mu_\beta \\ -\frac{g}{2}v_0\delta_{0\alpha} & \frac{g_2}{2}v_0\delta_{0\alpha} & -\mu_\alpha & 0_{\alpha\beta} \end{pmatrix}. \tag{C-10}$$

C.13 Mass terms for charged lepton-chargino

$$\begin{aligned}
& -M_2(-i\tilde{W}^+)(-i\tilde{W}^-) - \frac{1}{\sqrt{2}}g_2v_u(-i\tilde{W}^-)\tilde{h}_2^+ - \frac{1}{\sqrt{2}}g_2v_0(-i\tilde{W}^+)e_{L0} \\
& \quad -\mu_\alpha e_{L\alpha}\tilde{h}_2^+ + \frac{1}{\sqrt{2}}\lambda_{\alpha 0j}v_0e_{L\alpha}e_{Rj} - M_2^*(i\tilde{W}^+)(i\tilde{W}^-) \\
& -\frac{1}{\sqrt{2}}g_2v_u(i\tilde{W}^-)\bar{\tilde{h}}_2^+ - \frac{1}{\sqrt{2}}g_2v_0(i\tilde{W}^+)\bar{e}_{L0} - \mu_\alpha^*\bar{e}_{L\alpha}\bar{\tilde{h}}_2^+ + \frac{1}{\sqrt{2}}\lambda_{\alpha 0j}^*v_0\bar{e}_{L\alpha}\bar{e}_{Rj}
\end{aligned}$$

$$\begin{aligned}
\mathcal{L} \supset & - \begin{pmatrix} -i\tilde{W}^- & e_{L\alpha} \end{pmatrix} \mathcal{M}_c \begin{pmatrix} -i\tilde{W}^+ \\ \tilde{h}_2^+ \\ e_{Rk} \end{pmatrix} - \begin{pmatrix} i\tilde{W}^- & \bar{e}_{L\alpha} \end{pmatrix} \mathcal{M}_c^* \begin{pmatrix} i\tilde{W}^+ \\ \bar{\tilde{h}}_2^+ \\ \bar{e}_{Rk} \end{pmatrix} \\
& = - \begin{pmatrix} -i\tilde{W}^- & e_{L\alpha} \end{pmatrix} Z_- Z_-^\dagger \mathcal{M}_c Z_+ Z_+^\dagger \begin{pmatrix} -i\tilde{W}^+ \\ \tilde{h}_2^+ \\ e_{Rk} \end{pmatrix} \\
& \quad - \begin{pmatrix} i\tilde{W}^- & \bar{e}_{L\alpha} \end{pmatrix} Z_-^* Z_-^T \mathcal{M}_c^* Z_+^* Z_+^T \begin{pmatrix} i\tilde{W}^+ \\ \bar{\tilde{h}}_2^+ \\ \bar{e}_{Rk} \end{pmatrix} \\
& = -\hat{\mathcal{M}}_{cpq}\kappa_p^-\kappa_q^+ - \hat{\mathcal{M}}_{cpq}^*\bar{\kappa}_p^-\bar{\kappa}_q^+, \quad p, q = 1, \dots, 5 \tag{C-11}
\end{aligned}$$

where

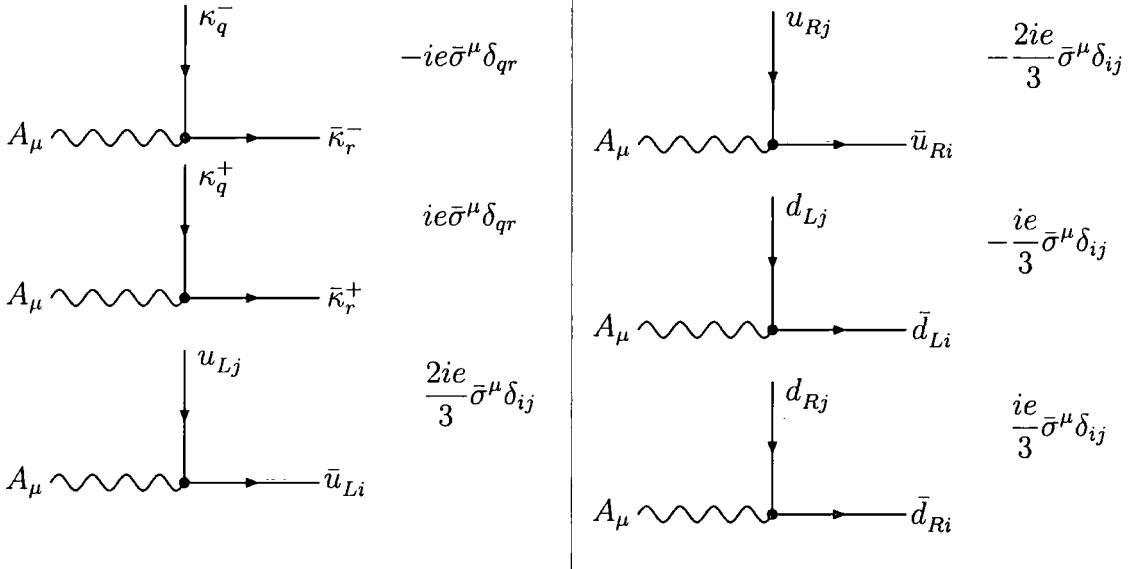
$$\mathcal{M}_c = \begin{pmatrix} M_2 & \frac{1}{\sqrt{2}}g_2v_u & 0 \\ \frac{1}{\sqrt{2}}g_2v_0\delta_{0\alpha} & \mu_\alpha & -\frac{1}{\sqrt{2}}\lambda_{\alpha 0k}v_0 \end{pmatrix}. \tag{C-12}$$

C.14 Mass terms for gluino

$$\mathcal{L} \supset \frac{1}{2}M_3\tilde{G}^R\tilde{G}^R + \frac{1}{2}M_3^*\tilde{G}^{\tilde{R}}\tilde{G}^{\tilde{R}}$$

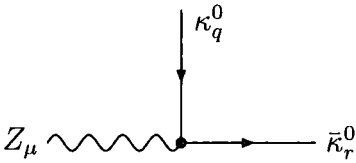
C.15 Fermion-Fermion-Photon interactions

$$\begin{aligned}
 \mathcal{L} \supset & -e\bar{e}_{L\alpha}\bar{\sigma}^\mu A_\mu e_{L\alpha} + e\bar{e}_{Ri}\bar{\sigma}^\mu A_\mu e_{Ri} + e\bar{h}_2^+\bar{\sigma}^\mu A_\mu \tilde{h}_2^+ \\
 & + g_2 s_w \tilde{W}^+ \bar{\sigma}^\mu A_\mu \tilde{W}^+ - g_2 s_w \tilde{W}^- \bar{\sigma}^\mu A_\mu \tilde{W}^- \\
 & - \frac{e}{3} \bar{d}_{Li}^x \bar{\sigma}^\mu A_\mu d_{Li}^x - \frac{2e}{3} \bar{u}_{Ri}^x \bar{\sigma}^\mu A_\mu u_{Ri}^x + \frac{e}{3} \bar{d}_{Ri}^x \bar{\sigma}^\mu A_\mu d_{Ri}^x + \frac{2e}{3} \bar{u}_{Li}^x \bar{\sigma}^\mu A_\mu u_{Li}^x
 \end{aligned}$$

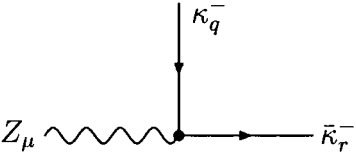


C.16 Fermion-Fermion-Z interactions

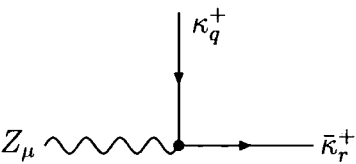
$$\begin{aligned}
\mathcal{L} \supset & \frac{g_2}{2c_W} \bar{\nu}_{L\alpha} \bar{\sigma}^\mu Z_\mu \nu_{L\alpha} - \frac{g_2}{c_W} \left(\frac{1}{2} - s_W^2 \right) \bar{e}_{L\alpha} \bar{\sigma}^\mu Z_\mu e_{L\alpha} \\
& - g s_w \bar{e}_{Ri} \bar{\sigma}^\mu Z_\mu e_{Ri} + \frac{g_2}{c_W} \left(\frac{1}{2} - s_W^2 \right) \bar{h}_2^+ \bar{\sigma}^\mu Z_\mu \tilde{h}_2^+ \\
& - \frac{g_2}{2c_w} \bar{h}_2^0 \bar{\sigma}^\mu Z_\mu \tilde{h}_2^0 \\
& + g_2 c_w \bar{W}^+ \bar{\sigma}^\mu Z_\mu \tilde{W}^+ - g_2 c_w \bar{W}^- \bar{\sigma}^\mu Z_\mu \tilde{W}^- \\
& - \frac{1}{3} g s_w \bar{d}_{Ri}^x \bar{\sigma}^\mu Z_\mu d_{Ri}^x - \frac{g_2}{c_w} \left(\frac{1}{2} - \frac{1}{3} s_W^2 \right) \bar{d}_{Li}^x \bar{\sigma}^\mu Z_\mu d_{Li}^x + \frac{2}{3} g s_w \bar{u}_{Ri}^x \bar{\sigma}^\mu Z_\mu u_{Ri}^x + \frac{g_2}{c_w} \left(\frac{1}{2} - \frac{2}{3} s_W^2 \right) \bar{u}_{Li}^x \bar{\sigma}^\mu Z_\mu u_{Li}^x
\end{aligned}$$



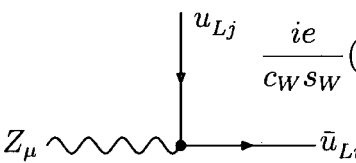
$$\frac{ie}{2s_W c_W} \left[Z_{N(4+\alpha)r}^* Z_{N(4+\alpha)q} - Z_{N3r}^* Z_{N3q} \right] \bar{\sigma}^\mu$$



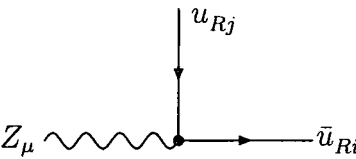
$$i \left[-\frac{e}{s_W c_W} \left(\frac{1}{2} - s_W^2 \right) Z_{-(2+\alpha)q}^* Z_{-(2+\alpha)r} - \frac{e c_W}{s_W} Z_{-1q}^* Z_{-1r} \right] \bar{\sigma}^\mu$$



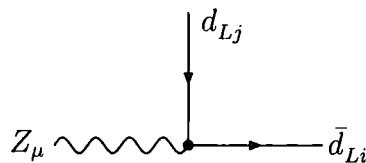
$$i \left[-\frac{e s_W}{c_W} Z_{+(2+i)r}^* Z_{+(2+i)q} + \frac{e}{s_W c_W} \left(\frac{1}{2} - s_W^2 \right) Z_{+2r}^* Z_{+2q} + \frac{e c_W}{s_W} Z_{+1r}^* Z_{+1q} \right] \bar{\sigma}^\mu$$



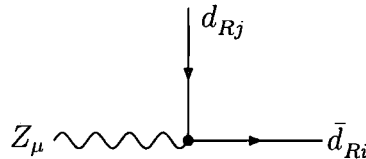
$$\frac{ie}{c_W s_W} \left(\frac{1}{2} - \frac{2}{3} s_W^2 \right) \bar{\sigma}^\mu \delta_{ij}$$



$$\frac{2ies_W}{3c_W} \bar{\sigma}^\mu \delta_{ij}$$



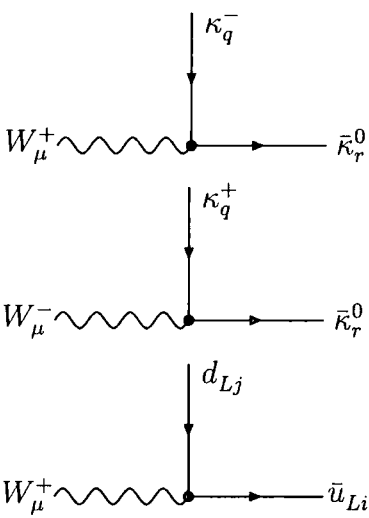
$$-\frac{ie}{c_W s_W} \left(\frac{1}{2} - \frac{1}{3} s_W^2 \right) \bar{\sigma}^\mu \delta_{ij}$$



$$-\frac{ies_W}{3c_W} \bar{\sigma}^\mu \delta_{ij}$$

C.17 Fermion-Fermion-W interactions

$$\begin{aligned}
 \mathcal{L} \supset & \frac{g_2}{\sqrt{2}} \bar{\nu}_{L\alpha} \bar{\sigma}^\mu W_\mu^+ e_{L\alpha} + \frac{g_2}{\sqrt{2}} \bar{e}_{L\alpha} \bar{\sigma}^\mu W_\mu^- \nu_{L\alpha} + \frac{g_2}{\sqrt{2}} \bar{h}_2^+ \bar{\sigma}^\mu W_\mu^+ \tilde{h}_2^0 + \frac{g_2}{\sqrt{2}} \bar{h}_2^0 \bar{\sigma}^\mu W_\mu^- \tilde{h}_2^+ \\
 & + g_2 \tilde{W}^0 \bar{\sigma}^\mu W_\mu^+ \tilde{W}^- - g_2 \tilde{W}^0 \bar{\sigma}^\mu W_\mu^- \tilde{W}^+ \\
 & + \frac{g_2}{\sqrt{2}} \bar{u}_{Li}^x \bar{\sigma}^\mu W_\mu^+ d_{Li}^x + \frac{g_2}{\sqrt{2}} \bar{d}_{Li}^x \bar{\sigma}^\mu W_\mu^- u_{Li}^x + g_2 \tilde{W}^- \bar{\sigma}^\mu W_\mu^- \tilde{W}^0 - g_2 \tilde{W}^+ \bar{\sigma}^\mu W_\mu^+ \tilde{W}^0
 \end{aligned}$$



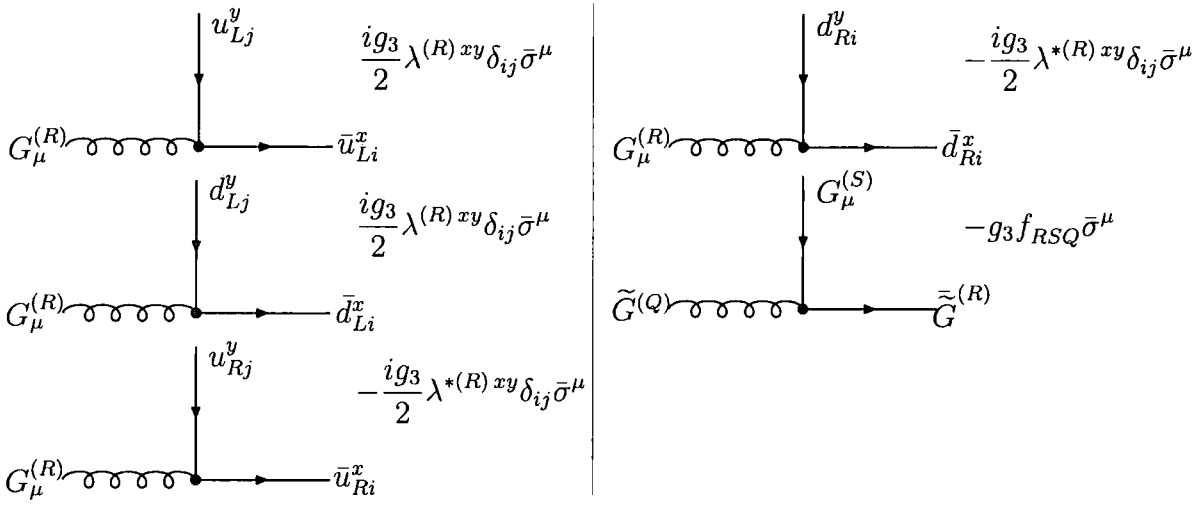
$$i \left[\frac{e}{\sqrt{2} s_W} Z_{N(4+\alpha)r}^* Z_{-(2+\alpha)q}^* + \frac{e}{s_W} Z_{N2r}^* Z_{-1q}^* \right] \bar{\sigma}^\mu$$

$$i \left[\frac{e}{\sqrt{2} s_W} Z_{N3r}^* Z_{+2q} - \frac{e}{s_W} Z_{N2r}^* Z_{+1q} \right] \bar{\sigma}^\mu$$

$$\frac{ie}{\sqrt{2} s_W} K_{ij} \bar{\sigma}^\mu$$

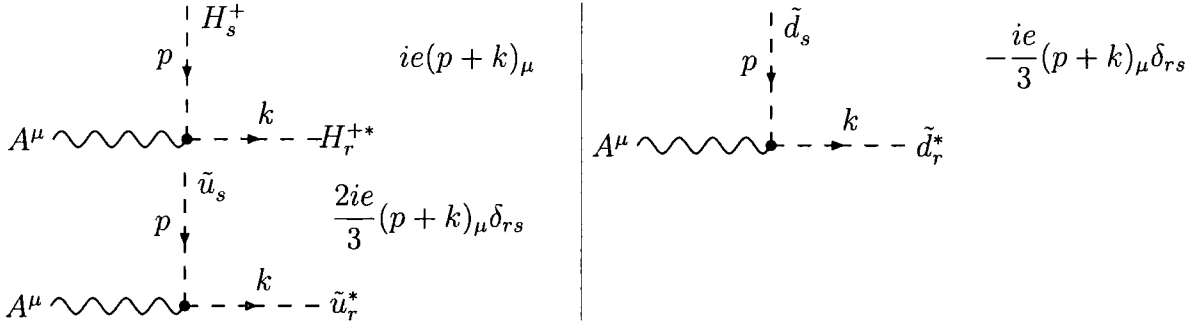
C.18 Fermion-Fermion-Gluon interactions

$$\begin{aligned} \mathcal{L} \supset & \frac{g_3}{2} \bar{u}_{Li}^x \bar{\sigma}^\mu G_\mu^{(R)} \lambda^{(R)xy} u_{Li}^y + \frac{g_3}{2} \bar{d}_{Li}^x \bar{\sigma}^\mu G_\mu^{(R)} \lambda^{(R)xy} d_{Li}^y \\ & - \frac{g_3}{2} \bar{u}_{Ri}^x \bar{\sigma}^\mu G_\mu^{(R)} \lambda^{*(R)xy} u_{Ri}^y - \frac{g_3}{2} \bar{d}_{Ri}^x \bar{\sigma}^\mu G_\mu^{(R)} \lambda^{*(R)xy} d_{Ri}^y + ig_3 f_{RSQ} \tilde{G}^{(R)} \bar{\sigma}^\mu G_\mu^{(S)} \tilde{G}^{(Q)} \end{aligned}$$



C.19 Scalar-Scalar-Photon interactions

$$\begin{aligned} & +ie\partial_\mu \tilde{e}_{L\alpha}^* A^\mu \tilde{e}_{L\alpha} - ieA_\mu \tilde{e}_{L\alpha}^* \partial^\mu \tilde{e}_{L\alpha} - ie\partial_\mu \tilde{e}_{Ri} A^\mu \tilde{e}_{Ri}^* + ieA_\mu \tilde{e}_{Ri} \partial^\mu \tilde{e}_{Ri}^* \\ & -ie\partial_\mu h_2^{+*} A^\mu h_2^+ + ieA_\mu h_2^{+*} \partial^\mu h_2^+ - \frac{2ie}{3} \partial_\mu \tilde{u}_{Li}^{*x} A^\mu \tilde{u}_{Li}^x \\ & + \frac{2ie}{3} A^\mu \tilde{u}_{Li}^{*x} \partial_\mu \tilde{u}_{Li}^x + \frac{ie}{3} \partial_\mu \tilde{d}_{Li}^{*x} A^\mu \tilde{d}_{Li}^x - \frac{ie}{3} A^\mu \tilde{d}_{Li}^{*x} \partial_\mu \tilde{d}_{Li}^x + \frac{2ie}{3} \partial_\mu \tilde{u}_{Ri}^x A^\mu \tilde{u}_{Ri}^{*x} \\ & - \frac{2ie}{3} A^\mu \tilde{u}_{Ri}^x \partial_\mu \tilde{u}_{Ri}^{*x} - \frac{ie}{3} \partial_\mu \tilde{d}_{Ri}^{*x} A^\mu \tilde{d}_{Ri}^x + \frac{ie}{3} A^\mu \tilde{d}_{Ri}^{*x} \partial_\mu \tilde{d}_{Ri}^x \end{aligned}$$



C.20 Scalar-Scalar-Z interactions

$$\begin{aligned}
& -\frac{ig_2}{2c_W} \partial_\mu \tilde{\nu}_{L\alpha}^* Z^\mu \tilde{\nu}_{L\alpha} + \frac{ig_2}{2c_W} Z_\mu \tilde{\nu}_{L\alpha}^* \partial^\mu \tilde{\nu}_{L\alpha} \\
& + \frac{ig_2}{c_W} \left(\frac{1}{2} - s_w^2 \right) \partial_\mu \tilde{e}_{L\alpha}^* Z^\mu \tilde{e}_{L\alpha} - \frac{ig_2}{c_W} \left(\frac{1}{2} - s_w^2 \right) Z_\mu \tilde{e}_{L\alpha}^* \partial^\mu \tilde{e}_{L\alpha} \\
& \quad - ig_s Z_\mu \tilde{e}_{Ri} \partial^\mu \tilde{e}_{Ri}^* + ig_s Z_\mu \tilde{e}_{Ri} \partial^\mu \tilde{e}_{Ri}^* \\
& - \frac{ig_2}{c_w} \left(\frac{1}{2} - s_w^2 \right) \partial_\mu h_2^{+*} Z^\mu h_2^+ + \frac{ig_2}{c_w} \left(\frac{1}{2} - s_w^2 \right) Z_\mu h_2^{+*} \partial^\mu h_2^+ \\
& \quad + \frac{ig_2}{2c_w} \partial_\mu h_2^{0*} Z^\mu h_2^0 - \frac{ig_2}{2c_w} Z_\mu h_2^{0*} \partial^\mu h_2^0 \\
& - \frac{ig_2}{c_w} \left(\frac{1}{2} - \frac{2}{3} s_w^2 \right) \partial_\mu \tilde{u}_{Li}^{*x} Z^\mu \tilde{u}_{Li}^x + \frac{ig_2}{c_w} \left(\frac{1}{2} - \frac{2}{3} s_w^2 \right) Z_\mu \tilde{u}_{Li}^{*x} \partial^\mu \tilde{u}_{Li}^x \\
& + \frac{ig_2}{c_w} \left(\frac{1}{2} - \frac{1}{3} s_w^2 \right) \partial_\mu \tilde{d}_{Li}^{*x} Z^\mu \tilde{d}_{Li}^x - \frac{ig_2}{c_w} \left(\frac{1}{2} - \frac{1}{3} s_w^2 \right) Z_\mu \tilde{d}_{Li}^{*x} \partial^\mu \tilde{d}_{Li}^x \\
& \quad - \frac{2i}{3} g_s Z_\mu \tilde{u}_{Ri}^x \partial^\mu \tilde{u}_{Ri}^{*x} + \frac{2i}{3} g_s Z_\mu \tilde{u}_{Ri}^x \partial^\mu \tilde{u}_{Ri}^{*x} \\
& \quad - \frac{i}{3} g_s Z_\mu \tilde{d}_{Ri}^x \partial^\mu \tilde{d}_{Ri}^{*x} + \frac{i}{3} g_s Z_\mu \tilde{d}_{Ri}^x \partial^\mu \tilde{d}_{Ri}^{*x}
\end{aligned}$$

	$i(p+k)_\mu \left[\frac{e}{c_W s_W} \left(\frac{1}{2} - s_W^2 \right) (Z_{H(2+\alpha)r}^* Z_{H(2+\alpha)q} + Z_{H1r}^* Z_{H1q}) - \frac{e s_W}{c_W} Z_{H(5+i)r}^* Z_{H(5+i)q} \right]$
	$i(p+k)_\mu \left[\frac{e}{c_W s_W} \left(\frac{1}{2} - \frac{2}{3} s_W^2 \right) Z_{\tilde{u}ir}^* Z_{\tilde{u}iq} - \frac{2e s_W}{3c_W} Z_{\tilde{u}(3+i)r}^* Z_{\tilde{u}(3+i)q} \right]$
	$i(p+k)_\mu \left[-\frac{e}{c_W s_W} \left(\frac{1}{2} - \frac{1}{3} s_W^2 \right) Z_{\tilde{d}ir} Z_{\tilde{d}iq}^* + \frac{e s_W}{3c_W} Z_{\tilde{d}(3+i)r} Z_{\tilde{d}(3+i)q}^* \right]$
	$\frac{e}{2s_W c_W} (p+k)_\mu [-Z_{R(2+\alpha)q} Z_{A(2+\alpha)s} + Z_{R1q} Z_{A1s}]$
	$\frac{e}{2s_W c_W} (p+k)_\mu [Z_{R(2+\alpha)s} Z_{A(2+\alpha)q} - Z_{R1s} Z_{A1q}]$

C.21 Scalar-Scalar-W

$$\begin{aligned}
& + \frac{ig_2}{\sqrt{2}} W_\mu^- \tilde{e}_{L\alpha}^* \partial^\mu \tilde{\nu}_{L\alpha} + \frac{ig_2}{\sqrt{2}} W_\mu^+ \tilde{\nu}_{L\alpha}^* \partial^\mu \tilde{e}_{L\alpha} + \frac{ig_2}{\sqrt{2}} W_\mu^- h_2^{0*} \partial^\mu h_2^+ \\
& + \frac{ig_2}{\sqrt{2}} W_\mu^+ h_2^{+*} \partial^\mu h_2^0 + \frac{ig_2}{\sqrt{2}} W_\mu^- \tilde{d}_{Li}^{*x} \partial^\mu \tilde{u}_{Li}^x + \frac{ig_2}{\sqrt{2}} W_\mu^+ \tilde{u}_{Li}^{*x} \partial^\mu \tilde{d}_{Li}^x \\
& - \frac{ig_2}{\sqrt{2}} \partial_\mu \tilde{e}_{L\alpha}^* W^{-\mu} \tilde{\nu}_{L\alpha} - \frac{ig_2}{\sqrt{2}} \partial_\mu h_2^{+*} W^{+\mu} h_2^0 - \frac{ig_2}{\sqrt{2}} \partial_\mu h_2^{0*} W^{-\mu} h_2^+ - \frac{ig_2}{\sqrt{2}} \partial_\mu \tilde{d}_{Li}^{*x} W^{-\mu} \tilde{u}_{Li}^x \\
& - \frac{ig_2}{\sqrt{2}} \partial_\mu \tilde{u}_{Li}^{*x} W^{+\mu} \tilde{d}_{Li}^x - \frac{ig_2}{\sqrt{2}} \partial_\mu \tilde{\nu}_{L\alpha}^* W^{+\mu} \tilde{e}_{L\alpha}
\end{aligned}$$

$$\begin{array}{l}
\begin{array}{c}
\text{---} H_q^+ \\
\downarrow p \\
W^{-\mu} \text{---} \bullet \text{---} H_r^0 \\
\uparrow k \\
\text{---} H_q^+ \\
\downarrow p \\
W^{-\mu} \text{---} \bullet \text{---} A_r^0 \\
\uparrow k \\
\text{---} \tilde{u}_q \\
\downarrow p \\
W^{-\mu} \text{---} \bullet \text{---} \tilde{d}_r^* \\
\uparrow k
\end{array}
\end{array}
\begin{array}{l}
-(p_\mu + k_\mu) \frac{e}{2s_W} i [Z_{H(2+\alpha)q} Z_{R(2+\alpha)r} - Z_{H1q} Z_{R1r}] \\
-(p_\mu + k_\mu) \frac{e}{2s_W} [-Z_{H(2+\alpha)q} Z_{A(2+\alpha)r} - Z_{H1q} Z_{A1r}] \\
\frac{ie}{\sqrt{2}s_W} Z_{\tilde{u}iq} Z_{\tilde{d}ir} (p_\mu + k_\mu)
\end{array}$$

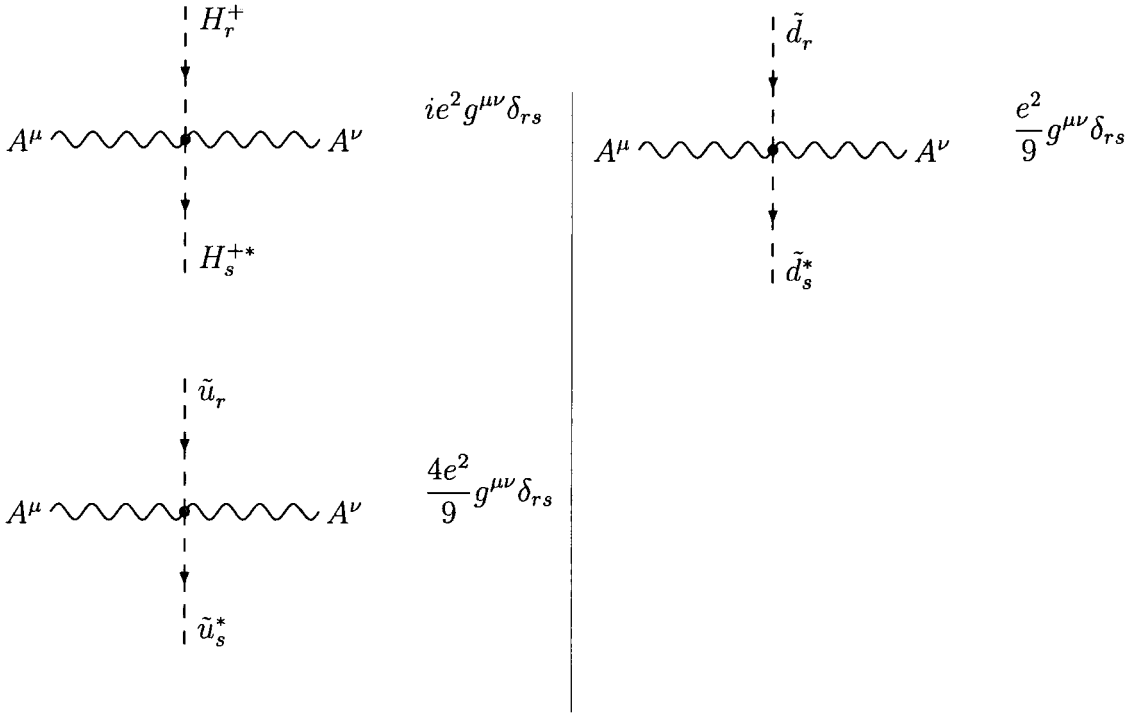
C.22 Scalar-Scalar-G

$$\begin{aligned}
& + \frac{ig_3}{2} G_\mu^{(R)} \tilde{u}_{Li}^{*z} \lambda^{(R)zx} \partial^\mu \tilde{u}_{Li}^x - \frac{ig_3}{2} \partial_\mu \tilde{u}_{Li}^{*x} G^{\mu(R)} \lambda^{(R)xy} \tilde{u}_{Li}^y \\
& + \frac{ig_3}{2} G_\mu^{(R)} \tilde{d}_{Li}^{*z} \lambda^{(R)zx} \partial^\mu \tilde{d}_{Li}^x - \frac{ig_3}{2} \partial_\mu \tilde{d}_{Li}^{*x} G^{\mu(R)} \lambda^{(R)xy} \tilde{d}_{Li}^y \\
& - \frac{ig_3}{2} G_\mu^{(R)} \tilde{u}_{Ri}^z \lambda^{*(R)zx} \partial^\mu \tilde{u}_{Ri}^{*x} + \frac{ig_3}{2} \partial_\mu \tilde{u}_{Ri}^x G^{\mu(R)} \lambda^{*(R)xy} \tilde{u}_{Ri}^{*y} \\
& - \frac{ig_3}{2} G_\mu^{(R)} \tilde{d}_{Ri}^z \lambda^{*(R)zx} \partial^\mu \tilde{d}_{Ri}^{*x} + \frac{ig_3}{2} \partial_\mu \tilde{d}_{Ri}^x G^{\mu(R)} \lambda^{*(R)xy} \tilde{d}_{Ri}^{*y}
\end{aligned}$$

$$\begin{array}{l}
\begin{array}{c}
\text{---} \tilde{u}_r^x \\
\downarrow p \\
G^{(R)\mu} \text{---} \bullet \text{---} \tilde{u}_r^{*z} \\
\uparrow k \\
\text{---} \tilde{d}_r^x \\
\downarrow p \\
G^{(R)\mu} \text{---} \bullet \text{---} \tilde{d}_r^{*z} \\
\uparrow k
\end{array}
\end{array}
\begin{array}{l}
\frac{ig_3}{2} \lambda^{(R)zx} (p+k)_\mu \\
\frac{ig_3}{2} \lambda^{(R)zx} (p+k)_\mu
\end{array}$$

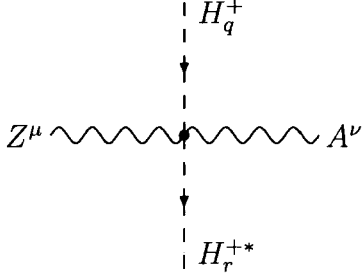
C.23 Scalar-Scalar-A-A

$$\begin{aligned}
 &+e^2 A_\mu \tilde{e}_{L\alpha}^* A^\mu \tilde{e}_{L\alpha} + e^2 A_\mu \tilde{e}_{Ri} A^\mu \tilde{e}_{Ri}^* + e^2 A_\mu h_2^{+*} A^\mu h_2^+ + \frac{4e^2}{9} A_\mu \tilde{u}_{Li}^* A^\mu \tilde{u}_{Li} \\
 &+ \frac{e^2}{9} A_\mu \tilde{d}_{Li}^* A^\mu \tilde{d}_{Li} + \frac{4e^2}{9} A_\mu \tilde{u}_{Ri}^* A^\mu \tilde{u}_{Ri} + \frac{e^2}{9} A_\mu \tilde{d}_{Ri}^* A^\mu \tilde{d}_{Ri}
 \end{aligned}$$

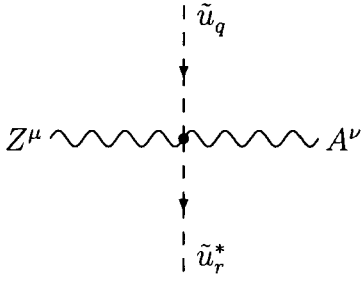


C.24 Scalar-Scalar-A-Z

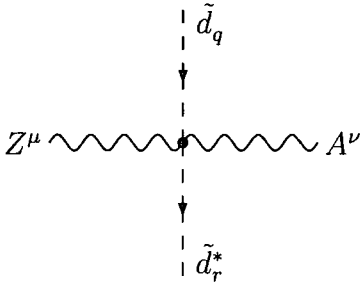
$$\begin{aligned}
 &+ \frac{2eg_2}{c_w} \left(\frac{1}{2} - s_w^2 \right) A_\mu \tilde{e}_{L\alpha}^* Z^\mu \tilde{e}_{L\alpha} - 2egs_w Z_\mu \tilde{e}_{Ri} A^\mu \tilde{e}_{Ri}^* \\
 &+ 2 \frac{eg_2}{c_w} \left(\frac{1}{2} - s_w^2 \right) Z_\mu h_2^{+*} A^\mu h_2^+ + \frac{4eg_2}{3c_w} \left(\frac{1}{2} - \frac{2}{3} s_w^2 \right) Z_\mu \tilde{u}_{Li}^* A^\mu \tilde{u}_{Li} \\
 &+ \frac{2eg_2}{3c_w} \left(\frac{1}{2} - \frac{1}{3} s_w^2 \right) Z_\mu \tilde{d}_{Li}^* A^\mu \tilde{d}_{Li} - \frac{8}{9} eg_s Z_\mu \tilde{u}_{Ri}^* A^\mu \tilde{u}_{Ri} - \frac{2}{9} eg_s Z_\mu \tilde{d}_{Ri}^* A^\mu \tilde{d}_{Ri}
 \end{aligned}$$



$$i\left[\frac{2e^2}{s_W c_W}\left(\frac{1}{2} - s_W^2\right)(Z_{H(2+\alpha)r}^* Z_{H(2+\alpha)q} + Z_{H1r}^* Z_{H1q}) - \frac{2e^2 s_W}{c_W} Z_{H(5+i)r}^* Z_{H(5+i)q}\right] g^{\mu\nu}$$



$$i\left[\frac{4e^2}{3s_W c_W}\left(\frac{1}{2} - \frac{2}{3}s_W^2\right)Z_{\tilde{u}ir}^* Z_{\tilde{u}iq} - \frac{8e^2 s_W}{9c_W} Z_{\tilde{u}(3+i)r}^* Z_{\tilde{u}(3+i)q}\right] g^{\mu\nu}$$

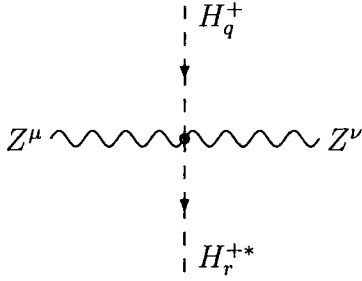


$$i\left[\frac{2e^2}{3s_W c_W}\left(\frac{1}{2} - \frac{1}{3}s_W^2\right)Z_{\tilde{d}iq}^* Z_{\tilde{d}ir} - \frac{2e^2 s_W}{9c_W} Z_{\tilde{d}(3+i)q}^* Z_{\tilde{d}(3+i)q}\right] g^{\mu\nu}$$

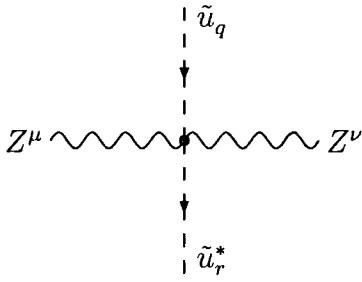
C.25 Scalar-Scalar-Z-Z

$$+\frac{g_2^2}{4c_w^2} Z_\mu \tilde{\nu}_{L\alpha}^* Z^\mu \tilde{\nu}_{L\alpha} + \frac{g_2^2}{c_w^2} \left(\frac{1}{2} - s_w^2\right)^2 Z_\mu \tilde{e}_{L\alpha}^* Z^\mu \tilde{e}_{L\alpha} + g^2 s_w^2 Z_\mu \tilde{e}_{Ri} Z^\mu \tilde{e}_{Ri}^* + \frac{g_2^2}{4c_w^2} Z_\mu h_2^{0*} Z^\mu h_2^0$$

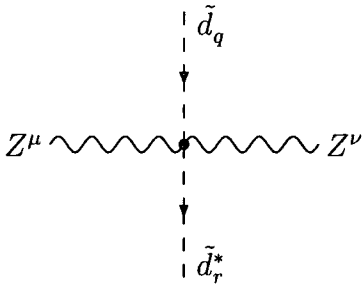
$$\begin{aligned}
& + \frac{g_2^2}{c_w^2} \left(\frac{1}{2} - s_w^2 \right)^2 Z_\mu h_2^{+*} Z^\mu h_2^+ + \frac{g_2^2}{c_w^2} \left(\frac{1}{2} - \frac{2}{3} s_w^2 \right)^2 Z_\mu \tilde{u}_{Li}^{*x} Z^\mu \tilde{u}_{Li}^x \\
& + \frac{g_2^2}{c_w^2} \left(\frac{1}{2} - \frac{1}{3} s_w^2 \right)^2 Z_\mu \tilde{d}_{Li}^{*x} Z^\mu \tilde{d}_{Li}^x + \frac{4}{9} g^2 s_w^2 Z_\mu \tilde{u}_{Ri}^x Z^\mu \tilde{u}_{Ri}^{*x} + \frac{1}{9} g^2 s_w^2 Z_\mu \tilde{d}_{Ri}^x Z^\mu \tilde{d}_{Ri}^{*x}
\end{aligned}$$



$$\begin{aligned}
& i \left[\frac{e^2}{s_W^2 c_W^2} \left(\frac{1}{2} - s_W^2 \right)^2 (Z_{H(2+\alpha)r}^* Z_{H(2+\alpha)q} + Z_{H1r}^* Z_{H1q}) \right. \\
& \left. + \frac{e^2 s_W^2}{c_W^2} Z_{H(5+i)r}^* Z_{H(5+i)q} \right] g^{\mu\nu}
\end{aligned}$$



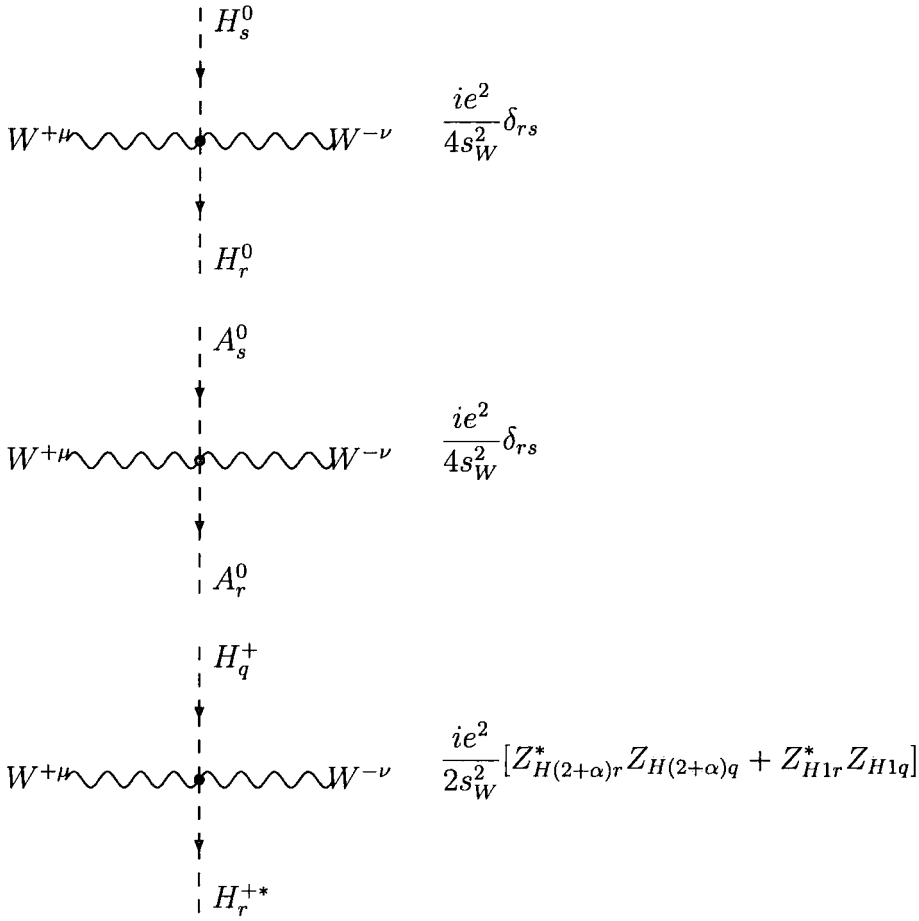
$$i \left[\frac{e^2}{s_W^2 c_W^2} \left(\frac{1}{2} - \frac{2}{3} s_W^2 \right)^2 Z_{\tilde{u}ir}^* Z_{\tilde{u}iq} + \frac{4e^2 s_W^2}{9c_W^2} Z_{\tilde{u}(3+i)r}^* Z_{\tilde{u}(3+i)q} \right] g^{\mu\nu}$$



$$i \left[\frac{e^2}{s_W^2 c_W^2} \left(\frac{1}{2} - \frac{1}{3} s_W^2 \right)^2 Z_{\tilde{d}iq}^* Z_{\tilde{d}ir} + \frac{e^2 s_W^2}{9c_W^2} Z_{\tilde{d}(3+i)q}^* Z_{\tilde{d}(3+i)r} \right] g^{\mu\nu}$$

C.26 Scalar-Scalar-W-W

$$\begin{aligned}
 & +\frac{g_2^2}{2}W_\mu^+\tilde{\nu}_{L\alpha}^*W^{-\mu}\tilde{\nu}_{L\alpha} + \frac{g_2^2}{2}W_\mu^-\tilde{e}_{L\alpha}^*W^{+\mu}\tilde{e}_{L\alpha} + \frac{g_2^2}{2}W_\mu^-h_2^{0*}W^{+\mu}h_2^0 + \frac{g_2^2}{2}W_\mu^+h_2^{+*}W^{-\mu}h_2^+ \\
 & +\frac{g_2^2}{2}W_\mu^-\tilde{d}_{Li}^{*x}W^{+\mu}\tilde{d}_{Li}^x + \frac{g_2^2}{2}W_\mu^+\tilde{u}_{Li}^{*x}W^{-\mu}\tilde{u}_{Li}^x
 \end{aligned}$$



$$\begin{array}{c}
\begin{array}{c}
\downarrow \tilde{d}_q \\
W^{+\mu} \text{---} \text{---} \text{---} W^{-\nu} \\
\downarrow \tilde{d}_r^* \\
\downarrow \tilde{u}_q \\
W^{+\mu} \text{---} \text{---} \text{---} W^{-\nu} \\
\downarrow \tilde{u}_r^*
\end{array}
\quad
\frac{ie^2}{2s_W^2} Z_{\tilde{d}iq}^* Z_{\tilde{d}ir} \\
\frac{ie^2}{2s_W^2} Z_{\tilde{u}ir}^* Z_{\tilde{u}iq}
\end{array}$$

C.27 Scalar-Scalar-A-W

$$\begin{aligned}
& -\frac{eg_2}{\sqrt{2}} A_\mu \tilde{e}_{L\alpha}^* W^{-\mu} \tilde{\nu}_{L\alpha} - \frac{eg_2}{\sqrt{2}} W_\mu^+ \tilde{\nu}_{L\alpha}^* A^\mu \tilde{e}_{L\alpha} + \frac{eg_2}{\sqrt{2}} A_\mu h_2^{+\ast} W^{+\mu} h_2^0 + \frac{eg_2}{\sqrt{2}} W_\mu^- h_2^{0\ast} A^\mu h_2^+ \\
& + \frac{1}{3\sqrt{2}} eg_2 W^{+\mu} \tilde{u}_{Li}^{\ast x} A_\mu \tilde{d}_{Li}^x + \frac{1}{3\sqrt{2}} eg_2 A_\mu \tilde{d}_{Li}^{\ast x} W^{-\mu} \tilde{u}_{Li}^x
\end{aligned}$$

$$\begin{array}{c}
\downarrow \tilde{d}_q \\
W_\mu^+ \text{---} \text{---} \text{---} A^\nu \\
\downarrow \tilde{u}_r^*
\end{array}
\quad
\frac{ie^2}{3\sqrt{2}s_W} Z_{\tilde{u}ir}^* Z_{\tilde{d}iq}^* g^{\mu\nu}$$

$$\begin{array}{c}
\begin{array}{c}
\downarrow H_q^+ \\
W_\mu^- \sim \text{wavy line} \quad A^\nu \\
\downarrow H_r^0
\end{array}
\end{array}
\quad \frac{ie^2}{2s_W} [-Z_{H(2+\alpha)q} Z_{R(2+\alpha)r} + Z_{H1q} Z_{R1r}] g^{\mu\nu}$$

$$\begin{array}{c}
\begin{array}{c}
\downarrow H_q^+ \\
W_\mu^- \sim \text{wavy line} \quad A^\nu \\
\downarrow A_r^0
\end{array}
\end{array}
\quad \frac{-ie^2}{2s_W} i [Z_{H(2+\alpha)q} Z_{A(2+\alpha)r} + Z_{H1q} Z_{A1r}] g^{\mu\nu}$$

C.28 Scalar-Scalar-Z-W

$$\begin{aligned}
& + \frac{eg}{\sqrt{2}} Z_\mu \tilde{\nu}_{L\alpha}^* W^{+\mu} \tilde{e}_{L\alpha} + \frac{eg}{\sqrt{2}} W^{-\mu} \tilde{e}_{L\alpha}^* Z_\mu \tilde{\nu}_{L\alpha} - \frac{eg}{\sqrt{2}} W^{+\mu} h_2^{+\ast} Z_\mu h_2^0 - \frac{eg}{\sqrt{2}} Z_\mu h_2^{0\ast} W^{-\mu} h_2^+ \\
& - \frac{eg}{3\sqrt{2}} Z_\mu \tilde{u}_{Li}^{\ast x} W^{+\mu} \tilde{d}_{Li}^x - \frac{eg}{3\sqrt{2}} W^{-\mu} \tilde{d}_{Li}^{\ast x} Z_\mu \tilde{u}_{Li}^x
\end{aligned}$$

.....

$$\begin{array}{c}
\begin{array}{c}
\downarrow \tilde{d}_q \\
W_\mu^+ \sim \text{wavy line} \quad Z^\nu \\
\downarrow \tilde{u}_r^*
\end{array}
\end{array}
\quad \frac{-ie^2}{3\sqrt{2}c_W} Z_{\tilde{u}ir}^* Z_{\tilde{d}iq}^* g^{\mu\nu}$$

$$\begin{array}{c}
\begin{array}{c}
\downarrow H_r^+ \\
W_\mu^- \sim \text{wavy line} \sim Z^\nu \\
\downarrow H_q^0
\end{array}
\end{array}
\quad \frac{ie^2}{2c_W} [Z_{H(2+\alpha)r} Z_{R(2+\alpha)q} - Z_{H1r} Z_{R1q}] g^{\mu\nu}$$

$$\begin{array}{c}
\begin{array}{c}
\downarrow H_r^+ \\
W_\mu^- \sim \text{wavy line} \sim Z^\nu \\
\downarrow A_q^0
\end{array}
\end{array}
\quad \frac{ie^2}{2c_W} i [Z_{H(2+\alpha)r} Z_{A(2+\alpha)q} + Z_{H1r} Z_{A1q}] g^{\mu\nu}$$

C.29 Scalar-Scalar-G-A

$$\begin{aligned}
& + \frac{2eg_3}{3} G^{(R)\mu} \tilde{u}_{Li}^{*z} \lambda^{(R)zx} A^\mu \tilde{u}_{Li}^x - \frac{eg_3}{3} G^{(R)\mu} \tilde{d}_{Li}^{*z} \lambda^{(R)zx} A^\mu \tilde{d}_{Li}^x \\
& + \frac{2eg_3}{3} G^{(R)\mu} \tilde{u}_{Ri}^z \lambda^{*(R)zx} A^\mu \tilde{u}_{Ri}^{*x} - \frac{eg_3}{3} G^{(R)\mu} \tilde{d}_{Ri}^z \lambda^{*(R)zx} A^\mu \tilde{d}_{Ri}^{*x}
\end{aligned}$$

$$\begin{array}{c}
\begin{array}{c}
\downarrow \tilde{u}_r^x \\
G^{(R)\mu} \sim \text{wavy line} \sim A^\nu \\
\downarrow \tilde{u}_s^{*z}
\end{array}
\end{array}
\quad \frac{2ieg_3}{3} \lambda^{(R)zx} g^{\mu\nu} \delta_{rs}$$

$$-\frac{eig_3}{3}\lambda^{(R)zx}g^{\mu\nu}\delta_{rs}$$

C.30 Scalar-Scalar-G-Z

$$+\frac{g_2g_3}{c_w}\left(\frac{1}{2}-\frac{2}{3}s_w^2\right)G_\mu^{(R)}\tilde{u}_{Li}^{*z}\lambda^{(R)zx}Z^\mu\tilde{u}_{Li}^x-\frac{g_2g_3}{c_w}\left(\frac{1}{2}-\frac{1}{3}s_w^2\right)G_\mu^{(R)}\tilde{d}_{Li}^{*z}\lambda^{(R)zx}Z^\mu\tilde{d}_{Li}^x$$

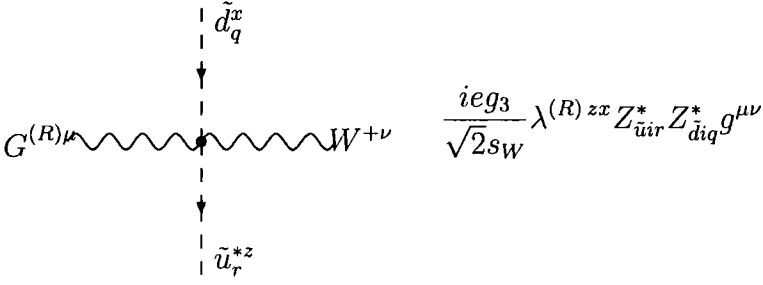
$$-\frac{2gg_3s_w}{3}G_\mu^{(R)}\tilde{u}_{Ri}^z\lambda^{*(R)zx}Z^\mu\tilde{u}_{Ri}^{*x}+\frac{gg_3s_w}{3}G_\mu^{(R)}\tilde{d}_{Ri}^z\lambda^{*(R)zx}Z^\mu\tilde{d}_{Ri}^{*x}$$

$$i\lambda^{(R)zx}\left[\frac{eg_3}{s_w c_w}\left(\frac{1}{2}-\frac{2}{3}s_w^2\right)Z_{\tilde{u}ir}^*Z_{\tilde{u}iq}-\frac{2eg_3s_w}{3c_w}Z_{\tilde{u}(3+i)r}^*Z_{\tilde{u}(3+i)q}\right]g^{\mu\nu}$$

$$i\lambda^{(R)zx}\left[\frac{-eg_3}{s_w c_w}\left(\frac{1}{2}-\frac{1}{3}s_w^2\right)Z_{\tilde{d}ir}Z_{\tilde{d}iq}^*+\frac{eg_3s_w}{3c_w}Z_{\tilde{d}(3+i)r}Z_{\tilde{d}(3+i)q}^*\right]g^{\mu\nu}$$

C.31 Scalar-Scalar-G-W

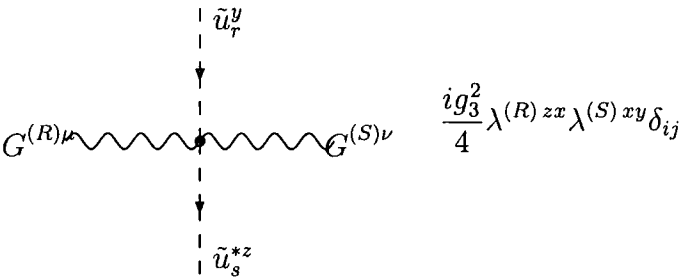
$$+\frac{g_2 g_3}{\sqrt{2}} G_\mu^{(R)} \tilde{u}_{Li}^{*z} \lambda^{(R)zx} W^{+\mu} \tilde{d}_{Li}^x + \frac{g_2 g_3}{\sqrt{2}} G_\mu^{(R)} \tilde{d}_{Li}^{*z} \lambda^{(R)zx} W^{-\mu} \tilde{u}_{Li}^x$$

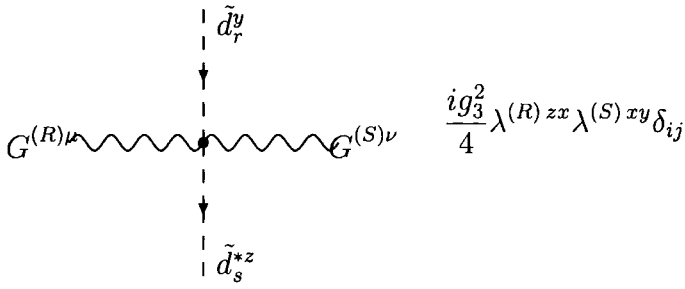


C.32 Scalar-Scalar-G-G

$$+\frac{g_3^2}{4} G_\mu^{(R)} \tilde{u}_{Li}^{*z} \lambda^{(R)zx} G_\mu^{(S)} \lambda^{(S)xy} \tilde{u}_{Li}^y + \frac{g_3^2}{4} G_\mu^{(R)} \tilde{d}_{Li}^{*z} \lambda^{(R)zx} G_\mu^{(S)} \lambda^{(S)xy} \tilde{d}_{Li}^y$$

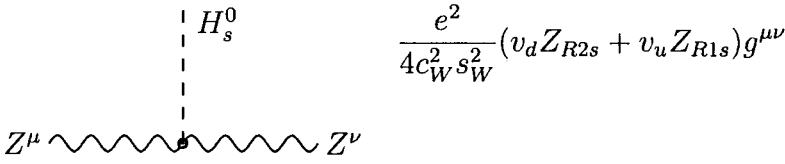
$$+\frac{g_3^2}{4} G_\mu^{(R)} \tilde{u}_{Ri}^z \lambda^{*(R)zx} G_\mu^{(S)} \lambda^{*(S)xy} \tilde{u}_{Ri}^{*y} + \frac{g_3^2}{4} G_\mu^{(R)} \tilde{d}_{Ri}^z \lambda^{*(R)zx} G_\mu^{(S)} \lambda^{*(S)xy} \tilde{d}_{Ri}^{*y}$$





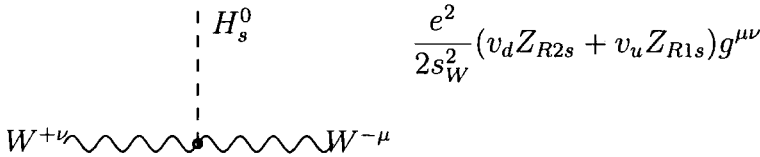
C.33 Scalar-Z-Z

$$+ \frac{1}{\sqrt{2}} \frac{g_2^2}{4c_w^2} Z_\mu v_0 Z^\mu \tilde{\nu}_{L0} + \frac{1}{\sqrt{2}} \frac{g_2^2}{4c_w^2} Z_\mu \tilde{\nu}_{L0}^* Z^\mu v_0 + \frac{1}{\sqrt{2}} \frac{g_2^2}{4c_w^2} Z_\mu v_u Z^\mu h_2^0 + \frac{1}{\sqrt{2}} \frac{g_2^2}{4c_w^2} Z_\mu h_2^{0*} Z^\mu v_u$$



C.34 Scalar-W-W

$$+ \frac{1}{\sqrt{2}} \frac{g_2^2}{2} W_\mu^+ v_0 W^{-\mu} \tilde{\nu}_{L0} + \frac{1}{\sqrt{2}} \frac{g_2^2}{2} W_\mu^+ \tilde{\nu}_{L0}^* W^{-\mu} v_0 + \frac{1}{\sqrt{2}} \frac{g_2^2}{2} W_\mu^- v_u W^{+\mu} h_2^0 + \frac{1}{\sqrt{2}} \frac{g_2^2}{2} W_\mu^- h_2^{0*} W^{+\mu} v_u$$



C.35 Scalar-A-W

$$-\frac{1}{\sqrt{2}}\frac{eg_2}{\sqrt{2}}A_\mu\tilde{e}_{L0}^*W^{-\mu}v_0-\frac{1}{\sqrt{2}}\frac{eg_2}{\sqrt{2}}W_\mu^+v_0A^\mu\tilde{e}_{L0}+\frac{eg_2}{2}A_\mu W^{-\mu}h_2^+v_u+\frac{1}{\sqrt{2}}\frac{eg_2}{\sqrt{2}}A_\mu h_2^{+*}W^{+\mu}v_u$$

.....

$$\begin{array}{c} | H_q^+ \\ | \\ \downarrow \\ | \\ A^\mu \sim \text{wavy line} \downarrow \text{wavy line} W^{-\nu} \end{array} \quad \frac{e^2}{2s_W}(-v_d Z_{H2q} + v_u Z_{H1q})g^{\mu\nu}$$

C.36 Scalar-Z-W

$$+\frac{1}{\sqrt{2}}\frac{eg}{\sqrt{2}}Z_\mu v_0 W^{+\mu}\tilde{e}_{L0}+\frac{1}{\sqrt{2}}\frac{eg}{\sqrt{2}}W^{-\mu}\tilde{e}_{L0}^*Z_\mu v_0-\frac{1}{\sqrt{2}}\frac{eg}{\sqrt{2}}W^{+\mu}h_2^{+*}Z_\mu v_u-\frac{1}{\sqrt{2}}\frac{eg}{\sqrt{2}}Z_\mu v_u W^{-\mu}h_2^+$$

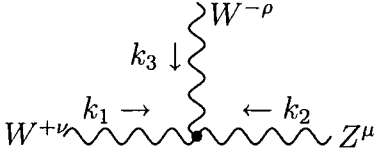
.....

$$\begin{array}{c} | H_q^+ \\ | \\ \downarrow \\ | \\ Z^\mu \sim \text{wavy line} \downarrow \text{wavy line} W^{-\nu} \end{array} \quad \frac{e^2}{2c_W}(v_d Z_{H2q} - v_u Z_{H1q})g^{\mu\nu}$$

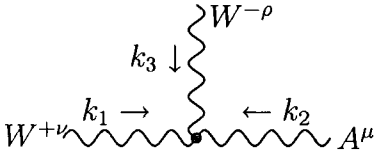
C.37 Gauge boson-Gauge boson-Gauge boson

$$\begin{aligned} &+ig_2c_w\partial_\mu Z_\nu W^{+\mu}W^{-\nu} - ig_2c_w\partial_\mu Z_\nu W^{-\mu}W^{+\nu} \\ &+ig_2c_w\partial_\mu W_\nu^+ W^{-\mu}Z^\nu - ig_2c_w\partial_\mu W_\nu^+ Z^\mu W^{-\nu} + ig_2c_w\partial_\mu W_\nu^- Z^\mu W^{+\nu} \\ &-ig_2c_w\partial_\mu W_\nu^- W^{+\mu}Z^\nu + ie\partial_\mu A_\nu W^{+\mu}W^{-\nu} - ie\partial_\mu A_\nu W^{-\mu}W^{+\nu} \\ &+ie\partial_\mu W_\nu^+ W^{-\mu}A^\nu - ie\partial_\mu W_\nu^+ A^\mu W^{-\nu} + ie\partial_\mu W_\nu^- A^\mu W^{+\nu} \\ &-ie\partial_\mu W_\nu^- W^{+\mu}A^\nu \end{aligned}$$

$$-g_3 f_{RSQ} \partial^\mu G^{(R)\nu} G_\mu^{(S)} G_\nu^{(Q)}$$



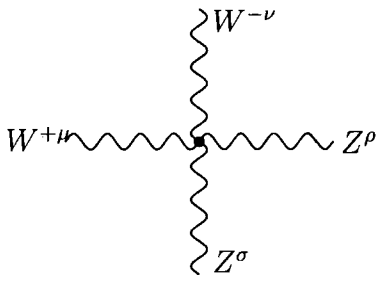
$$\frac{ie c_w}{s_w} [g_{\mu\rho}(k_3 - k_2)_\nu + g_{\nu\rho}(k_2 - k_1)_\mu + g_{\mu\nu}(k_1 - k_3)_\rho]$$



$$-ie [g_{\mu\rho}(k_3 - k_2)_\nu + g_{\nu\rho}(k_2 - k_1)_\mu + g_{\mu\nu}(k_1 - k_3)_\rho]$$

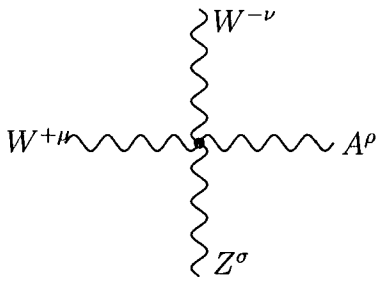
C.38 Gauge boson-Gauge boson-Gauge boson-Gauge boson

$$\begin{aligned} & -2eg_2 c_w A_\mu Z^\mu W_\nu^- W^{+\nu} + eg_2 c_w Z_\mu A^\nu W_\nu^- W^{+\mu} \\ & + eg_2 c_w Z_\mu A^\nu W_\nu^+ W^{-\mu} - g_2^2 c_w^2 Z_\mu Z^\mu W_\nu^- W^{+\nu} \\ & + g_2^2 c_w^2 Z_\mu Z^\nu W_\nu^- W^{+\mu} - e^2 A_\mu A^\mu W_\nu^- W^{+\nu} \\ & + e^2 A_\mu A^\nu W_\nu^- W^{+\mu} + \frac{1}{2} g_2^2 W_\mu^+ W^{+\mu} W_\nu^- W^{-\nu} - \frac{1}{2} g_2^2 W_\mu^+ W^{-\mu} W_\nu^+ W^{-\nu} \\ & - \frac{g_3^2}{4} f_{RSQ} f_{RTW} G_\mu^{(S)} G_\nu^{(Q)} G^{(T)\mu} G^{(W)\nu} \end{aligned}$$



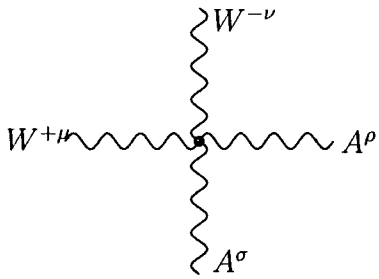
A Feynman diagram showing a central vertex with four external lines. A wavy line labeled $W^{+\mu}$ enters from the left. A wavy line labeled $W^{-\nu}$ exits upwards. A wavy line labeled Z^ρ exits to the right. A wavy line labeled Z^σ exits downwards.

$$\frac{-ie^2 c_w^2}{s_w^2} [2g_{\mu\nu}g_{\sigma\rho} - g_{\nu\rho}g_{\mu\sigma} - g_{\rho\mu}g_{\nu\sigma}]$$



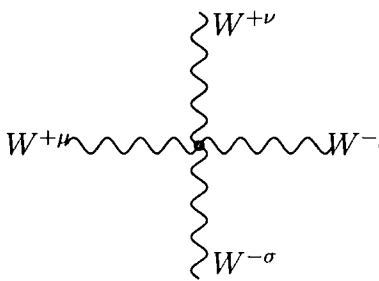
A Feynman diagram showing a central vertex with four external lines. A wavy line labeled $W^{+\mu}$ enters from the left. A wavy line labeled $W^{-\nu}$ exits upwards. A wavy line labeled A^ρ exits to the right. A wavy line labeled Z^σ exits downwards.

$$\frac{ie^2 c_w}{s_w} [2g_{\mu\nu}g_{\sigma\rho} - g_{\nu\rho}g_{\mu\sigma} - g_{\rho\mu}g_{\nu\sigma}]$$



A Feynman diagram showing a central vertex with four external lines. A wavy line labeled $W^{+\mu}$ enters from the left. A wavy line labeled $W^{-\nu}$ exits upwards. A wavy line labeled A^ρ exits to the right. A wavy line labeled A^σ exits downwards.

$$-ie^2 [2g_{\mu\nu}g_{\sigma\rho} - g_{\nu\rho}g_{\mu\sigma} - g_{\rho\mu}g_{\nu\sigma}]$$

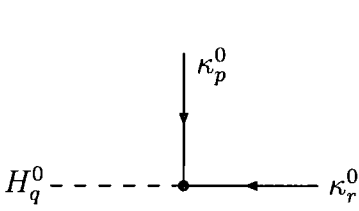


A Feynman diagram showing a central vertex with four external lines. A wavy line labeled $W^{+\mu}$ enters from the left. A wavy line labeled $W^{+\nu}$ exits upwards. A wavy line labeled $W^{-\rho}$ exits to the right. A wavy line labeled $W^{-\sigma}$ exits downwards.

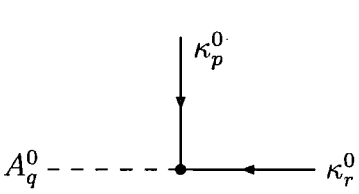
$$\frac{ie^2}{s_w^2} [2g_{\mu\nu}g_{\sigma\rho} - g_{\nu\rho}g_{\mu\sigma} - g_{\rho\mu}g_{\nu\sigma}]$$

C.39 Neutral Scalar - Neutral Fermion - Neutral Fermion interactions

$$\begin{aligned}
& +\frac{ig}{\sqrt{2}}h_2^{0*}\tilde{h}_2^0\tilde{B} - \frac{ig}{\sqrt{2}}h_2^0\tilde{h}_2^{\bar{0}}\tilde{B} - \frac{ig_2}{\sqrt{2}}h_2^{0*}\tilde{W}^0\tilde{h}_2^0 + \frac{ig_2}{\sqrt{2}}h_2^0\tilde{W}^{\bar{0}}\tilde{h}_2^{\bar{0}} \\
& -\frac{ig}{\sqrt{2}}\tilde{\nu}_{L\alpha}^*\nu_{L\alpha}\tilde{B} + \frac{ig}{\sqrt{2}}\tilde{\nu}_{L\alpha}\bar{\nu}_{L\alpha}\tilde{B} + \frac{ig_2}{\sqrt{2}}\tilde{\nu}_{L\alpha}^*\tilde{W}^0\nu_{L\alpha} - \frac{ig_2}{\sqrt{2}}\tilde{\nu}_{L\alpha}\tilde{W}^{\bar{0}}\bar{\nu}_{L\alpha}
\end{aligned}$$



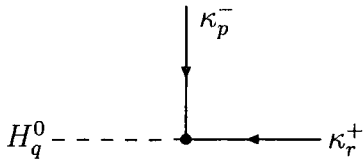
$$\begin{aligned}
& -\frac{ie}{2c_W}Z_{R1q}Z_{N3p}Z_{N1r} + \frac{ie}{2s_W}Z_{R1q}Z_{N2p}Z_{N3r} \\
& +\frac{ie}{2c_W}Z_{R(2+\alpha)q}Z_{N(4+\alpha)p}Z_{N1r} - \frac{ie}{2s_W}Z_{R(2+\alpha)q}Z_{N2p}Z_{N(4+\alpha)r} \\
& -\frac{ie}{2c_W}Z_{R1q}Z_{N3r}Z_{N1p} + \frac{ie}{2s_W}Z_{R1q}Z_{N2r}Z_{N3p} \\
& +\frac{ie}{2c_W}Z_{R(2+\alpha)q}Z_{N(4+\alpha)r}Z_{N1p} - \frac{ie}{2s_W}Z_{R(2+\alpha)q}Z_{N2r}Z_{N(4+\alpha)p}
\end{aligned}$$



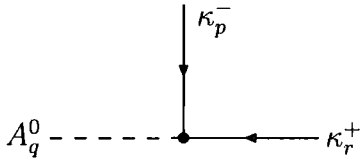
$$\begin{aligned}
& -\frac{e}{2c_W}Z_{A1q}Z_{N3p}Z_{N1r} + \frac{e}{2s_W}Z_{A1q}Z_{N2p}Z_{N3r} \\
& +\frac{e}{2c_W}Z_{A(2+\alpha)q}Z_{N(4+\alpha)p}Z_{N1r} - \frac{e}{2s_W}Z_{A(2+\alpha)q}Z_{N2p}Z_{N(4+\alpha)r} \\
& -\frac{e}{2c_W}Z_{A1q}Z_{N3r}Z_{N1p} + \frac{e}{2s_W}Z_{A1q}Z_{N2r}Z_{N3p} \\
& +\frac{e}{2c_W}Z_{A(2+\alpha)q}Z_{N(4+\alpha)r}Z_{N1p} - \frac{e}{2s_W}Z_{A(2+\alpha)q}Z_{N2r}Z_{N(4+\alpha)p}
\end{aligned}$$

C.40 Neutral Scalar - Charged Fermion - Charged Fermion interactions

$$\begin{aligned}
& +ig_2h_2^{0*}\tilde{W}^-\tilde{h}_2^+ - ig_2h_2^0\tilde{W}^{\bar{-}}\tilde{h}_2^{\bar{+}} + ig_2\tilde{\nu}_{L\alpha}^*\tilde{W}^+e_{L\alpha} - ig_2\tilde{\nu}_{L\alpha}\tilde{W}^{\bar{+}}\bar{e}_{L\alpha} \\
& +\lambda_{\alpha\beta j}\tilde{\nu}_{L\beta}e_{L\alpha}e_{Rj} + \lambda_{\alpha\beta j}^*\tilde{\nu}_{L\beta}^*\bar{e}_{L\alpha}\bar{e}_{Rj}
\end{aligned}$$



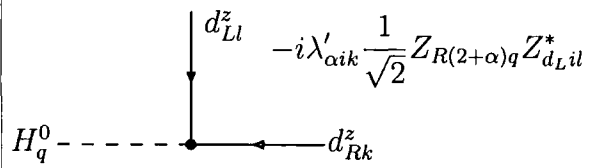
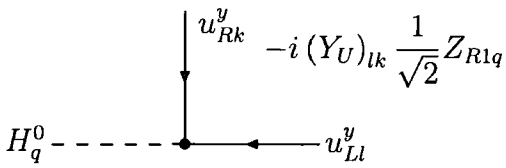
$$-\frac{ie}{s_W} \frac{1}{\sqrt{2}} Z_{R1q} Z_{-1p}^* Z_{+2r} - \frac{ie}{s_W} \frac{1}{\sqrt{2}} Z_{R(2+\alpha)q} Z_{+1r} Z_{-(2+\alpha)p}^* + i\lambda_{\alpha\beta j} \frac{1}{\sqrt{2}} Z_{R(2+\beta)q} Z_{-(2+\alpha)p}^* Z_{+(2+j)r}$$

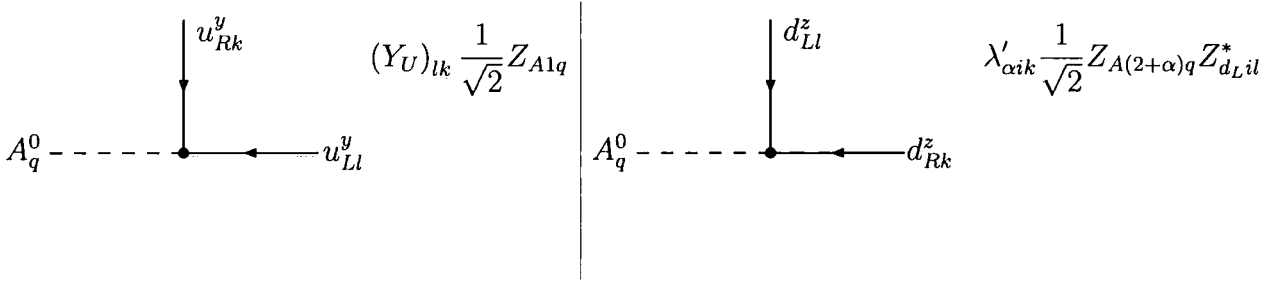


$$-\frac{e}{s_W} \frac{1}{\sqrt{2}} Z_{A1q} Z_{-1p}^* Z_{+2r} - \frac{e}{s_W} \frac{1}{\sqrt{2}} Z_{A(2+\alpha)q} Z_{+1r} Z_{-(2+\alpha)p}^* - \lambda_{\alpha\beta j} \frac{1}{\sqrt{2}} Z_{A(2+\beta)q} Z_{-(2+\alpha)p}^* Z_{+(2+j)r}$$

C.41 Neutral Scalar-Quark-Quark interactions

$$-(Y_U)_{ij} h_2^0 u_{Rj}^y u_{Li}^y - (Y_U)_{ij}^* h_2^{0*} \bar{u}_{Rj}^y \bar{u}_{Li}^y - \lambda'_{\alpha ij} \tilde{\nu}_{L\alpha} d_{Li}^z d_{Rj}^z - \lambda'_{\alpha ij}{}^* \tilde{\nu}_{L\alpha}^* \bar{d}_{Li}^z \bar{d}_{Rj}^z$$

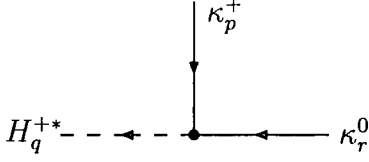




C.42 Charged Scalar - Neutral Fermion - Charged Fermion interactions

$$\begin{aligned}
& -\frac{ig}{\sqrt{2}} \tilde{e}_{L\alpha}^* e_{L\alpha} \tilde{B} + \frac{ig}{\sqrt{2}} \tilde{e}_{L\alpha} \bar{e}_{L\alpha} \tilde{B} + ig_2 \tilde{e}_{L\alpha}^* \tilde{W}^- \nu_{L\alpha} - \frac{ig_2}{\sqrt{2}} \tilde{e}_{L\alpha}^* \tilde{W}^0 e_{L\alpha} \\
& -ig_2 \tilde{e}_{L\alpha} \tilde{W}^- \bar{\nu}_{L\alpha} + \frac{ig_2}{\sqrt{2}} \tilde{e}_{L\alpha} \tilde{W}^0 \bar{e}_{L\alpha} - \lambda_{\alpha\beta j} \tilde{e}_{L\beta} e_{Rj} \nu_{L\alpha} - \lambda_{\alpha\beta j}^* \tilde{e}_{L\beta}^* \bar{e}_{Rj} \bar{\nu}_{L\alpha} \\
& +i\sqrt{2}g \tilde{e}_{Ri} e_{Ri} \tilde{B} - i\sqrt{2}g \tilde{e}_{Ri}^* \bar{e}_{Ri} \tilde{B} - \lambda_{\alpha\beta j} \tilde{e}_{Rj}^* e_{L\beta} \nu_{L\alpha} - \lambda_{\alpha\beta j}^* \tilde{e}_{Rj} \bar{e}_{L\beta} \bar{\nu}_{L\alpha} \\
& +\frac{ig}{\sqrt{2}} h_2^{+*} \tilde{h}_2^+ \tilde{B} - \frac{ig}{\sqrt{2}} h_2^+ \tilde{h}_2^+ \tilde{B} + \frac{ig_2}{\sqrt{2}} h_2^{+*} \tilde{W}^0 \tilde{h}_2^+ + ig_2 h_2^{+*} \tilde{W}^+ \tilde{h}_2^0 \\
& -\frac{ig_2}{\sqrt{2}} h_2^+ \tilde{W}^0 \tilde{h}_2^{+*} - ig_2 h_2^+ \tilde{W}^+ \tilde{h}_2^0
\end{aligned}$$

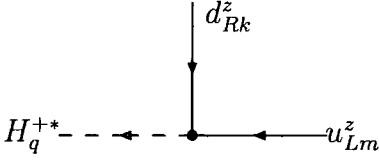
$$\begin{aligned}
& -i \frac{e}{s_W} Z_{H(2+\alpha)q} Z_{-1p}^* Z_{N(4+\alpha)r} \\
& -i \lambda_{\alpha\beta j} Z_{H(5+j)q} Z_{-(2+\beta)p}^* Z_{N(4+\alpha)r} \\
& +i \frac{e}{\sqrt{2}c_W} Z_{H(2+\alpha)q} Z_{-(2+\alpha)p}^* Z_{N1r} \\
& +i \frac{e}{\sqrt{2}s_W} Z_{H(2+\alpha)q} Z_{N2r} Z_{-(2+\alpha)p}^*
\end{aligned}$$



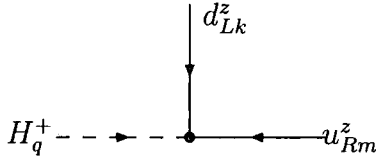
$$\begin{aligned}
& -i\lambda_{\alpha\beta j} Z_{H(2+\beta)q}^* Z_{+(2+j)p} Z_{N(4+\alpha)r} \\
& -i\sqrt{2}\frac{e}{c_W} Z_{H(5+i)q}^* Z_{+(2+i)p} Z_{N1r} \\
& -i\frac{e}{\sqrt{2}c_W} Z_{H1q}^* Z_{+2p} Z_{N1r} - i\frac{e}{s_W} Z_{H1q}^* Z_{+1p} Z_{N3r} \\
& -i\frac{e}{\sqrt{2}s_W} Z_{H1q}^* Z_{N2r} Z_{+2p}
\end{aligned}$$

C.43 Charged Scalar - Quark - Quark interactions

$$+i\lambda'_{\alpha ij} \tilde{e}_{L\alpha} d_{Rj}^z u_{Li}^z + \lambda'_{\alpha ij} \tilde{e}_{L\alpha}^* \bar{d}_{Rj}^z \bar{u}_{Li}^z + (Y_U)_{ij} h_2^+ d_{Li}^z u_{Rj}^z + (Y_U)_{ij}^* h_2^{+*} \bar{d}_{Li}^z \bar{u}_{Rj}^z$$



$$+i\lambda'_{\alpha mk} Z_{H(2+\alpha)q}^*$$



$$+i(Y_U)_{im} Z_{H1q} Z_{d_L ik}^*$$

C.44 Squark - Neutral Fermion - Quark interactions

$$+\frac{ig}{3\sqrt{2}} \tilde{u}_{Li}^* u_{Li} \tilde{B} - \frac{ig}{3\sqrt{2}} \tilde{u}_{Li} \bar{u}_{Li} \tilde{B} + \frac{ig_2}{\sqrt{2}} \tilde{u}_{Li}^* \tilde{W}^0 u_{Li} - \frac{ig_2}{\sqrt{2}} \tilde{u}_{Li} \tilde{W}^0 \bar{u}_{Li}$$

$$\begin{aligned}
& - (Y_U)_{ij} \tilde{u}_{Li}^y u_{Rj}^y \tilde{h}_2^0 - (Y_U)^*_{ij} \tilde{u}_{Li}^{*y} \bar{u}_{Rj}^y \bar{h}_2^0 - \frac{2ig\sqrt{2}}{3} \tilde{u}_{Ri} u_{Ri} \tilde{B} + \frac{2ig\sqrt{2}}{3} \tilde{u}_{Ri}^* \bar{u}_{Ri} \tilde{B} \\
& + \frac{ig}{3\sqrt{2}} \tilde{d}_{Li}^* d_{Li} \tilde{B} - \frac{ig}{3\sqrt{2}} \tilde{d}_{Li} \bar{d}_{Li} \tilde{B} - (Y_U)^*_{ij} \tilde{u}_{Rj}^y \bar{u}_{Li}^y \bar{h}_2^0 - (Y_U)_{ij} \tilde{u}_{Rj}^* u_{Li}^y \tilde{h}_2^0 - \frac{ig_2}{\sqrt{2}} \tilde{d}_{Li}^* \tilde{W}^0 d_{Li} \\
& + \frac{ig_2}{\sqrt{2}} \tilde{d}_{Li} \tilde{W}^0 \bar{d}_{Li} - \lambda'_{\alpha ij} \tilde{d}_{Li}^y \nu_{L\alpha} d_{Rj}^y - \lambda'_{\alpha ij} \tilde{d}_{Li}^{*y} \bar{\nu}_{L\alpha} \bar{d}_{Rj}^y + \frac{ig\sqrt{2}}{3} \tilde{d}_{Ri} d_{Ri} \tilde{B} \\
& - \frac{ig\sqrt{2}}{3} \tilde{d}_{Ri}^* \bar{d}_{Ri} \tilde{B} - \lambda'_{\alpha ij} \tilde{d}_{Rj}^{*y} \nu_{L\alpha} d_{Li}^y - \lambda'_{\alpha ij} \tilde{d}_{Rj}^y \bar{\nu}_{L\alpha} \bar{d}_{Li}^y
\end{aligned}$$

$$\begin{aligned}
& -i\lambda'_{\alpha jk} Z_{\tilde{d}(3+k)q} Z_{N(4+\alpha)p} - i\frac{e}{3\sqrt{2}c_W} Z_{\tilde{d}jq} Z_{N1p} \\
& + i\frac{e}{\sqrt{2}s_W} Z_{\tilde{d}jq} Z_{N2p}
\end{aligned}$$

$$-i\lambda'_{\alpha ij} Z_{\tilde{d}iq}^* Z_{N(4+\alpha)p} - i\frac{e\sqrt{2}}{3c_W} Z_{\tilde{d}(3+j)q}^* Z_{N1p}$$

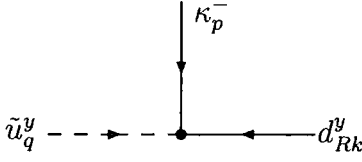
$$\begin{aligned}
& -i\frac{e}{3\sqrt{2}c_W} Z_{\tilde{u}jq}^* Z_{N1p} - i(Y_U)_{jk} Z_{\tilde{u}(3+k)q}^* Z_{N3p} \\
& -i\frac{e}{\sqrt{2}s_W} Z_{\tilde{u}jq}^* Z_{N2p}
\end{aligned}$$

$$i\frac{2e\sqrt{2}}{3c_W} Z_{\tilde{u}(3+k)q} Z_{N1p} - i(Y_U)_{ik} Z_{\tilde{u}iq} Z_{N3p}$$

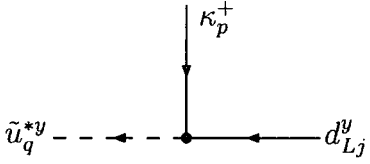
C.45 Squark - Charged Fermion - Quark interactions

$$\begin{aligned}
& +ig_2\tilde{u}_{Li}^*\tilde{W}^+d_{Li} - ig_2\tilde{u}_{Li}\tilde{W}^+\bar{d}_{Li} + \lambda'_{\alpha ij}\tilde{u}_{Li}^ye_{L\alpha}d_{Rj}^y + \lambda'^*_{\alpha ij}\tilde{u}_{Li}^*e_{L\alpha}\bar{d}_{Rj}^y \\
& + (Y_U)^*_{ij}\tilde{u}_{Rj}^yd_{Li}^y\tilde{h}_2^+ + ig_2\tilde{d}_{Li}^*\tilde{W}^-u_{Li} - ig_2\tilde{d}_{Li}\tilde{W}^-\bar{u}_{Li} + (Y_U)_{ij}\tilde{d}_{Li}^yu_{Rj}^y\tilde{h}_2^+ \\
& + (Y_U)^*_{ij}\tilde{d}_{Li}^*u_{Rj}^y\tilde{h}_2^+ + \lambda'_{\alpha ij}\tilde{d}_{Rj}^*e_{L\alpha}u_{Li}^y + \lambda'^*_{\alpha ij}\tilde{d}_{Rj}^ye_{L\alpha}\bar{u}_{Li}^y + (Y_U)_{ij}\tilde{u}_{Rj}^*d_{Li}^y\tilde{h}_2^+
\end{aligned}$$

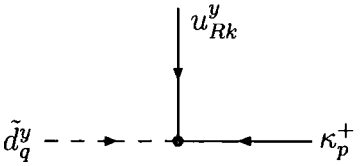
.....



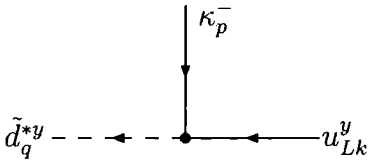
$$+i\lambda'_{\alpha ik}Z_{\tilde{u}iq}Z_{-(2+\alpha)p}^*$$



$$-i\frac{e}{S_W}Z_{\tilde{u}iq}^*Z_{+1q}Z_{d_Lij}^* + i(Y_U)_{ik}Z_{\tilde{u}(3+k)q}^*Z_{d_Lij}^*Z_{+2q}$$



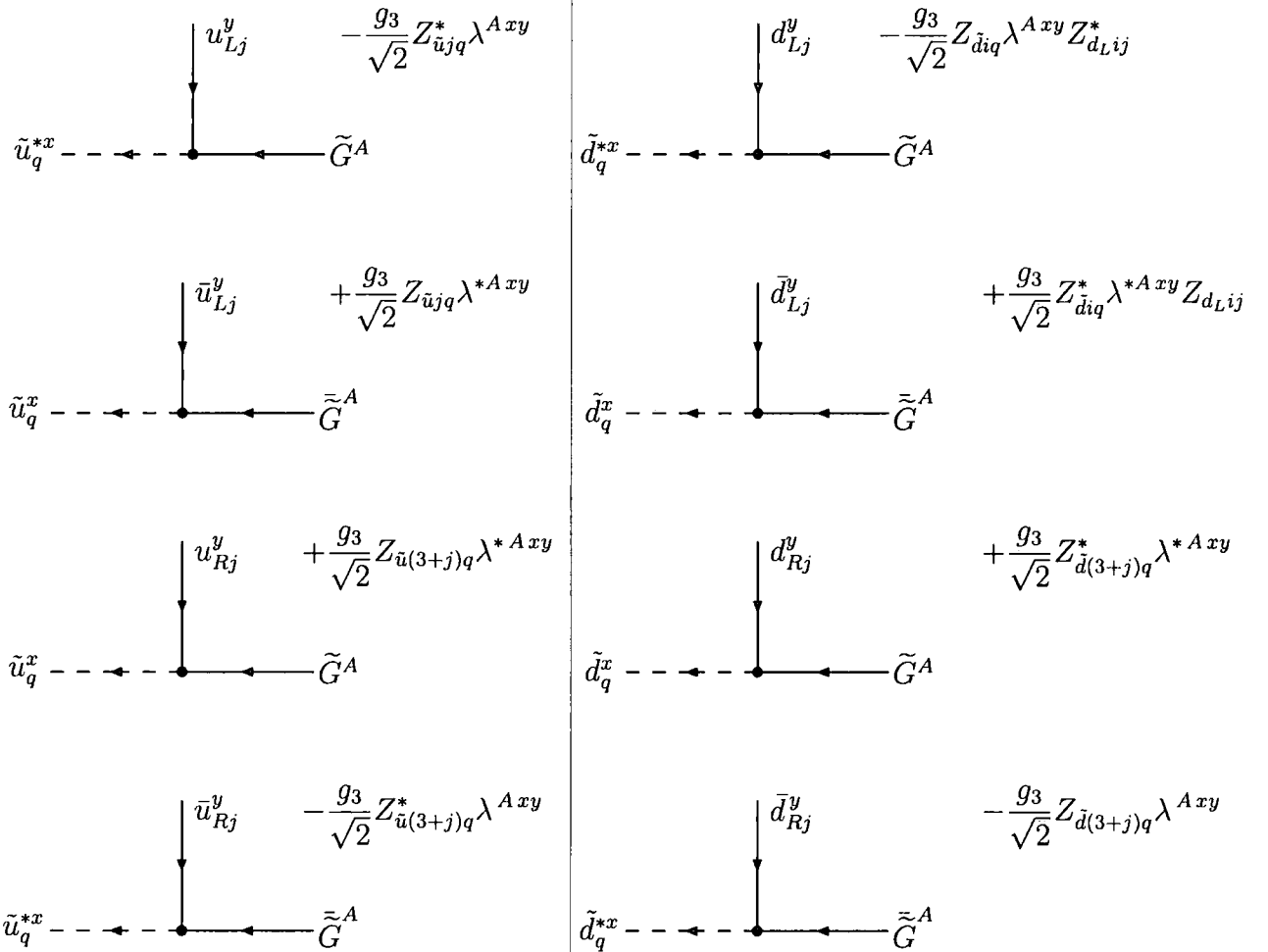
$$+i(Y_U)_{ik}Z_{\tilde{d}iq}^*Z_{+2p}$$



$$+i\lambda'_{\alpha kj}Z_{\tilde{d}(3+j)q}^*Z_{-(2+\alpha)p}^* - i\frac{e}{S_W}Z_{\tilde{d}kq}Z_{-1p}^*$$

C.46 Squark - Gluino - Quark interactions

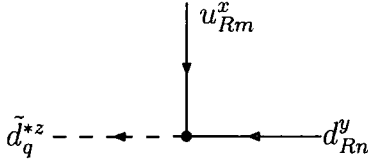
$$\begin{aligned}
 & + \frac{ig_3}{\sqrt{2}} \tilde{u}_{Li}^{*x} \lambda^{Axy} u_{Li}^y \tilde{G}^A - \frac{ig_3}{\sqrt{2}} \tilde{u}_{Li}^x \lambda^{*Axy} \bar{u}_{Li}^y \tilde{G}^A - \frac{ig_3}{\sqrt{2}} \tilde{u}_{Ri}^x \lambda^{*Axy} u_{Ri}^y \tilde{G}^A + \frac{ig_3}{\sqrt{2}} \tilde{u}_{Ri}^{*x} \lambda^{Axy} \bar{u}_{Ri}^y \tilde{G}^A \\
 & + \frac{ig_3}{\sqrt{2}} \tilde{d}_{Li}^{*x} \lambda^{Axy} d_{Li}^y \tilde{G}^A - \frac{ig_3}{\sqrt{2}} \tilde{d}_{Li}^x \lambda^{*Axy} \bar{d}_{Li}^y \tilde{G}^A - \frac{ig_3}{\sqrt{2}} \tilde{d}_{Ri}^x \lambda^{*Axy} d_{Ri}^y \tilde{G}^A + \frac{ig_3}{\sqrt{2}} \tilde{d}_{Ri}^{*x} \lambda^{Axy} \bar{d}_{Ri}^y \tilde{G}^A
 \end{aligned}$$



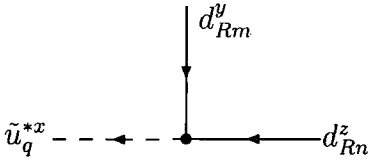
C.47 Squark - Quark - Quark interactions

$$-\frac{1}{2}\varepsilon_{xyz}\lambda''_{ijk}\tilde{u}_{Ri}^{*x}d_{Rj}^yd_{Rk}^z-\frac{1}{2}\varepsilon_{xyz}\lambda''_{ijk}\tilde{u}_{Ri}^x\bar{d}_{Rj}^y\bar{d}_{Rk}^z-\varepsilon_{xyz}\lambda''_{ijk}\tilde{d}_{Rk}^{*z}u_{Ri}^xd_{Rj}^y-\varepsilon_{xyz}\lambda''_{ijk}\tilde{d}_{Rk}^z\bar{u}_{Ri}^x\bar{d}_{Rj}^y$$

.....



$$-i\varepsilon_{xyz}\lambda''_{mnk}Z_{\tilde{d}(3+k)q}$$



$$-i\frac{1}{2}\varepsilon_{xyz}\lambda''_{imn}Z_{\tilde{u}(3+i)q}^*+i\frac{1}{2}\varepsilon_{xyz}\lambda''_{inm}Z_{\tilde{u}(3+i)q}^*$$

C.48 Neutral Scalar - Neutral Scalar - Neutral Scalar - Neutral Scalar

$$+\frac{g^2}{4}\tilde{\nu}_{L\alpha}^*\tilde{\nu}_{L\alpha}h_2^{0*}h_2^0+\frac{g_2^2}{4}h_2^{0*}h_2^0\tilde{\nu}_{L\alpha}^*\tilde{\nu}_{L\alpha}-\frac{g^2}{8}h_2^{0*}h_2^0h_2^{0*}h_2^0-\frac{g_2^2}{8}h_2^{0*}h_2^0h_2^{0*}h_2^0$$

$$-\frac{g^2}{8}\tilde{\nu}_{L\alpha}^*\tilde{\nu}_{L\alpha}\tilde{\nu}_{L\beta}^*\tilde{\nu}_{L\beta}-\frac{g_2^2}{8}\tilde{\nu}_{L\alpha}^*\tilde{\nu}_{L\alpha}\tilde{\nu}_{L\beta}^*\tilde{\nu}_{L\beta}$$

.....

$$\begin{array}{c}
\begin{array}{c}
H_r^0 \\
| \\
H_q^0 \text{---} \bullet \text{---} H_s^0 \\
| \\
H_t^0
\end{array}
\quad -\frac{ie^2}{32c_W^2 s_W^2} (\delta_{qs} - 2Z_{R1q}Z_{R1s})(\delta_{rt} - 2Z_{R1r}Z_{R1t}) \\
\\
\begin{array}{c}
A_r^0 \\
| \\
A_q^0 \text{---} \bullet \text{---} A_s^0 \\
| \\
A_t^0
\end{array}
\quad -\frac{ie^2}{32c_W^2 s_W^2} (\delta_{qs} - 2Z_{A1q}Z_{A1s})(\delta_{rt} - 2Z_{A1r}Z_{A1t}) \\
\\
\begin{array}{c}
H_s^0 \\
| \\
H_q^0 \text{---} \bullet \text{---} A_r^0 \\
| \\
A_t^0
\end{array}
\quad -\frac{ie^2}{16c_W^2 s_W^2} (\delta_{qs} - 2Z_{R1q}Z_{R1s})(\delta_{rt} - 2Z_{A1r}Z_{A1t})
\end{array}$$

C.49 Neutral Scalar - Neutral Scalar - Charged Scalar - Charged Scalar

$$\begin{aligned}
& -\frac{g_2^2}{4} h_2^{0*} h_2^0 h_2^{+*} h_2^+ - \frac{g_2^2}{2} h_2^{+*} \tilde{\nu}_{L\alpha} h_2^0 \tilde{e}_{L\alpha}^* - \frac{g_2^2}{4} h_2^{0*} \tilde{e}_{L\alpha} h_2^0 \tilde{e}_{L\alpha}^* - \frac{g^2}{4} h_2^{+*} h_2^+ h_2^{0*} h_2^0 \\
& \quad - \frac{g_2^2}{2} h_2^{0*} \tilde{e}_{L\alpha} h_2^+ \tilde{\nu}_{L\alpha}^* + \frac{g^2}{4} \tilde{e}_{L\alpha}^* \tilde{e}_{L\alpha} h_2^{0*} h_2^0 - \frac{g^2}{2} \tilde{e}_{Ri}^* \tilde{e}_{Ri} h_2^{0*} h_2^0 \\
& + \frac{g^2}{4} \tilde{\nu}_{L\alpha}^* \tilde{\nu}_{L\alpha} h_2^{+*} h_2^+ - \frac{g_2^2}{4} h_2^{+*} \tilde{\nu}_{L\alpha} h_2^+ \tilde{\nu}_{L\alpha}^* + \frac{g^2}{2} \tilde{\nu}_{L\alpha}^* \tilde{\nu}_{L\alpha} \tilde{e}_{Rj}^* \tilde{e}_{Rj} - \frac{g^2}{4} \tilde{e}_{L\alpha}^* \tilde{e}_{L\alpha} \tilde{\nu}_{L\beta}^* \tilde{\nu}_{L\beta}
\end{aligned}$$

$$-\frac{g_2^2}{2}\tilde{e}_{L\alpha}^*\tilde{\nu}_{L\alpha}\tilde{\nu}_{L\beta}^*\tilde{e}_{L\beta}+\frac{g_2^2}{4}\tilde{e}_{L\alpha}^*\tilde{e}_{L\alpha}\tilde{\nu}_{L\beta}^*\tilde{\nu}_{L\beta}-\lambda_{\alpha\beta j}\lambda_{\alpha\gamma q}^*\tilde{\nu}_{L\beta}\tilde{e}_{Rj}^*\tilde{\nu}_{L\gamma}^*\tilde{e}_{Rq}-\lambda_{\alpha\beta k}\lambda_{\delta\gamma k}^*\tilde{\nu}_{L\alpha}\tilde{e}_{L\beta}\tilde{\nu}_{L\delta}^*\tilde{e}_{L\gamma}$$

.....

	$ \begin{aligned} & -\left[-\frac{\lambda_{\alpha\beta j}\lambda_{\alpha\gamma k}^*}{2}Z_{H(5+k)t}^*Z_{H(5+j)r}(Z_{R(2+\gamma)q}Z_{A(2+\beta)s}-Z_{R(2+\beta)q}Z_{A(2+\gamma)s})\right. \\ & -\frac{\lambda_{\alpha\beta k}\lambda_{\delta\gamma k}^*}{2}Z_{H(2+\beta)t}^*Z_{H(2+\gamma)r}(Z_{R(2+\delta)q}Z_{A(2+\alpha)s}-Z_{R(2+\alpha)q}Z_{A(2+\delta)s}) \\ & -\frac{e^2}{4s_W^2}Z_{H(2+\beta)t}^*Z_{H(2+\alpha)r}(Z_{R(2+\beta)q}Z_{A(2+\alpha)s}-Z_{R(2+\alpha)q}Z_{A(2+\beta)s}) \\ & -\frac{e^2}{4s_W^2}Z_{H1t}^*Z_{H(2+\alpha)r}(Z_{R(2+\alpha)q}Z_{A1s}+Z_{R1q}Z_{A(2+\alpha)s}) \\ & \left. +\frac{e^2}{4s_W^2}Z_{H(2+\alpha)t}^*Z_{H1r}(Z_{R1q}Z_{A(2+\alpha)s}+Z_{R(2+\alpha)q}Z_{A1s})\right] \end{aligned} $
--	--

	$ \begin{aligned} & i\left[-\frac{\lambda_{\alpha\beta j}\lambda_{\alpha\gamma k}^*}{2}Z_{H(5+k)t}^*Z_{H(5+j)r}Z_{R(2+\beta)q}Z_{R(2+\gamma)s}\right. \\ & -\frac{\lambda_{\alpha\beta k}\lambda_{\delta\gamma k}^*}{2}Z_{H(2+\beta)t}^*Z_{H(2+\gamma)r}Z_{R(2+\alpha)q}Z_{R(2+\delta)s} \\ & -\frac{e^2(1-2s_W^2)}{8c_W^2s_W^2}Z_{H(2+\alpha)t}^*Z_{H(2+\alpha)r}(\delta_{qs}-2Z_{R1q}Z_{R1s}) \\ & +\frac{e^2}{4c_W^2}Z_{H(5+j)t}^*Z_{H(5+j)r}(\delta_{qs}-2Z_{R1q}Z_{R1s}) \\ & +\frac{e^2}{8c_W^2}Z_{H1t}^*Z_{H1r}(\delta_{qs}-2Z_{R1q}Z_{R1s}) \\ & -\frac{e^2}{4s_W^2}Z_{H(2+\beta)t}^*Z_{H(2+\alpha)r}Z_{R(2+\alpha)q}Z_{R(2+\beta)s} \\ & -\frac{e^2}{8s_W^2}Z_{H1t}^*Z_{H1r}\delta_{qs}-\frac{e^2}{4s_W^2}Z_{H1t}^*Z_{H(2+\alpha)r}Z_{R(2+\alpha)q}Z_{R1s}x \\ & \left. -\frac{e^2}{4s_W^2}Z_{H(2+\alpha)t}^*Z_{H1r}Z_{R(2+\alpha)q}Z_{R1s}\right] \end{aligned} $
--	---

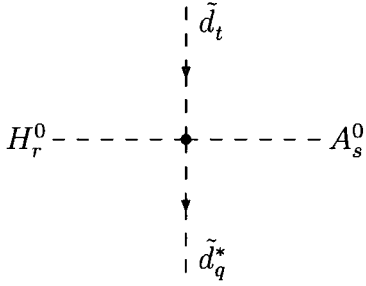
$$\begin{array}{c}
H_r^+ \\
\vdots \\
A_q^0 \text{ --- } \bullet \text{ --- } A_s^0 \\
\vdots \\
H_t^{+*}
\end{array}$$

$$\begin{aligned}
& i \left[-\frac{\lambda_{\alpha\beta j} \lambda_{\alpha\gamma k}^*}{2} Z_{H(5+k)t}^* Z_{H(5+j)r} Z_{A(2+\beta)q} Z_{A(2+\gamma)s} \right. \\
& - \frac{\lambda_{\alpha\beta k} \lambda_{\delta\gamma k}^*}{2} Z_{H(2+\beta)t}^* Z_{H(2+\gamma)r} Z_{A(2+\alpha)q} Z_{A(2+\delta)s} \\
& - \frac{e^2(1-2s_W^2)}{8c_W^2 s_W^2} Z_{H(2+\alpha)t}^* Z_{H(2+\alpha)r} (\delta_{qs} - 2Z_{A1q} Z_{A1s}) \\
& + \frac{e^2}{4c_W^2} Z_{H(5+j)t}^* Z_{H(5+j)r} (\delta_{qs} - 2Z_{A1q} Z_{A1s}) \\
& + \frac{e^2}{8c_W^2} Z_{H1t}^* Z_{H1r} (\delta_{qs} - 2Z_{A1q} Z_{A1s}) \\
& - \frac{e^2}{4s_W^2} Z_{H(2+\beta)t}^* Z_{H(2+\alpha)r} Z_{A(2+\alpha)q} Z_{A(2+\beta)s} \\
& - \frac{e^2}{8s_W^2} Z_{H1t}^* Z_{H1r} \delta_{qs} \\
& + \frac{e^2}{4s_W^2} Z_{H1t}^* Z_{H(2+\alpha)r} Z_{A(2+\alpha)q} Z_{A1s} \\
& \left. + \frac{e^2}{4s_W^2} Z_{H(2+\alpha)t}^* Z_{H1r} Z_{A(2+\alpha)q} Z_{A1s} \right]
\end{aligned}$$

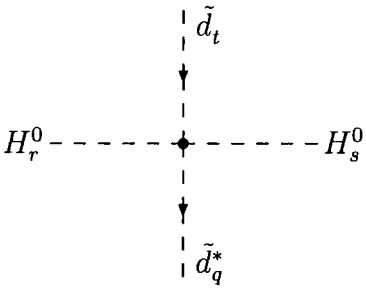
C.50 Neutral Scalar - Neutral Scalar - Squark - Squark

$$\begin{aligned}
& - (Y_U)_{ik} (Y_U)_{pk}^* \tilde{u}_{Li}^x h_2^0 \tilde{u}_{Lp}^{*x} h_2^{0*} - (Y_U)_{ij} (Y_U)_{iq}^* h_2^0 \tilde{u}_{Rj}^{*y} h_2^{0*} \tilde{u}_{Rq}^y - \frac{g^2}{12} h_2^{0*} h_2^0 \tilde{u}_{Lj}^{*y} \tilde{u}_{Lj}^y + \frac{g^2}{4} h_2^{0*} h_2^0 \tilde{u}_{Li}^{*x} \tilde{u}_{Li}^x \\
& + \frac{g^2}{12} \tilde{\nu}_{L\alpha}^* \tilde{\nu}_{L\alpha} \tilde{u}_{Lj}^{*y} \tilde{u}_{Lj}^y - \frac{g^2}{4} \tilde{\nu}_{L\alpha}^* \tilde{u}_{Lj}^x \tilde{\nu}_{L\alpha} \tilde{u}_{Lj}^{*x} + \frac{g^2}{3} h_2^{0*} h_2^0 \tilde{u}_{Rj}^{*y} \tilde{u}_{Rj}^y - \frac{g^2}{12} h_2^{0*} h_2^0 \tilde{d}_{Lj}^{*y} \tilde{d}_{Lj}^y \\
& - \frac{g^2}{4} h_2^{0*} \tilde{d}_{Li}^x h_2^0 \tilde{d}_{Li}^{*x} - \frac{g^2}{6} h_2^{0*} h_2^0 \tilde{d}_{Rj}^{*y} \tilde{d}_{Rj}^y - \lambda'_{\alpha ij} \lambda_{\beta iq}^* \tilde{\nu}_{L\alpha} \tilde{d}_{Rj}^{*y} \tilde{\nu}_{L\beta}^* \tilde{d}_{Rq}^y + \frac{g^2}{6} \tilde{\nu}_{L\alpha}^* \tilde{\nu}_{L\alpha} \tilde{d}_{Rj}^{*y} \tilde{d}_{Rj}^y \\
& - \lambda'_{\alpha ik} \lambda_{\beta pk}^* \tilde{\nu}_{L\alpha} \tilde{d}_{Li}^z \tilde{\nu}_{L\beta}^* \tilde{d}_{Lp}^{*z} + \frac{g^2}{12} \tilde{\nu}_{L\alpha}^* \tilde{\nu}_{L\alpha} \tilde{d}_{Lj}^{*y} \tilde{d}_{Lj}^y + \frac{g^2}{4} \tilde{\nu}_{L\alpha}^* \tilde{\nu}_{L\alpha} \tilde{d}_{Lj}^{*x} \tilde{d}_{Lj}^x - \frac{g^2}{3} \tilde{\nu}_{L\alpha}^* \tilde{\nu}_{L\alpha} \tilde{u}_{Rj}^{*y} \tilde{u}_{Rj}^y
\end{aligned}$$

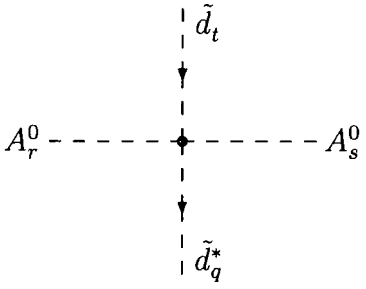
.....



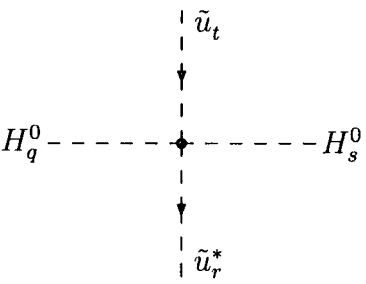
$$\left(\frac{\lambda'_{\alpha ij} \lambda'_{\beta ik}^*}{2} Z_{\tilde{d}(3+j)q} Z_{\tilde{d}(3+k)t}^* + \frac{\lambda'_{\alpha ik} \lambda'_{\beta jk}^*}{2} Z_{\tilde{d}jq} Z_{\tilde{d}it}^* \right) (Z_{R(2+\beta)r} Z_{A(2+\alpha)s} - Z_{R(2+\alpha)r} Z_{A(2+\beta)s})$$



$$i \left[-\frac{\lambda'_{\alpha ij} \lambda'_{\beta ik}^*}{2} Z_{\tilde{d}(3+j)q} Z_{\tilde{d}(3+k)t}^* Z_{R(2+\alpha)r} Z_{R(2+\beta)s} - \frac{\lambda'_{\alpha ik} \lambda'_{\beta jk}^*}{2} Z_{\tilde{d}jq} Z_{\tilde{d}it}^* Z_{R(2+\alpha)r} Z_{R(2+\beta)s} + \frac{e^2(1+2c_W^2)}{24c_W^2 s_W^2} Z_{\tilde{d}jq} Z_{\tilde{d}jt}^* (\delta_{rs} - 2Z_{R1s} Z_{R1r}) + \frac{e^2}{12c_W^2} Z_{\tilde{d}(3+j)q} Z_{\tilde{d}(3+j)t}^* (\delta_{rs} - 2Z_{R1s} Z_{R1r}) \right]$$



$$i \left[-\frac{\lambda'_{\alpha ij} \lambda'_{\beta ik}^*}{2} Z_{\tilde{d}(3+j)q} Z_{\tilde{d}(3+k)t}^* Z_{A(2+\alpha)r} Z_{A(2+\beta)s} - \frac{\lambda'_{\alpha ik} \lambda'_{\beta jk}^*}{2} Z_{\tilde{d}jq} Z_{\tilde{d}it}^* Z_{A(2+\alpha)r} Z_{A(2+\beta)s} + \frac{e^2(1+2c_W^2)}{24c_W^2 s_W^2} Z_{\tilde{d}jq} Z_{\tilde{d}jt}^* (\delta_{rs} - 2Z_{A1s} Z_{A1r}) + \frac{e^2}{12c_W^2} Z_{\tilde{d}(3+j)q} Z_{\tilde{d}(3+j)t}^* (\delta_{rs} - 2Z_{A1s} Z_{A1r}) \right]$$

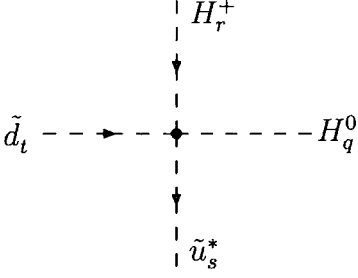


$$i \left[-\frac{(Y_U)_{ij} (Y_U)_{ik}^*}{2} Z_{\tilde{u}(3+j)r} Z_{\tilde{u}(3+k)t}^* Z_{R1q} Z_{R1s} - \frac{(Y_U)_{ik} (Y_U)_{jk}^*}{2} Z_{\tilde{u}jr} Z_{\tilde{u}it}^* Z_{R1q} Z_{R1s} + \frac{e^2(1-4c_W^2)}{24c_W^2 s_W^2} Z_{\tilde{u}jr} Z_{\tilde{u}jt}^* (\delta_{qs} - 2Z_{R1s} Z_{R1q}) - \frac{e^2}{6c_W^2} Z_{\tilde{u}(3+j)r} Z_{\tilde{u}(3+j)t}^* (\delta_{qs} - 2Z_{R1s} Z_{R1q}) \right]$$

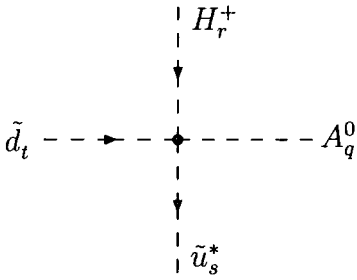
$$\begin{array}{c}
\vdots \tilde{u}_t \\
\downarrow \\
A_q^0 \text{---} \bullet \text{---} A_s^0 \\
\uparrow \\
\vdots \tilde{u}_r^*
\end{array}
\quad
\begin{aligned}
& i \left[-\frac{(Y_U)_{ij} (Y_U)_{ik}^*}{2} Z_{\tilde{u}(3+j)r}^* Z_{\tilde{u}(3+k)t} Z_{A1q} Z_{A1s} \right. \\
& - \frac{(Y_U)_{ik} (Y_U)_{jk}^*}{2} Z_{\tilde{u}jr}^* Z_{\tilde{u}it} Z_{A1q} Z_{A1s} \\
& + \frac{e^2(1-4c_W^2)}{24c_W^2 s_W^2} Z_{\tilde{u}jr}^* Z_{\tilde{u}jt} (\delta_{qs} - 2Z_{A1s} Z_{A1q}) \\
& \left. - \frac{e^2}{6c_W^2} Z_{\tilde{u}(3+j)r}^* Z_{\tilde{u}(3+j)t} (\delta_{qs} - 2Z_{A1s} Z_{A1q}) \right]
\end{aligned}$$

C.51 Neutral Scalar - Charged Scalar - Squark - Squark

$$\begin{aligned}
& -\lambda_{\alpha\beta j} \lambda'_{\alpha p q} \tilde{\nu}_{L\beta} \tilde{e}_{Rj}^* \tilde{u}_{Lp}^{*z} \tilde{d}_{Rq}^z - \lambda'_{\alpha ij} \lambda_{\alpha\gamma q}^* \tilde{u}_{Li}^y \tilde{d}_{Rj}^{*y} \tilde{\nu}_{L\gamma}^* \tilde{e}_{Rq} + \lambda'_{\alpha ik} \lambda_{\beta p k}^* \tilde{\nu}_{L\alpha} \tilde{d}_{Li}^z \tilde{e}_{L\beta}^* \tilde{u}_{Lp}^{*z} \\
& + \lambda'_{\alpha ik} \lambda_{\beta p k}^* \tilde{e}_{L\alpha} \tilde{u}_{Li}^z \tilde{\nu}_{L\beta}^* \tilde{d}_{Lp}^{*z} + (Y_U)_{ik} (Y_U)_{pk}^* \tilde{u}_{Li}^x h_2^0 \tilde{d}_{Lp}^{*x} h_2^{+*} + (Y_U)_{ik} (Y_U)_{pk}^* \tilde{d}_{Li}^x h_2^+ \tilde{u}_{Lp}^{*x} h_2^{0*} \\
& + (Y_U)_{ij} \lambda_{\alpha iq}^* h_2^+ \tilde{u}_{Rj}^{*y} \tilde{\nu}_{L\alpha}^* \tilde{d}_{Rq}^y + \lambda'_{\alpha ij} (Y_U)_{iq}^* \tilde{\nu}_{L\alpha} \tilde{d}_{Rj}^{*y} h_2^{+*} \tilde{u}_{Rq}^y \\
& + (Y_U)_{ij} \lambda_{\alpha iq}^* h_2^0 \tilde{u}_{Rj}^{*y} \tilde{e}_{L\alpha}^* \tilde{d}_{Rq}^y + \lambda'_{\alpha ij} (Y_U)_{iq}^* \tilde{e}_{L\alpha} \tilde{d}_{Rj}^{*y} h_2^{0*} \tilde{u}_{Rq}^y - \frac{g_2^2}{2} h_2^{+*} \tilde{u}_{Li}^x h_2^0 \tilde{d}_{Li}^{*x} \\
& - \frac{g_2^2}{2} h_2^{0*} \tilde{d}_{Li}^x h_2^+ \tilde{u}_{Li}^{*x} - \frac{g_2^2}{2} \tilde{\nu}_{L\alpha}^* \tilde{u}_{Lj}^y \tilde{e}_{L\alpha} \tilde{d}_{Lj}^{*y} - \frac{g_2^2}{2} \tilde{e}_{L\alpha}^* \tilde{d}_{Lj}^y \tilde{\nu}_{L\alpha} \tilde{u}_{Lj}^{*y}
\end{aligned}$$



$$\begin{aligned}
& i \left[-\frac{\lambda_{\alpha\beta j} \lambda'_{\alpha k m}}{\sqrt{2}} Z_{\tilde{u}ks}^* Z_{\tilde{d}(3+m)t}^* Z_{H(5+j)r} Z_{R(2+\beta)q} \right. \\
& + \frac{(Y_U)_{ij} \lambda'_{\alpha ik}}{\sqrt{2}} Z_{\tilde{u}(3+j)s}^* Z_{\tilde{d}(3+k)t}^* Z_{H1r} Z_{R(2+\alpha)q} \\
& + \frac{\lambda'_{\alpha ik} \lambda'_{\beta jk}}{\sqrt{2}} Z_{\tilde{u}js}^* Z_{\tilde{d}it}^* Z_{H(2+\beta)r} Z_{R(2+\alpha)q} \\
& - \frac{e^2}{2\sqrt{2}s_W^2} Z_{\tilde{u}is}^* Z_{\tilde{d}it}^* Z_{H1r} Z_{R1q} \\
& - \frac{e^2}{2\sqrt{2}s_W^2} Z_{\tilde{u}is}^* Z_{\tilde{d}it}^* Z_{H(2+\alpha)r} Z_{R(2+\alpha)q} \\
& + \frac{(Y_U)_{ij} \lambda'_{\alpha ik}}{\sqrt{2}} Z_{\tilde{u}(3+j)s}^* Z_{\tilde{d}(3+k)t}^* Z_{H(2+\alpha)r} Z_{R1q} \\
& \left. + \frac{(Y_U)_{ik} (Y_U)_{jk}^*}{\sqrt{2}} Z_{\tilde{u}js}^* Z_{\tilde{d}it}^* Z_{H1r} Z_{R1q} \right]
\end{aligned}$$

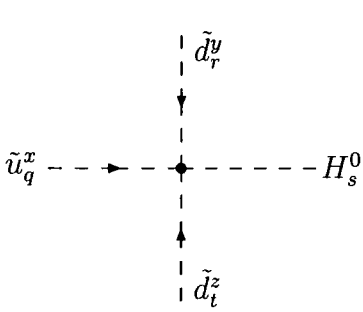


$$\begin{aligned}
& - \left[-\frac{\lambda_{\alpha\beta j} \lambda'_{\alpha k m}}{\sqrt{2}} Z_{\tilde{u}ks}^* Z_{\tilde{d}(3+m)t}^* Z_{H(5+j)r} Z_{A(2+\beta)q} \right. \\
& - \frac{(Y_U)_{ij} \lambda'_{\alpha ik}}{\sqrt{2}} Z_{\tilde{u}(3+j)s}^* Z_{\tilde{d}(3+k)t}^* Z_{H1r} Z_{A(2+\alpha)q} \\
& + \frac{\lambda'_{\alpha ik} \lambda'_{\beta jk}}{\sqrt{2}} Z_{\tilde{u}js}^* Z_{\tilde{d}it}^* Z_{H(2+\beta)r} Z_{A(2+\alpha)q} \\
& + \frac{e^2}{2\sqrt{2}s_W^2} Z_{\tilde{u}is}^* Z_{\tilde{d}it}^* Z_{H1r} Z_{A1q} \\
& - \frac{e^2}{2\sqrt{2}s_W^2} Z_{\tilde{u}is}^* Z_{\tilde{d}it}^* Z_{H(2+\alpha)r} Z_{A(2+\alpha)q} \\
& + \frac{(Y_U)_{ij} \lambda'_{\alpha ik}}{\sqrt{2}} Z_{\tilde{u}(3+j)s}^* Z_{\tilde{d}(3+k)t}^* Z_{H(2+\alpha)r} Z_{A1q} \\
& \left. - \frac{(Y_U)_{ik} (Y_U)_{jk}^*}{\sqrt{2}} Z_{\tilde{u}js}^* Z_{\tilde{d}it}^* Z_{H1r} Z_{A1q} \right]
\end{aligned}$$

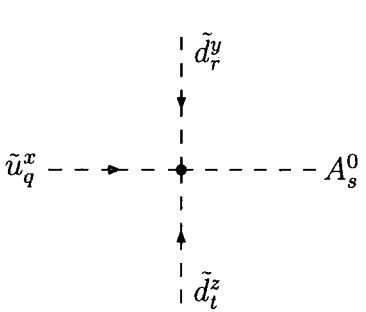
C.52 Neutral Scalar - Squark - Squark - Squark

$$\begin{aligned}
 & - (Y_U)_{ik} \frac{1}{2} \varepsilon_{xvw} \lambda''^{*}{}_{kpq} \tilde{u}_{Li}^x h_2^0 \tilde{d}_{Rp}^v \tilde{d}_{Rq}^w - \frac{1}{2} \varepsilon_{xyz} \lambda''_{kij} (Y_U)_{pk}^* \tilde{d}_{Ri}^{*y} \tilde{d}_{Rj}^{*z} \tilde{u}_{Lp}^{*x} h_2^{0*} \\
 & - \lambda'_{\alpha ik} \varepsilon_{vwx} \lambda''^{*}{}_{pqk} \tilde{\nu}_{L\alpha} \tilde{d}_{Li}^z \tilde{u}_{Rp}^v \tilde{d}_{Rq}^w - \varepsilon_{xyz} \lambda''_{ijk} \lambda'^{*}{}_{\alpha pk} \tilde{u}_{Ri}^{*x} \tilde{d}_{Rj}^{*y} \tilde{\nu}_{L\alpha}^* \tilde{d}_{Lp}^{*z}
 \end{aligned}$$

.....



$$\begin{aligned}
 & i \varepsilon_{xyz} \left[- \frac{(Y_U)_{ik} \lambda''^{*}{}_{kjm}}{2\sqrt{2}} Z_{\tilde{u}iq} Z_{\tilde{d}(3+j)r}^* Z_{\tilde{d}(3+m)t}^* Z_{R1s} \right. \\
 & \left. - \frac{\lambda'_{\alpha ik} \lambda''^{*}{}_{jmk}}{\sqrt{2}} Z_{\tilde{u}(3+j)q} Z_{\tilde{d}(3+m)r}^* Z_{\tilde{d}it}^* Z_{R(2+\alpha)s} \right]
 \end{aligned}$$



$$\begin{aligned}
 & i \varepsilon_{xyz} \left[- \frac{(Y_U)_{ik} \lambda''^{*}{}_{kjm}}{2\sqrt{2}} Z_{\tilde{u}iq} Z_{\tilde{d}(3+j)r}^* Z_{\tilde{d}(3+m)t}^* Z_{A1s} \right. \\
 & \left. - \frac{\lambda'_{\alpha ik} \lambda''^{*}{}_{jmk}}{\sqrt{2}} Z_{\tilde{u}(3+j)q} Z_{\tilde{d}(3+m)r}^* Z_{\tilde{d}it}^* Z_{A(2+\alpha)s} \right]
 \end{aligned}$$

C.53 Charged Scalar - Charged Scalar - Charged Scalar - Charged Scalar

$$-\lambda_{\alpha\beta j} \lambda_{\alpha\gamma q}^* \tilde{e}_{L\beta} \tilde{e}_{Rj}^* \tilde{e}_{L\gamma} \tilde{e}_{Rq} - \frac{g^2}{8} \tilde{e}_{L\alpha}^* \tilde{e}_{L\alpha} \tilde{e}_{L\beta}^* \tilde{e}_{L\beta} + \frac{g^2}{4} \tilde{e}_{L\alpha}^* \tilde{e}_{L\alpha} h_2^{*+} h_2^+ - \frac{g^2}{8} \tilde{e}_{L\alpha}^* \tilde{e}_{L\alpha} \tilde{e}_{L\beta}^* \tilde{e}_{L\beta}$$

$$\begin{aligned}
& + \frac{g_2^2}{4} h_2^{+\ast} h_2^+ \tilde{e}_{L\alpha}^* \tilde{e}_{L\alpha} - \frac{g^2}{2} \tilde{e}_{Ri}^* \tilde{e}_{Ri} \tilde{e}_{Rj}^* \tilde{e}_{Rj} - \frac{g^2}{2} \tilde{e}_{Ri}^* \tilde{e}_{Ri} h_2^{+\ast} h_2^+ - \frac{g^2}{8} h_2^{+\ast} h_2^+ h_2^{+\ast} h_2^+ \\
& - \frac{g_2^2}{8} h_2^{+\ast} h_2^+ h_2^{+\ast} h_2^+ + \frac{g^2}{2} \tilde{e}_{L\alpha}^* \tilde{e}_{L\alpha} \tilde{e}_{Rj}^* \tilde{e}_{Rj}
\end{aligned}$$

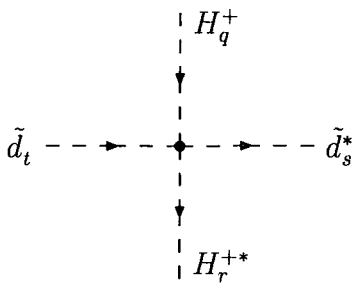
.....

$$\begin{aligned}
& i[\lambda_{\alpha\beta j} \lambda_{\alpha\gamma k}^* Z_{H(2+\beta)r}^* Z_{H(5+k)t}^* Z_{H(5+j)q} Z_{H(2+\gamma)s} \\
& - \frac{e^2}{8c_W^2 s_W^2} Z_{H(2+\alpha)r}^* Z_{H(2+\beta)t}^* Z_{H(2+\alpha)q} Z_{H(2+\beta)s} \\
& + \frac{e^2}{2c_W^2} Z_{H(2+\alpha)r}^* Z_{H(5+j)t}^* Z_{H(2+\alpha)q} Z_{H(5+j)s} \\
& + \frac{e^2}{4c_W^2 s_W^2} Z_{H(2+\alpha)r}^* Z_{H1t}^* Z_{H(2+\alpha)q} Z_{H1s} \\
& - \frac{e^2}{2c_W^2} Z_{H(5+i)r}^* Z_{H(5+j)t}^* Z_{H(5+i)q} Z_{H(5+j)s} \\
& - \frac{e^2}{2c_W^2} Z_{H(5+i)r}^* Z_{H1t}^* Z_{H(5+i)q} Z_{H1s} \\
& - \frac{e^2}{8c_W^2 s_W^2} Z_{H1r}^* Z_{H1t}^* Z_{H1q} Z_{H1s}]
\end{aligned}$$

C.54 Charged Scalar - Charged Scalar - Squark - Squark

$$\begin{aligned}
& -\lambda_{\alpha\beta j} \lambda_{\alpha p q}^* \tilde{e}_{L\beta} \tilde{e}_{Rj}^* \tilde{d}_{Lp}^{\ast z} \tilde{d}_{Rq}^{\ast z} - \lambda'_{\alpha i j} \lambda_{\alpha\gamma q}^* \tilde{d}_{Li}^y \tilde{d}_{Rj}^{\ast y} \tilde{e}_{L\gamma} \tilde{e}_{Rq} - \lambda'_{\alpha i j} \lambda_{\beta i q}^* \tilde{e}_{L\alpha} \tilde{d}_{Rj}^{\ast y} \tilde{e}_{L\beta} \tilde{d}_{Rq}^y - \lambda'_{\alpha i k} \lambda_{\beta p k}^* \tilde{e}_{L\alpha} \tilde{u}_{Li}^z \tilde{e}_{L\beta} \tilde{u}_{Lp}^{\ast z} \\
& + \frac{g^2}{12} \tilde{e}_{L\alpha}^* \tilde{e}_{L\alpha} \tilde{u}_{Lj}^{\ast y} \tilde{u}_{Lj}^y + \frac{g^2}{12} \tilde{e}_{L\alpha}^* \tilde{e}_{L\alpha} \tilde{d}_{Lj}^{\ast y} \tilde{d}_{Lj}^y - \frac{g^2}{3} \tilde{e}_{L\alpha}^* \tilde{e}_{L\alpha} \tilde{u}_{Rj}^{\ast y} \tilde{u}_{Rj}^y + \frac{g^2}{6} \tilde{e}_{L\alpha}^* \tilde{e}_{L\alpha} \tilde{d}_{Rj}^{\ast y} \tilde{d}_{Rj}^y \\
& - \frac{g_2^2}{4} \tilde{e}_{L\alpha}^* \tilde{d}_{Lj}^y \tilde{e}_{L\alpha} \tilde{d}_{Lj}^{\ast y} + \frac{g_2^2}{4} \tilde{e}_{L\alpha}^* \tilde{e}_{L\alpha} \tilde{u}_{Lj}^{\ast x} \tilde{u}_{Lj}^x - \frac{g^2}{6} \tilde{e}_{Ri}^* \tilde{e}_{Ri} \tilde{u}_{Lj}^{\ast y} \tilde{u}_{Lj}^y - \frac{g^2}{6} \tilde{e}_{Ri}^* \tilde{e}_{Ri} \tilde{d}_{Lj}^{\ast y} \tilde{d}_{Lj}^y
\end{aligned}$$

$$\begin{aligned}
& + \frac{2g^2}{3} \tilde{e}_{Ri}^* \tilde{e}_{Ri} \tilde{u}_{Rj}^* \tilde{u}_{Rj}^y - \frac{g^2}{3} \tilde{e}_{Ri}^* \tilde{e}_{Ri} \tilde{d}_{Rj}^* \tilde{d}_{Rj}^y - (Y_U)_{ik} (Y_U)_{pk}^* \tilde{d}_{Li}^x h_2^+ \tilde{d}_{Lp}^{*x} h_2^{+*} - \frac{g^2}{12} h_2^{+*} h_2^+ \tilde{d}_{Lj}^* \tilde{d}_{Lj}^y \\
& + \frac{g^2}{4} h_2^{+*} h_2^+ \tilde{d}_{Li}^* \tilde{d}_{Li}^x - \frac{g^2}{6} h_2^{+*} h_2^+ \tilde{d}_{Rj}^* \tilde{d}_{Rj}^y - (Y_U)_{ij} (Y_U)_{iq}^* h_2^+ \tilde{u}_{Rj}^* h_2^{+*} \tilde{u}_{Rq}^y - \frac{g^2}{12} h_2^{+*} h_2^+ \tilde{u}_{Lj}^* \tilde{u}_{Lj}^y \\
& \quad + \frac{g^2}{3} h_2^{+*} h_2^+ \tilde{u}_{Rj}^* \tilde{u}_{Rj}^y - \frac{g^2}{4} h_2^{+*} \tilde{u}_{Li}^x h_2^+ \tilde{u}_{Li}^{*x}
\end{aligned}$$



$$\begin{aligned}
& i[-\lambda_{\alpha\beta j} \lambda_{\alpha ki}^* Z_{\tilde{d}ks} Z_{\tilde{d}(3+i)t}^* Z_{H(2+\beta)r}^* Z_{H(5+j)q} \\
& - \lambda'_{\alpha ij} \lambda_{\alpha\gamma k}^* Z_{\tilde{d}(3+j)s} Z_{\tilde{d}it}^* Z_{H(5+k)r}^* Z_{H(2+\gamma)q} \\
& - \lambda'_{\alpha ij} \lambda_{\beta ik}^* Z_{\tilde{d}(3+j)s} Z_{\tilde{d}(3+k)t}^* Z_{H(2+\alpha)r}^* Z_{H(2+\beta)q} \\
& - (Y_U)_{ik} (Y_U)_{jk}^* Z_{\tilde{d}js} Z_{\tilde{d}it}^* Z_{H1r}^* Z_{H1q} \\
& + \frac{e^2(1-4c_W^2)}{12c_W^2 s_W^2} Z_{\tilde{d}js} Z_{\tilde{d}jt}^* Z_{H(2+\alpha)r}^* Z_{H(2+\alpha)q} \\
& + \frac{e^2}{6c_W^2} Z_{\tilde{d}(3+j)s} Z_{\tilde{d}(3+j)t}^* Z_{H(2+\alpha)r}^* Z_{H(2+\alpha)q} \\
& - \frac{e^2}{6c_W^2} Z_{\tilde{d}js} Z_{\tilde{d}jt}^* Z_{H(5+i)r}^* Z_{H(5+i)q} \\
& - \frac{e^2}{3c_W^2} Z_{\tilde{d}(3+j)s} Z_{\tilde{d}(3+j)t}^* Z_{H(5+i)r}^* Z_{H(5+i)q} \\
& + \frac{e^2(4c_W^2-1)}{12c_W^2 s_W^2} Z_{\tilde{d}js} Z_{\tilde{d}jt}^* Z_{H1r}^* Z_{H1q} \\
& - \frac{e^2}{6c_W^2} Z_{\tilde{d}(3+j)s} Z_{\tilde{d}(3+j)t}^* Z_{H1r}^* Z_{H1q}]
\end{aligned}$$

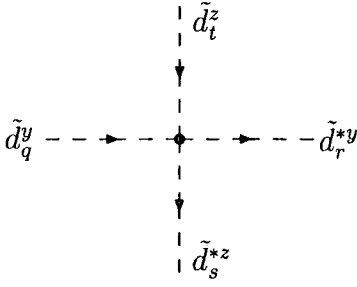
C.55 Charged Scalar - Squark - Squark - Squark

$$\begin{aligned}
& + \lambda'_{\alpha ik} \varepsilon_{vuz} \lambda''_{pqk} \tilde{e}_{L\alpha} \tilde{u}_{Li}^z \tilde{u}_{Rp}^v \tilde{d}_{Rq}^w + \varepsilon_{xyz} \lambda''_{ijk} \lambda'_{\alpha pk} \tilde{u}_{Ri}^{*x} \tilde{d}_{Rj}^{*y} \tilde{e}_{L\alpha} \tilde{u}_{Lp}^{*z} \\
& + (Y_U)_{ik} \frac{1}{2} \varepsilon_{xvw} \lambda''_{kpq} \tilde{d}_{Li}^x h_2^+ \tilde{d}_{Rp}^v \tilde{d}_{Rq}^w + \frac{1}{2} \varepsilon_{xyz} \lambda''_{kij} (Y_U)_{pk}^* \tilde{d}_{Ri}^{*y} \tilde{d}_{Rj}^{*z} \tilde{d}_{Lp}^{*x} h_2^{+*}
\end{aligned}$$

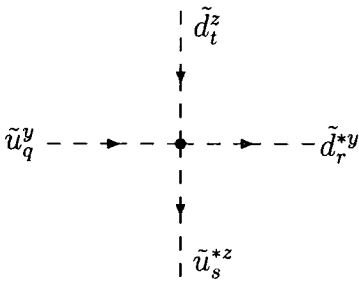
$$\begin{array}{c}
\tilde{d}_s^y \\
\downarrow \\
\tilde{d}_q^x \text{ --- } \bullet \text{ --- } \tilde{d}_t^z \\
\uparrow \\
H_r^+
\end{array}
\quad i\epsilon_{xyz} \frac{1}{2} (Y_U)_{ik} \lambda''_{kjm} Z_{\tilde{d}_{iq}}^* Z_{\tilde{d}_{(3+j)s}}^* Z_{\tilde{d}_{(3+m)t}}^* Z_{H1r}$$

C.56 Squark - Squark - Squark - Squark

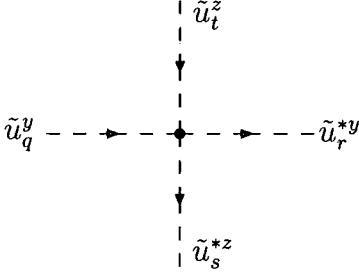
$$\begin{aligned}
& -\lambda'_{\alpha ij} \lambda''_{\alpha pq} \tilde{d}_{Li}^y \tilde{d}_{Rj}^{*y} \tilde{d}_{Lp}^{*z} \tilde{d}_{Rq}^z - (Y_U)_{ij} (Y_U)_{pq}^* \tilde{d}_{Li}^y \tilde{u}_{Rj}^{*y} \tilde{d}_{Lp}^{*z} \tilde{u}_{Rq}^z - \frac{g^2}{72} \tilde{d}_{Li}^{*x} \tilde{d}_{Li}^x \tilde{d}_{Lj}^{*y} \tilde{d}_{Lj}^y - \frac{g^2}{18} \tilde{d}_{Li}^{*x} \tilde{d}_{Li}^x \tilde{d}_{Rj}^{*y} \tilde{d}_{Rj}^y \\
& - \frac{g^2}{8} \tilde{d}_{Li}^{*y} \tilde{d}_{Li}^y \tilde{d}_{Lj}^{*z} \tilde{d}_{Lj}^z - \frac{g^2}{4} \tilde{d}_{Li}^{*x} \tilde{d}_{Li}^x \tilde{d}_{Lj}^{*v} \tilde{d}_{Lj}^v + \frac{g^2}{12} \tilde{d}_{Li}^{*y} \tilde{d}_{Li}^y \tilde{d}_{Lj}^{*v} \tilde{d}_{Lj}^v + \frac{g^2}{2} \tilde{d}_{Li}^{*x} \tilde{d}_{Li}^x \tilde{d}_{Rj}^{*v} \tilde{d}_{Rj}^v \\
& - \frac{g^2}{6} \tilde{d}_{Li}^{*x} \tilde{d}_{Li}^x \tilde{d}_{Rj}^{*v} \tilde{d}_{Rj}^v - \frac{1}{4} \lambda''_{kij} \lambda''_{kpq} \tilde{d}_{Ri}^{*y} \tilde{d}_{Rj}^{*z} \tilde{d}_{Rp}^y \tilde{d}_{Rq}^z + \frac{1}{4} \lambda''_{kij} \lambda''_{kpq} \tilde{d}_{Ri}^{*y} \tilde{d}_{Rj}^{*z} \tilde{d}_{Rp}^z \tilde{d}_{Rq}^y - \frac{g^2}{18} \tilde{d}_{Ri}^{*x} \tilde{d}_{Ri}^x \tilde{d}_{Rj}^{*y} \tilde{d}_{Rj}^y \\
& - \frac{g^2}{4} \tilde{d}_{Ri}^{*x} \tilde{d}_{Ri}^x \tilde{d}_{Rj}^{*v} \tilde{d}_{Rj}^v + \frac{g^2}{12} \tilde{d}_{Ri}^{*y} \tilde{d}_{Ri}^y \tilde{d}_{Rj}^{*v} \tilde{d}_{Rj}^v - (Y_U)_{ij} (Y_U)_{pq}^* \tilde{u}_{Li}^y \tilde{u}_{Rj}^{*y} \tilde{u}_{Lp}^{*z} \tilde{u}_{Rq}^z - \frac{g^2}{72} \tilde{u}_{Li}^{*x} \tilde{u}_{Li}^x \tilde{u}_{Lj}^{*y} \tilde{u}_{Lj}^y \\
& + \frac{g^2}{9} \tilde{u}_{Li}^{*x} \tilde{u}_{Li}^x \tilde{u}_{Rj}^{*y} \tilde{u}_{Rj}^y - \frac{g^2}{8} \tilde{u}_{Li}^{*y} \tilde{u}_{Li}^y \tilde{u}_{Lj}^{*z} \tilde{u}_{Lj}^z - \frac{g^2}{4} \tilde{u}_{Li}^{*x} \tilde{u}_{Li}^x \tilde{u}_{Lj}^{*v} \tilde{u}_{Lj}^v + \frac{g^2}{12} \tilde{u}_{Li}^{*y} \tilde{u}_{Li}^y \tilde{u}_{Lj}^{*v} \tilde{u}_{Lj}^v \\
& + \frac{g^2}{2} \tilde{u}_{Li}^{*x} \tilde{u}_{Li}^x \tilde{u}_{Rj}^{*v} \tilde{u}_{Rj}^v - \frac{g^2}{6} \tilde{u}_{Li}^{*x} \tilde{u}_{Li}^x \tilde{u}_{Rj}^{*v} \tilde{u}_{Rj}^v - \frac{2g^2}{9} \tilde{u}_{Ri}^{*x} \tilde{u}_{Ri}^x \tilde{u}_{Rj}^{*y} \tilde{u}_{Rj}^y - \frac{g^2}{4} \tilde{u}_{Ri}^{*x} \tilde{u}_{Ri}^x \tilde{u}_{Rj}^{*v} \tilde{u}_{Rj}^v \\
& + \frac{g^2}{12} \tilde{u}_{Ri}^{*y} \tilde{u}_{Ri}^y \tilde{u}_{Rj}^{*v} \tilde{u}_{Rj}^v - \frac{g^2}{36} \tilde{u}_{Li}^{*x} \tilde{u}_{Li}^x \tilde{d}_{Lj}^{*y} \tilde{d}_{Lj}^y + \frac{g^2}{9} \tilde{d}_{Li}^{*x} \tilde{d}_{Li}^x \tilde{u}_{Rj}^{*y} \tilde{u}_{Rj}^y - \frac{g^2}{2} \tilde{u}_{Li}^{*y} \tilde{d}_{Li}^y \tilde{d}_{Lj}^{*z} \tilde{u}_{Lj}^z \\
& + \frac{g^2}{4} \tilde{u}_{Li}^{*y} \tilde{d}_{Li}^y \tilde{d}_{Lj}^{*z} \tilde{u}_{Lj}^z + \frac{g^2}{2} \tilde{d}_{Li}^{*x} \tilde{d}_{Li}^x \tilde{u}_{Rj}^{*v} \tilde{u}_{Rj}^v - \frac{g^2}{6} \tilde{d}_{Li}^{*x} \tilde{d}_{Li}^x \tilde{u}_{Rj}^{*v} \tilde{u}_{Rj}^v - \frac{g^2}{2} \tilde{u}_{Li}^{*x} \tilde{u}_{Li}^x \tilde{d}_{Lj}^{*y} \tilde{d}_{Lj}^y \\
& + \frac{g^2}{6} \tilde{u}_{Li}^{*x} \tilde{u}_{Li}^x \tilde{d}_{Lj}^{*z} \tilde{d}_{Lj}^z - \lambda'_{\alpha ij} \lambda''_{\alpha pq} \tilde{u}_{Li}^y \tilde{d}_{Rj}^{*y} \tilde{u}_{Lp}^{*z} \tilde{d}_{Rq}^z - \lambda''_{ijk} \lambda''_{pqk} \tilde{u}_{Ri}^{*x} \tilde{d}_{Rj}^{*y} \tilde{u}_{Rp}^x \tilde{d}_{Rq}^y + \lambda''_{ijk} \lambda''_{pqk} \tilde{u}_{Ri}^{*x} \tilde{d}_{Rj}^{*y} \tilde{u}_{Rp}^y \tilde{d}_{Rq}^x \\
& - \frac{g^2}{18} \tilde{u}_{Li}^{*x} \tilde{u}_{Li}^x \tilde{d}_{Rj}^{*y} \tilde{d}_{Rj}^y + \frac{2g^2}{9} \tilde{u}_{Ri}^{*x} \tilde{u}_{Ri}^x \tilde{d}_{Rj}^{*y} \tilde{d}_{Rj}^y + \frac{g^2}{2} \tilde{u}_{Li}^{*x} \tilde{u}_{Li}^x \tilde{d}_{Rj}^{*v} \tilde{d}_{Rj}^v - \frac{g^2}{6} \tilde{u}_{Li}^{*x} \tilde{u}_{Li}^x \tilde{d}_{Rj}^{*v} \tilde{d}_{Rj}^v \\
& + \frac{g^2}{6} \tilde{u}_{Ri}^{*x} \tilde{u}_{Ri}^x \tilde{d}_{Rj}^{*v} \tilde{d}_{Rj}^v - \frac{g^2}{2} \tilde{d}_{Ri}^{*x} \tilde{d}_{Ri}^x \tilde{u}_{Rj}^{*v} \tilde{u}_{Rj}^v
\end{aligned}$$



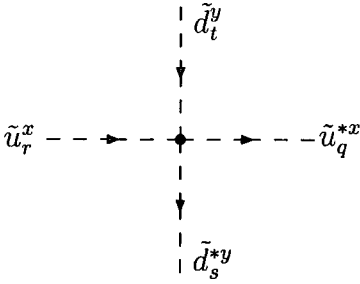
$$\begin{aligned}
& i[-\lambda'_{\alpha ij} \lambda'^{*}_{\alpha km} Z_{\bar{d}(3+j)r} Z_{\bar{d}i q}^* Z_{\bar{d}ks} Z_{\bar{d}(3+m)t}^* \\
& - \frac{1}{4} \lambda''_{kij} \lambda''^{*}_{klm} Z_{\bar{d}(3+i)r} Z_{\bar{d}(3+l)q}^* Z_{\bar{d}(3+j)s} Z_{\bar{d}(3+m)t}^* \\
& + \frac{1}{4} \lambda''_{kij} \lambda''^{*}_{klm} Z_{\bar{d}(3+i)r} Z_{\bar{d}(3+m)q}^* Z_{\bar{d}(3+j)s} Z_{\bar{d}(3+l)t}^* \\
& - \frac{e^2(1+8c_W^2)}{72c_W^2 s_W^2} Z_{\bar{d}ir} Z_{\bar{d}i q}^* Z_{\bar{d}js} Z_{\bar{d}jt}^* \\
& - \frac{e^2}{18c_W^2} Z_{\bar{d}ir} Z_{\bar{d}i q}^* Z_{\bar{d}(3+j)s} Z_{\bar{d}(3+j)t}^* \\
& - \frac{e^2}{18c_W^2} Z_{\bar{d}(3+i)r} Z_{\bar{d}(3+i)q}^* Z_{\bar{d}(3+j)s} Z_{\bar{d}(3+j)t}^* \\
& - \frac{g_3^2}{4} (Z_{\bar{d}ir} Z_{\bar{d}it}^* - Z_{\bar{d}(3+i)r} Z_{\bar{d}(3+i)t}^*) (Z_{\bar{d}is} Z_{\bar{d}i q}^* - Z_{\bar{d}(3+i)s} Z_{\bar{d}(3+i)q}^*) \\
& + \frac{g_3^2}{12} (Z_{\bar{d}ir} Z_{\bar{d}i q}^* - Z_{\bar{d}(3+i)r} Z_{\bar{d}(3+i)q}^*) (Z_{\bar{d}is} Z_{\bar{d}it}^* - Z_{\bar{d}(3+i)s} Z_{\bar{d}(3+i)t}^*)
\end{aligned}$$



$$\begin{aligned}
& i[-\lambda'_{\alpha ij} \lambda'^{*}_{\alpha km} Z_{\bar{d}(3+j)r} Z_{\bar{u}i q} Z_{\bar{u}ks} Z_{\bar{d}(3+m)t}^* \\
& - (Y_U)_{ij} (Y_U)_{km}^* Z_{\bar{d}kr} Z_{\bar{u}(3+m)q} Z_{\bar{u}(3+j)s} Z_{\bar{d}it}^* \\
& + \lambda''_{ijk} \lambda''^{*}_{lmk} Z_{\bar{d}(3+j)r} Z_{\bar{u}(3+l)q} Z_{\bar{u}(3+i)s} Z_{\bar{d}(3+m)t}^* \\
& - \frac{e^2}{2s_W^2} Z_{\bar{d}jr} Z_{\bar{u}jq} Z_{\bar{u}is} Z_{\bar{d}it}^* \\
& - \frac{g_3^2}{2} (Z_{\bar{d}ir} Z_{\bar{d}it}^* - Z_{\bar{d}(3+i)r} Z_{\bar{d}(3+i)t}^*) (Z_{\bar{u}is} Z_{\bar{u}i q} - Z_{\bar{u}(3+i)s} Z_{\bar{u}(3+i)q})
\end{aligned}$$



$$\begin{aligned}
& i[-(Y_U)_{ij}(Y_U)_{km}^* Z_{\tilde{u}(3+j)r}^* Z_{\tilde{u}iq} Z_{\tilde{u}ks}^* Z_{\tilde{u}(3+m)t} \\
& - \frac{e^2(1+8c_W^2)}{72c_W^2 s_W^2} Z_{\tilde{u}ir}^* Z_{\tilde{u}iq} Z_{\tilde{u}js}^* Z_{\tilde{u}jt} \\
& + \frac{e^2}{9c_W^2} Z_{\tilde{u}ir}^* Z_{\tilde{u}iq} Z_{\tilde{u}(3+j)s}^* Z_{\tilde{u}(3+j)t} \\
& - \frac{2e^2}{9c_W^2} Z_{\tilde{u}(3+i)r}^* Z_{\tilde{u}(3+i)q} Z_{\tilde{u}(3+j)s}^* Z_{\tilde{u}(3+j)t} \\
& - \frac{g_3^2}{4} (Z_{\tilde{u}ir}^* Z_{\tilde{u}it} - Z_{\tilde{u}(3+i)r}^* Z_{\tilde{u}(3+i)t}) (Z_{\tilde{u}is}^* Z_{\tilde{u}iq} - Z_{\tilde{u}(3+i)s}^* Z_{\tilde{u}(3+i)q}) \\
& + \frac{g_3^2}{12} (Z_{\tilde{u}ir}^* Z_{\tilde{u}iq} - Z_{\tilde{u}(3+i)r}^* Z_{\tilde{u}(3+i)q}) (Z_{\tilde{u}is}^* Z_{\tilde{u}it} - Z_{\tilde{u}(3+i)s}^* Z_{\tilde{u}(3+i)t})]
\end{aligned}$$



$$\begin{aligned}
& i[-\lambda''_{ijk} \lambda''_{mlk}^* Z_{\tilde{u}(3+i)q}^* Z_{\tilde{u}(3+m)r} Z_{\tilde{d}(3+j)s} Z_{\tilde{d}(3+l)t}^* \\
& + \frac{e^2(10c_W^2-1)}{36c_W^2 s_W^2} Z_{\tilde{u}iq}^* Z_{\tilde{u}ir} Z_{\tilde{d}js} Z_{\tilde{d}jt}^* \\
& - \frac{e^2}{18c_W^2} Z_{\tilde{u}iq}^* Z_{\tilde{u}ir} Z_{\tilde{d}(3+j)s} Z_{\tilde{d}(3+j)t}^* \\
& + \frac{e^2}{9c_W^2} Z_{\tilde{u}(3+j)q}^* Z_{\tilde{u}(3+j)r} Z_{\tilde{d}is} Z_{\tilde{d}it}^* \\
& + \frac{2e^2}{9c_W^2} Z_{\tilde{u}(3+i)q}^* Z_{\tilde{u}(3+i)r} Z_{\tilde{d}(3+j)s} Z_{\tilde{d}(3+j)t}^* \\
& + \frac{g_3^2}{6} (Z_{\tilde{u}iq}^* Z_{\tilde{u}ir} - Z_{\tilde{u}(3+i)q}^* Z_{\tilde{u}(3+i)r}) (Z_{\tilde{d}is} Z_{\tilde{d}it}^* - Z_{\tilde{d}(3+i)s} Z_{\tilde{d}(3+i)t}^*)]
\end{aligned}$$

C.57 Neutral Scalar - Neutral Scalar - Neutral Scalar

$$\begin{aligned}
& + \frac{1}{\sqrt{2}} \frac{g^2}{4} v_0 \tilde{\nu}_{L0} h_2^{0*} h_2^0 + \frac{1}{\sqrt{2}} \frac{g^2}{4} \tilde{\nu}_{L0}^* v_0 h_2^{0*} h_2^0 + \frac{1}{\sqrt{2}} \frac{g^2}{4} \tilde{\nu}_{L\alpha}^* \tilde{\nu}_{L\alpha} v_u h_2^0 + \frac{1}{\sqrt{2}} \frac{g^2}{4} \tilde{\nu}_{L\alpha}^* \tilde{\nu}_{L\alpha} h_2^{0*} v_u \\
& + \frac{1}{\sqrt{2}} \frac{g_2^2}{4} h_2^{0*} h_2^0 \tilde{\nu}_{L0}^* v_0 - \frac{1}{\sqrt{2}} \frac{g^2}{8} h_2^{0*} h_2^0 h_2^{0*} v_u - \frac{1}{\sqrt{2}} \frac{g^2}{8} h_2^{0*} h_2^0 v_u h_2^0 - \frac{1}{\sqrt{2}} \frac{g^2}{8} h_2^{0*} v_u h_2^{0*} h_2^0 \\
& - \frac{1}{\sqrt{2}} \frac{g^2}{8} v_u h_2^0 h_2^{0*} h_2^0 - \frac{1}{\sqrt{2}} \frac{g_2^2}{8} h_2^{0*} h_2^0 h_2^{0*} v_u - \frac{1}{\sqrt{2}} \frac{g_2^2}{8} h_2^{0*} h_2^0 v_u h_2^0 - \frac{1}{\sqrt{2}} \frac{g_2^2}{8} h_2^{0*} v_u h_2^{0*} h_2^0 \\
& - \frac{1}{\sqrt{2}} \frac{g_2^2}{8} v_u h_2^0 h_2^{0*} h_2^0 - \frac{1}{\sqrt{2}} \frac{g^2}{8} \tilde{\nu}_{L\alpha}^* \tilde{\nu}_{L\alpha} \tilde{\nu}_{L0}^* v_0 - \frac{1}{\sqrt{2}} \frac{g^2}{8} \tilde{\nu}_{L\alpha}^* \tilde{\nu}_{L\alpha} v_0 \tilde{\nu}_{L0} - \frac{1}{\sqrt{2}} \frac{g^2}{8} \tilde{\nu}_{L0}^* v_0 \tilde{\nu}_{L\beta}^* \tilde{\nu}_{L\beta} \\
& - \frac{1}{\sqrt{2}} \frac{g^2}{8} v_0 \tilde{\nu}_{L0} \tilde{\nu}_{L\beta}^* \tilde{\nu}_{L\beta} - \frac{1}{\sqrt{2}} \frac{g_2^2}{8} \tilde{\nu}_{L\alpha}^* \tilde{\nu}_{L\alpha} \tilde{\nu}_{L0}^* v_0 - \frac{1}{\sqrt{2}} \frac{g_2^2}{8} \tilde{\nu}_{L\alpha}^* \tilde{\nu}_{L\alpha} v_0 \tilde{\nu}_{L0} - \frac{1}{\sqrt{2}} \frac{g_2^2}{8} \tilde{\nu}_{L0}^* v_0 \tilde{\nu}_{L\beta}^* \tilde{\nu}_{L\beta} \\
& - \frac{1}{\sqrt{2}} \frac{g_2^2}{8} v_0 \tilde{\nu}_{L0} \tilde{\nu}_{L\beta}^* \tilde{\nu}_{L\beta} + \frac{1}{\sqrt{2}} \frac{g_2^2}{4} v_u h_2^0 \tilde{\nu}_{L\alpha}^* \tilde{\nu}_{L\alpha} + \frac{1}{\sqrt{2}} \frac{g_2^2}{4} v_u h_2^{0*} \tilde{\nu}_{L\alpha}^* \tilde{\nu}_{L\alpha} + \frac{1}{\sqrt{2}} \frac{g_2^2}{4} h_2^{0*} h_2^0 v_0 \tilde{\nu}_{L0}
\end{aligned}$$

.....

$$\begin{array}{ccc}
& & \begin{array}{c} -ie^2 \\ 8c_W^2 s_W^2 (\delta_{rs} - 2Z_{R1r} Z_{R1s}) (v_d Z_{R2q} - v_u Z_{R1q}) \end{array} \\
\begin{array}{c} H_r^0 \\ | \\ H_q^0 \text{---} \bullet \text{---} H_s^0 \\ | \\ A_r^0 \end{array} & & \begin{array}{c} -ie^2 \\ 8c_W^2 s_W^2 (\delta_{rs} - 2Z_{A1r} Z_{A1s}) (v_d Z_{R2q} - v_u Z_{R1q}) \end{array} \\
\begin{array}{c} H_q^0 \text{---} \bullet \text{---} A_s^0 \end{array} & &
\end{array}$$

C.58 Neutral Scalar - Charged Scalar - Charged Scalar

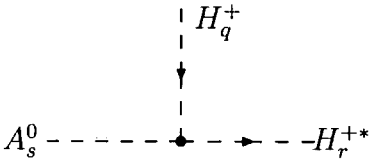
$$\begin{aligned}
& - \frac{1}{\sqrt{2}} \frac{g_2^2}{4} h_2^{+*} \tilde{\nu}_{L\alpha} v_u \tilde{e}_{L\alpha}^* - \frac{1}{\sqrt{2}} \frac{g_2^2}{4} v_u \tilde{\nu}_{L\alpha}^* v_u \tilde{e}_{L\alpha} - \frac{1}{\sqrt{2}} \frac{g_2^2}{4} v_u \tilde{e}_{L\alpha} h_2^0 \tilde{e}_{L\alpha}^* - \frac{1}{\sqrt{2}} \frac{g_2^2}{4} v_u \tilde{e}_{L\alpha}^* h_2^{0*} \tilde{e}_{L\alpha} \\
& - \frac{1}{\sqrt{2}} \frac{g_2^2}{2} h_2^{+*} v_0 h_2^0 \tilde{e}_{L0}^* - \frac{1}{\sqrt{2}} \frac{g^2}{4} h_2^{+*} h_2^+ h_2^{0*} v_u - \frac{1}{\sqrt{2}} \frac{g_2^2}{2} h_2^{0*} \tilde{e}_{L0} h_2^+ v_0 + \frac{1}{\sqrt{2}} \frac{g^2}{4} \tilde{e}_{L\alpha}^* \tilde{e}_{L\alpha} h_2^{0*} v_u
\end{aligned}$$

$$\begin{aligned}
& -\frac{1}{\sqrt{2}} \frac{g^2}{2} \tilde{e}_{Ri}^* \tilde{e}_{Ri} h_2^{0*} v_u + \mu_\alpha \lambda_{\alpha\gamma q}^* h_2^0 \tilde{e}_{L\gamma}^* \tilde{e}_{Rq} - \frac{1}{\sqrt{2}} \frac{g^2}{4} h_2^{++*} h_2^+ v_u h_2^0 \\
& + \lambda_{\alpha\beta j} \mu_\alpha^* \tilde{e}_{L\beta} \tilde{e}_{Rj}^* h_2^{0*} + \frac{1}{\sqrt{2}} \frac{g^2}{4} \tilde{e}_{L\alpha}^* \tilde{e}_{L\alpha} v_u h_2^0 - \frac{1}{\sqrt{2}} \frac{g^2}{2} \tilde{e}_{Ri}^* \tilde{e}_{Ri} v_u h_2^0 \\
& + \frac{1}{\sqrt{2}} \frac{g^2}{4} v_0 \tilde{\nu}_{L0} h_2^{++*} h_2^+ + \frac{1}{\sqrt{2}} \frac{g^2}{4} \tilde{\nu}_{L0}^* v_0 h_2^{++*} h_2^+ - \frac{1}{\sqrt{2}} \frac{g_2^2}{4} h_2^{++*} v_0 h_2^+ \tilde{\nu}_{L0}^* - \frac{1}{\sqrt{2}} \frac{g_2^2}{4} h_2^{++*} \tilde{\nu}_{L0} h_2^+ v_0 \\
& - \frac{1}{\sqrt{2}} \lambda_{\alpha 0j} \lambda_{\alpha\gamma q}^* v_0 \tilde{e}_{Rj}^* \tilde{\nu}_{L\gamma}^* \tilde{e}_{Rq} - \frac{1}{\sqrt{2}} \lambda_{\alpha\beta j} \lambda_{\alpha 0q}^* \tilde{\nu}_{L\beta} \tilde{e}_{Rj}^* v_0 \tilde{e}_{Rq} + \frac{1}{\sqrt{2}} \frac{g^2}{2} v_0 \tilde{\nu}_{L0} \tilde{e}_{Rj}^* \tilde{e}_{Rj} + \frac{1}{\sqrt{2}} \frac{g^2}{2} \tilde{\nu}_{L0}^* v_0 \tilde{e}_{Rj}^* \tilde{e}_{Rj} \\
& - \frac{1}{\sqrt{2}} \lambda_{0\beta k} \lambda_{\delta\gamma k}^* v_0 \tilde{e}_{L\beta} \tilde{\nu}_{L\delta}^* \tilde{e}_{L\gamma}^* - \frac{1}{\sqrt{2}} \lambda_{\alpha\beta k} \lambda_{0\gamma k}^* \tilde{\nu}_{L\alpha} \tilde{e}_{L\beta} v_0 \tilde{e}_{L\gamma}^* - \frac{1}{\sqrt{2}} \frac{g^2}{4} \tilde{e}_{L\alpha}^* \tilde{e}_{L\alpha} v_0 \tilde{\nu}_{L0} - \frac{1}{\sqrt{2}} \frac{g^2}{4} \tilde{e}_{L\alpha}^* \tilde{e}_{L\alpha} \tilde{\nu}_{L0}^* v_0 \\
& - \frac{1}{\sqrt{2}} \frac{g_2^2}{2} \tilde{e}_{L0}^* v_0 \tilde{\nu}_{L\beta}^* \tilde{e}_{L\beta} - \frac{1}{\sqrt{2}} \frac{g_2^2}{2} \tilde{e}_{L\alpha}^* \tilde{\nu}_{L\alpha} v_0 \tilde{e}_{L0} + \frac{1}{\sqrt{2}} \frac{g_2^2}{4} \tilde{e}_{L\alpha}^* \tilde{e}_{L\alpha} v_0 \tilde{\nu}_{L0} + \frac{1}{\sqrt{2}} \frac{g_2^2}{4} \tilde{e}_{L\alpha}^* \tilde{e}_{L\alpha} \tilde{\nu}_{L0}^* v_0 \\
& + \lambda_{\alpha\beta j} \mu_\alpha^* \tilde{\nu}_{L\beta} \tilde{e}_{Rj}^* h_2^{++*} + \mu_\alpha \lambda_{\alpha\gamma q}^* h_2^+ \tilde{\nu}_{L\gamma}^* \tilde{e}_{Rq} - h_{\alpha\beta k} \tilde{\nu}_{L\alpha} \tilde{e}_{L\beta} \tilde{e}_{Rk}^* - h_{\alpha\beta k}^* \tilde{\nu}_{L\alpha}^* \tilde{e}_{L\beta} \tilde{e}_{Rk} \\
& - \frac{1}{\sqrt{2}} \frac{g_2^2}{4} v_u h_2^0 h_2^{++*} h_2^+ - \frac{1}{\sqrt{2}} \frac{g_2^2}{4} v_u h_2^{0*} h_2^{++*} h_2^+
\end{aligned}$$

$$\begin{array}{ccc}
& & H_q^+ \\
& & \vdots \\
& & \downarrow \\
H_s^0 & \cdots \cdots \cdots & \bullet & \cdots \cdots \cdots & H_r^{++*}
\end{array}$$

$$\begin{aligned}
& i \left[\frac{\lambda_{\alpha\beta j} \mu_\alpha^*}{\sqrt{2}} Z_{H1r}^* Z_{H(5+j)q} Z_{R(2+\beta)s} \right. \\
& + \frac{\lambda_{\alpha\beta j} \mu_\alpha^*}{\sqrt{2}} Z_{H(2+\beta)r}^* Z_{H(5+j)q} Z_{R1s} \\
& + \frac{\lambda_{\alpha\gamma k}^* \mu_\alpha}{\sqrt{2}} Z_{H(5+k)r}^* Z_{H(2+\gamma)q} Z_{R1s} \\
& + \frac{\lambda_{\alpha\gamma i}^* \mu_\alpha}{\sqrt{2}} Z_{H(5+i)r}^* Z_{H1q} Z_{R(2+\gamma)s} \\
& - \frac{h_{\alpha\beta k}}{\sqrt{2}} Z_{H(2+\beta)r}^* Z_{H(5+k)q} Z_{R(2+\alpha)s} \\
& - \frac{h_{\alpha\beta k}^*}{\sqrt{2}} Z_{H(5+k)r}^* Z_{H(2+\beta)q} Z_{R(2+\alpha)s} \\
& - \frac{\lambda_{\alpha 0j} \lambda_{\alpha\gamma i}^* v_d}{2} Z_{H(5+i)r}^* Z_{H(5+j)q} Z_{R(2+\gamma)s} \\
& - \frac{\lambda_{\alpha\beta j} \lambda_{\alpha 0i}^* v_d}{2} Z_{H(5+i)r}^* Z_{H(5+j)q} Z_{R(2+\beta)s} \\
& - \frac{\lambda_{0\beta k} \lambda_{\delta\gamma k}^* v_d}{2} Z_{H(2+\beta)r}^* Z_{H(2+\gamma)q} Z_{R(2+\delta)s} \\
& \left. - \frac{\lambda_{\alpha\beta k} \lambda_{0\gamma k}^* v_d}{2} Z_{H(2+\beta)r}^* Z_{H(2+\gamma)q} Z_{R(2+\alpha)s} \right]
\end{aligned}$$

$$\begin{aligned}
& -\frac{e^2 v_d (1 - 2c_W^2)}{4c_W^2 s_W^2} Z_{H(2+\alpha)r}^* Z_{H(2+\alpha)q} Z_{R2s} \\
& + \frac{e^2 v_u (1 - 2c_W^2)}{4c_W^2 s_W^2} Z_{H(2+\alpha)r}^* Z_{H(2+\alpha)q} Z_{R1s} \\
& + \frac{e^2 v_d}{2c_W^2} Z_{H(5+j)r}^* Z_{H(5+j)q} Z_{R2s} \\
& + \frac{e^2 v_d (1 - 2c_W^2)}{4c_W^2 s_W^2} Z_{H1r}^* Z_{H1q} Z_{R2s} \\
& - \frac{e^2 v_u}{2c_W^2} Z_{H(5+i)r}^* Z_{H(5+i)q} Z_{R1s} \\
& - \frac{e^2 v_u}{4c_W^2 s_W^2} Z_{H1r}^* Z_{H1q} Z_{R1s} \\
& - \frac{e^2 v_d}{4s_W^2} Z_{H(2+\beta)r}^* Z_{H2q} Z_{R(2+\beta)s} \\
& - \frac{e^2 v_d}{4s_W^2} Z_{H2r}^* Z_{H(2+\alpha)q} Z_{R(2+\alpha)s} \\
& - \frac{e^2 v_d}{4s_W^2} Z_{H1r}^* Z_{H2q} Z_{R1s} \\
& - \frac{e^2 v_u}{4s_W^2} Z_{H1r}^* Z_{H(2+\alpha)q} Z_{R(2+\alpha)s} \\
& - \frac{e^2 v_d}{4s_W^2} Z_{H2r}^* Z_{H1q} Z_{R1s} \\
& - \frac{e^2 v_u}{4s_W^2} Z_{H(2+\alpha)r}^* Z_{H1q} Z_{R(2+\alpha)s}]
\end{aligned}$$



$$\begin{aligned}
& - \left[\frac{\lambda_{\alpha\beta j} \mu_\alpha^*}{\sqrt{2}} Z_{H1r}^* Z_{H(5+j)q} Z_{A(2+\beta)s} \right. \\
& - \frac{\lambda_{\alpha\beta j} \mu_\alpha^*}{\sqrt{2}} Z_{H(2+\beta)r}^* Z_{H(5+j)q} Z_{A1s} \\
& + \frac{\lambda_{\alpha\gamma k} \mu_\alpha^*}{\sqrt{2}} Z_{H(5+k)r}^* Z_{H(2+\gamma)q} Z_{A1s} \\
& - \frac{\lambda_{\alpha\gamma i} \mu_\alpha^*}{\sqrt{2}} Z_{H(5+i)r}^* Z_{H1q} Z_{A(2+\gamma)s} \\
& \left. - \frac{h_{\alpha\beta k}}{\sqrt{2}} Z_{H(2+\beta)r}^* Z_{H(5+k)q} Z_{A(2+\alpha)s} \right]
\end{aligned}$$

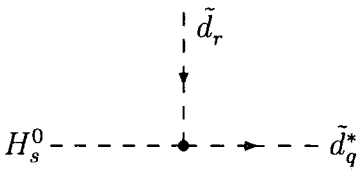
$$\begin{aligned}
& + \frac{h_{\alpha\beta k}^*}{\sqrt{2}} Z_{H(5+k)r}^* Z_{H(2+\beta)q} Z_{A(2+\alpha)s} \\
& + \frac{\lambda_{\alpha 0j} \lambda_{\alpha\gamma i}^* v_d}{2} Z_{H(5+i)r}^* Z_{H(5+j)q} Z_{A(2+\gamma)s} \\
& - \frac{\lambda_{\alpha\beta j} \lambda_{\alpha 0i}^* v_d}{2} Z_{H(5+i)r}^* Z_{H(5+j)q} Z_{A(2+\beta)s} \\
& + \frac{\lambda_{0\beta k} \lambda_{\delta\gamma k}^* v_d}{2} Z_{H(2+\beta)r}^* Z_{H(2+\gamma)q} Z_{A(2+\delta)s} \\
& - \frac{\lambda_{\alpha\beta k} \lambda_{0\gamma k}^* v_d}{2} Z_{H(2+\beta)r}^* Z_{H(2+\gamma)q} Z_{A(2+\alpha)s} \\
& + \frac{e^2 v_d}{4s_W^2} Z_{H(2+\beta)r}^* Z_{H2q} Z_{A(2+\beta)s} \\
& - \frac{e^2 v_d}{4s_W^2} Z_{H2r}^* Z_{H(2+\alpha)q} Z_{A(2+\alpha)s} \\
& - \frac{e^2 v_d}{4s_W^2} Z_{H1r}^* Z_{H2q} Z_{A1s} \\
& - \frac{e^2 v_u}{4s_W^2} Z_{H1r}^* Z_{H(2+\alpha)q} Z_{A(2+\alpha)s} \\
& + \frac{e^2 v_d}{4s_W^2} Z_{H2r}^* Z_{H1q} Z_{A1s} \\
& + \frac{e^2 v_u}{4s_W^2} Z_{H(2+\alpha)r}^* Z_{H1q} Z_{A(2+\alpha)s}]
\end{aligned}$$

C.59 Neutral Scalar - Squark - Squark

$$\begin{aligned}
& - \frac{1}{\sqrt{2}} \frac{g_2^2}{4} v_u \tilde{d}_{Li}^x h_2^0 \tilde{d}_{Li}^{*x} - \frac{1}{\sqrt{2}} \frac{g_2^2}{4} h_2^{0*} \tilde{d}_{Li}^x v_u \tilde{d}_{Li}^{*x} + \frac{1}{\sqrt{2}} \frac{g_2^2}{4} v_u h_2^0 \tilde{u}_{Li}^{*x} \tilde{u}_{Li}^x + \frac{1}{\sqrt{2}} \frac{g_2^2}{4} h_2^{0*} v_u \tilde{u}_{Li}^{*x} \tilde{u}_{Li}^x \\
& - \frac{1}{\sqrt{2}} \frac{g^2}{3} v_0 \tilde{\nu}_{L0} \tilde{u}_{Rj}^{*y} \tilde{u}_{Rj}^y - \frac{1}{\sqrt{2}} \frac{g^2}{3} \tilde{\nu}_{L0}^* v_0 \tilde{u}_{Rj}^{*y} \tilde{u}_{Rj}^y - \frac{1}{\sqrt{2}} \lambda'_{0ij} \lambda'_{\beta iq} \lambda_{\beta iq}^* v_0 \tilde{d}_{Rj}^{*y} \tilde{\nu}_{L\beta}^* \tilde{d}_{Rq}^y - \frac{1}{\sqrt{2}} \lambda'_{\alpha ij} \lambda'_{0iq} \lambda_{0iq}^* \tilde{\nu}_{L\alpha} \tilde{d}_{Rj}^{*y} v_0 \tilde{d}_{Rq}^y \\
& + \frac{1}{\sqrt{2}} \frac{g^2}{6} v_0 \tilde{\nu}_{L0} \tilde{d}_{Rj}^{*y} \tilde{d}_{Rj}^y + \frac{1}{\sqrt{2}} \frac{g^2}{6} \tilde{\nu}_{L0}^* v_0 \tilde{d}_{Rj}^{*y} \tilde{d}_{Rj}^y - \frac{1}{\sqrt{2}} \lambda'_{0ik} \lambda'_{\beta pk} \lambda_{\beta pk}^* v_0 \tilde{d}_{Li}^z \tilde{\nu}_{L\beta}^* \tilde{d}_{Lp}^{*z} - \frac{1}{\sqrt{2}} \lambda'_{\alpha ik} \lambda'_{0pk} \lambda_{0pk}^* \tilde{\nu}_{L\alpha} \tilde{d}_{Li}^z v_0 \tilde{d}_{Lp}^{*z}
\end{aligned}$$

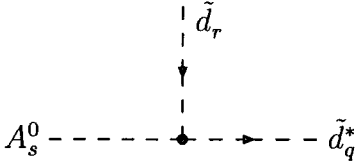
$$\begin{aligned}
& + \frac{1}{\sqrt{2}} \frac{g^2}{12} v_0 \tilde{\nu}_{L0} \tilde{d}_{Lj}^{*y} \tilde{d}_{Lj}^y + \frac{1}{\sqrt{2}} \frac{g^2}{12} \tilde{\nu}_{L0}^* v_0 \tilde{d}_{Lj}^{*y} \tilde{d}_{Lj}^y + \frac{1}{\sqrt{2}} \frac{g_2^2}{4} v_0 \tilde{\nu}_{L0} \tilde{d}_{Lj}^{*x} \tilde{d}_{Lj}^x + \frac{1}{\sqrt{2}} \frac{g_2^2}{4} \tilde{\nu}_{L0}^* v_0 \tilde{d}_{Lj}^{*x} \tilde{d}_{Lj}^x \\
& - (h_u)_{ij} \tilde{u}_{Li}^y h_2^0 \tilde{u}_{Rj}^{*y} - (h_u^*)_{ij} \tilde{u}_{Li}^{*y} h_2^0 \tilde{u}_{Rj}^y + (Y_U)_{ij} \mu_\beta^* \tilde{u}_{Li}^y \tilde{u}_{Rj}^{*y} \tilde{\nu}_{L\beta}^* + \mu_\alpha (Y_U)_{pq}^* \tilde{\nu}_{L\alpha} \tilde{u}_{Lp}^{*z} \tilde{u}_{Rq}^z \\
& \quad + \lambda'_{\alpha ij} \mu_\alpha^* \tilde{d}_{Li}^y \tilde{d}_{Rj}^{*y} h_2^{0*} + \mu_\alpha \lambda'_{\alpha pq} h_2^0 \tilde{d}_{Lp}^{*z} \tilde{d}_{Rq}^z - h'_{\alpha jk} \tilde{\nu}_{L\alpha} \tilde{d}_{Lj} \tilde{d}_{Rk}^* \\
& - h'_{\alpha jk} \tilde{\nu}_{L\alpha}^* \tilde{d}_{Lj} \tilde{d}_{Rk} - \frac{1}{\sqrt{2}} \frac{g^2}{12} v_u h_2^0 \tilde{d}_{Lj}^{*y} \tilde{d}_{Lj}^y - \frac{1}{\sqrt{2}} \frac{g^2}{12} h_2^{0*} v_u \tilde{d}_{Lj}^{*y} \tilde{d}_{Lj}^y - \frac{1}{\sqrt{2}} \frac{g^2}{6} v_u h_2^0 \tilde{d}_{Rj}^{*y} \tilde{d}_{Rj}^y \\
& \quad - \frac{1}{\sqrt{2}} \frac{g^2}{6} h_2^{0*} v_u \tilde{d}_{Rj}^{*y} \tilde{d}_{Rj}^y - \frac{1}{2} \frac{g^2}{6} v_u v_u \tilde{d}_{Rj}^{*y} \tilde{d}_{Rj}^y \\
& - \frac{1}{\sqrt{2}} (Y_U)_{ik} (Y_U)_{pk}^* \tilde{u}_{Li}^x v_u \tilde{u}_{Lp}^{*x} h_2^{0*} - \frac{1}{\sqrt{2}} (Y_U)_{ik} (Y_U)_{pk}^* \tilde{u}_{Li}^x h_2^0 \tilde{u}_{Lp}^{*x} v_u \\
& - \frac{1}{\sqrt{2}} \frac{g^2}{12} v_u h_2^0 \tilde{u}_{Lj}^{*y} \tilde{u}_{Lj}^y - \frac{1}{\sqrt{2}} \frac{g^2}{12} h_2^{0*} v_u \tilde{u}_{Lj}^{*y} \tilde{u}_{Lj}^y + \frac{1}{\sqrt{2}} \frac{g^2}{12} v_0 \tilde{\nu}_{L0} \tilde{u}_{Lj}^{*y} \tilde{u}_{Lj}^y + \frac{1}{\sqrt{2}} \frac{g^2}{12} \tilde{\nu}_{L0}^* v_0 \tilde{u}_{Lj}^{*y} \tilde{u}_{Lj}^y \\
& - \frac{1}{\sqrt{2}} \frac{g_2^2}{4} v_0 \tilde{u}_{Lj}^x \tilde{\nu}_{L0} \tilde{u}_{Lj}^{*x} - \frac{1}{\sqrt{2}} \frac{g_2^2}{4} \tilde{\nu}_{L0}^* \tilde{u}_{Lj}^x v_0 \tilde{u}_{Lj}^{*x} - \frac{1}{\sqrt{2}} (Y_U)_{ij} (Y_U)_{iq}^* v_u \tilde{u}_{Rj}^{*y} h_2^0 \tilde{u}_{Rq}^y \\
& - \frac{1}{\sqrt{2}} (Y_U)_{ij} (Y_U)_{iq}^* h_2^0 \tilde{u}_{Rj}^{*y} v_u \tilde{u}_{Rq}^y + \frac{1}{\sqrt{2}} \frac{g^2}{3} v_u h_2^0 \tilde{u}_{Rj}^{*y} \tilde{u}_{Rj}^y + \frac{1}{\sqrt{2}} \frac{g^2}{3} h_2^{0*} v_u \tilde{u}_{Rj}^{*y} \tilde{u}_{Rj}^y
\end{aligned}$$

.....



$$\begin{aligned}
& i \left[\frac{\lambda'_{\alpha ij} \mu_\alpha^*}{\sqrt{2}} Z_{\tilde{d}(3+j)q} Z_{\tilde{d}ir}^* Z_{R1s} \right. \\
& \quad + \frac{\lambda'_{\alpha ki} \mu_\alpha}{\sqrt{2}} Z_{\tilde{d}kq} Z_{\tilde{d}(3+i)r}^* Z_{R1s} \\
& \quad - \frac{h'_{\alpha jk}}{\sqrt{2}} Z_{\tilde{d}jr}^* Z_{\tilde{d}(3+k)q} Z_{R(2+\alpha)s} \\
& \quad - \frac{h'_{\alpha jk}}{\sqrt{2}} Z_{\tilde{d}(3+k)r}^* Z_{\tilde{d}jq} Z_{R(2+\alpha)s} \\
& \quad \left. - \frac{\lambda'_{0ij} \lambda'_{\beta ik} v_d}{2} Z_{\tilde{d}(3+k)r}^* Z_{\tilde{d}(3+j)q} Z_{R(2+\beta)s} \right]
\end{aligned}$$

$$\begin{aligned}
& -\frac{\lambda'_{\alpha ij} \lambda'_{0 ik} v_d}{2} Z_{\tilde{d}(3+k)r}^* Z_{\tilde{d}(3+j)q} Z_{R(2+\alpha)s} \\
& -\frac{\lambda'_{0 ik} \lambda'_{\beta jk} v_d}{2} Z_{\tilde{d}ir}^* Z_{\tilde{d}jq} Z_{R(2+\beta)s} \\
& -\frac{\lambda'_{\alpha ik} \lambda'_{0 jk} v_d}{2} Z_{\tilde{d}ir}^* Z_{\tilde{d}jq} Z_{R(2+\alpha)s} \\
& +\frac{e^2 v_d (1 + 2c_W^2)}{12c_W^2 s_W^2} Z_{\tilde{d}jq} Z_{\tilde{d}jr}^* Z_{R2s} \\
& +\frac{e^2 v_d}{6c_W^2} Z_{\tilde{d}(3+j)q} Z_{\tilde{d}(3+j)r}^* Z_{R2s} \\
& -\frac{e^2 v_u (1 + 2c_W^2)}{12c_W^2 s_W^2} Z_{\tilde{d}jq} Z_{\tilde{d}jr}^* Z_{R1s} \\
& -\frac{e^2 v_u}{6c_W^2} Z_{\tilde{d}(3+j)q} Z_{\tilde{d}(3+j)r}^* Z_{R1s}]
\end{aligned}$$



$$\begin{aligned}
& -\left[-\frac{\lambda'_{\alpha ij} \mu_\alpha}{\sqrt{2}} Z_{\tilde{d}(3+j)q} Z_{\tilde{d}ir}^* Z_{A1s} \right. \\
& +\frac{\lambda'_{\alpha ki} \mu_\alpha}{\sqrt{2}} Z_{\tilde{d}kq} Z_{\tilde{d}(3+i)r}^* Z_{A1s} \\
& -\frac{h'_{\alpha jk}}{\sqrt{2}} Z_{\tilde{d}jr}^* Z_{\tilde{d}(3+k)q} Z_{A(2+\alpha)s} \\
& +\frac{h'_{\alpha jk}}{\sqrt{2}} Z_{\tilde{d}(3+k)r}^* Z_{\tilde{d}jq} Z_{A(2+\alpha)s} \\
& \left. +\frac{\lambda'_{0 ij} \lambda'_{\beta ik} v_d}{2} Z_{\tilde{d}(3+k)r}^* Z_{\tilde{d}(3+j)q} Z_{A(2+\beta)s} \right]
\end{aligned}$$

$$\begin{aligned}
& -\frac{\lambda'_{\alpha ij} \lambda'_{0 ik} v_d}{2} Z_{\tilde{d}(3+k)r}^* Z_{\tilde{d}(3+j)q} Z_{A(2+\alpha)s} \\
& +\frac{\lambda'_{0 ik} \lambda'_{\beta jk} v_d}{2} Z_{\tilde{d}ir}^* Z_{\tilde{d}jq} Z_{A(2+\beta)s} \\
& -\frac{\lambda'_{\alpha ik} \lambda'_{0 jk} v_d}{2} Z_{\tilde{d}ir}^* Z_{\tilde{d}jq} Z_{A(2+\alpha)s}]
\end{aligned}$$

$$\begin{aligned}
& i\left[\frac{(Y_U)_{ij} \mu_\beta^*}{\sqrt{2}} Z_{\tilde{u}(3+j)q}^* Z_{\tilde{u}ir} Z_{R(2+\beta)s} \right. \\
& + \frac{(Y_U)_{ij}^* \mu_\beta}{\sqrt{2}} Z_{\tilde{u}iq}^* Z_{\tilde{u}(3+j)r} Z_{R(2+\beta)s} \\
& - \frac{(h_U)_{ij}}{\sqrt{2}} Z_{\tilde{u}(3+j)q}^* Z_{\tilde{u}ir} Z_{R1s} \\
& - \frac{(h_U^*)_{ij}}{\sqrt{2}} Z_{\tilde{u}iq}^* Z_{\tilde{u}(3+j)r} Z_{R1s} \\
& \left. - (Y_U)_{ij} (Y_U)_{ik}^* v_u Z_{\tilde{u}(3+j)q}^* Z_{\tilde{u}(3+k)r} Z_{R1s} \right. \\
& - (Y_U)_{ik} (Y_U)_{jk}^* v_u Z_{\tilde{u}jq}^* Z_{\tilde{u}ir} Z_{R1s} \\
& + \frac{e^2 v_d (1 - 4c_W^2)}{12c_W^2 s_W^2} Z_{\tilde{u}jq}^* Z_{\tilde{u}jr} Z_{R2s} \\
& - \frac{e^2 v_d}{3c_W^2} Z_{\tilde{u}(3+j)q}^* Z_{\tilde{u}(3+j)r} Z_{R2s} \\
& - \frac{e^2 v_u (1 - 4c_W^2)}{12c_W^2 s_W^2} Z_{\tilde{u}jq}^* Z_{\tilde{u}jr} Z_{R1s} \\
& + \frac{e^2 v_u}{3c_W^2} Z_{\tilde{u}(3+j)q}^* Z_{\tilde{u}(3+j)r} Z_{R1s} \\
& \left. - \left[-\frac{(Y_U)_{ij} \mu_\beta^*}{\sqrt{2}} Z_{\tilde{u}(3+j)q}^* Z_{\tilde{u}ir} Z_{A(2+\beta)s} \right. \right. \\
& + \frac{(Y_U)_{ij}^* \mu_\beta}{\sqrt{2}} Z_{\tilde{u}iq}^* Z_{\tilde{u}(3+j)r} Z_{A(2+\beta)s} \\
& - \frac{(h_U)_{ij}}{\sqrt{2}} Z_{\tilde{u}(3+j)q}^* Z_{\tilde{u}ir} Z_{A1s} \\
& \left. + \frac{(h_U^*)_{ij}}{\sqrt{2}} Z_{\tilde{u}iq}^* Z_{\tilde{u}(3+j)r} Z_{A1s} \right]
\end{aligned}$$

C.60 Charged Scalar - Squark - Squark

$$\begin{aligned}
& -\frac{1}{\sqrt{2}} \frac{g_2^2}{2} v_u \tilde{d}_{Li}^* h_2^+ \tilde{u}_{Li}^* - \frac{1}{\sqrt{2}} \frac{g_2^2}{2} v_u \tilde{d}_{Li}^* h_2^+ \tilde{u}_{Li} + (Y_U)_{ij} \mu_\beta^* \tilde{d}_{Li}^y \tilde{u}_{Rj}^{*y} \tilde{e}_{L\beta}^* + \mu_\alpha (Y_U)_{pq}^* \tilde{e}_{L\alpha} \tilde{d}_{Lp}^{*z} \tilde{u}_{Rq}^z \\
& + h'_{\alpha jk} \tilde{e}_{L\alpha} \tilde{u}_{Lj} \tilde{d}_{Rk}^* + h'^*_{\alpha jk} \tilde{e}_{L\alpha}^* \tilde{u}_{Lj}^* \tilde{d}_{Rk} + (h_u)_{ij} \tilde{d}_{Li}^y h_2^+ \tilde{u}_{Rj}^{*y} + (h_u^*)_{ij} \tilde{d}_{Li}^{*y} h_2^+ \tilde{u}_{Rj}^y
\end{aligned}$$

$$\begin{aligned}
& + \lambda'_{\alpha ij} \mu_\alpha^* \tilde{u}_{Li}^y \tilde{d}_{Rj}^{*y} h_2^{+*} + \mu_\alpha \lambda'_{\alpha pq} h_2^+ \tilde{u}_{Lp}^{*z} \tilde{d}_{Rq}^z - \frac{1}{\sqrt{2}} \lambda_{\alpha 0j} \lambda'_{\alpha pq} v_0 \tilde{e}_{Rj}^* \tilde{u}_{Lp}^{*z} \tilde{d}_{Rq}^z - \frac{1}{\sqrt{2}} \lambda'_{\alpha ij} \lambda_{\alpha 0q} \tilde{u}_{Li}^y \tilde{d}_{Rj}^{*y} v_0 \tilde{e}_{Rq} \\
& + \frac{1}{\sqrt{2}} \lambda'_{0ik} \lambda_{\beta pk}^* v_0 \tilde{d}_{Li}^z \tilde{e}_{L\beta}^* \tilde{u}_{Lp}^{*z} + \frac{1}{\sqrt{2}} \lambda'_{\alpha ik} \lambda_{0pk}^* \tilde{e}_{L\alpha} \tilde{u}_{Li}^z v_0 \tilde{d}_{Lp}^{*z} \\
& + \frac{1}{\sqrt{2}} (Y_U)_{ik} (Y_U)_{pk}^* \tilde{u}_{Li}^x v_u \tilde{d}_{Lp}^{*x} h_2^{+*} + \frac{1}{\sqrt{2}} (Y_U)_{ik} (Y_U)_{pk}^* \tilde{d}_{Li}^x h_2^+ \tilde{u}_{Lp}^{*x} v_u \\
& - \frac{1}{\sqrt{2}} \frac{g_2^2}{2} v_0 \tilde{u}_{Lj}^y \tilde{e}_{L0} \tilde{d}_{Lj}^{*y} - \frac{1}{\sqrt{2}} \frac{g_2^2}{2} \tilde{e}_{L0}^* \tilde{d}_{Lj}^y v_0 \tilde{u}_{Lj}^{*y} + \frac{1}{\sqrt{2}} (Y_U)_{ij} \lambda_{0iq}^* h_2^+ \tilde{u}_{Rj}^{*y} v_0 \tilde{d}_{Rq}^y \\
& + \frac{1}{\sqrt{2}} \lambda'_{0ij} (Y_U)_{iq}^* v_0 \tilde{d}_{Rj}^{*y} h_2^{+*} \tilde{u}_{Rq}^y + \frac{1}{\sqrt{2}} (Y_U)_{ij} \lambda'_{\alpha iq} v_u \tilde{u}_{Rj}^{*y} \tilde{e}_{L\alpha}^* \tilde{d}_{Rq}^y + \frac{1}{\sqrt{2}} \lambda'_{\alpha ij} (Y_U)_{iq}^* \tilde{e}_{L\alpha} \tilde{d}_{Rj}^{*y} v_u \tilde{u}_{Rq}^y
\end{aligned}$$

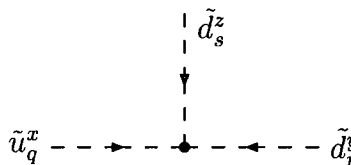
.....

$$\begin{aligned}
& i[\lambda'_{\alpha ij} \mu_\alpha^* Z_{\tilde{u}iq} Z_{\tilde{d}(3+j)r} Z_{H1s}^* \\
& + \mu_\alpha (Y_U)_{ij}^* Z_{\tilde{u}(3+j)q} Z_{\tilde{d}ir} Z_{H(2+\alpha)s}^* \\
& + h'_{\alpha jk} Z_{\tilde{u}jq} Z_{\tilde{d}(3+k)r} Z_{H(2+\alpha)s}^* \\
& + (h_u^*)_{ij} Z_{\tilde{u}(3+j)q} Z_{\tilde{d}ir} Z_{H1s}^* \\
& - \frac{\lambda'_{\alpha ij} \lambda_{\alpha 0k}^* v_d}{\sqrt{2}} Z_{\tilde{u}iq} Z_{\tilde{d}(3+j)r} Z_{H(5+k)s}^* \\
& + \frac{\lambda'_{\alpha ij} (Y_U)_{ik}^* v_u}{\sqrt{2}} Z_{\tilde{u}(3+k)q} Z_{\tilde{d}(3+j)r} Z_{H(2+\alpha)s}^* \\
& + \frac{(Y_U)_{ik} (Y_U)_{jk}^* v_u}{\sqrt{2}} Z_{\tilde{u}iq} Z_{\tilde{d}jr} Z_{H1s}^* \\
& + \frac{\lambda'_{0ij} (Y_U)_{ik}^* v_d}{\sqrt{2}} Z_{\tilde{u}(3+k)q} Z_{\tilde{d}(3+j)r} Z_{H1s}^* \\
& + \frac{\lambda'_{\alpha ik} \lambda_{0jk}^* v_d}{\sqrt{2}} Z_{\tilde{u}iq} Z_{\tilde{d}jr} Z_{H(2+\alpha)s}^* \\
& - \frac{e^2 v_u}{2\sqrt{2} s_W^2} Z_{\tilde{u}iq} Z_{\tilde{d}ir} Z_{H1s}^* - \frac{e^2 v_d}{2\sqrt{2} s_W^2} Z_{\tilde{u}jq} Z_{\tilde{d}jr} Z_{H2s}^*]
\end{aligned}$$

C.61 Squark - Squark - Squark

$$-\frac{1}{2} \varepsilon_{xyz} h''_{ijk} \tilde{u}_{Ri}^{*x} \tilde{d}_{Rj}^{*y} \tilde{d}_{Rk}^z - \frac{1}{2} \varepsilon_{xyz} h''_{ijk} \tilde{u}_{Ri}^x \tilde{d}_{Rj}^y \tilde{d}_{Rk}^z$$

$$\begin{aligned}
& -\frac{1}{\sqrt{2}} \lambda'_{0ik} \varepsilon_{vwz} \lambda''_{pqk} v_0 \tilde{d}_{Li}^z \tilde{u}_{Rp}^v \tilde{d}_{Rq}^w - \frac{1}{\sqrt{2}} \varepsilon_{xyz} \lambda''_{ijk} \lambda'_{0pk} \tilde{u}_{Ri}^{*x} \tilde{d}_{Rj}^{*y} v_0 \tilde{d}_{Lp}^{*z} \\
& -\frac{1}{\sqrt{2}} (Y_U)_{ik} \frac{1}{2} \varepsilon_{xvw} \lambda''_{kpq} \tilde{u}_{Li}^x v_u \tilde{d}_{Rp}^v \tilde{d}_{Rq}^w - \frac{1}{\sqrt{2}} \frac{1}{2} \varepsilon_{xyz} \lambda''_{kij} (Y_U)_{pk} \tilde{d}_{Ri}^{*y} \tilde{d}_{Rj}^{*z} \tilde{u}_{Lp}^{*x} v_u
\end{aligned}$$



$$\begin{aligned}
& i \varepsilon_{xyz} \left[-\frac{1}{2} h''_{ijk} Z_{\tilde{u}(3+i)q} Z_{\tilde{d}(3+j)r}^* Z_{\tilde{d}(3+k)s}^* \right. \\
& - \frac{(Y_U)_{ik} \lambda''_{kjm} v_u}{2\sqrt{2}} Z_{\tilde{u}iq} Z_{\tilde{d}(3+j)r}^* Z_{\tilde{d}(3+m)s}^* \\
& \left. - \frac{\lambda'_{0ik} \lambda''_{jmk} v_d}{\sqrt{2}} Z_{\tilde{u}(3+j)q} Z_{\tilde{d}is}^* Z_{\tilde{d}(3+m)r}^* \right]
\end{aligned}$$

Appendix D

Summary of rotation matrix definitions

We draw together the definitions of the rotation matrices, which describe the transformation from interaction basis to mass eigenbasis, as determined by the forms of the mass matrices.

Charged scalars

$$\begin{pmatrix} h_2^+ \\ \tilde{e}_{L\alpha}^* \\ \tilde{e}_{Ri}^* \end{pmatrix} = Z_H \begin{pmatrix} H_1^+ \\ \vdots \\ H_8^+ \end{pmatrix}$$

$$h_2^+ = Z_{H1q} H_q^+$$

$$\tilde{e}_{L\alpha}^* = Z_{H(2+\alpha)q} H_q^+$$

$$\tilde{e}_{Ri}^* = Z_{H(5+i)q} H_q^+$$

Neutral scalars

$$\begin{aligned} \begin{pmatrix} \text{Re} h_2^0 \\ \text{Re} \tilde{\nu}_{L\alpha} \end{pmatrix} &= \frac{1}{\sqrt{2}} Z_R \begin{pmatrix} H_1^0 \\ \vdots \\ H_5^0 \end{pmatrix} \\ &= \frac{1}{\sqrt{2}} Z_R \begin{pmatrix} h^0 \\ H^0 \\ \tilde{\nu}_{+i} \end{pmatrix} \end{aligned}$$

$$\begin{aligned} \begin{pmatrix} \text{Im} h_2^0 \\ \text{Im} \tilde{\nu}_{L\alpha} \end{pmatrix} &= \frac{1}{\sqrt{2}} Z_A \begin{pmatrix} A_1^0 \\ \vdots \\ A_5^0 \end{pmatrix} \\ &= \frac{1}{\sqrt{2}} Z_A \begin{pmatrix} A^0 \\ G^0 \\ \tilde{\nu}_{-i} \end{pmatrix} \end{aligned}$$

$$h_2^0 = \frac{1}{\sqrt{2}} (Z_{R1q} H_q^0 + i Z_{A1q} A_q^0)$$

$$\tilde{\nu}_{L\alpha} = \frac{1}{\sqrt{2}} (Z_{R(2+\alpha)q} H_q^0 + i Z_{A(2+\alpha)q} A_q^0)$$

Charginos

$$\begin{pmatrix} -i\widetilde{W}^+ \\ \tilde{h}_2^+ \\ e_{Ri} \end{pmatrix} = Z_+ \begin{pmatrix} \kappa_1^+ \\ \vdots \\ \kappa_5^+ \end{pmatrix}$$

$$\begin{pmatrix} -i\widetilde{W}^- \\ e_{L\alpha} \end{pmatrix} = Z_-^* \begin{pmatrix} \kappa_1^- \\ \vdots \\ \kappa_5^- \end{pmatrix}$$

$$\widetilde{W}^+ = iZ_{+1q}\kappa_q^+$$

$$\widetilde{W}^- = iZ_{-1q}^*\kappa_q^-$$

$$\tilde{h}_2^+ = Z_{+2q}\kappa_q^+$$

$$e_{Ri} = Z_{+(2+i)q}\kappa_q^+$$

$$e_{L\alpha} = Z_{-(2+\alpha)q}^*\kappa_q^-$$

Neutralinos

$$\begin{pmatrix} -i\tilde{B} \\ -i\widetilde{W}^0 \\ \tilde{h}_2^0 \\ \nu_{L\alpha} \end{pmatrix} = Z_N \begin{pmatrix} \kappa_1^0 \\ \vdots \\ \kappa_7^0 \end{pmatrix}$$

$$\tilde{B} = iZ_{N1q}\kappa_q^0$$

$$\widetilde{W}^0 = iZ_{N2q}\kappa_q^0$$

$$\tilde{h}_2^0 = Z_{N3q}\kappa_q^0$$

$$\nu_{L\alpha} = Z_{N(4+\alpha)q}\kappa_q^0$$

Up-type Squarks

$$\begin{pmatrix} \tilde{u}_{Li}^x \\ \tilde{u}_{Rj}^x \end{pmatrix} = Z_{\tilde{u}} \begin{pmatrix} \tilde{u}_1^x \\ \vdots \\ \tilde{u}_6^x \end{pmatrix}$$

$$\tilde{u}_{Li}^x = Z_{\tilde{u}iq}\tilde{u}_q^x$$

$$\tilde{u}_{Rj}^x = Z_{\tilde{u}(3+j)q}\tilde{u}_q^x$$

Down-type Squarks

$$\begin{pmatrix} \tilde{d}_{Li}^x \\ \tilde{d}_{Rj}^x \end{pmatrix} = Z_{\tilde{d}}^* \begin{pmatrix} \tilde{d}_1^x \\ \vdots \\ \tilde{d}_6^x \end{pmatrix} \quad \left| \quad \begin{aligned} \tilde{d}_{Li}^x &= Z_{\tilde{d}iq}^* \tilde{d}_q^x \\ \tilde{d}_{Rj}^x &= Z_{\tilde{d}(3+j)q}^* \tilde{d}_q^x \end{aligned} \right.$$

Quarks

$$\begin{aligned} u_{Li}^x &= Z_{uLij} u_{Lj}^x, & d_{Li}^x &= Z_{dLij}^* d_{Lj}^x \\ u_{Ri}^x &= Z_{uRij}^* u_{Rj}^x, & d_{Ri}^x &= Z_{dRij} d_{Rj}^x \end{aligned}$$

where ‘primed’ fields are the quarks in the interaction basis and ‘unprimed’ fields give the fields in the mass basis.

Appendix E

Courant-Fischer theorem

Consider A an $n \times n$, hermitian matrix, with real eigenvalues $\lambda_1 \geq \lambda_2 \geq \dots \geq \lambda_n$ and U defined such that

$$U^\dagger A U = D = \text{diag}(\lambda_1, \lambda_2, \dots, \lambda_n) \quad (\text{E-1})$$

Consider two subspaces; \mathcal{F} is the subspace spanned by the basis vectors $\{e_1, \dots, e_i\}$ and \mathcal{V} an unspecified subspace which has dimension $(n - i + 1)$. $S_{\mathcal{V}}$ is the set of all unit vectors in \mathcal{V} . $S'_{\mathcal{V}}$ is the set of all unit vectors which live in both \mathcal{F} and \mathcal{V} .

Consider a particular \mathcal{V} and any unit vector from $S'_{\mathcal{V}}, y$

$$y^\dagger D y = \sum_{j=1}^i \lambda_j y_j^* y_j \geq \lambda_i \sum_{j=1}^i y_j^* y_j = \lambda_i \quad \text{for any unit vector in } S'_{\mathcal{V}} \quad (\text{E-2})$$

It is possible to find the specific y from $S'_{\mathcal{V}}$ which gives the greatest value for $y^\dagger D y$ and as all the elements of $S'_{\mathcal{V}}$ also appear in $S_{\mathcal{V}}$, it is clear that

$$\max_{S_{\mathcal{V}}} \{y^\dagger D y\} \geq \max_{S'_{\mathcal{V}}} \{y^\dagger D y\} \geq \lambda_i \quad (\text{E-3})$$

Now, each possible \mathcal{V} is considered and the specific \mathcal{V} which gives the lowest value

for $\overset{\max}{S_{\mathcal{V}}}\{y^\dagger Dy\}$ is selected.

$$\overset{\min\max}{\mathcal{V}S_{\mathcal{V}}}\{y^\dagger Dy\} \geq \lambda_i \quad (\text{E-4})$$

$\tilde{\mathcal{V}}$ is defined to be the subspace spanned by all the basis vectors orthogonal to $\{e_1, \dots, e_{i-1}\}$. $S_{\tilde{\mathcal{V}}}$ is the set of unit vectors in $\tilde{\mathcal{V}}$. Consider y , a unit vector from $S_{\tilde{\mathcal{V}}}$

$$y^\dagger Dy = \sum_{j=i}^n \lambda_j y_j^* y_j \leq \lambda_i \sum_{j=i}^n y_j^* y_j = \lambda_i \quad \text{for any unit vector in } S_{\tilde{\mathcal{V}}} \quad (\text{E-5})$$

As all y satisfy this relation, the particular y which gives the greatest value for $y^\dagger Dy$ satisfies

$$\overset{\max}{S_{\tilde{\mathcal{V}}}}\{y^\dagger Dy\} \leq \lambda_i \quad (\text{E-6})$$

Noting that $\tilde{\mathcal{V}}$ is a specific \mathcal{V} and comparing with (E-4)

$$\overset{\min\max}{\mathcal{V}S_{\tilde{\mathcal{V}}}}\{y^\dagger Dy\} \leq \overset{\max}{S_{\tilde{\mathcal{V}}}}\{y^\dagger Dy\} \leq \lambda_i \quad \longrightarrow \quad \overset{\min\max}{\mathcal{V}S_{\tilde{\mathcal{V}}}}\{y^\dagger Dy\} = \lambda_i \quad (\text{E-7})$$

The process can be repeated, choosing \mathcal{F} to be the subspace spanned by $\{e_{i+1}, \dots, n\}$ and $\tilde{\mathcal{V}}$ to be the subspace orthogonal to $\{e_{i+1}, \dots, n\}$. To obtain

$$\overset{\max\min}{\mathcal{V}S_{\tilde{\mathcal{V}}}}\{y^\dagger Dy\} = \lambda_i \quad (\text{E-8})$$

It is now possible to perform a basis rotation $y = U^\dagger x$, leaving

$$\overset{\min}{\mathcal{V}_{n-i+1}} \overset{\max}{S_{\mathcal{V}}}\{x^\dagger Ax\} = \lambda_i \quad (\text{E-9})$$

$$\overset{\max\min}{\mathcal{V}_i S_{\mathcal{V}}}\{x^\dagger Ax\} = \lambda_i \quad (\text{E-10})$$

E.1 Interlaced eigenvalues

Consider two hermitian matrices; A , $n \times n$ with eigenvalues $\lambda_1 \geq \lambda_2 \dots \geq \lambda_n$ and B , $(n+1) \times (n+1)$ with eigenvalues $\beta_1 \geq \beta_2 \geq \dots \geq \beta_{n+1}$.

$$\begin{aligned}
 U^\dagger A U &= D = \text{diag}(\lambda_1, \lambda_2, \dots, \lambda_n) & V &= \begin{pmatrix} U & 0 \\ 0 & 1 \end{pmatrix} \\
 B &= \begin{pmatrix} A & c \\ c^\dagger & \alpha \end{pmatrix} & \tilde{B} &= V^\dagger B V = \begin{pmatrix} D & U^\dagger c \\ c^\dagger U & \alpha \end{pmatrix}
 \end{aligned} \tag{E-11}$$

The eigenvalues of \tilde{B} are equal to those of B as the transformation is unitary.

Consider an i -dimension subspace, \mathcal{F} , defined as being the space spanned by basis vectors $\{e_1, \dots, e_i\}$ where $i \leq n$. Choose any unit vector, x , which lives in this subspace, then find the x which gives the smallest value for $x^\dagger \tilde{B} x$

$$x^\dagger \tilde{B} x = \sum_{j=1}^i \lambda_j x_j^* x_j \geq \lambda_i \sum_{j=1}^i x_j^* x_j \quad \longrightarrow \quad \min_{\mathcal{F}} \{x^\dagger \tilde{B} x\} \geq \lambda_i \tag{E-12}$$

Using the Courant-Fischer theorem for β_i , noting \mathcal{F} is a particular \mathcal{V} and comparing with (E-12) shows

$$\beta_i = \max_{\mathcal{V}} \min_{\mathcal{V}} \{x^\dagger \tilde{B} x\} \geq \min_{\mathcal{F}} \{x^\dagger \tilde{B} x\} \quad \longrightarrow \quad \beta_i \geq \lambda_i \tag{E-13}$$

Consider an $(n-i)$ -dimensional subspace, \mathcal{T} , defined to be the subspace spanned by $\{e_{i-1}, \dots, e_n\}$. Choose any unit vector which lives in the subspace, x .

$$\begin{aligned}
 x^\dagger \tilde{B} x &= \sum_{j=i-1}^n \lambda_j x_j^* x_j \leq \lambda_{i-1} \sum_{j=i-1}^n x_j^* x_j \\
 \max_{\mathcal{T}} \{x^\dagger \tilde{B} x\} &\leq \lambda_{i-1}
 \end{aligned} \tag{E-14}$$

Using the Courant-Fischer theorem for β_i , noting \mathcal{T} is a specific \mathcal{V} and comparing

with (E-14) gives

$$\beta_i = \min_{\mathcal{V}} \max_{\mathcal{V}} \{x^\dagger \tilde{B}x\} \leq \max_{\mathcal{T}} \{x^\dagger \tilde{B}x\} \longrightarrow \lambda_{i-1} \geq \beta_i \quad (\text{E-15})$$

Consider a 1-dim subspace, \mathcal{K} which spans $\{e_n\}$ and any unit vector in this subspace x .

$$\max_{\mathcal{K}} \{x^\dagger \tilde{B}x\} = \lambda_n \quad (\text{E-16})$$

Using the Courant-Fischer theorem for β_i implies

$$\beta_{n+1} = \min_{\mathcal{V}} \max_{\mathcal{V}} \{x^\dagger \tilde{B}x\} \leq \max_{\mathcal{K}} \{x^\dagger \tilde{B}x\} \longrightarrow \lambda_n \geq \beta_{n+1}$$

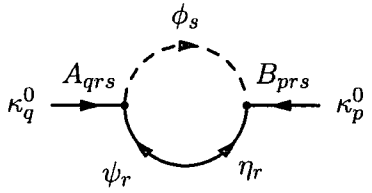
Combining the results

$$\beta_1 \geq \lambda_1 \geq \beta_2 \geq \lambda_2 \geq \dots \geq \lambda_{n-1} \geq \beta_n \geq \lambda_n \quad (\text{E-17})$$

Appendix F

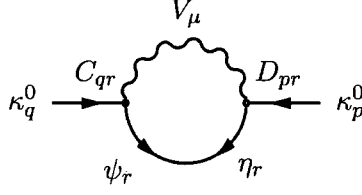
Self-energy one-loop corrections

We now proceed in calculating the general self energies of (5.1,5.2). The 1PI self energy, Σ^D , obtains corrections from diagrams which have either gauge particles or scalar particles in the loop. The scalar contributions for general scalar-fermion vertices iA_{qrs} and iB_{prs} is



$$\Sigma_{pq}^D(m_{\kappa_q^0}^2) = iB_{prs}A_{qrs}m_{\psi\eta_r} \frac{i\pi^2}{(2\pi)^4\mu^{4-D}} B_0(m_{\kappa_q^0}^2, m_{\phi_s}^2, m_{\psi\eta_r}^2), \quad (\text{F-1})$$

where $m_{\psi\eta_r}$ denotes the physical mass of the mass eigenstate which is composed out of the interaction eigenstates ψ_r and η_r . The corresponding neutrino self energy arising from vector boson contributions with generic vertices $iC_{qr}\bar{\sigma}^\mu$ and $iD_{qr}\bar{\sigma}^\mu$ is



$$\begin{aligned} \Sigma_{pq}^D(m_{\kappa_q^0}^2) &= iD_{pr}C_{qr}m_{\psi\eta_r} \frac{i\pi^2}{(2\pi)^4\mu^{4-D}} \left\{ (\xi + 3)B_0(m_{\kappa_q^0}^2, m_V^2, m_{\psi\eta_r}^2) + \right. \\ &\quad \left. + (\xi - 1)\xi m_V^2 C_0(0, m_{\kappa_q^0}^2, m_{\kappa_q^0}^2, m_V^2, \xi m_V^2, m_{\psi\eta_r}^2) \right\}, \end{aligned} \quad (\text{F-2})$$

where ξ is the gauge fixing parameter, m_V is the mass of the vector boson and B_0, C_0 are the Passarino-Veltman functions [90] in the notation of Ref. [91],

$$B_0(q^2, m_\phi^2, m_\psi^2) = \frac{(2\pi)^4\mu^{4-D}}{i\pi^2} \int \frac{d^D k}{(2\pi)^D} \frac{1}{(k^2 - m_\phi^2) ([q + k]^2 - m_\psi^2)}, \quad (\text{F-3})$$

$$C_0(0, q^2, q^2, m_V^2, \xi m_V^2, m_\psi^2) = \frac{(2\pi)^4\mu^{4-D}}{i\pi^2} \int \frac{d^D k}{(2\pi)^D} \frac{1}{(k^2 - m_V^2) (k^2 - \xi m_V^2) ([q + k]^2 - m_\psi^2)}. \quad (\text{F-4})$$

Finally, self energy corrections to the Weyl fermion kinetic terms read as

$$\Sigma_{pq}^L(m_{\kappa_q^0}^2) = iA_{prs}^* A_{qrs} \frac{i\pi^2}{(2\pi)^4\mu^{4-D}} B_1(m_{\kappa_q^0}^2, m_{\psi_r}^2, m_{\phi_s}^2), \quad (\text{F-5})$$

and

$$\begin{aligned} \Sigma_{pq}^L(m_{\kappa_q^0}^2) &= iC_{pr}^* C_{qr} \frac{i\pi^2}{(2\pi)^4\mu^{4-D}} \\ &\quad \left\{ -(\xi + 1)B_0(m_{\kappa_q^0}^2, m_V^2, m_{\psi_r}^2) - 2B_1(m_{\kappa_q^0}^2, m_V^2, m_{\psi_r}^2) \right\} \end{aligned}$$

$$- (\xi - 1)\xi m_V^2 C_0(0, m_{\kappa_q}^2, m_{\kappa_q}^2, m_V^2, \xi m_V^2, m_{\psi_r}^2) (\xi - 1)(m_{\kappa_q}^2 - m_{\psi_r}^2) C_2(0, m_{\kappa_q}^2, m_{\kappa_q}^2, m_V^2, \xi m_V^2, m_{\psi_r}^2) \Big\},$$

(F-6)

where B_1, C_2 are defined in [91].

Appendix G

One-loop calculation for radiative decays

In this appendix, details of the calculation of the radiative decay of charged leptons are presented.

We first consider all terms which are proportional to the product $A_{iks}B_{jks}$, where A is the Feynman rule associated with the e_L -fermion-scalar vertex and B is the rule associated with the e_R -fermion-scalar vertex. Terms of this nature arise from seven diagrams. Two diagrams where the photon is attached to the internal fermion G.1; one diagram where the photon is attached to the scalar in the loop G.2; and four diagrams where the photon vertex appears on an external leg G.3.

We assume that $m_j \ll m_i \ll m_\varphi, m_\psi$, where m_i is the mass of the initial state lepton, m_j is the mass of the final state lepton, m_φ is the mass of the scalar in the loop, and m_ψ is the mass of the fermion in the loop. We further impose that the initial and final state particles are on-shell, $q^2 = m_i^2$, $(p-q)^2 = m_j^2$ and $p^2 = 0$, where

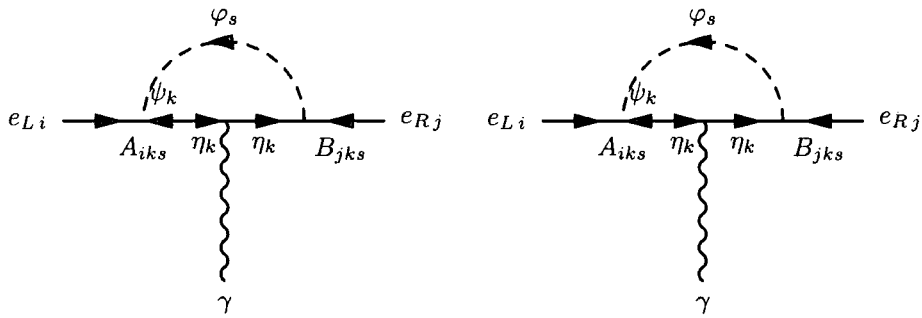


Figure G.1: *Two diagrams with the photon attached to the internal fermion which give a contribution proportional to $A_{iks}B_{jks}$*

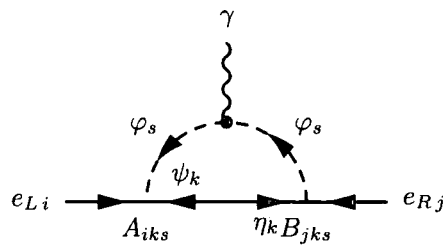


Figure G.2: *The diagram with the photon attached to the internal scalar which gives a contribution proportional to $A_{iks}B_{jks}$*

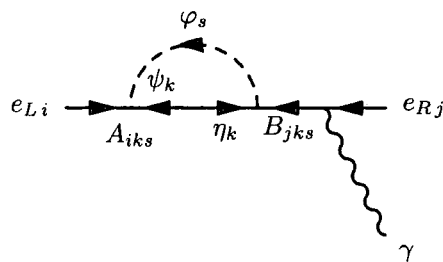


Figure G.3: *One of the diagrams with the photon attached to the external leg which give a contribution proportional to $A_{iks}B_{jks}$. The photon can be attached to the other leg, and the arrow on the initial/final state fermion can be reversed for each leg.*

p is the photon momentum and q is the momentum of the initial state fermion. Under these conditions, we write down the contributions for the seven Feynman diagrams. The contribution from the diagrams where the photon is attached to the internal fermion is given by,

$$i\mathcal{M}_1 = A_{iks}B_{jks}Q_\psi m_\psi \int \frac{d^4k}{(2\pi)^4} \frac{y(p-q)[2k \cdot \varepsilon - 2\sigma^{\mu\nu}p_\nu \varepsilon_\mu]x(q)}{([k-q]^2 - m_\psi^2)(k^2 - m_\psi^2)([k-p]^2 - m_\varphi^2)}. \quad (\text{G-1})$$

The contribution from the diagram where the photon is attached to the internal scalar is given by,

$$i\mathcal{M}_2 = A_{iks}B_{jks}Q_\varphi m_\psi \int \frac{d^4k}{(2\pi)^4} \frac{y(p-q)[2k \cdot \varepsilon]x(q)}{([k-p]^2 - m_\psi^2)(k^2 - m_\psi^2)([k-q]^2 - m_\varphi^2)}. \quad (\text{G-2})$$

Finally, the contribution from attaching the photon to the external leg is given by,

$$i\mathcal{M}_3 = A_{iks}B_{jks}[Q_\psi + Q_\varphi]m_\psi \int \frac{d^4k}{(2\pi)^4} \left[\frac{y(p-q)[\sigma \cdot \varepsilon \bar{\sigma} \cdot q]x(q)}{(m_i^2 - m_j^2)(k^2 - m_\psi^2)([k-q]^2 - m_\varphi^2)} + \frac{y(p-q)[\sigma \cdot \varepsilon \bar{\sigma} \cdot q]x(q)}{(m_j^2 - m_i^2)(k^2 - m_\psi^2)([k-q+p]^2 - m_\varphi^2)} \right]. \quad (\text{G-3})$$

To evaluate these contributions we determine the integrand as a Taylor series. Under the assumption $p^2, q^2 \ll m_a^2, m_b^2$, we can expand expressions as follows,

$$\frac{1}{(k^2 - m_a^2)([k-p]^2 - m_b^2)} = \frac{1}{AB} + \frac{2p \cdot k}{AB^2} + \frac{4(k \cdot p)^2}{AB^3} - \frac{p^2}{AB^2} - \frac{4(k \cdot p)p^2}{AB^3} + \frac{8(k \cdot p)^3}{AB^4}, \quad (\text{G-4})$$

and, similarly,

$$\frac{1}{(k^2 - m_a^2)([k-p]^2 - m_a^2)([k-q]^2 - m_b^2)} = \frac{1}{A^2B} + \frac{2p \cdot k}{A^3B} + \frac{2q \cdot k}{A^2B^2} - \frac{p^2}{A^3B} + \frac{4(p \cdot k)^2}{A^4B} - \frac{q^2}{A^2B^2} + \frac{4(q \cdot k)^2}{A^2B^3} + \frac{4(k \cdot p)(k \cdot q)}{A^3B^2}, \quad (\text{G-5})$$

where $A = k^2 - m_a^2$ and $B = k^2 - m_b^2$.

Expanding the contributions $\mathcal{M}_{1,2,3}$ in this manner gives,

$$\begin{aligned} i\mathcal{M}_1 &= A_{iks}B_{jks}Q_\psi m_\psi \int \frac{d^4k}{(2\pi)^4} y(p-q) \left(\frac{-2\sigma^{\mu\nu}p_\nu\varepsilon_\mu}{\Psi^2\Phi} + \frac{\varepsilon \cdot q k^2}{\Phi^2\Psi^2} \right) x(q), \\ i\mathcal{M}_2 &= -A_{iks}B_{jks}Q_\varphi m_\psi \int \frac{d^4k}{(2\pi)^4} y(p-q) \left(\frac{\varepsilon \cdot q k^2}{\Phi^2\Psi^2} \right) x(q), \\ i\mathcal{M}_3 &= A_{iks}B_{jks}[Q_\psi + Q_\phi]m_\psi \int \frac{d^4k}{(2\pi)^4} y(p-q)[2q \cdot \varepsilon - 2\sigma^{\mu\nu}p_\nu\varepsilon_\mu]x(q) \left(\frac{k^2}{\Phi\Psi^3} - \frac{1}{\Phi\Psi^2} \right), \end{aligned}$$

where $\Phi = k^2 - m_\varphi^2$ and $\Psi = k^2 - m_\psi^2$. We can evaluate integrals of this form using the following change of variables,

$$\begin{aligned} \int_{-\infty}^{\infty} \frac{d^4k}{(2\pi)^4} \frac{(k^2)^n}{(k^2 - m_1) \dots (k^2 - m_i)} &= \int_0^{\infty} \frac{2\pi^2}{(2\pi)^4} d|k| |k|^3 \frac{|k|^{2n}}{(|k|^2 - m_1) \dots (|k|^2 - m_i)} \\ &\stackrel{u=-|k|^2}{=} (-1)^n \int_0^{-\infty} \frac{2\pi^2}{(2\pi)^4} \frac{1}{2} du u \frac{u^n}{(-u - m_1) \dots (-u - m_i)} \\ &= (-1)^n (-1)^i \int_0^{-\infty} \frac{1}{(4\pi)^2} \frac{du u^{n+1}}{(u + m_1) \dots (u + m_i)}. \end{aligned}$$

Before deriving explicit expressions for integrals of this form, we note that relations between such integrals can be produced by employing integration by parts,

$$\begin{aligned} \int \frac{d^4k}{(2\pi)^4} \frac{k^2}{\Phi^2\Psi^2} &= - \int_0^{-\infty} \frac{du}{(4\pi)^2} \frac{1}{(u + m_\varphi^2)^2} \frac{u^2}{(u + m_\psi^2)^2} \\ &= - \int_0^{-\infty} \frac{du}{(4\pi)^2} \frac{-2u^2}{(u + m_\varphi^2)(u + m_\psi^2)^3} + \frac{2u}{(u + m_\varphi^2)(u + m_\psi^2)^2} = - \int \frac{d^4k}{(2\pi)^4} \frac{2k^2}{\Phi\Psi^3} + \frac{2}{\Phi\Psi^2}, \end{aligned}$$

Finally, we note the explicit form of two particular integrals of this type.

$$\begin{aligned} \int \frac{d^4k}{(2\pi)^4} \frac{k^2}{A^2B^2} &= - \int_0^{-\infty} \frac{du}{(2\pi)^4} \frac{u^2}{(u+a)^2(u+b)^2} \\ &= - \int_0^{-\infty} \frac{du}{(2\pi)^2} \frac{-2ab}{(b-a)^3} \left(\frac{1}{u+a} - \frac{1}{u+b} \right) + \frac{a^2}{(b-a)^2} \frac{1}{(u+a)^2} + \frac{b^2}{(b-a)^2} \frac{1}{(u+b)^2} \end{aligned}$$

$$= \frac{2ab}{(b-a)^3} \ln \left[\frac{b}{a} \right] - \frac{b}{(b-a)^2} - \frac{a}{(b-a)^2}.$$

Similarly, it can be shown that,

$$\int \frac{d^4k}{(2\pi)^4} \frac{1}{A^2B} = \frac{-b}{(b-a)^2} \ln \left[\frac{b}{a} \right] + \frac{1}{b-a}.$$

Combining all these results allows us to write down a contribution to the following effective Lagrangian,

$$\mathcal{L}_{\text{eff}} \supset 2\Lambda_{Rij} e_{Rj} \sigma^{\mu\nu} e_{Li} F_{\mu\nu} + 2\Lambda_{Lij} \bar{e}_{Lj} \bar{\sigma}^{\mu\nu} \bar{e}_{Ri} F_{\mu\nu},$$

where the contribution to Λ_R is,

$$\begin{aligned} \Lambda_R \supset & \frac{1}{(4\pi)^2} A_{iks} B_{jks} Q_{\psi_k} m_{\psi_k} \left[-\frac{m_{\psi_k}^2 - 3m_{\phi_s}^2}{4(m_{\psi_k}^2 - m_{\phi_s}^2)^2} + \frac{m_{\phi_s}^4}{(m_{\psi_k}^2 - m_{\phi_s}^2)^3} \ln \left[\frac{m_{\phi_s}}{m_{\psi_k}} \right] \right] \\ & + \frac{1}{2(4\pi)^2} A_{iks} B_{jks} Q_{\phi_s} m_{\psi_k} \left[-\frac{m_{\psi_k}^2 + m_{\phi_s}^2}{2(m_{\psi_k}^2 - m_{\phi_s}^2)^2} + \frac{2m_{\psi_k}^2 m_{\phi_s}^2}{(m_{\psi_k}^2 - m_{\phi_s}^2)^3} \ln \left[\frac{m_{\phi_s}}{m_{\psi_k}} \right] \right]. \end{aligned}$$

We now consider contributions proportional to $B_{iks}^* B_{jks}$, which also contribute to Λ_R . Terms proportional to $A_{jks}^* B_{iks}^*$ and $A_{jks}^* A_{iks}$ contribute to Λ_L . Again, we consider the contributions from diagrams in which the photon is attached to the fermion in the loop, \mathcal{M}_4 , the scalar in the loop, \mathcal{M}_5 , and the external legs, \mathcal{M}_6 and expand as before, giving,

$$\begin{aligned} i\mathcal{M}_4 = & \frac{1}{2} B_{iks}^* B_{jks} Q_{\psi} \int \frac{d^4k}{(2\pi)^4} y(p-q) m_i k^2 \sigma \cdot p \bar{\sigma} \cdot \varepsilon \sigma \cdot q \bar{y} q \left(\frac{k^4}{3\Psi^2\Phi^3} - \frac{k^2}{2\Psi^2\Phi^2} + \frac{k^4}{6\Psi^3\Phi^2} \right) \\ & + y(p-q) \sigma \cdot \varepsilon \bar{y}(q) \left(\frac{-1}{\Psi\Phi} + \frac{k^2}{2\Psi^2\Phi} + \frac{m_i^2}{\Phi^2\Psi} - \frac{k^2 m_i^2}{2\Phi^2\Psi^2} + \frac{2k^4 m_i^2}{3\Psi^2\Phi^3} + \frac{k^4 m_i^2}{3\Psi^3\Phi^2} - \frac{k^2 m_i^2}{\Psi\Phi^3} - \frac{k^2 m_i^2}{2\Psi^2\Phi^2} \right), \end{aligned}$$

$$i\mathcal{M}_5 = -B_{iks}^* B_{jks} Q_\psi \int \frac{d^4 k}{(2\pi)^4} y(p-q) m_i k^2 \sigma \cdot p \bar{\sigma} \cdot \varepsilon \sigma \cdot q \bar{y} q \left(\frac{k^4}{3\Phi^2\Psi^3} - \frac{k^2}{2\Psi^2\Phi^2} + \frac{k^4}{6\Phi^3\Psi^2} \right) \\ + y(p-q) \sigma \cdot \varepsilon \bar{y}(q) \left(\frac{k^2}{2\Phi^2\Psi} - \frac{k^2 m_i^2}{\Phi^2\Psi^2} + \frac{2k^4 m_i^2}{3\Psi^2\Phi^3} + \frac{k^4 m_i^2}{3\Phi^3\Psi^2} \right),$$

and,

$$i\mathcal{M}_6 = B_{iks}^* B_{jks} Q_\psi \int \frac{d^4 k}{(2\pi)^4} + y(p-q) \sigma \cdot \varepsilon \bar{y}(q) \left(\frac{1}{\Psi\Phi} - \frac{k^2}{2\Psi^2\Phi} - \frac{m_i^2}{\Psi^2\Phi} + \frac{2m_i^2 k^2}{\Psi^3\Phi} - \frac{k^4 m_i^2}{\Psi^4\Phi} \right).$$

We use integration by parts in a similar manner as before to determine three further relations between integrals of this form,

$$\int \frac{d^4 k}{(2\pi)^4} \left[\frac{k^2}{\Phi^2\Psi} = \int \frac{d^4 k}{(2\pi)^4} - \frac{k^2}{\Phi\Psi^2} + \frac{2}{\Phi\Psi} \right],$$

$$\int \frac{d^4 k}{(2\pi)^4} \left[\frac{2k^4}{3\Phi^3\Psi^2} = \int \frac{d^4 k}{(2\pi)^4} \frac{k^2}{\Phi^2\Psi^2} - \frac{2k^4}{3\Phi^2\Psi^3} \right],$$

$$\int \frac{d^4 k}{(2\pi)^4} \left[\frac{k^4}{3\Phi^2\Psi^3} = \int \frac{d^4 k}{(2\pi)^4} \frac{k^2}{\Phi\Psi^3} - \frac{k^4}{\Phi\Psi^4} \right].$$

One further explicit expression must also be determined,

$$\int \frac{d^4 k}{(2\pi)^4} \frac{k^4}{A^2 B^3} = \frac{3a^2 b}{(b-a)^4} \ln \left[\frac{b}{a} \right] - \frac{a^2}{(b-a)^3} + \frac{b^2 - 3ab}{(b-a)^3} - \frac{b}{2(b-a)^2}.$$

Combining these results gives a contribution to the branching ratio in the form.

$$\Lambda_R \supset -\frac{1}{2(4\pi)^2} B_{iks}^* B_{jks} Q_{\psi_k} m_i \left[-\frac{m_{\psi_k}^4 - 5m_{\psi_k}^2 m_{\phi_s}^2 - 2m_{\phi_s}^4}{12(m_{\psi_k}^2 - m_{\phi_s}^2)^3} + \frac{m_{\psi_k}^2 m_{\phi_s}^4}{(m_{\psi_k}^2 - m_{\phi_s}^2)^4} \ln \left[\frac{m_{\phi_s}}{m_{\psi_k}} \right] \right] \\ - \frac{1}{2(4\pi)^2} B_{iks}^* B_{jks} Q_{\phi_s} m_i \left[\frac{m_{\phi_s}^4 - 5m_{\psi_k}^2 m_{\phi_s}^2 - 2m_{\psi_k}^4}{12(m_{\psi_k}^2 - m_{\phi_s}^2)^3} - \frac{m_{\phi_s}^2 m_{\psi_k}^4}{(m_{\psi_k}^2 - m_{\phi_s}^2)^4} \ln \left[\frac{m_{\phi_s}}{m_{\psi_k}} \right] \right].$$

It can be seen that the terms proportional to $A_{jks}^* B_{iks}^*$ and $A_{jks}^* A_{iks}$ take the same form as $A_{iks} B_{jks}$ and $B_{iks}^* B_{jks}$, respectively. As such, the result for Λ_L can be seen immediately to be,

$$\begin{aligned} \Lambda_L = & \frac{1}{(4\pi)^2} A_{jks}^* B_{iks}^* Q_{\psi_k} m_{\psi_k} \left[-\frac{m_{\psi_k}^2 - 3m_{\phi_s}^2}{4(m_{\psi_k}^2 - m_{\phi_s}^2)^2} + \frac{m_{\phi_s}^4}{(m_{\psi_k}^2 - m_{\phi_s}^2)^3} \ln \left[\frac{m_{\phi_s}}{m_{\psi_k}} \right] \right] \\ & + \frac{1}{2(4\pi)^2} A_{jks}^* B_{iks}^* Q_{\phi_s} m_{\psi_k} \left[-\frac{m_{\psi_k}^2 + m_{\phi_s}^2}{2(m_{\psi_k}^2 - m_{\phi_s}^2)^2} + \frac{2m_{\psi_k}^2 m_{\phi_s}^2}{(m_{\psi_k}^2 - m_{\phi_s}^2)^3} \ln \left[\frac{m_{\phi_s}}{m_{\psi_k}} \right] \right] \\ & - \frac{1}{2(4\pi)^2} A_{jks}^* A_{iks} Q_{\psi_k} m_i \left[-\frac{m_{\psi_k}^4 - 5m_{\psi_k}^2 m_{\phi_s}^2 - 2m_{\phi_s}^4}{12(m_{\psi_k}^2 - m_{\phi_s}^2)^3} + \frac{m_{\psi_k}^2 m_{\phi_s}^4}{(m_{\psi_k}^2 - m_{\phi_s}^2)^4} \ln \left[\frac{m_{\phi_s}}{m_{\psi_k}} \right] \right] \\ & - \frac{1}{2(4\pi)^2} A_{jks}^* A_{iks} Q_{\phi_s} m_i \left[\frac{m_{\phi_s}^4 - 5m_{\psi_k}^2 m_{\phi_s}^2 - 2m_{\psi_k}^4}{12(m_{\psi_k}^2 - m_{\phi_s}^2)^3} - \frac{m_{\phi_s}^2 m_{\psi_k}^4}{(m_{\psi_k}^2 - m_{\phi_s}^2)^4} \ln \left[\frac{m_{\phi_s}}{m_{\psi_k}} \right] \right]. \end{aligned}$$

Finally, we calculate the resulting branching ratio of the process. The effective vertex is given by,

$$\mathcal{L}_{\text{eff}} \supset 2\Lambda_{Rij} e_{Rj} \sigma^{\mu\nu} e_{Li} F_{\mu\nu} + 2\Lambda_{Lij} \bar{e}_{Lj} \bar{\sigma}^{\mu\nu} \bar{e}_{Ri} F_{\mu\nu},$$

from which it follows that the matrix element takes the form,

$$i\mathcal{M} = 2\Lambda_R p_\mu \varepsilon_\nu y(p-q) \sigma^\mu \bar{\sigma}^\nu x(q) + 2\Lambda_L p_\mu \varepsilon_\nu \bar{y}(p-q) \bar{\sigma}^\mu \sigma^\nu \bar{x}(q).$$

The matrix element is then squared, averaging over initial spin states to give,

$$\frac{1}{2} |\mathcal{M}|^2 = 16 (|\Lambda_R|^2 + |\Lambda_L|^2) (p \cdot q)^2$$

The general result for the decay $A \rightarrow 1 + 2$ is given by [92],

$$\Gamma(A \rightarrow 1 + 2) = \frac{p_f}{32\pi^2 m_A^2} \int |\mathcal{M}_{\text{spin-averaged}}|^2 d\Omega,$$

where p_f is the momentum of a final state particle in the centre-of-mass frame. For the radiative decay of charged leptons, the resulting branching ratio is given by,

$$\Gamma(l_i \rightarrow l_j \gamma) = \frac{m_i^3}{4\pi} (|\Lambda_R|^2 + |\Lambda_L|^2) .$$

It is convenient to present this in terms of the following branching ratio [92],

$$\Gamma(l_i \rightarrow l_j \nu_i \bar{\nu}_j) = \frac{G_F^2 m_i^5}{192\pi^3} ,$$

resulting in the following expression for the decay rate $l_i \rightarrow l_j \gamma$,

$$\Gamma(l_i \rightarrow l_j \gamma) = \frac{48\pi^2}{G_F^2 m_i^2} [|\Lambda_L|^2 + |\Lambda_R|^2] \Gamma(l_i \rightarrow l_j \nu_i \bar{\nu}_j) .$$

Bibliography

- [1] W. M. Yao *et al.* [Particle Data Group], “Review of particle physics,” J. Phys. G **33** (2006) 1.
- [2] N. Cabibbo, “Unitary Symmetry and Leptonic Decays,” Phys. Rev. Lett. **10** (1963) 531.
- [3] M. Kobayashi and T. Maskawa, “CP Violation In The Renormalizable Theory Of Weak Interaction,” Prog. Theor. Phys. **49** (1973) 652.
- [4] H. P. Nilles, “Supersymmetry, Supergravity And Particle Physics,” Phys. Rept. **110** (1984) 1; H. E. Haber and G. L. Kane, “The Search For Supersymmetry: Probing Physics Beyond The Standard Model,” Phys. Rept. **117**, 75 (1985); S. P. Martin, “A supersymmetry primer,” arXiv:hep-ph/9709356.
- [5] J. Wess and J. Bagger, “Supersymmetry and supergravity,” Princeton Series in Physics, 2nd Edition.
- [6] L. Girardello and M. T. Grisaru, “Soft Breaking Of Supersymmetry,” Nucl. Phys. B **194**, 65 (1982).

- [7] G. Feinberg, P. Kabir and S. Weinberg, "Transformation Of Muons Into Electrons," *Phys. Rev. Lett.* **3** (1959) 527. See also S. Weinberg, "The Quantum Theory Of Fields. Vol. I: Foundations" *Cambridge, UK: Univ. Pr. (2000)*.
- [8] L. E. Ibanez and G. G. Ross, "Discrete Gauge Symmetries And The Origin Of Baryon And Lepton Number Conservation In Supersymmetric Versions Of The Standard Model," *Nucl. Phys. B* **368** (1992) 3.
- [9] H. K. Dreiner, C. Luhn and M. Thormeier, "What is the discrete gauge symmetry of the MSSM?," arXiv:hep-ph/0512163.
- [10] P. Fayet, "Spontaneously Broken Supersymmetric Theories Of Weak, Electromagnetic And Strong Interactions," *Phys. Lett. B* **69**, 489 (1977);
G. R. Farrar and P. Fayet, "Phenomenology Of The Production, Decay, And Detection Of New Hadronic States Associated With Supersymmetry," *Phys. Lett. B* **76** (1978) 575;
- [11] S. Weinberg, "Supersymmetry At Ordinary Energies. 1. Masses And Conservation Laws," *Phys. Rev. D* **26**, 287 (1982).
- [12] For reviews of the topic, see, H. K. Dreiner, "An introduction to explicit R-parity violation," arXiv:hep-ph/9707435;
G. Bhattacharyya, "R-parity-violating supersymmetric Yukawa couplings: A mini-review," *Nucl. Phys. Proc. Suppl.* **52A** (1997) 83 [arXiv:hep-ph/9608415];
M. Chemtob, "Phenomenological constraints on broken R parity symmetry in supersymmetry models," *Prog. Part. Nucl. Phys.* **54** (2005) 71 [arXiv:hep-ph/0406029].

- [13] Y. Grossman and H. E. Haber, “The would-be majoron in R-parity violating supersymmetry,” *Phys. Rev. D* **67** (2003) 036002 [arXiv:hep-ph/0210273].
- [14] B. C. Allanach, A. Dedes and H. K. Dreiner, “The R parity violating minimal supergravity model,” *Phys. Rev. D* **69** (2004) 115002 [arXiv:hep-ph/0309196].
- [15] Phenomenology of the $\Delta L = 1$ terms $LL\bar{E}$, $LQ\bar{D}$ and LH_2 were first considered in L. J. Hall and M. Suzuki, “Explicit R Parity Breaking In Supersymmetric Models,” *Nucl. Phys. B* **231** (1984) 419. Phenomenology of the $\Delta B = 1$ term $\bar{U}\bar{D}\bar{D}$ in the superpotential was first considered in F. Zwirner, “Observable Delta B = 2 Transitions Without Nucleon Decay In A Minimal Supersymmetric Extension Of The Standard Model,” *Phys. Lett. B* **132** (1983) 103.
- [16] T. Banks, Y. Grossman, E. Nardi and Y. Nir, “Supersymmetry without R-parity and without lepton number,” *Phys. Rev. D* **52** (1995) 5319 [arXiv:hep-ph/9505248].
- [17] R. Hempfling, “Neutrino Masses and Mixing Angles in SUSY-GUT Theories with explicit R-Parity Breaking,” *Nucl. Phys. B* **478** (1996) 3 [arXiv:hep-ph/9511288].
- [18] M. Nowakowski and A. Pilaftsis, “W and Z boson interactions in supersymmetric models with explicit R-parity violation,” *Nucl. Phys. B* **461** (1996) 19 [arXiv:hep-ph/9508271].
- [19] F. de Campos, M. A. Garcia-Jareno, A. S. Joshipura, J. Rosiek and J. W. F. Valle, “Novel scalar boson decays in SUSY with broken r parity,” *Nucl. Phys. B* **451**, 3 (1995) [arXiv:hep-ph/9502237];

- [20] M. Hirsch, M. A. Diaz, W. Porod, J. C. Romao and J. W. F. Valle, “Neutrino masses and mixings from supersymmetry with bilinear R-parity violation: A theory for solar and atmospheric neutrino oscillations,” *Phys. Rev. D* **62** (2000) 113008 [Erratum-ibid. *D* **65** (2002) 119901] [arXiv:hep-ph/0004115].
- [21] D. W. Jung, S. K. Kang, J. D. Park and E. J. Chun, “Neutrino oscillations and collider test of the R-parity violating minimal supergravity model,” *JHEP* **0408** (2004) 017 [arXiv:hep-ph/0407106].
- [22] M. Bisset, O. C. W. Kong, C. Macesanu and L. H. Orr, “A simple phenomenological parametrization of supersymmetry without R-parity,” *Phys. Lett. B* **430**, 274 (1998) [arXiv:hep-ph/9804282].
- [23] Y. Grossman and H. E. Haber, “(S)neutrino properties in R-parity violating supersymmetry. I: CP-conserving phenomena,” *Phys. Rev. D* **59**, 093008 (1999) [arXiv:hep-ph/9810536].
- [24] A. Dedes, S. Rimmer, J. Rosiek and M. Schmidt-Sommerfeld, “On the neutral scalar sector of the general R-parity violating MSSM,” *Phys. Lett. B* **627** (2005) 161 [arXiv:hep-ph/0506209].
- [25] S. Davidson, M. Losada and N. Rius, “Neutral Higgs sector of the MSSM without R(p),” *Nucl. Phys. B* **587** (2000) 118 [arXiv:hep-ph/9911317].
- [26] Y. Grossman and H. E. Haber, “Basis-independent analysis of the sneutrino sector in R-parity violating supersymmetry,” *Phys. Rev. D* **63** (2001) 075011 [arXiv:hep-ph/0005276].

- [27] S. Davidson and H. E. Haber, “Basis-independent methods for the two-Higgs-doublet model,” arXiv:hep-ph/0504050.
- [28] M. Masip and A. Rasin, “Minimal supersymmetric scenarios for spontaneous CP violation,” Phys. Rev. D **58** (1998) 035007 [arXiv:hep-ph/9803271].
- [29] A. Pilaftsis, “CP-odd tadpole renormalization of Higgs scalar-pseudoscalar mixing,” Phys. Rev. D **58** (1998) 096010 [arXiv:hep-ph/9803297]; D. A. Demir, “Effects of the supersymmetric phases on the neutral Higgs sector,” Phys. Rev. D **60** (1999) 055006 [arXiv:hep-ph/9901389].
- [30] See for instance, R. A. Horn and C. R. Johnson, *Topics in Matrix analysis*, Cambridge University Press, 1991; Carl D. Meyer, *Matrix Analysis and Applied Linear Algebra*, Siam, 2000.
- [31] S. Davidson and M. Losada, “Neutrino masses in the R(p) violating MSSM,” JHEP **0005** (2000) 021 [arXiv:hep-ph/0005080].
- [32] A. Abada, S. Davidson and M. Losada, “Neutrino masses and mixings in the MSSM with soft bilinear R(p) violation,” Phys. Rev. D **65** (2002) 075010 [arXiv:hep-ph/0111332].
- [33] M. A. Diaz, M. Hirsch, W. Porod, J. C. Romao and J. W. F. Valle, “Solar neutrino masses and mixing from bilinear R-parity broken supersymmetry: Analytical versus numerical results,” Phys. Rev. D **68** (2003) 013009 [Erratum-ibid. D **71** (2005) 059904] [arXiv:hep-ph/0302021].
- [34] Y. Grossman and S. Rakshit, “Neutrino masses in R-parity violating supersymmetric models,” Phys. Rev. D **69** (2004) 093002 [arXiv:hep-ph/0311310].

- [35] J. Rosiek, "Complete Set Of Feynman Rules For The Minimal Supersymmetric Extension Of The Standard Model," *Phys. Rev. D* **41** (1990) 3464; Erratum [arXiv:hep-ph/9511250](https://arxiv.org/abs/hep-ph/9511250).
- [36] S. A. Abel and C. A. Savoy, "On metastability in supersymmetric models," *Nucl. Phys. B* **532** (1998) 3 [[arXiv:hep-ph/9803218](https://arxiv.org/abs/hep-ph/9803218)].
- [37] L. J. Hall and M. Suzuki, "Explicit R Parity Breaking In Supersymmetric Models," *Nucl. Phys. B* **231** (1984) 419.
- [38] A. S. Joshipura and M. Nowakowski, "'Just so' oscillations in supersymmetric standard model," *Phys. Rev. D* **51**, 2421 (1995) [[arXiv:hep-ph/9408224](https://arxiv.org/abs/hep-ph/9408224)].
- [39] D. E. Kaplan and A. E. Nelson, "Solar and atmospheric neutrino oscillations from bilinear R-parity violation," *JHEP* **0001** (2000) 033 [[arXiv:hep-ph/9901254](https://arxiv.org/abs/hep-ph/9901254)].
- [40] Y. Grossman and H. E. Haber, "Sneutrino mixing phenomena," *Phys. Rev. Lett.* **78** (1997) 3438 [[arXiv:hep-ph/9702421](https://arxiv.org/abs/hep-ph/9702421)].
- [41] B. de Carlos and P. L. White, "R-parity Violation Effects through Soft Supersymmetry Breaking Terms and the Renormalisation Group," *Phys. Rev. D* **54** (1996) 3427 [[arXiv:hep-ph/9602381](https://arxiv.org/abs/hep-ph/9602381)].
- [42] E. Nardi, "Renormalization group induced neutrino masses in supersymmetry without R-parity," *Phys. Rev. D* **55** (1997) 5772 [[arXiv:hep-ph/9610540](https://arxiv.org/abs/hep-ph/9610540)].

- [43] F. M. Borzumati, Y. Grossman, E. Nardi and Y. Nir, “Neutrino masses and mixing in supersymmetric models without R parity,” *Phys. Lett. B* **384** (1996) 123 [arXiv:hep-ph/9606251].
- [44] M. Drees, S. Pakvasa, X. Tata and T. ter Veldhuis, “A supersymmetric resolution of solar and atmospheric neutrino puzzles,” *Phys. Rev. D* **57** (1998) 5335 [arXiv:hep-ph/9712392].
- [45] E. J. Chun, S. K. Kang, C. W. Kim and U. W. Lee, “Supersymmetric neutrino masses and mixing with R-parity violation,” *Nucl. Phys. B* **544** (1999) 89 [arXiv:hep-ph/9807327].
- [46] A. S. Joshipura and S. K. Vempati, “Sneutrino vacuum expectation values and neutrino anomalies through trilinear R-parity violation,” *Phys. Rev. D* **60** (1999) 111303 [arXiv:hep-ph/9903435].
- [47] K. Choi, K. Hwang and E. J. Chun, “Atmospheric and solar neutrino masses from horizontal U(1) symmetry,” *Phys. Rev. D* **60**, 031301 (1999) [arXiv:hep-ph/9811363].
- [48] O. C. W. Kong, “Neutrino oscillations and flavor structure of supersymmetry without R-parity,” *Mod. Phys. Lett. A* **14** (1999) 903 [arXiv:hep-ph/9808304].
- [49] S. Rakshit, G. Bhattacharyya and A. Raychaudhuri, “R-parity-violating trilinear couplings and recent neutrino data,” *Phys. Rev. D* **59** (1999) 091701 [arXiv:hep-ph/9811500].

- [50] R. Adhikari and G. Omanovic, “LSND, solar and atmospheric neutrino oscillation experiments, and R-parity violating supersymmetry,” *Phys. Rev. D* **59** (1999) 073003.
- [51] A. Abada, G. Bhattacharyya and M. Losada, “A general analysis with trilinear and bilinear R-parity violating couplings in the light of recent SNO data,” *Phys. Rev. D* **66** (2002) 071701 [arXiv:hep-ph/0208009]; A. Abada and M. Losada, “Constraints on both bilinear and trilinear R-parity violating couplings from neutrino laboratories and astrophysics data,” *Phys. Lett. B* **492** (2000) 310 [arXiv:hep-ph/0007041].
- [52] S. Rakshit, “Neutrino masses and R-parity violation,” *Mod. Phys. Lett. A* **19** (2004) 2239 [arXiv:hep-ph/0406168].
- [53] A. Dedes, S. Rimmer and J. Rosiek, “Neutrino masses in the lepton number violating MSSM,” *JHEP* **0608** (2006) 005 [arXiv:hep-ph/0603225].
- [54] Z. Maki, M. Nakagawa and S. Sakata, “Remarks On The Unified Model Of Elementary Particles,” *Prog. Theor. Phys.* **28** (1962) 870; B. Pontecorvo, “Neutrino Experiments And The Question Of Leptonic-Charge Conservation,” *Sov. Phys. JETP* **26** (1968) 984 [*Zh. Eksp. Teor. Fiz.* **53** (1967) 1717].
- [55] J. Schechter and J. W. F. Valle, “Neutrino Decay And Spontaneous Violation Of Lepton Number,” *Phys. Rev. D* **25** (1982) 774.
- [56] M. Gell-Mann, M. P. Ramond and R. Slansky, 1979, in *Supergravity*, edited by P. van Nieuwenhuizen and D.Z. Freedman (North Holland); T Yanagida, in *Proceedings of Workshop on Unified Theory and Baryon Number in the*

- Universe, edited by O. Sawada and A. Sugamoto (KEK); R. N. Mohapatra and G. Senjanovic, "Neutrino Mass And Spontaneous Parity Nonconservation," *Phys. Rev. Lett.* **44** (1980) 912.
- [57] S. Y. Choi, J. Kalinowski, G. Moortgat-Pick and P. M. Zerwas, "Analysis of the neutralino system in supersymmetric theories," *Eur. Phys. J. C* **22**, 563 (2001) [Addendum-*ibid.* C **23**, 769 (2002)] [arXiv:hep-ph/0108117].
- [58] H. Haber, "*Practical Methods for treating Majorana fermions*", lecture given at Pre-SUSY 2005, <http://www.ippp.dur.ac.uk/pre-SUSY05/> . See also, H.K. Dreiner, H. E. Haber and S. P. Martin, *unpublished*.
- [59] B. A. Kniehl and A. Pilaftsis, "Mixing Renormalization in Majorana Neutrino Theories," *Nucl. Phys. B* **474**, 286 (1996) [arXiv:hep-ph/9601390]; A. Pilaftsis, "Gauge and scheme dependence of mixing matrix renormalization," *Phys. Rev. D* **65**, 115013 (2002) [arXiv:hep-ph/0203210].
- [60] M. Misiak, S. Pokorski and J. Rosiek, "Supersymmetry and FCNC effects," *Adv. Ser. Direct. High Energy Phys.* **15** (1998) 795 [arXiv:hep-ph/9703442].
- [61] M. Hirsch, H. V. Klapdor-Kleingrothaus and S. G. Kovalenko, "B-L violating masses in softly broken supersymmetry," *Phys. Lett. B* **398**, 311 (1997) [arXiv:hep-ph/9701253].
- [62] F. Borzumati and J. S. Lee, "Novel constraints on $\Delta(L) = 1$ interactions from neutrino masses," *Phys. Rev. D* **66**, 115012 (2002) [arXiv:hep-ph/0207184].
- [63] T. Schwetz, "Neutrino oscillations: Current status and prospects," *Acta Phys. Polon. B* **36** (2005) 3203 [arXiv:hep-ph/0510331].

- [64] P. F. Harrison, D. H. Perkins and W. G. Scott, “Tri-bimaximal mixing and the neutrino oscillation data,” *Phys. Lett. B* **530**, 167 (2002) [arXiv:hep-ph/0202074].
- [65] B. C. Allanach *et al.*, “The Snowmass points and slopes: Benchmarks for SUSY searches,” in *Proc. of the APS/DPF/DPB Summer Study on the Future of Particle Physics (Snowmass 2001)* ed. N. Graf, *Eur. Phys. J. C* **25** (2002) 113 [eConf **C010630** (2001) P125] [arXiv:hep-ph/0202233].
- [66] B. C. Allanach, “SOFTSUSY: A C++ program for calculating supersymmetric spectra,” *Comput. Phys. Commun.* **143**, 305 (2002) [arXiv:hep-ph/0104145].
- [67] B. C. Allanach, A. Dedes and H. K. Dreiner, “Bounds on R-parity violating couplings at the weak scale and at the GUT scale,” *Phys. Rev. D* **60** (1999) 075014 [arXiv:hep-ph/9906209].
- [68] S. A. Abel, A. Dedes and H. K. Dreiner, “Dipole moments of the electron, neutrino and neutron in the MSSM without R-parity symmetry,” *JHEP* **0005** (2000) 013 [arXiv:hep-ph/9912429].
- [69] T. Schwetz, “Global fits to neutrino oscillation data,” *Phys. Scripta* **T127** (2006) 1 [arXiv:hep-ph/0606060].
- [70] T. P. Cheng and L. F. Li, “Nonconservation Of Separate Mu - Lepton And E - Lepton Numbers In Gauge Theories With V+A Currents,” *Phys. Rev. Lett.* **38** (1977) 381.
- [71] F. Borzumati and A. Masiero, “Large Muon And Electron Number Violations In Supergravity Theories,” *Phys. Rev. Lett.* **57** (1986) 961.

- [72] B. de Carlos, J. A. Casas and J. M. Moreno, “Constraints on supersymmetric theories from $\mu \rightarrow e \gamma$,” *Phys. Rev. D* **53** (1996) 6398 [arXiv:hep-ph/9507377].
- [73] J. Hisano and K. Tobe, “Neutrino masses, muon $g-2$, and lepton-flavour violation in the supersymmetric see-saw model,” *Phys. Lett. B* **510**, 197 (2001) [arXiv:hep-ph/0102315].
- [74] S. Lavignac, I. Masina and C. A. Savoy, “ $\tau \rightarrow \mu \gamma$ and $\mu \rightarrow e \gamma$ as probes of neutrino mass models,” *Phys. Lett. B* **520**, 269 (2001) [arXiv:hep-ph/0106245].
- [75] J. A. Casas and A. Ibarra, “Oscillating neutrinos and $\mu \rightarrow e, \gamma$,” *Nucl. Phys. B* **618**, 171 (2001) [arXiv:hep-ph/0103065].
- [76] A. de Gouvea, S. Lola and K. Tobe, “Lepton flavor violation in supersymmetric models with trilinear R-parity violation,” *Phys. Rev. D* **63**, 035004 (2001) [arXiv:hep-ph/0008085].
- [77] S. Rimmer, “ $l \rightarrow l' \gamma$ in the lepton number violating MSSM,” arXiv:hep-ph/0610406.
- [78] M. Ahmed *et al.* [MEGA Collaboration], “Search for the lepton-family-number nonconserving decay $\mu^+ \rightarrow e^+ \gamma$,” *Phys. Rev. D* **65**, 112002 (2002) [arXiv:hep-ex/0111030].
- [79] B. Aubert *et al.* [BABAR Collaboration], “Search for lepton flavor violation in the decay $\tau \rightarrow \mu \gamma$,” *Phys. Rev. Lett.* **95**, 041802 (2005) [arXiv:hep-ex/0502032].

- [80] B. Aubert *et al.* [BABAR Collaboration], “Search for lepton flavor violation in the decay $\tau^\pm \rightarrow e^\pm \gamma$,” *Phys. Rev. Lett.* **96** (2006) 041801 [arXiv:hep-ex/0508012].
- [81] Y. Mori *et al.* [PRISM/PRIME working group], LOI-25 [<http://psux1.kek.jp/~jhfnp/LOIlist/LOIlist.html>].
- [82] M. A. Giorgi [SuperB group], “SuperB: a High Luminosity Flavour Factory”, [<http://www.infn.it/csn1/Roadmap/Super%20B.pdf>].
- [83] L. Calibbi, A. Faccia, A. Masiero and S. K. Vempati, “Lepton flavour violation from SUSY-GUTs: Where do we stand for MEG, PRISM / PRIME and a super flavour factory,” arXiv:hep-ph/0605139.
- [84] A. Brignole and A. Rossi, “Anatomy and phenomenology of mu tau lepton flavour violation in the MSSM,” *Nucl. Phys. B* **701** (2004) 3 [arXiv:hep-ph/0404211].
- [85] A. Dedes, H. Haber and J. Rosiek, *in preparation*
- [86] D. F. Carvalho, M. E. Gomez and J. C. Romao, “Charged lepton flavor violation in supersymmetry with bilinear R-parity violation,” *Phys. Rev. D* **65** (2002) 093013 [arXiv:hep-ph/0202054].
- [87] V. D. Barger, G. F. Giudice and T. Han, “SOME NEW ASPECTS OF SUPER-SYMMETRY R PARITY VIOLATING INTERACTIONS,” *Phys. Rev. D* **40** (1989) 2987.

- [88] K. Huitu, J. Maalampi, M. Raidal and A. Santamaria, “New constraints on R-parity violation from $\mu \rightarrow e$ conversion in nuclei,” *Phys. Lett. B* **430** (1998) 355 [arXiv:hep-ph/9712249].
- [89] B. C. Allanach, M. A. Bernhardt, H. K. Dreiner, C. H. Kom and P. Richardson, “Mass spectrum in R-parity violating mSUGRA and benchmark points,” arXiv:hep-ph/0609263.
- [90] G. Passarino and M. J. G. Veltman, “One Loop Corrections For $E^+ E^-$ Annihilation Into $\mu^+ \mu^-$ In The Weinberg Model,” *Nucl. Phys. B* **160** (1979) 151;
- [91] T. Hahn and M. Perez-Victoria, “Automatized one-loop calculations in four and D dimensions,” *Comput. Phys. Commun.* **118**, 153 (1999) [arXiv:hep-ph/9807565]. See also “*LoopTools user guide*” in <http://www.feynarts.de/looptools/>.
- [92] F. Halzen and A. D. Martin, “Quarks And Leptons: An Introductory Course In Modern Particle Physics,” *Phys. Rev. D* **66** (2002) 010001.

